THÈSE POUR OBTENIR LE GRADE DE DOCTEUR DE L'UNIVERSITÉ DE MONTPELLIER

En Biologie Santé

École doctorale Sciences Chimiques et Biologiques pour la Santé (CBS2)

Unité de recherche UMR5235

CARACTÉRISATION MOLÉCULAIRE DE L'INVASION DES BRADYZOITES ET ÉVALUATION DE CANDIDATS VACCINS CIBLANT LA JONCTION MOBILE DE *TOXOPLASMA GONDII*

Présentée par Rania Najm
Le 5 mars 2021

Sous la direction de Maryse Lebrun
et co-direction Hiba El Hajj

Devant le jury composé de

Mr Rogerio Amino, Directeur d'unité, Malaria Infection & Immunity, Institut Pasteur Paris	Rapporteur
Mr Furio Spano, Staff Scientist, Département Maladies Infectieuses, Instituto Superiore di Sanità, Rome (IT)	Rapporteur
Mr Olivier Silvie, DR2, Inserm, Université Pierre et Marie Curie	Examinateur
Mr Jean François Dubremetz, DR1, CNRS, Université de Montpellier	Président
Mme Maryse Lebrun, DR1, CNRS, Université de Montpellier	Directeur
Mme Hiba El Hajj, Associate Pr, Département de Microbiologie, Université Américaine de Beirut (Liban)	Co-Directeur

UNIVERSITÉ DE MONTPELLIER

ACKNOWLEDGEMENTS

Foremost, I would like to express my sincere appreciation to my thesis director Dr Maryse Lebrun and thesis co-director Dr Hiba El Hajj for their continuous support and guidance. This tremendous collaborative supervision was more than I ever asked for in a back and forth PhD program.

For that, I am extremely thankful and pay my gratitude to my guide Dr Maryse for her encouragement, immense knowledge and enthusiasm. I benefited a lot from her constructive scientific comments. Thank you for your constant support throughout my PhD and I look forward to continue working with you. I am also ineffably indebted to my role model Dr Hiba for her patience, conscientious guidance and uplifting motivation. Your profound proficiency and scientific knowledge reinforced my research skills. Thank you for believing in me since day one and pushing me to become the best version of myself. You assisted me on a professional level as much as you did on a personal level and I am forever grateful for that.

I am very thankful to Dr Martin Boulanger for supplying us with the recombinant proteins. Without him this work would not have been possible. I would like to thank Dr Mathieu Gissot for helping us in our *in vivo* experiments. I am also grateful to Dr Sebastien Besteiro who was the first to assist me with my experiments during my first arrival to the ML lab.

My sincere gratitude goes to the Jury members Drs Jean François Dubremetz, Olivier Silvie, Rogerio Amino and Furio Spano for accepting to judge this work. I am confident that I will benefit from their insightful comments and expertise in the field.

I would like to extend my gratitude to all Dr Maryse's and Dr Hiba's lab members who were of tremendous help during my journey with their constructive ideas and stimulating discussions.

My deep appreciation goes to my beloved friends and colleagues, Rana El Hajj and Sara Moadad for their continuous motivation, true friendship that turned into a sisterhood and unforgettable dear memories.

A warm thank you to my dear friends Marta Cova, Eleonora Aquilini, Aude Cerutti, Daniela Sparvoli, Sarah Pamukcu, Diana Penarete Vargas, Justine Heckendorn, and Margarida Ruivo for their support, technical help whenever needed, and a delightful and pleasant environment.

I finally acknowledge with deep sense of reverence, my gratitude to my family, my lovely parents and little sister for their tenacious support throughout my life. This kind of achievement would not have been possible without you by my side.

Résumé

La toxoplasmose est une infection parasitaire négligée nécessitant un contrôle de santé publique. Elle est due au parasite intracellulaire obligatoire, *Toxoplasma gondii*. Une des voies d'infection est l'ingestion orale de kystes tissulaires contenant des bradyzoïtes. Ces derniers envahissent les entérocytes et se transforment en tachyzoïtes, responsables de la toxoplasmose aiguë. Sous le contrôle de la réponse immunitaire de l'hôte, les tachyzoïtes se retransforment en bradyzoïtes, forme dormante enkystée dans le cerveau et les muscles, et conduisant à la toxoplasmose chronique. Chez les immunodéprimés, cette forme chronique peut se réactiver et devenir fatale, si non traitée. L'invasion par le toxoplasme engage la formation d'une jonction mobile (JM), correspondant à une connexion étroite entre les membranes du parasite et de sa cellule hôte. Chez les tachyzoïtes, la JM est moléculairement bien caractérisée. Elle est formée par l'interaction d'une protéine de micronème, AMA1, et une protéine du col des rhoptries, RON2, elle-même associée à d'autres protéines RONs. Quant aux bradyzoïtes, la présence de JM et l'invasion demeurent énigmatiques. Dans cette étude, nous avons montré que les protéines de JM caractérisées chez le tachyzoïte, sont également exprimées dans la JM des bradyzoïtes, révélant pour la première fois, que les bradyzoïtes établissent une JM lors de leur invasion. Nous avons également montré qu'AMA2, AMA4 et $RON2_{L1}$, des protéines homologues à AMA1 et RON2 mais quasiment pas exprimées au stade tachyzoïte, l'étaient en revanche fortement au stade bradyzoïte. Notamment, nous avons détecté AMA4 et AMA2 à la JM des bradyzoïtes, soulignant que la JM de ces stades présente une composition protéique différente de celle des tachyzoïtes. Nous avons aussi généré des parasites knock-out AMA4 et montré l'importance d'AMA4 lors de l'invasion des tachyzoïtes, mais surtout son rôle prédominant lors de l'invasion des bradyzoïtes et de l'établissement de la toxoplasmose chronique.

En absence d'un vaccin approuvé contre la toxoplasmose humaine, et en vue des résultats prometteurs de la stratégie de vaccination contre le paludisme basée sur l'immunisation avec le complexe AMA1-RON2, nous visions à cibler les complexes moléculaires de la JM des stades tachyzoïtes et bradyzoïtes, afin d'élucider la protection éventuelle contre la toxoplasmose. L'immunisation par la protéine recombinante AMA1, en complexe avec un peptide RON2, montra une efficacité protectrice élevée se manifestant par 80% de réduction du nombre de kystes après une épreuve kystique par voie orale, et 80% d'augmentation de survie des souris infectées par une dose létale de tachyzoïtes par voie intrapéritonéale. Cependant, le complexe AMA4 lié à son peptide $RON2_{L1}$ n'a conféré aucune

protection contre l'infection aiguë, un résultat cohérent avec sa faible expression chez le tachyzoïte. Cependant, le complexe AMA4-RON2$_{L1}$ protégeait principalement les souris contre l'infection chronique après une épreuve par voie orale de kystes, supportant son rôle essentiel dans l'invasion des bradyzoïtes. De plus, l'immunisation avec les complexes AMA-RON2 s'avérait plus efficace que celle par les protéines AMA seules. Finalement, les immunoglobulines G contre l'un ou l'autre des complexes inhibaient la formation de la JM et l'invasion *in vitro*, suggérant que l'inhibition de l'invasion puisse être un des mécanismes de protection *in vivo*. En outre, nous avons démontré que les anticorps générés contre le complexe AMA1-RON2 ciblent surtout l'invasion des tachyzoïtes alors que ceux générés contre le complexe AMA4-RON2$_{L1}$ visent préférentiellement l'invasion des bradyzoïtes; soutenant ainsi le rôle prédominant du complexe AMA1-RON2 dans l'invasion des tachyzoïtes et celui du complexe AMA4-RON2$_{L1}$ dans l'invasion des bradyzoïtes. Globalement, nos résultats identifient et valident différents complexes de JM comme candidats potentiels pour la vaccination contre la toxoplasmose.

Mots clés: Toxoplasmose, invasion, jonction mobile, AMA4-RON2$_{L1}$, AMA1-RON2, vaccin

ABSTRACT

Toxoplasmosis is classified as a neglected parasitic infection necessitating public health control. It is due to *Toxoplasma gondii*, an obligatory intracellular parasite. One route of infection occurs following the oral ingestion of bradyzoite tissue cysts. Thereupon, bradyzoites invade enterocytes and convert rapidly to tachyzoites, leading to the acute infection. Under the tight control of host immune response, tachyzoites transform back into bradyzoites which sustain a lifelong chronic disease. If left untreated, chronic toxoplasmosis may reactivate and become fatal in immunocompromised patients. Invasion of *Toxoplasma* involves the formation of a tight connection between the parasite and the host cell membranes, referred to a structure called Moving Junction (MJ). In tachyzoites, the MJ is shaped by the assembly of a microneme protein, AMA1, and a rhoptry neck protein, RON2, as part of a complex involving additional RONs. Whilst the MJ process is well characterized in tachyzoites, invasion in bradyzoites remains underexplored. Here, we demonstrated that tachyzoite MJ proteins are also expressed at the MJ of invading bradyzoites, showing for the first time that bradyzoites do form a MJ during their invasion. We also characterized more paralogs of MJ proteins, which are barely expressed in tachyzoites, and demonstrated that AMA2, AMA4 and $RON2_{L1,}$ are highly expressed in bradyzoites. Remarkably, we found AMA4 and AMA2 at the MJ of invading bradyzoites, highlighting that bradyzoite MJ exhibits a different protein composition than that of invading tachyzoites. Moreover, we generated AMA4 knockout parasites and unraveled the importance of AMA4 for invasion in tachyzoites in some extent, but its predominant role for bradyzoite invasion and for establishing the chronic phase of infection.

In light of the absence of an approved vaccine against human toxoplasmosis and the promises of a vaccine strategy based on immunization with AMA1-RON2 complex against *Plasmodium*, we built on the importance of MJ in invasion of both tachyzoite and bradyzoite stages, and interrogated the potential protection against toxoplasmosis by targeting MJ complexes. Immunization with recombinant AMA1 protein in complex with a RON2 peptide, revealed a high protective efficacy both after oral challenge of mice with bradyzoites (≈80% reduction of cysts burden) or intraperitoneal challenge with a lethal dose of tachyzoites (80% increased mice survival). Yet, AMA4 in complex with its binding $RON2_{L1}$ peptide did not protect against acute infection, a consistent result with its low expression and function in tachyzoites. In contrast, supporting its role in the invasion of bradyzoites, AMA4-$RON2_{L1}$ complex mainly protected against chronic infection. In both cases, immunization with AMA-RON2 complexes is more efficient than immunization with AMA alone. Finally, IgG against

either complexes inhibited MJ formation and invasion *in vitro*, suggesting that the inhibition of invasion may be one plausible mechanism for *in vivo* protection. Importantly, antibodies against AMA1-RON2 are more efficient to inhibit the invasion of tachyzoites while antibodies against AMA4-RON2$_{L1}$ target preferentially the invasion of bradyzoites; both supporting a predominant role of AMA1-RON2 in tachyzoites and AMA4-RON2$_{L1}$ in bradyzoites. Altogether, these results validate different MJ complexes as potential vaccine candidates to protect against toxoplasmosis.

Keywords: Toxoplasmosis, invasion, moving junction, AMA4-RON2$_{L1}$, AMA1-RON2, vaccine

LIST OF ABREVIATIONS

Tg	*Toxoplasma gondii*	Mbp	Megabase pair
MJ	Moving Junction	PCR-RFLP	polymerase chain reaction-restriction fragment length polymorphism
AMA	Apical membrane Antigen	Br	Brazil
RON	Rhoptry Neck Protein	AIDS	Acquired immunodeficiency syndrome
IL	Interleukin	LD	Lethal Dose
Co	Conoid	CNTNAP	Contactin-associated protein-like
Go	Golgi complex	GABA	neurotransmitter gamma-aminobutyric acid
Mn	Microneme	GABAR	neurotransmitter gamma-aminobutyric acid receptor
Rh	Rhoptry	HIV	human immunodeficiency virus
Dg	Electron-dense granule	BBB	Blood-brain barrier
Pv	Parasitophorous vacuole	CNS	Central nervous system
PVM	Parasitophorous vacuole membrane	Ca^{2+}	Calcium
Cw	Cyst wall	IFN	Interferon
Ga	Golgi adjunct (apicoplast)	NO	Nitric oxide
Am	Amylopectin	KO	Knock out
IDO	indoleamine 2,3-dioxygenase	GAP	gliding-associated integral membrane glycoprotein
TNF	Tumor Necrosis Factor	MLC	Myosin Light Chain
CDA	Autoantigen-1	IAP	IMC-associated protein
AP2	Apetala2	ACT	Actin
ApiAP2	Apicomplexan Apetala2	F-actin	Filamentous actin
MIC	Microneme protein	ELC	Essential Light Chain

PPM	Parasite Plasma Membrane	PCR	Pre-conoidal rings
IMC	Inner Membrane Complex	APR	Apical polar ring
GAC	glideosome-associated connector	MTs	Microtubules
Myo	Myosin	AKMT	lysine (K) methyltransferase
CaM	Calmodulin	SAG	Surface Antigen Glycoprotein
GPI	Glycosylphosphatidylinositol	SRS	SAG-related sequence proteins
TRAP	Thrombospondin-related anonymous protein	M2AP	MIC2-associated protein
EGF	Epidermal growth factor	EGFR	Epidermal growth factor receptor
ROM	Rhomboid-like protease 4	CLAMP	claudin-like apicomplexan microneme protein
K^+	Potassium	cGMP	cyclic guanosine monophosphate
H^+	Hydrogen	PKG	cGMP associated protein kinase G
IP_3	Inositol triphosphate	cAMP	cyclic adenosine monophosphate
PIP_2	Phosphatidyl inositol diphosphate	APH	acylated pleckstrin homology domain
PI-PLC	phosphoinositide phospholipase C	CHO	Chinese hamster ovary cells
CDPK	Calcium dependent protein kinase	HCM	Host cell plasmalemma
Pf	*Plasmodium falciparum*	*Pv*	*Plasmodium vivax*
Trp	Tryptophan	CD2AP	CD2-associated protein
Tyr	Tyrosine	TSG101	tumor susceptibility gene 101 protein
CIN85	CBL-interacting protein	ALIX	ALG2-interacting protein X
sporo	Sporozoite	CTD	C-terminal domain
CDC	Centers for Disease Control	TMP-SMX	trimethoprim–sulfamethoxazole
GRA	Dense granule antigen	MHC	major histocompatibility complex
VLP	virus-like particle	HSP	Heat shock protein

ROP	Rhoptry bulb protein	EF	Elongation factor
ADF	actin depolymerizing factor	ASP	Aspartic protease
PGAM	phosphoglycerate mutase	Prx	Peroxiredoxin
mRNA	messenger RNA	miRNA	microRNA
NPs	Nanoparticles	TLR	Toll like receptor
DMEM	Dulbecco's Modified Eagle's Medium	CAT	Chloramphenicol acetyltransferase
Pru	Prugnaud	DHFR	dihydrofolate reductase
YFP	Yellow fluorescent protein	gRNA	guide RNA
HA3	Triple Hemagglutinin tag	CRISPR	clusters of regularly interspaced short palindromic repeats
PBS	Phosphate-buffered saline	Cas9	CRISPR associated protein 9
HFF	Human foreskin fibroblasts	NaHCO3	sodium bicarbonate
TEV	Tobacco Etch Virus	HBSS	Hanks' Balanced Salt Solution
DBA	*Dolichos biflorus* agglutinin		

LIST OF FIGURES

Figure 1	Phylogenetic tree of Apicompla	16
Figure 2	Transmission electron micrograph showing the structure of *Toxoplasma gondii* tachyzoite	18
Figure 3	Structure of bradyzoite in tissue cyst	20
Figure 4	*Toxoplasma gondii* oocysts	22
Figure 5	*Toxoplasma gondii* life cycle	25
Figure 6	A schematic representation of a gliding and invading parasite	41
Figure 7	Schematic representation of the glideosome	43
Figure 8	Moving junction formation by *Plasmodium* merozoite and *Toxoplasma* tachyzoite *in vitro*	49
Figure 9	Scheme presenting the composition of the moving junction during invasion in tachyzoites	50
Figure 10	AMA1-RON2 complex in *T. gondii*	54
Figure 11	Structures of *Tg*AMA family members	60
Figure 12	*In vivo* transcriptome analysis of *T. gondii* during acute and chronic infection	91
Figure 13	Expression of AMA1, RON2, RON4, RON5, RON8 and $RON4_{L1}$ in the bradyzoite stage	92
Figure 14	Tagging of the rhoptry neck protein $RON4_{L1}$ at its N-terminal end	93
Figure 15	Localization of AMA1, RON2, RON4, RON5, RON8, and $RON4_{L1}$ at the moving junction of invading bradyzoites	96
Figure 16	Expression of alternative *Tg*AMA-*Tg*RON complex in bradyzoites	98
Figure 17	Tagging of the microneme protein AMA2 at the C-terminal end	99
Figure 18	Disruption and knock out of *AMA4* locus in RH*Δku80* and Pru respectively	101
Figure 19	AMA4 does not have a role during acute phase in type I RH *Δku80* strain	102
Figure 20	AMA4 plays are role in tachyzoite invasion and establishment of chronic toxoplasmosis	105

Figure 21	Vaccination strategy using rAMA$_1$ protein or rAMA1-RON$_2$D3 complex	107
Figure 22	Immunization with rAMA1 or rAMA1-RON2D3 induce a strong and specific immune response against AMA1 in C57BL/6 mice	110
Figure 23	Immunization with rAMA1-RON2D3 induces higher protective efficacy against acute and chronic toxoplasmosis	111
Figure 24	Vaccination strategy using rAMA4 protein or rAMA1-RON2$_{L1}$D3 complex	112
Figure 25	Immunization with rAMA4 or rAMA4-RON2$_{L1}$D3 induce a strong and specific immune response in C57BL/6 mice	115
Figure 26	Immunization with rAMA4-RON2$_{L1}$D3 induces higher protective efficacy after oral challenge with cysts	116
Figure 27	Immunization with both rAMA1-RON2D3 and rAMA4-RON2$_{L1}$D3 enhances protection against chronic toxoplasmosis	117
Figure 28	Immunization with the complexes induce more potent inhibitory antibodies	119
Figure 29	Inhibitory antibodies induces abortive invasion	121
Figure 30	Inhibitory antibodies targeting the invasion complexes inhibit bradyzoite invasion	124
Figure 31	Localization of *Tg*ROP1 and RON5 in bradyzoites 30 min after invasion	129
Figure 32	*In vivo* transcriptome analysis of *T. gondii* in tachyzoite and day 5 merozoite stages	138

LIST OF TABLES

Table 1	Comparison between tachyzoite and bradyzoite stages	20
Table 2	Ultrastructural differentiation of *T. gondii* tachyzoites and types B–E schizonts of merozoites	22
Table 3	Summary of most effective live-attenuated vaccines	65
Table 4	Summary of most effective protein vaccines	66
Table 5	Summary of most effective DNA vaccines	68
Table 6	List of primers used for the generarion of *KO-AMA4* in RH*Δku80* and Pru backgrounds	77
Table 7	List of primers used for the verification of $RON4_{L1}$ and *AMA2 HA3* tagging in Pru background	78
Table 8	List of antibodies used in IFA	80
Table 9	List of antibodies used in western blot analysis	80

Table of Contents

ACKNOWLEDGEMENTS 1
Résumé 2
ABSTRACT 4
LIST OF ABREVIATIONS 6
LIST OF FIGURES 9
LIST OF TABLES 11
1.1. *Toxoplasma gondii* 15
1.1.1. *Toxoplasma gondii*: Taxonomy 15
1.1.2. The phylum Apicomplexa 16
1.2. Stages of *Toxoplasma gondii* 17
1.2.1. The tachyzoite stage 18
1.2.2. The Bradyzoite stage 18
1.2.3. The Merozoites stage 21
1.2.4. Sporozoites 22
1.3. Life cycle 23
1.3.1. Sexual life cycle 23
1.3.2. Asexual life cycle 24
1.4. Modes of Transmission 25
1.5. Genetic overview and virulence of *T. gondii* strains 26
1.6. Toxoplasmosis 27
1.6.1 Toxoplasmosis in immunocompetent individuals 27
1.6.1.1. Cancers associated with *T. gondii* 28
1.6.1.2. Psychiatric Disorders Associated with *T. gondii* 28
1.6.2. Toxoplasmosis in immunocompromised patients 29
1.6.3. Congenital toxoplasmosis 30
1.7. The impact of bradyzoites on the central nervous system 31
1.7.1. Molecular mechanisms of conversion of tachyzoites to bradyzoites 32
1.7.1.1. Immunity factors 32
1.7.1.2. Host cell factors 34
1.7.1.3. Parasitic factors 35
1.7.2. Reactivation of bradyzoites to tachyzoites 36
1.8. Invasion of *Toxoplasma gondii* 37
1.8.1. Structures involved during invasion of *T. gondii* 40

1.8.1.1. Glideosome machinery 41
1.8.1.2 Conoid 43
1.8.2. Secretory organelles associated with invasion 44
1.8.2.1. Molecular mechanisms of secretory organelles secretion 46
1.8.2.1. Moving junction 48
1.8.2.1.1. Molecular organization of the Moving junction 49
1.8.2.1.1.1. Moving junction composition in tachyzoites 50
1.8.2.1.1.1.1. Importance of moving junction proteins during invasion 54
1.8.2.1.1.2. Moving junction in sporozoite stage 57
1.9. Vaccination and Toxoplasmosis 60
1.9.1. Vaccination approaches against toxoplasmosis 61
1.9.1.1. Live-attenuated Vaccines 63
1.9.1.2. Protein vaccines 65
1.9.1.3. DNA vaccines 66
1.9.1.4. RNA vaccines 68
1.9.1.5. Nanoparticle-Based Vaccines 69
1.9.1.6. Exosome-Based Vaccines 70
1.9.1.7. Carbohydrate-Based Vaccines 71
1.9.1.8. AMA1 vaccines 71
1.9.2. Challenges for developing vaccines 73
CHAPTER 2: MATERIALS AND METHODS 75
2.1. Parasite and cell culture 75
2.2. Generation of parasite lines 75
2.2.1. Knock out strategy 75
2.2.1.1. KO-AMA4 in RH*Δku80* 75
2.2.1.2. KO-AMA4 in Pru 76
2.2.2. Tagging strategy 77
2.2.2.1. *RON4$_{L1}$-HA$_3$* tagging 77
2.2.2.2. *AMA2-HA$_3$* tagging 78
2.3. Immunofluorescence assay (IFA) 78
2.4. Western blot analysis 80
2.5. *In vitro* bradyzoite differentiation assay 81
2.6. Generation of individual proteins and complexes 81
2.6.1. Cloning and purification of individual proteins 81
2.6.2. Purification of the complexes 82
2.8. Brain cyst purification using Percoll gradient 83

2.9. Mice survival and burden of cysts in the brains of infected mice 83
2.10. Immunization study 84
2.11. Bradyzoite isolation and invasion assay 85
2.12. Invasion Inhibition Assay and e-vacuoles quantification 85
2.13. Plaque assay 86
2.14. ELISA (Enzyme-linked Immunosorbent Assay) 87
2.15. Statistical Analysis 88
CHAPTER 3: RESULTS 89
Part I: Deciphering the invasion process and molecular players in bradyzoites 91
3.1.1. Moving Junction proteins are expressed in bradyzoites 91
3.1.2. Bradyzoites invade in a moving junction-dependent fashion 94
3.1.3. AMA2, AMA4 and RON2$_{L1}$ are up-regulated in the bradyzoite stage and AMA2 and AMA4 decorate the moving junction of invading bradyzoites 96
3.1.4. AMA4 plays a role in invasion and establishment of chronic infection 100
Part II. Vaccination using AMA-RON MJ complexes 107
3.2.1. AMA1 in complex with RON2 exhibits a strong protective effect against acute and chronic infection with *Toxoplasma gondii* 107
3.2.2. AMA1 in complex with RON2 peptide induces a protective immunization for acute and chronic phase 110
3.2.3. AMA4-RON2$_{L1}$ complex is another vaccine candidate against chronic toxoplasmosis 112
3.2.4. AMA-RON complexes induce invasion inhibitory antibodies 117
3.2.5. AMA1-RON2 but mostly AMA4-RON2$_{L1}$ are involved in bradyzoite invasion 122
CHAPTER 4: DISCUSSION AND PERSPECTIVES 125
4.1. Bradyzoites use a MJ to invade but its molecular composition is slightly different than that of tachyzoites 126
4.2. Role of AMA4 in invasion of bradyzoites 130
4.3. AMA-RON2 complexes as a strategy to vaccinate against toxoplasmosis 132
4.4. The vaccine study as a tool to decipher the function of AMA-RONs complexes at different stages 138
4.5. Presence of different MJ paralogs in the same parasitic stage 140
Annexe 195
Résumé français de la thèse 220

CHAPTER 1: INTRODUCTION

1.1. *Toxoplasma gondii*

The discovery of *Toxoplasma gondii* goes back to 1908, when Nicolle and Manceaux described it in an African hamster-like rodent called *Ctenoductylus gundi,* used for *Leishmania* research at the Pasteur Institute in Tunis (NICOLLE, 1908). This parasite was also described by Splendore in a rabbit in the same year (Splendore, 1908). Yet, its complete life cycle was not clearly unraveled until the late 1960s (Frenkel et al., 1970). *T. gondii* is an obligate intracellular protozoan parasite, belonging to the class of Coccidia and the phylum of Apicomplexa (Dubey et al., 1998). This phylum comprises a diverse group of intracellular parasites characterized by the presence of an apical complex and a conserved way of host cell invasion. Infection by *T. gondii* has a dreadful prevalence ranging between 25 to 80% of the worldwide population (Robert-Gangneux & Dardé, 2012), in addition to warm-blooded vertebrates and avian species (Skariah et al., 2010). Moreover, this infection has a negative impact on livestock, mainly goats and sheep, where *T. gondii* leads to stillbirth and abortion, yielding durable outcomes in agricultural economies (Robert-Gangneux & Dardé, 2012).

1.1.1. *Toxoplasma gondii*: Taxonomy

The systematic classification of *T. gondii* goes back to 1980 (Figure 1). Advancements in electron microscopy yielded the identification of a complex structure and a number of unique organelles, and unraveled similarities with *Plasmodium* and *Eimeria* species, previously considered as unrelated parasites (Scholtyseck & Mehlhorn, 1970). Since then, the classification of Protozoa was revisited, and a new Phylum, named the Apicomplexan phylum, emerged, and encompassed the relatedness between parasites of the genera *Babesia, Theileria,*

Plasmodium, Eimeria, Toxoplasma, Neospora, and *Cryptosporidium* (David J. P. Ferguson, 2009).

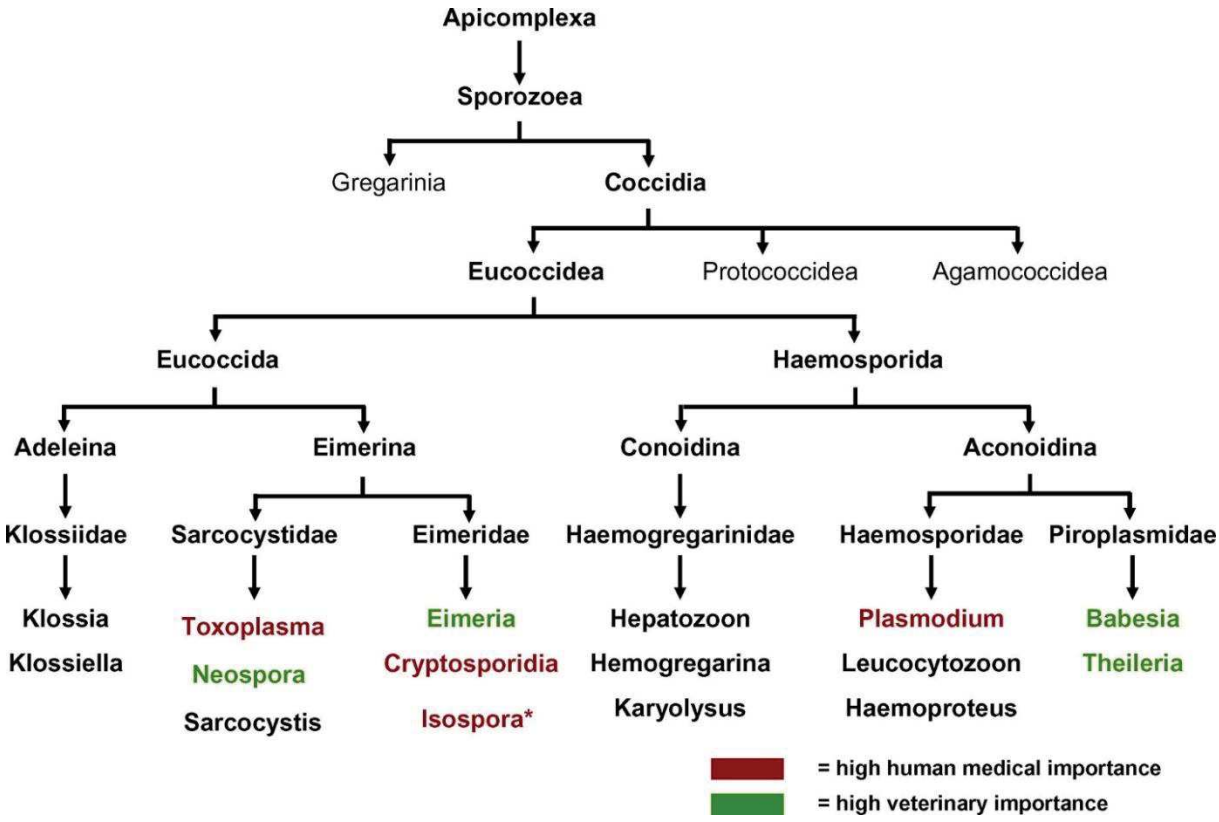


Figure 1: Phylogenetic tree of Apicompla (H.-P. Beck et al., 2009).

1.1.2. The phylum Apicomplexa

The phylum Apicomplexa includes the malaria-causing parasite (*Plasmodium* spp.), several major animal pathogens (e.g. *Eimeria* spp., *Theileria* spp., *Babesia* spp., *Neospora caninum*) and the causative agents of toxoplasmosis (*Toxoplasma gondii*) and cryptosporidiosis (*Cryptosporidium* spp.) (Figure 1). These parasites are responsible for some of the deadliest parasitic diseases afflicting humans, including malaria and toxoplasmosis. They are also responsible for many diseases of veterinary and economic importance, and exhibit a complex life cycle and a coordinated cell cycle-dependent expression program. A general similarity among all the members of this phylum is the complexity of their life cycles, which for most,

involve multiple host organisms. In addition, all the members of this phylum are obligate intracellular parasites. This property confers them a considerably safe route to evade the immune system of the host (Blader & Saeij, 2009). In case of *T. gondii*, this is primarily achieved by infecting macrophages and dendritic cells mainly, affecting the secretion of pro-inflammatory cytokines such as IL-12 and activating anti-apoptotic machinery, hence securing a safe low profile vehicle to spread to various tissues (Blader & Saeij, 2009).

1.2. Stages of *Toxoplasma gondii*

T. gondii is an obligate eukaryotic intracellular protozoan parasite where a living host cell is detrimentally essential to support its life cycle's continuity. Like all eukaryotes, it possesses mitochondria, endoplasmic reticulum, nucleus, Golgi complex and ribosomes. *T. gondii* presents also a plastid-derived structure known as apicoplast, which is a vital endosymbiotic organelle inherited from symbiotic algae (Dubey et al., 1998; McFadden & Yeh, 2017). It is essential for the parasite survival because of its involvement in key metabolic pathways such as isoprenoid, and type II fatty acids precursors synthesis among others (Dubey et al., 1998; Sheiner et al., 2013). *T. gondii* apical complex contains secretory organelles including microneme and rhoptries along with the conoid, which is a specialized cytoskeletal structure used for cell invasion (Dubey, 1998).

Throughout its life cycle, *T. gondii* exhibits distinct stages: the tachyzoite, the bradyzoite, the sporozoite and the merozoite.

1.2.1. The tachyzoite stage

In Greek 'tachy' stands for 'fast, rapid'. Tachyzoites, named so by Frenkel (Frenkel, 1973), are the 2 µm lunate/crescent forms initially discovered in the *gundi* rodent by Nicolle and Manceaux in 1909. Tachyzoites are the anteriorly pointed and posteriorly rounded proliferative intracellular forms (Figure 2). Following invasion of a host cell, each tachyzoite divides into two daughter tachyzoites, as a result of a process called endodyogeny. The process continues until the host cell can no longer embrace the huge number of proliferating tachyzoites, and bursts releasing these stages, to infect neighboring cells (Goldman et al., 1958). Tachyzoites are the fast replicating forms responsible for the acute phase of infection. Their structural integrity and motility are regulated by the cytoskeleton limited by a complex membrane called the pellicle (Dubey et al., 1998) (detailed in section 1.8.1).

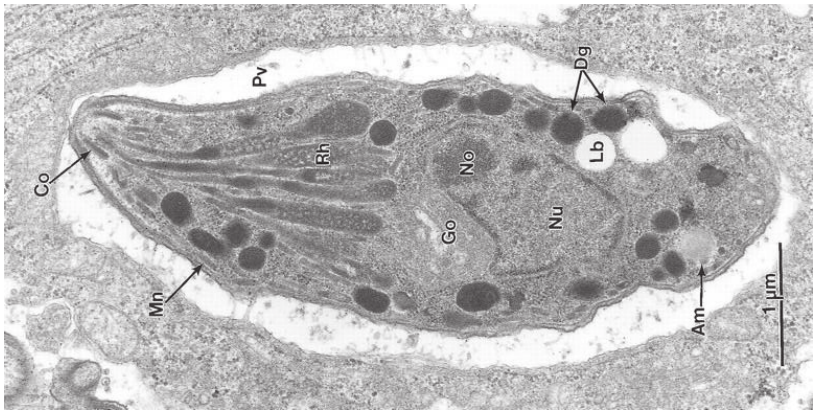


Figure 2: Transmission electron micrograph showing the structure of *Toxoplasma gondii* tachyzoite. Co, conoid; Go, Golgi complex; Mn, microneme; Rh, rhoptry; Dg, electron-dense granule; Nu, nucleus; No, nucleolus; Pv, parasitophorous vacuole; Am, amylopectin (Dubey et al., 1998).

1.2.2. The Bradyzoite stage

In 1973, Frenkel proposed the term "bradyzoite", with "brady" meaning "slow" in Greek, to describe the slow growing/dormant or non-proliferative developmental stage of *T. gondii,* encysting in tissues. Bradyzoites (Figure 3*A*) result from the conversion of tachyzoite

stages, to evade the pressure of the host immune system. They form cysts (Figure 3*B*) in brain and in muscle cells and are responsible for the chronic phase of infection (D. J. P. Ferguson, 2004). Importantly, these tissue cysts remain mainly dormant as long as the host is immunocompetent. Upon immunosuppression, the bradyzoites reactivate back to tachyzoites. These later are capable of infecting all nucleated cells and hence, may become life threatening. Moreover, ingestion of these bradyzoite cysts contribute to the transmission of the parasite between hosts (Mai et al., 2009).

Bradyzoites cysts show propensity for muscle and neural tissues, and can be detected in eyes, brain, cardiac and skeletal muscles (Dubey, 1998). Although these cysts were seen in astrocytes, microglia and neurons (D. J. Ferguson et al., 1989; D. J. Ferguson & Hutchison, 1987b, 1987a), recent studies showed that they mainly associate with neurons in mouse models (Cabral et al., 2016; Koshy et al., 2012). The size of immature cysts is around 5 μm. These contain a minimum of two parasites, and are surrounded by a cyst wall formed during bradyzoites early development (Dzierszinski et al., 2004; K. Kim & Weiss, 2004). The size of mature cysts varies from about 10 μm to 70 μm for brain cysts and 100 μm for muscle cysts, and these may contain thousands of bradyzoites (Dubey, 1998). Bradyzoite stages were known to be quiescent, until a study showed that *in vitro* parasites are capable of exiting cysts and invade new host cells creating new cysts (Dzierszinski et al., 2004). This phenomenon could elucidate the presence of cyst clusters and the increased burden *in vivo* during the chronic phase of infection (E. Watts et al., 2015). More recently, clusters of parasites were shown to endure asynchronous cell division in subset of cysts, highlighting that these cysts are dynamic structures (E. Watts et al., 2015).

Several differences distinguish tachyzoites and bradyzoites (Table 1). Bradyzoites are more gracile compared to tachyzoites and have a noticeable crescent shape (Mehlhorn & Frenkel, 1980). Bradyzoites have their nucleus located at the posterior end and contain several

micronemes, and electron dense rhoptries (Dubey, 1998; D. J. Ferguson & Hutchison, 1987a; Weiss & Kim, 2000). Moreover, they contain amylopectin granules (Dubey, 1998). Mature bradyzoites are in a growth-arrested stage carrying a uniform 1N content of nuclear DNA (J. Wang et al., 2014).

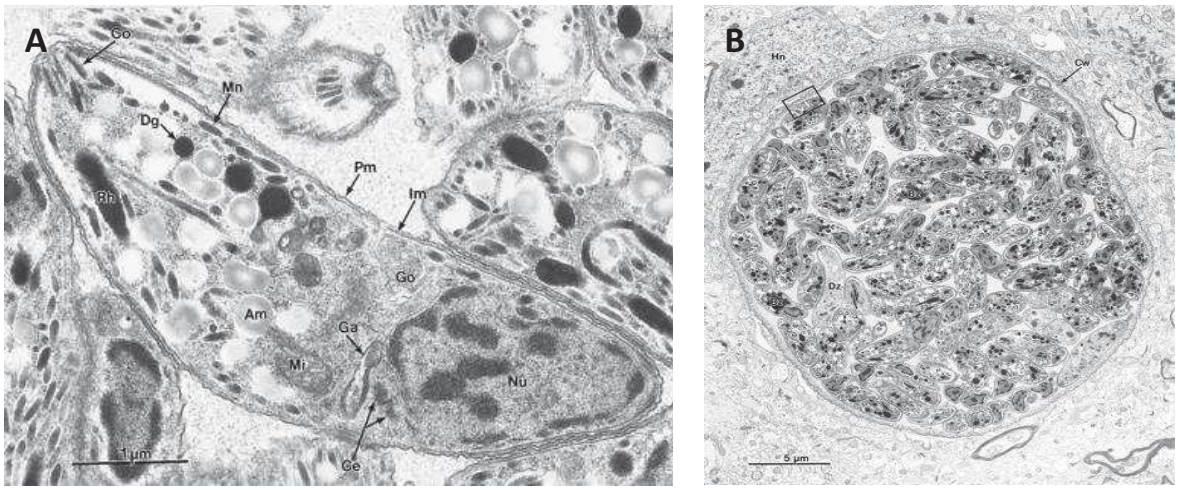


Figure 3: A) Structure of a bradyzoite in tissue cyst. Im, inner membrane complex; Pm, plasmalemma; Nu, nucleus; Mi, mitochondrion, Go, Golgi complex, Ga, Golgi adjunct (apicoplast); Ce, centrioles; Co, conoid; Am, amylopectin granule; Mn, microneme; Rh, rhoptry; Dg, electron-dense granule. **B) Structure of a tissue cyst positioned in the cytoplasm of host cell and surrounded by a cyst wall** (Cw) (Dubey et al., 1998).

Tachyzoites	Bradyzoites
Fast replicating forms	Slowly replicating forms
More centrally located nucleus	Posteriorly located nucleus
Apicoplast present	Apicoplast maybe lost
Synchronous replication	Synchronous and asynchronous replication
Labyrinthine rhoptries	Solid rhoptries
Absent or few amylopectin granules	Numerous amylopectin granules
Occasionally presence of lipid bodies	Absence of lipid bodies
More susceptible to destruction by proteolytic enzymes	Less susceptible to destruction by proteolytic enzymes

Table 1: Comparison between tachyzoite and bradyzoite stages.

1.2.3. The Merozoites stage

The presence of this stage in feline intestines restricts our knowledge of its properties and molecular characteristics. However, a recent study illustrated that the lack of delta-6-desaturase activity, involved in lipid metabolism, in feline intestine is essential for *T. gondii* sexual cycle (Genova et al., 2019). This enabled the development of a mouse model capable of inducing the sexual stage, through conversion of bradyzoites to schizonts upon inhibiting this enzyme. This model might help in further characterization of merozoites.

After ingestion of oocysts or tissue cysts by felids, sporozoites and bradyzoites infect the intestinal epithelium. This leads to the development of asexual entero-epithelial stages named schizonts, corresponding to several generations of *T. gondii* merozoites. Morphologically, there are five different types (A to E) of schizonts in the cat intestinal epithelium (Dubey & Frenkel, 1972). During schizogony, consecutive nuclear divisions of the parasite take place, then the inner membranes are formed individualizing each daughter cell known as merozoite. Upon rupture of enterocytes, many merozoites are released, infect surrounding enterocytes, and divide further by schizogony (Dubey & Frenkel, 1972). The ultrastructure differences between the different types of schizonts and merozoites compared to that of tachyzoites are listed in table 2.

Characteristic	Parasite or schizont Type				
	Tachyzoites	B	C	D	E
Location	Lamina propria	Epithelium, lamina propria	Epithelium, lamina propria	Epithelium	Epithelium
Division	Endodyogeny, asynchronous	Endodyogeny, asynchronous	Endopolygeny, synchronous	Endopolygeny, synchronous	Endopolygeny, synchronous
Parasitophorous vacuole					
TMN	Present	Present	Absent	Absent	Absent
PVM	Thin	Thin	Thin	Thick	Thick
Granular material	Absent	Absent	Present	Absent	Absent
Residual body	Absent	Absent	Present	Present	Present
Schizont size, number measured		26×17 μm, 10	16×10 μm, 8	7.3×5.6 μm, 6	12×8.8 μm, 10
Number of merozoites per schizont		2–48	24–36	12–18	50–80
Tachyzoites or merozoites					
Size, number measured	4.7×2.1 μm, 10	5.8×2.9 μm, 10	6.1×1.5 μm, 8	5.8×1.3 μm, 10	4.5×1.1 μm, 10
Amylopectin	Few	Few	Several	Few	Few
Rhoptries	Labyrinthine	Labyrinthine	Electron-dense	Electron-dense	Electron-dense
Granular vacuole	Absent	Absent	Absent	Present	Absent
Granular body	Absent	Absent	Absent	Absent	Present

Table 2: Ultrastructural differentiation of *T. gondii* tachyzoites and types B–E schizonts of merozoites (Speer & Dubey, 2005).

1.2.4. Sporozoites

Sporozoites are the stages found inside a structure called oocyst, which is the result of the sexual part of the parasite's life cycle. This later occurs in the intestine of feline hosts and results in shedding oocysts in felines' feces, to the environment (Dubey et al., 1998; Dubey & Frenkel, 1972). Upon excretion, oocysts are unsporulated at first (Figure 4*A*), then sporulation follows within 1 to 5 days of excretion, depending upon aeration and temperature conditions (Dubey, 1998). A sporulated oocyst contains two sporocysts (Figure 4*B*), each of which with four infective sporozoites. Oocysts can survive and remain infective for years in fresh water (Dumètre & Dardé, 2003) and for at least 24 months in salt water (Lindsay & Dubey, 2009).

Once ingested by an intermediate host in contaminated food, these sporulated infective oocysts rupture by the digestive enzymes of the gastro-intestinal tract and liberate the sporozoites, which then rapidly invade the enterocytes and transform into merozoites (Furtado et al., 2013).

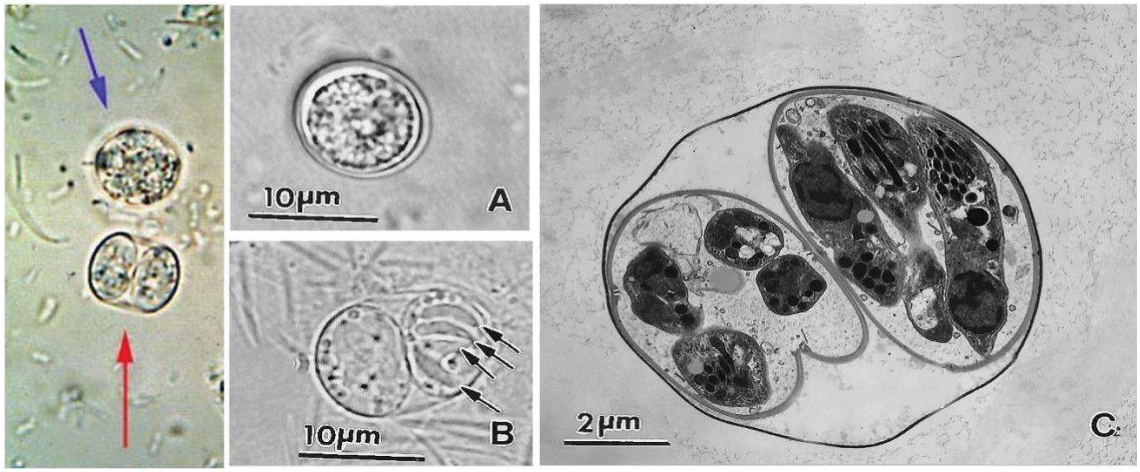


Figure 4: ***Toxoplasma gondii* oocysts**. An unsporulated oocyst (blue arrow) and a sporulated oocyst (red arrow) seen at high power (40 X). (A) Unsporulated oocyst. Note the central mass (sporont) occupying most of the oocyst. (B) Sporulated oocyst with two sporocysts. Four sporozoites (arrows) are visible in one of the sporocysts. (C) Transmission electron micrograph of a sporulated oocyst. Note the thin oocyst wall (large arrow), two sporocysts (arrowheads), and sporozoites, one of which is cut longitudinally (small arrows) (Dubey et al., 1998).

1.3. Life cycle

T. gondii spans its life cycle between a definitive host (a felid) where sexual reproduction takes place, and an intermediate host (any warm-blooded animal) where its asexual reproduction occurs (Figure 5). This parasite can undergo all means of transmission, from definitive to intermediate hosts, between intermediate hosts themselves or between definitive hosts (Afonso et al., 2006).

1.3.1. Sexual life cycle

The sexual reproduction takes place only in felids intestine (Figure 5*A*). These include the wild and domestic cats. Upon feeding on an infected prey, bradyzoite cysts are destroyed by digestive enzymes. Hence, bradyzoites are released and occupy the felids enterocytes, then differentiate and give rise to five different morphological types of schizonts. Within 2 days in the intestinal epithelium, schizonts become merozoites. After which, merozoites undergo rounds of replication, limited from two to four times before gametogony (Dubey, 1998). Gametogony takes place and sexual development leads to the formation of male and female gametes (David J. P. Ferguson, 2002). Oocysts form after fertilization of the female macrogamete and the male microgamete in the enterocytes. Once the intestinal lining cells are disrupted, unsporulated oocysts are shed in cats' feces. Few days later, sporulation takes place in the external environment (Figure 5*B*), through mitotic division and some morphological changes, and infective sporulated oocysts, composed of two sporocysts containing each four haploid sporozoites are formed (Figures 4B and 5*B*) (Dubey & Frenkel, 1972).

1.3.2. Asexual life cycle

Once a sporulated oocyst is ingested by an intermediate host, sporozoites are liberated following the lysis of its thick wall by the gastric enzymes. Thereafter, sporozoites will invade enterocytes and rapidly transform into tachyzoites, capable of infecting all nucleated cells. Tachyzoites rapidly multiply by endodyogeny and disseminate to different body parts. 7 to 10 days after infection and due to the host immune response, tachyzoites convert into bradyzoites that hide, mostly in brain and muscle cells, for a life span in immunocompetent patients. Latency of the encysted form may be provided by the cyst wall acting as a physical barrier and hence is poorly recognized by the immune system (Weiss & Kim, 2000). When an intermediate host consumes contaminated undercooked or raw meat, the cyst ruptures in the digestive tract and bradyzoites are released in the new host (Dubey, 1998) (Figure 5C). When a cyst is ingested by a feline host following ingestion of an infected prey, sexual reproduction takes place and a new cycle begins.

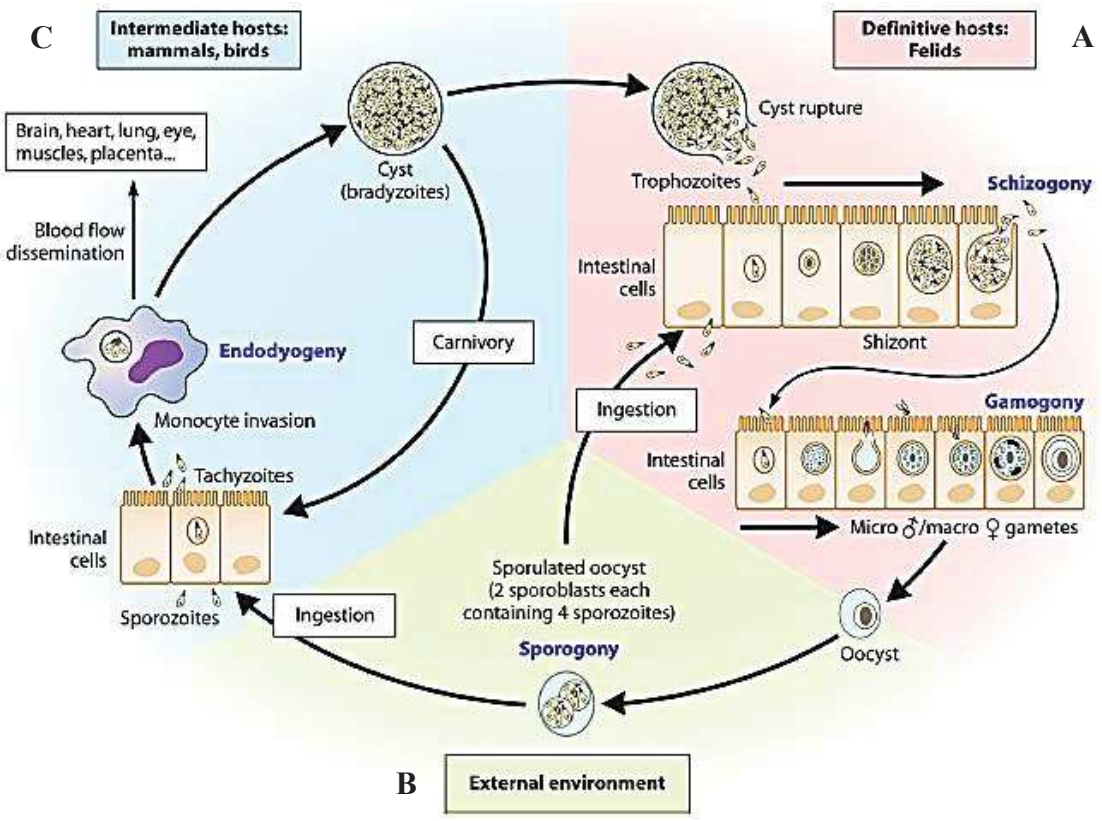


Figure 5: ***Toxoplasma gondii* life cycle** (Robert-Gangneux & Dardé, 2012). (A) Sexual life cycle of *T. gondii* occurs in definitive hosts upon ingestion of tissue cysts containing bradyzoites and results in the production of oocyst via gamogony. (B) Maturation of oocyst containing sporozoites in external environment via sporogony (C) Asexual life cycle of *T. gondii* in intermediate hosts occurs upon ingestion of oocyst (sporozoites) or tissue cysts (bradyzoites) leading to emergence of tachyzoites and dissemination of *T. gondii* to the host's organ.

1.4. Modes of Transmission

Intermediate and definitive hosts can contract an infection with *T. gondii,* mainly *via* one of two main modes of transmission:

(1) The horizontal mode of transmission following oral ingestion of infectious sporulated oocysts in food contaminated by cats' feces, or through ingestion of tissue cysts present in raw or undercooked meat.

(2) The vertical mode of transmission *via* the placental spread of tachyzoites from a pregnant primo-infected mother to her fetus/baby.

These routes of transmission allow a high level of sustainability of *T. gondii* in the environment. In addition to transmission between intermediate and definitive hosts, the asexual life cycle can sustain the parasites existence indefinitely *via* the transmission of tissue cysts in-between intermediate hosts. Same applies for the infectious oocysts able to support a continuity through the sexual life cycle in-between definitive hosts (Tenter et al., 2000).

1.5. Genetic overview and virulence of *T. gondii* strains

T. gondii genome was fully sequenced by the J. Craig Venter Institute and is available on www.ToxoDB.org. It is an 87 Mbp nuclear genome, haploid for most of the parasite's life cycle and only exhibits a brief diploid phase in the cat intestine before meiosis. *T. gondii* genome consists of 11 chromosomes designed by Roman numerals and ranging in size from approximately 1.8 Mbp to > 10 Mbp.

At a first glance, *T. gondii* appears to be a parasite of immunocompromised individuals where it leads to severe infections. This idea of opportunistic parasitism has changed thereafter (Dubremetz & Lebrun, 2012) and many parameters of virulence were thus associated with the success of the parasite to invade host cells. The first forefront line is the host immune response and the capacity of the parasite to modulate it. Not only the parasite can affect the expression of immunity related signaling factors (Hunter & Sibley, 2012), but it can also act on the intracellular effectors of the primary immune response (Melo et al., 2011).

While at first, three main types of strains were described, PCR-RFLP on *T. gondii* samples worldwide revealed the presence of 189 different genotypes, all currently available on ToxoDB (Hosseini et al., 2018). The new genotypes are distinct form the three main genotypes (type I, II, and III), and were classified as exotic, recombinant, atypical and non-archetypal genotypes (Ajzenberg et al., 2004). Recently, substantial genotypes including type 12 (#4, #5), type Br I (#6), type Br III (#8), Chinese 1 (#9), type Br II (#11), and type IV (#17)

were introduced to type I, II, III and atypical genotypes (Sharif et al., 2017; Shwab et al., 2014). As per clonal genotyping, around 58% of the population are infected with the most prevalent genotype of type II strain (Hosseini et al., 2018). Indeed, Type II strain prevalence is 41.7%, 62.1%, and 64.3% in patients with ocular toxoplasmosis, congenital toxoplasmosis and AIDS, respectively (Hosseini et al., 2018). Intriguingly, *T. gondii* strains in Africa and Asia are distinguished by low genetic diversity, yet are of a wide diversity in North and South America (Hosseini et al., 2018).

While virulence of *T. gondii* is related to the reciprocal interplay between the parasite and its host-mediated immunity, it was always associated with the amount of tachyzoites needed to kill a mouse (Saeij et al., 2005). Although strains of *T. gondii* are genetically quite similar, they show strong phenotypic differences in laboratory mouse models. In that sense, infection with type I strains is fatal (LD_{50} = 1) in all strains of laboratory mice, whereas infection with type II ($LD_{50} \sim 10^2$) or type III ($LD_{50} \sim 10^3$) strains generally results in controlled persistent infections (Sibley & Boothroyd, 1992).

1.6. Toxoplasmosis

1.6.1 Toxoplasmosis in immunocompetent individuals

Toxoplasmosis is a benign and self-limiting disease, usually asymptomatic in up to 80% of immunocompetent individuals (Halonen & Weiss, 2013; Yazdani et al., 2018). During the acute phase of primary infection with *T. gondii*, patients may experience mononucleosis-like symptoms along with asthenia and myalgias. Anemia, lymphocytosis, splenomegaly and leucopenia are less frequently encountered (Neves et al., 2009). Another clinical symptom is lymphadenopathy that may occur in the head and neck region. It may also involve retroperitoneal, axillary, inguinal, and mesenteric lymph nodes. Lymphadenopathy associated with sore throat, fever, rash, malaise, and hepatosplenomegaly (Halonen & Weiss, 2013).

Additionally, severity of cases is correlated with the genotype of the parasitic strain. As such, patients infected with "Atypical" strains isolated in French Guiana, manifested weight loss, lymphadenopathy pneumopathy, headache, elevated and prolonged fever and, hepatic cytolysis. More signs including retinochoroiditis, myositis, rash, myocarditis, and neurologic disorders, were also detected during toxoplasmosis (Carme et al., 2009). Although, retinochoroiditis is rare in immunocompetent individuals, its occurrence doesn't require immunosuppression. It may cause decreased visual acuity (Matias et al., 2014) and blindness in severe cases (de Boer et al., 2003).

1.6.1.1. Cancers associated with *T. gondii*

Patients with toxoplasmosis presented an increased risk for brain cancer (Thomas et al., 2012). The incidence of adult brain cancers was also reported higher in countries where the *T. gondii* infection is common (B.-K. Jung et al., 2016; Thomas et al., 2012). Indeed, a positive correlation between seropositivity for *T. gondii* and incidence of brain cancer demonstrated that *Toxoplasma* increases the potential for brain cancer occurrence by interfering with the miRNA machinery in brain cells (Zeiner et al., 2010). Yet, the miRNAs specifically deregulated by *Toxoplasma* and associated with brain cancers are yet to be identified (Thirugnanam et al., 2013).

Toxoplasmosis is also correlated with other cancers, including oral cancer (Zhou et al., 2018), leukemia (Y. Huang et al., 2016), breast and colorectal cancers (Falih & Saheb, 2017), lung, cervical and endometrial cancers (Cong et al., 2015).

1.6.1.2. Psychiatric Disorders Associated with *T. gondii*

Infection with *Toxoplasma*, was thought to be highly innocuous, in immunocompetent individuals. However, animal models showed behavioral changes following infection with *Toxoplasma* (Webster, 2007). In humans, a similar association of *T. gondii* infection with

behavioral and mental disorders including mood disorders, cognitive impairments and, personality changes was unraveled (Fekadu et al., 2010; Flegr, 2007; Pearce et al., 2014; Webster, 2001). Indeed, some genes related to neuropsychiatric illnesses are associated with susceptibility to toxoplasmosis. These include the two related schizophrenia genes, Contactin-associated protein-like 2 (*CNTNAP2)* and GABA receptor 2 (*GABAR2)* (A. W. Wang et al., 2019). The partial expression of GABBR2 in *Toxoplasma* encephalitis (Sahu et al., 2014) is also reported in patients with schizophrenia. Lately, a major mental illness-related susceptibility factor, the "Disrupted in schizophrenia" (DISC1), was shown to contribute in host immune responses against toxoplasmosis. In that sense, a DISC1 genotype induced an elevated antibody response targeting the parasite (Kano et al., 2020). Interestingly, several treatments targeting schizophrenia and other mental illnesses, including the antipsychotic drug haloperidol, and the mood stabilizer valproic acid, showed growth inhibition of the parasite *in vitro* (Jones-Brando et al., 2003). Yet, the relatedness of *T. gondii* to behavioral modifications and neurodegenerative diseases in both humans and rodents is still a conflicting topic. Indeed, contradictory findings make it unclear as to what extent *T. gondii* affects host behavior or causes a secondary disease. In rodents, some studies suggested that behavioral changes in infected animals are mostly due to neuroinflammation, defects in neurotransmitter release, and cyst location in the brain (H. J. Johnson & Koshy, 2020). In humans, contradictory studies are also reported and behavioral changes might be linked to individual genetic background or to factors pertaining to infection including *T. gondii* strain type, and route of infection among others (H. J. Johnson & Koshy, 2020).

1.6.2. Toxoplasmosis in immunocompromised patients

Chronic toxoplasmosis is an opportunistic disease that may evolve to fatality in immunocompromised patients (Bannoura et al., 2018; Kodym et al., 2015). Under normal

conditions, the host immune system controls tachyzoites replication and maintains tissue cysts. However, patients receiving treatment against cancers and immune-mediated inflammatory diseases, are at risk of developing *Toxoplasma* encephalitis, not only upon latent cyst reactivation, but also during primary infection (Gharamti et al., 2018). As such, in immunocompromised individuals, tissue cysts rupture and bradyzoites are released leading to recrudescent infections and several neurological symptoms (W. J. Sullivan et al., 2009). The most frequent symptoms are cerebral mass lesions, confusion, headaches, seizures, diffuse encephalopathy, poor co-ordination, and meningoencephalitis. During advanced stages, symptoms manifest as visual disturbance, respiratory problems, high grade fever and hence mortality (Bannoura et al., 2018; Luft & Remington, 1992; Prandota, 2009). Reactivation due to the impairment of protective immune response may also occur following cancer immunotherapy, HIV infection, immunosuppressive therapies delivered upon hematopoietic stem cells or solid organ transplants (Kollu et al., 2018; Roche et al., 2018; Xu et al., 2018). As an example, rituximab therapy associates with several cases of reactivation of cerebral toxoplasmosis (Ramezani et al., 2016; Safa & Darrieux, 2013).

1.6.3. Congenital toxoplasmosis

Congenital toxoplasmosis entitles the spectrum of complications resulting from the placental passage of *T. gondii* from a primo-infected mother to the fetus. Severity of associated conditions depends on the time of acquisition of the parasitic infection by the mother (Yamamoto et al., 2017), whereby the occurrence of the infection in a late gestational age decreases its clinical consequences (Dunn et al., 1999). During the first trimester, 10 to 25% of the mother's parasitic infection leads to fetal infection which leads to abortion in dreadful cases or contributes to stillbirth associated with severe abnormalities in the brain and eyes, deafness, hydrocephalus, intracranial calcification, mental retardation, seizures, retinochoroiditis, and

blindness (Robert-Gangneux & Dardé, 2012; Singh, 2016; Swisher et al., 1994). If the infection occurs in the second trimester, 30% of affected fetuses suffer from mental retardation along with hydrocephalus and microcephaly. In the third trimester infection may be asymptomatic and only retinochoroiditis can manifest several years after birth (Weiss & Dubey, 2009).

1.7. The impact of bradyzoites on the central nervous system

One of the parasites' features for pathogenesis is the ability to cross highly restricted barriers such as the blood-brain barrier (BBB), the placenta and the eye of infected hosts (K. S. Harker et al., 2015). *Toxoplasma* can cross the BBB through one of several mechanisms: one is the trans-endothelial migration through the vascular endothelium by infected monocytes containing tachyzoites (Lachenmaier et al., 2011; Ueno et al., 2014). Free parasites are also capable of crossing the endothelium (Katherine S. Harker et al., 2014) and the extracellular parasites attached to the endothelium represent the majority of tachyzoites crossing the BBB (Konradt et al., 2016). The entry of these tachyzoites may be either through crossing intracellular junctions by paracytosis or through a pinocytic-derived vesicle by transcytosis (Furtado et al., 2012; Wohlfert et al., 2017). This involves the replication of tachyzoites followed by lysis of underlying endothelial cells and thus reaching the central nervous system (CNS) (Konradt et al., 2016). While the host immune response eliminates most of tachyzoites, some manage to escape through modifying signaling or transcriptional pathways (Hakimi et al., 2017; Lima & Lodoen, 2019). These uncleared tachyzoites convert into encysted bradyzoites mostly concentrated in the basal ganglia, hippocampus, amygdala and cerebral cortex (Melzer et al., 2010). It is now admitted that bradyzoites are continuous replicating entities (E. Watts et al., 2015). These stages are active and remodel constantly, appearing in certain brain regions and disappearing from others (Lyons et al., 2002). Moreover, encysted bradyzoites inhibit apoptosis of the infected neurons allowing their persistence for a long time

in the brain (Boothroyd, 2009). This persistence may cause neurodegeneration or inflammation in susceptible individuals. *T. gondii* has also a direct effect on the neurons, where it depletes Ca^{2+} of the endoplasmic reticulum and reduces potassium uptake. As a result, bradyzoites and tachyzoites inhibit the function of infected neurons (Haroon et al., 2012). The parasites also alter dopamine metabolism (Martin et al., 2015), and their direct effect exhibits obstruction of neurotransmitter expression, myelinated fibers loss and alteration in calcium signaling (Parlog et al., 2015).

1.7.1. Molecular mechanisms of conversion of tachyzoites to bradyzoites

1.7.1.1. Immunity factors

Host immune response-induced stress is pivotal for the conversion from the tachyzoite to the bradyzoite stage (Cerutti et al., 2020). In immunocompetent host, cell-mediated immunity is responsible for establishing chronic toxoplasmosis (Dupont et al., 2012). $CD4^+$ and $CD8^+$ T cells contribute to long-term survival of the infected host by preventing reactivation of cysts and the developing immunity against reinfection (Hwang & Khan, 2015). An increased vulnerability to *Toxoplasma* infection was documented in mice lacking B cells, $CD4^+$, or $CD8^+$ T cells and in patients with impaired T-cells (L. L. Johnson & Sayles, 2002; Kang et al., 2000). It was later shown that resistance to *T. gondii* infection necessitates a complementarity in activity between $CD4^+$, $CD8^+$ T and B cells (Khan et al., 2019). Moreover, $CD4^+$ T cells are vital for maintaining $CD8^+$ T cells activity during chronic toxoplasmosis (Combe et al., 2005; Lütjen et al., 2006). A key mediator of *T. gondii* clearance is interferon gamma (IFN-γ) which is an essential cytokine produced by activated $CD4^+$ T cells (R. T. Gazzinelli et al., 1991), $CD8^+$ T cells (Y. Suzuki et al., 1988), NK cells, in addition to innate immune cells like microglia and macrophages (Kang & Suzuki, 2001; Yasuhiro Suzuki et al., 2005; X. Wang & Suzuki, 2007). In a recent study, $CD4^+$ T cells were shown to be the main

interferon gamma producing cells and essential for protection against toxoplasmosis in $CD8^+$ T deficient mice (Tussiwand et al., 2020).The importance of this cytokine in the context of *T. gondii* infection was documented in mice, where IFN-$\gamma^{-/-}$ mice weren't able to survive infection with an avirulent *T. gondii* strain (Scharton-Kersten et al., 1996). Treatment of mice with anti-IFN-γ monoclonal antibodies abrogated the establishment of the chronic phase of infection (R. T. Gazzinelli et al., 1994; Y. Suzuki et al., 1988). These findings demonstrate the key role of this cytokine in the context of toxoplasmosis and tachyzoite to bradyzoite conversion. Importantly, IFN-γ stimulates the production of reactive oxygen species and nitric oxide (NO) by-products in astrocyte, macrophages, and microglial cells in both humans and mice (Chao et al., 1993; Langermans et al., 1992; P. K. Peterson et al., 1995). IFN-γ produced by the brain-resident microglia, is involved in activation and the production of nitric oxide by those cell thereby contributing in the control latent infection (Blanchard et al., 2015). Apparently, NO metabolite is vital to suppress parasite replication and leads to bradyzoite development (Ibrahim et al., 2009; Lüder et al., 2003). Furthermore, inducible nitric oxide synthase converts arginine into citrulline upon production of NO. Thus, in activated macrophages, *T. gondii* undergoes stage conversion since it is auxotrophic for arginine which is limited in this case (Lüder & Seeber, 2016).Yet, NO is not a key factor for bradyzoite formation *in vivo.* Indeed, tissue cysts can normally form in inducible nitric oxide synthase KO mice (Scharton-Kersten et al., 1996) or in mice treated with aminoguanidine, an inhibitor of NO producing enzyme (Hayashi et al., 1996).

In *T. gondii* infected human fibroblasts, and brain macrovascular endothelial cells, tryptophan degradation in response to IFN-γ has been reported (Däubener et al., 1996, 2001; Gupta et al., 1994). Moreover, treatment of *T. gondii* infected cells with IFN-γ induced an upregulation of indoleamine 2,3-dioxygenase 1 and 2 (IDO1 and IDO2), which are host enzymes mediating tryptophan degradation (Divanovic et al., 2012; Murray et al., 1989;

Pfefferkorn, 1984). IDO1 and IDO2 upregulation limits the availability of host tryptophan inhibiting parasite replication (Sibley et al., 1994), while adding exogenous tryptophan leads to re-establishment of parasite replication (Schmitz et al., 1989). Inhibition of IDO *in vivo* did not affect IFN-γ production 30 days following *Toxoplasma* infection. Nevertheless inhibiting IDO in chronically infected mice caused an increase in cyst burden and induced reactivation of the disease (Divanovic et al., 2012).

Tumor Necrosis Factor α (TNFα) is another effector that contributes to initiating chronic toxoplasmosis (Dirk Schlüter et al., 2003; Yap et al., 1998). Moreover, Interleukin 6 (IL-6) also increases the number of cysts i*n vitro* (Weiss et al., 1995), and is involved in controlling the acute and chronic phases of the disease *in vivo* (R. T. Gazzinelli et al., 1993; Y. Suzuki et al., 1988).

1.7.1.2. Host cell factors

Host cell background impact bradyzoite conversion besides the specific *in vivo* local immune response that aids in cyst formation (Wiendl et al., 2005). As such, mature skeletal muscle cells and neurons are known to be highly differentiated and post-mitotic cells that cannot reenter the cell cycle (Deneris & Hobert, 2014; Frade & Ovejero-Benito, 2015). Moreover, cyst conversion may be due to presumably an ineffective immune responses in these tissues (L. A. Jones et al., 2006). Thus, there are higher frequency of neurons infected with *T. gondii* compared to astrocytes in the brain (Cabral et al., 2016). This was related to IFN-γ that activates astrocytes leading to the reduction in number of infected astrocytes either by inhibiting interaction of astrocytes with *T. gondii* or killing of intracellular parasites (Cabral et al., 2016). Moreover, a recent study confirmed that the distribution of tissue cyst is affected by IFN-γ-dependent signaling in astrocytes (Hidano et al., 2016). Although, IFN-γ signaling

induce killing of intracellular parasites by astrocytes (Halonen et al., 2001), IFN-γ and/or TNF do not obstruct the parasite replication in neurons *in vitro* (D. Schlüter et al., 2001).

Alternately, cells and organs' type-specific factors that stimulates parasite differentiation and cyst formation may be involved enhancing parasite persistence in tissues. For instance, human cell division autoantigen-1 gene (CDA-1) that is involved in cell proliferation, has a role in altering parasite replication thereby inducing parasite cell cycle arrest and the expression of bradyzoite genes. This highlights the direct involvement of host cell factors in inducing the conversion of tachyzoites into bradyzoites (J. R. Radke et al., 2006). In addition, it was lately reported that the host cell metabolic state and non-immune secreted metabolites, may appoint host cells to be resistant or permissive to bradyzoite formation (Mahamed et al., 2012; Weilhammer et al., 2012).

1.7.1.3. Parasitic factors

The conversion between tachyzoite and bradyzoite stages entails prominent alterations in parasite gene expression. In that sense, three to four weeks post-infection, *in vivo* cyst transcriptomic analyses revealed the changes in the expression of hundreds of genes (Buchholz et al., 2011; Pittman et al., 2014). However, transcription profiles remained primarily unchanged between 3 and 4 months post-infection, which may imply that the parasites attain a steady state at 90 days post infection (Garfoot et al., 2019). Gene expression is regulated by a machinery of transcriptional complexes (K. Kim, 2018), and histones epigenetic modifications which contribute to modulating the tachyzoite/bradyzoite interconversion (Bougdour et al., 2009; Naguleswaran et al., 2010; Saksouk et al., 2005; Weiss et al., 1995). *Toxoplasma* lacks many identifiable specific eukaryotic transcription factors and rather possesses various members of the plant-like ApiAP2 DNA-binding family which are apicoplast proteins (Balaji et al., 2005). Several ApiAP2 transcription factors regulate bradyzoite conversion. This occurs

through a complex interchange between bradyzoite-specific and tachyzoite-specific ApiAP2 factors leading to activation or repression of bradyzoite differentiation, respectively. For instance, AP2IX-9 mainly represses bradyzoite development since its depletion leads to an increased cyst number (Hong et al., 2017). In contrary, AP2XI-4 (Walker et al., 2013), AP2IV-3 (Hong et al., 2017), and AP2IV-4(J. B. Radke et al., 2018) are implicated in bradyzoite development. Nevertheless, none of these factors can entirely control the differentiation process, since depletion of these AP2 transcription leads only to a decrease in parasites ability to generate tissue cysts *in vivo* (Hong et al., 2017; S. Huang et al., 2017; J. B. Radke et al., 2013, 2018). Intriguingly, a recently identified a Myb-like transcription factor (BFD1), not related to the ApiAP2 family, seems to be sufficient and necessary for tachyzoites conversion into bradyzoites. During stress, BFD1 accumulates and binds the promoter of stage-specific genes thereby promoting differentiation of *T. gondii* (Waldman et al., 2020). This underlines the complexity and factor diversity of the differentiation mechanism.

1.7.2. Reactivation of bradyzoites to tachyzoites

The reactivation of tissue cyst was not broadly studied. Cell-mediated immunity is a key factor in the reactivation of toxoplasmosis. HIV patients having low numbers of $CD4^+$ T cells, witness reactivation of toxoplasmosis (Montoya & Liesenfeld, 2004). Mice lacking $CD4^+$ and $CD8^+$ T cells show similar reactivation at the chronic stage of the disease (R. Gazzinelli et al., 1992; L. L. Johnson & Sayles, 2002). A recent study illustrated that $CD4^+$ T cells depletion leads to reactivation of chronic toxoplasmosis due to dysfunctional $CD8^+$ T cells. Interestingly, the function of $CD8^+$ T cells was restored and reactivation could not occur upon treating infected hosts with antigen-specific non-exhausted $CD4^+$ T cells (Khan et al., 2019).

IFN- γ is not only important in the conversion from tachyzoites to bradyzoites, but also plays a pivotal role in the reactivation process. Inhibition of IFN-γ leads to cyst reactivation in

chronically infected mice (Ildiko R. Dunay et al., 2009; Y. Suzuki & Joh, 1994). IFN-γ removal from murine brain astrocyte cultures containing cysts, lead to cysts rupture and appearance of tachzyoites (T. C. Jones et al., 1986). Chronically-infected mice treated with anti-IFNγ also showed reactivation of tissue cysts (R. Gazzinelli et al., 1992). A suggested hypothesis for the role of IFN-γ in inhibiting the reactivation is that IFN-γ may induce an anti-parasitic stimulation in astrocytes, leading to cell cycle arrest that is related to bradyzoite differentiation (J. Wang et al., 2014). In addition, IFNγ and $CD8^+$ T-cells are requisite for the control of tachyzoites proliferation (Mammari et al., 2015; Y. Suzuki & Remington, 1990). Concisely, tissue cysts are not likely to prompt vital pathological damage, since stochastic bradyzoites release may be eradicated by the host immune system. On the other hand, in certain cases, rupture of cysts can contribute to pathogenesis of toxoplasmic encephalitis (S.-B. Lee & Lee, 2017).

1.8. Invasion of *Toxoplasma gondii*

Invasion of *T. gondii* is an orchestrated multi-step process that is conserved among apicomplexan parasites (Morisaki et al., 1995). It takes place rapidly in around 25-40 seconds (Morisaki et al., 1995). The parasite starts gliding as soon as it egresses from the host cell. The gliding motility is an active process required for the invasion. It consists of three perceptible forms: upright twirling, circular gliding and helical rotation (Håkansson et al., 1999). It is then accompanied by a short decrease in motion upon the formation of a moving junction (detailed in section 1.8.2.1) at the host cell-parasite interphase, previous to entering by rotational progression (Bichet et al., 2014). The parasite penetrates by actively dragging the transmembrane MJ posteriorly, leading to the invagination of the host plasma membrane and creation of the parasitophorous vacuole (Mordue et al., 1999). When the parasite is completely in the host cell, it twists by rotating physically. Membrane scission occurs thereafter, at the

moving junction/plasma membrane interface. As such, the PV becomes sealed and separated from the host plasma membrane (Pavlou et al., 2018).

In 1995, a study emphasized on the difference between the active invasion of *T. gondii* tachyzoites and phagocytosis. Using a video microscopy, tachyzoite invades without ruffling the host cell membrane and reorganizing the actin microfilaments of CHO cells and bone marrow-derived macrophages, and ending up in a parasitophorous vacuole. Conversely, phagocytosis of the parasite by macrophages was associated with an immense ruffling of the membrane and reorganization of the cytoskeleton where *T. gondii* was introduced in a loose-fitting phagosome. Yet some parasites were able to escape from the phagosome (Morisaki et al., 1995). As such, one of the novel features of *T. gondii* is the formation of a non-fusogenic PVM during invasion, which allows it to escape the endocytic processing (Morisaki et al., 1995). This feature was related to the exclusion of host cell transmembrane proteins by the MJ during invasion (Mordue et al., 1999).

First studies on invasion were mainly conducted using virulent type I RH tachyzoite. Although a major step in invasion of type I strain is the MJ formation (detailed in section 1.8.2.1), type II avirulent strains exploit a noncanonical pathway called "phagosome to vacuole invasion (PTVI)" in macrophages (Y. Zhao et al., 2014). In this process, tachyzoites are first internalized *via* phagocytosis, followed by MJ formation upon active invasion from within a phagosomal compartment to form the classical specialized PV (Y. Zhao et al., 2014). As such, the PTVI strategy might be the route implemented in utilizing phagocytic cells as a Trojan horse to escape the immune system and disseminate to establish chronic toxoplasmosis thereafter.

Unlike tachyzoites, the invasion of sporozoites has been poorly investigated. In 1997, Speer et al descrived the initial invasion of sporozites in cardio-pulmonary-artery endothelial cells (CPA) with no formation of a MJ or constirction of the parastise during penetration,

whereby they settled in the first parasitophorous vacuole (PV1). Following this step, some sporozoites were detected moving in the cytoplasm and later leave the host cell, thereby causing a small bleb in the host cell. The constriction of parasites was then documented upon movement from PV1 to a second vacuole, PV2. An ultrastructural assessment of several extracellular sporozoites that were presumed to have exited the host cell, showed a thin layer of cytoplasm surrounded by a plasma membrane from the host. Notalby, PV1 was large and marked with tubulovesicular membrane network (TMN) absence, however PV2 was smaller, had TMN and a distinct parasitophorous membrane (PVM), where sporozoites proceeded in replication and formed tachyzoites (Speer et al., 1997). Morever, most of the intracellular sporozoites were found in PV1, 2 to 18 hours after infection of CPA cells. Yet, this vacuole disappeared in later time ponits and the parasites settled in a typical PV (Speer et al., 1995, 1997). Another study using electron microscopy, suggested that sporozoites are capable of traversing cells, thus passing from one cell to another. At 2h post-infection of Swiss-Webster mice most of the parasites were detected in ileal enterocytes and occasionally in goblet cells. However, sporozoites were exclusively found in cells of the underlying lamina propria, 6–12 h post-infection (Speer & Dubey, 1998), supporting the idea of sporozoite migation between cells (Dubey, 1997; Speer & Dubey, 1998). Yet, the process behind this passage was not understood. In a recent study, Tartarelli *et al* provided for the first time an ultrastructural evidence for cell-to-cell migration of sporozoites. As such finger-like protrustions were formed upon exiting the host cell by traversing parasites. At the end, parasites were surrounded by two membranes presenting the original PVM and a more external host derived membrane. Those double-layered extracellular sporozoites were later shown to invade a new host cell by invaginating the plasma membrane (Tartarelli et al., 2020). Interestingly, this study addressed the formation of a moving junction by invading sporozoites. This was accompanied by an unusual long membranous tail at the posterior end of invaded parasites present in their PVM. Thus, the

propelling of sporozoites in the host cell was proposed to be related to the force-producing mechanism by this tail (Tartarelli et al., 2020).

On the other hand, one single study addressed the invasion of bradyzoites where electron microscopy was used to assess invasion after 60 min of inoculating host cells. Electron micrographs showed no clear evidence of a MJ and no constriction in the parasite membrane upon invasion. Since the detection of MJ is particularly challenging by electron-microscopy, this conclusion should be taken with caution (Sasono & Smith, 1998).

1.8.1. Structures involved during invasion of *T. gondii*

Invasion of *Toxoplasma* is a fast and active process requiring gliding motility, conoid extrusion, microneme and rhoptry secretion. (Besteiro et al., 2011; V. B. Carruthers & Sibley, 1999; Dubremetz, 2007; Mondragon & Frixione, 1996; Santos et al., 2009; Soldati et al., 2001; Dawn M. Wetzel et al., 2004). Findings pertaining to the invasion machinery are discussed in the following sections and are mostly based on studies of tachzyoites' invasion.

T. gondii movement is established by a rudimentary actin-myosin motor, propelling invasion-related proteins and adhesins through rearward translocation along the plasma membrane during invasion. This actin-myosin motor is known as the glideosome which is conserved in the Apicomplexan phylum and empowers the parasites motility, invasion and egress (Frénal et al., 2017; Jacot et al., 2016; Keeley & Soldati, 2004; Santos et al., 2009). The system is fixed on the inner membrane complex (Opitz & Soldati, 2002) and connected to actin filaments that pull adhesin molecules (MIC), located on the plasma membrane of the parasite but fixed to host cell (for invasion) or substrate (for gliding), leading to their anterior-to-posterior translocation to drive parasite motion (Figure 6*A*). Thus, it is thought that the actin-myosin motor of parasite powers invasion (Figure 6*A*) and the MJ anchors it to the host cell (Figure 6*B*) (detailed in sections 1.8.1.1 and 1.8.2.1).

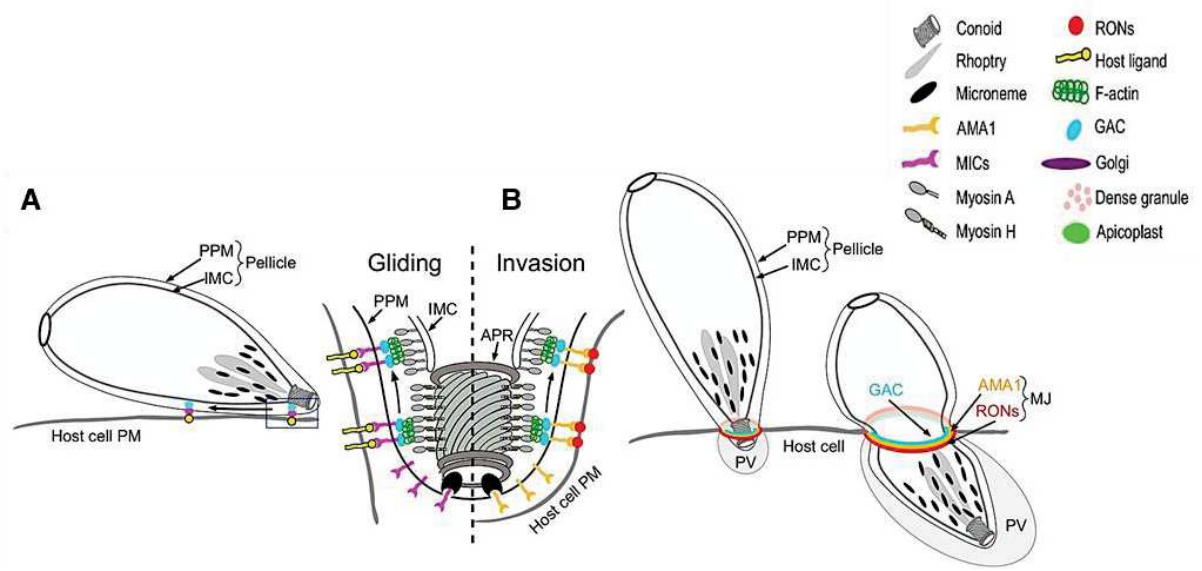


Figure 6: A schematic representation of a gliding and invading parasite (Tosetti et al., 2019). A) The parasite plasma membrane (PPM) and the inner membrane complex (IMC) create the pellicle. During gliding, the micronmes secrete MICs that are transmembrane adhesins which will interact with host cell ligands. On the other side, MICs will interact with GAC that is connected to F-actin. MyoH and MyoA aids in the rearward translocation of the GAC-adhesin complexes hence resulting forward movement of the parasite. B) During invasion, rhoptry neck proteins (RONs) are secreted by rhoptries into the host plasma membrane. Micronemal apical membrane antigen 1 (AMA1) distributed on the surface of the parasite with interact with these RONs, thus forming the moving junction. The entry of the parasite will result into invagination of the host plasma membrane and formation of the parasitophorous vacuole (PVM).

1.8.1.1. Glideosome machinery

The glideosome is located between the inner membrane complex (IMC) and the plasma membrane (PM) at the pellicle (Opitz & Soldati, 2002). A class XIV myosin A (*Tg*MyoA), a myosin light chain (*Tg*MLC1) and three additional gliding-associated integral membrane glycoprotein *Tg*GAP45, *Tg*GAP50 and *Tg*GAP40 form the glideosomal structure (Frénal et al., 2010; Gaskins et al., 2004). The association of *Tg*MyoA with *Tg*MLC1 and *Tg*GAP45, leads to the formation of a bridge between the PM and IMC which maintains an appropriate distance to preserve the pellicle integrity during motility (Frénal et al., 2010). *Tg*MLC1 light chain interacts with two essential light chains (ELC1 and ELC2) leading to stabilization of *Tg*MyoA neck domain (Figure 7). This intermolecular interaction is induced by Ca^{2+} which regulates

*Tg*MyoA activity (Q. Tang et al., 2014). Additionally, a *Tg*GAP45 homolog, *Tg*GAP70 aids in the recruitment of the glideosomal complex to the parasite's apical cap (Frénal et al., 2010).

Another type of glideosome can be assembled through the recruitment of class XIV myosin C (*Tg*MyoC), which possesses the same myosin light chains found in *Tg*MyoA, by GAP80 to the basal polar rings. *Tg*MyoC interacts with GAP50 and GAP40 as well. In addition, the IMC-associated protein 1 (IAP1) is a component of this complex that strictly localizes *Tg*MyoC to the posterior end. MyoA-glideosome and MyoC-glideosome have a high level of plasticity to secure the parasite survival. In that sense, depleting *Tg*MyoA leads to *Tg*MyoC relocalizatoin to the apical ring as a compensatory mechanism to secure infection (Frénal et al., 2014).

Addionally, a recently identified essential class, XIVc myosin motor protein (*Tg*MyoH), functions upstream of *Tg*MyoA and *Tg*MyoC. *Tg*MyoH tail is anchored to the conoid and is indispensable for initiating motility by this organelle. Moreover, it is essential for the displacement of receptor-adhesin complexes from the tip of the parasite, on the exocytosis site of secretory organelles. As such *Tg*MyoH is necessary for invasion, motility and egress (Graindorge et al., 2016). Although gliding motility is a result of the glideosome complex, osmotic forces created in the cytosol of the parasite may contribute to residual motility (Egarter et al., 2014).

Actin is one major protein of the motor-complex protein. *Toxoplasma* actin polymers are unstable and are about 100 nm in length (D. M. Wetzel et al., 2003). Unlike an ordinary system, polymerization of new actin filaments is what regulates motility instead of changing myosin activation states (D. M. Wetzel et al., 2003). Consequently, stabilization of *Toxoplasma* actin ACT1 (TgACT1) impairs gliding (Skillman et al., 2011), and its depletion demonstrated its crucial role in motility, invasion and egress (Andenmatten et al., 2013; Drewry & Sibley, 2015). Yet, Tg*ACT-1* knock-out parasites propagated for several days in culture

(Egarter et al., 2014; Whitelaw et al., 2017). This suggested the presence of an actin-independent machinery for motility. The movement of filamentous actin (F-actin) originate at the apical end by conoidal formin 1 that polymerizes actin and depends on myosin (Tosetti et al., 2019). Importantly, F-actin filamentous actin and adhesins (MIC2) are connected to glideosome machinery via a glideosome-associated connector (GAC). As such, GAC is essential for gliding motility, invasion, and egress (Jacot et al., 2016).

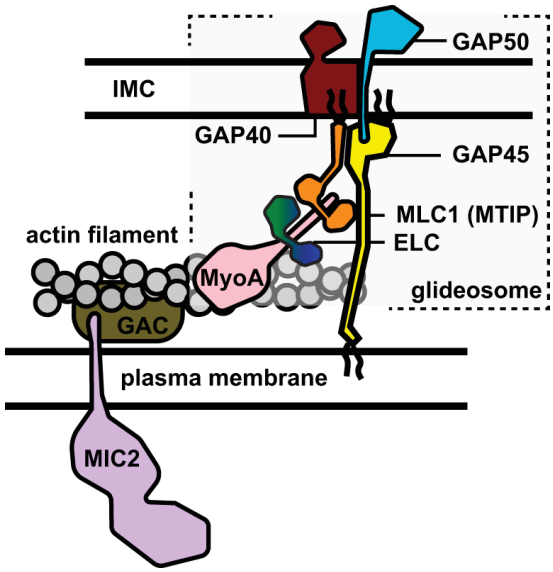


Figure 7: Schematic representation of the glideosome. MyoA interacts with MLC1 (myosin light chain) and ELC (essential light chain) in addition to glideosome associated proteins GAP40, GAP45 and GAP50, anchoring the glideosome to the IMC. On the other side, the GAC (glideosome associated connector) associates actin filaments with transmembrane proteins including MIC2 (Pazicky et al., 2020)

1.8.1.2 Conoid

The conoid is a motile structure that is linked to two pre-conoidal rings (PCR) from the top and an apical polar ring (APR) from the bottom, which aids in the organization of polarized microtubule to form the apical complex (Hu et al., 2006). Furthermore, it is constructed from twenty-two subpellicular microtubules (MTs) protruding from the APR. Those microtubules are organized in spiraling filaments with a counter-clockwise fashion to form a cone-shaped

assembly which confer the rigidity and polarity of *Toxoplasma* (Hu et al., 2002; Morrissette & Sibley, 2002). Additionally, it extends and retracts during the movement of the parasite along the host cell surface in a repetitive manner. Although conoid extrusion was thought to control invasion and motility (Mondragon & Frixione, 1996), inhibiting conoid protrusion has no effect on motility (Carey et al., 2004).

Activation of motility and hence invasion is controlled by an apical complex lysine (K) methyltransferase (AKMT) that re-localized in the apical complex and body of the parasite to activate motility (Heaslip et al., 2011). Recently, Ca^{2+} binding Calmodulin (CaM)-like proteins (CaM1, CaM2 and CaM3) were identified to overlap with MyoH in the conoid. This family was shown to be essential for motility, invasion and egress. More importantly, CaMs act downstream of rhoptry and microneme secretion (Long et al., 2017).

1.8.2. Secretory organelles associated with invasion

Invasion is initiated with a lateral low affinity interaction between the parasite and its host. This is carried out by profuse and highly distributed surface antigen glycoproteins (SAGs) also named SAG-related sequence proteins (SRS) which are GPI-anchored adhesins found on the surface of *T. gondii* during several stages of its life cycle (C. Jung et al., 2004; Lekutis et al., 2001). They interact with host-surface glycosaminoglycans, that are exploited as receptors during the parasite invasion (Vern B. Carruthers et al., 2000).

This step is followed by the successive and sequential exocytosis of two apical organelles called micronemes and rhoptries (V. B. Carruthers and Sibley 1997). Micronemes are numerous, small, membrane-bound, rod-shaped structures, located at the apical portion of the parasite and are the first to secrete their content (V. B. Carruthers & Sibley, 1997). An increase in the level of intracellular calcium (V. B. Carruthers & Sibley, 1999) induces the release of mironeme proteins known as MICs (recently reviewed in Lebrun, Carruthers, and

Cesbron-Delauw 2020). Some MICs are involved in *T. gondii* recognition, gliding, adhesion to the host cells and invasion, or in inducing the next step of rhoptry secretion (Lebrun, Carruthers, and Cesbron-Delauw 2020). It is worth noting that MICs form complexes in the endoplasmic reticulum before being transported to the micronemes. There are at least three crucial complexes that aid in the attachment of *Toxoplasma* to its host cell. The first is a heterohexameric complex composed of a member of the conserved TRAP family, the microneme protein 2 (*Tg*MIC2) which interacts with MIC2-associated protein (*Tg*M2AP). This later engages in the attachment of host cell and gliding motility (Huynh and Carruthers 2006; Jewett and Sibley 2004). The second complex important for invasion and rhoptry secretion is formed by complexing of *Tg*MIC8 (Kessler et al. 2008) with *Tg*MIC3 (Cérède et al. 2005). *Tg*MIC8 is involved in rhoptry secretion (Kessler et al. 2008) while *Tg*MIC3 interacts with host cell though a lectin-like binding motif (Cérède et al. 2005). The third is a multimeric complex formed by binding of *Tg*MIC6 with two adhesins, *Tg*MIC4 and *Tg*MIC1, which impart to invasion *in vitro* and virulence *in vivo* (Cérède et al., 2005; Marchant et al., 2012; Sawmynaden et al., 2008). The EGF domains of *Tg*MIC3 and *Tg*MIC6 maintain a non-fusogenic parasitophorous vacuole feature that does not fuse with lysosomes. This is attained through host cell signaling and activation of epidermal growth factor receptor (EGFR) (Muniz-Feliciano et al., 2013). These microneme adhesins contribute to the apical interaction of the parasite with its host. MICs are shed at the posterior end by the action of rhomboid protease. In *T. gondii*, the intramembrane serine rhomboid-like protease 4 (*Tg*ROM4) belonging to rhomboid family protease cleaves adhesins at their transmembrane domain, thus contributing to the disentanglement of interaction between host receptor and parasite ligand (Buguliskis et al., 2010; Rugarabamu et al., 2015; Shen et al., 2014). This creates a concentration gradient contributing to parasite reorientation in order to face its apex with the host cell during invasion.

Among the key players of *Tg*MIC is the apical membrane antigen 1 (AMA1). In collaboration with rhoptry proteins, it plays a role for MJ formation and invasion (detailed in section 1.8.2.1.1.). Another essential microneme protein is claudin-like apicomplexan microneme protein (CLAMP). It is necessary for invasion (Sidik et al., 2016), likely in participating in rhoptry secretion.

1.8.2.1. Molecular mechanisms of secretory organelles secretion

Microneme secretion is controlled by downstream signaling pathways which is established through second messages. These include intracellular calcium levels that are released form intracellular stores (V. B. Carruthers & Sibley, 1999; Dawn M. Wetzel et al., 2004), purine cyclic nucleotides (cGMP and cAMP) (Ono et al., 2008; Wiersma et al., 2004) and phosphatidic acid (PA) (Bullen & Soldati-Favre, 2016). Extracellular stimuli involved in micronemes secretion include serum albumin (Brown et al., 2016), drop in extracellular K^+ (Moudy et al., 2001), increase in extracellular Ca^{2+} (Pace et al., 2014), and increase in H^+ (Roiko et al., 2014).

Although the signaling pathways involving Ca^{2+} for micronemal secretion are not yet fully understood, some kinases contributing to this process were identified. The level of cytosolic Ca^{2+} is elevated during migration, invasion and egress but retained at low levels during immotile replicative stages (Lourido & Moreno, 2015). It has been suggested that inositol triphosphate (IP_3) produced from phosphatidyl inositol diphosphate (PIP_2) cleavage by phosphoinositide phospholipase C (PI-PLC) opens an IP_3-sensitive Ca^{2+} channel (Garcia et al., 2017; Lovett et al., 2002). Upon the release of cytosolic Ca^{2+}, a calcium dependent protein kinase 1 (*Tg*CDPK1) is activated (Lourido et al., 2010), and interacts with a human redox chaperone protein homologue (*Tg*DJ-1). This association leads to an enhanced kinase activity of *Tg*CDPK1 for attachment and secretion of micronemes (Child et al., 2017). This increase in

intracellular Ca^{2+} is mainly controlled by a cGMP associated protein kinase G (PKG) that induces an elevated microneme secretion (Brown et al., 2016). Mainly PKGI, is important for the survival of the parasite and microneme secretion in a calcium independent matter (Brown et al., 2017). A recent study showed that phosphatidic acid is an indispensable lipid mediator for microneme discharge which acts in a calcium-dependent matter. The importance of phosphatidic acid is correlated with acylated pleckstrin homology domain-containing protein (APH), found on micronemes surface and binds phosphatidic acid by its pleckstrin domain. When APH is depleted, microneme discharge is extremely blocked and lead to glideosome function abolition (Bullen et al., 2016).

The molecular mechanism behind the secretion of rhoptries remains ambiguous. A study conducted by Revindran *et al.* proposed the involvement of phospholipase. Given that the treatment with 4-bromophenacyl bromide, phospholipase A2s inhibitor, altered rhoptry secretion with no effect on that of the micronemes (Ravindran et al., 2009). Lately, *Toxoplasma* Ferlin 2 was shown to play a role in rhoptry secretion and invasion (Coleman et al., 2018). It possess potential lipid-calcium binding domains and is part of a eukaryotic ferlin protein family that is involved in vesicle trafficking, membrane fusion and repair (Lek et al., 2012). The content of rhoptry is injected into the host cell (Håkansson et al., 2001; Miller et al., 1979). A recent study showed that rhoptry exocytosis require multiple Non-discharge (Nd) proteins that are conserved in superphylum Alveolata. Nds are involved in the formation of intramembranous particles in the form of a rosette that is submerged in the plasma membrane at the apex of the parasite. Additionally, they are associated with an apical vesicle at the site of exocytosis. Interestingly, the apical vesicle is located between the tip of the rhoptry and the rosette, thereby illustrating for the first time that rhoptry secretion is linked to a vesicle through which exocytosis occurs (Aquilini and Cova et al, 2021 in press).

When the invasion is complete, a burst of dense granules is secreted inside the parasitophorous vacuole (PV), and then persists during the intracellular life of the parasite. As for rhoptries, the mechanisms behind dense granules secretion is enigmatic. A recent study, elaborated that dense granule secretion is negatively regulated by calcium and that this Ca^{2+}-mediated response is contingent on the function of calcium-dependent protein kinases *Tg*CDPK1 and *Tg*CDPK3 (Katris et al., 2019).

1.8.2.1. Moving junction

Around 40 years ago, the moving junction (MJ) was first perceived during erythrocyte invasion of *P. knowlesi* merozoites using electron microscopy (Figure 8*A*) (Aikawa et al., 1978). In this study, the MJ morphology was visualized as a circumferential zone affixing the erythrocyte membrane with the invading merozoite (Figure 8*B*). As invasion proceeds, the MJ moves along the invaginating membrane and maintains the position of the parasite at the site of entry (Aikawa et al., 1978). Later, the same ring shaped MJ was described during the invasion of *T. gondii* in nucleated and red blood cells (PORCHET-HENNERE & TORPIER, 1983). It appeared with thickening of the membrane from the side of the host cell and accumulation of integral membrane proteins from the host plasma membrane protoplasmic face (David J. P. Ferguson & Dubremetz, 2020) (Figure 8*C*).

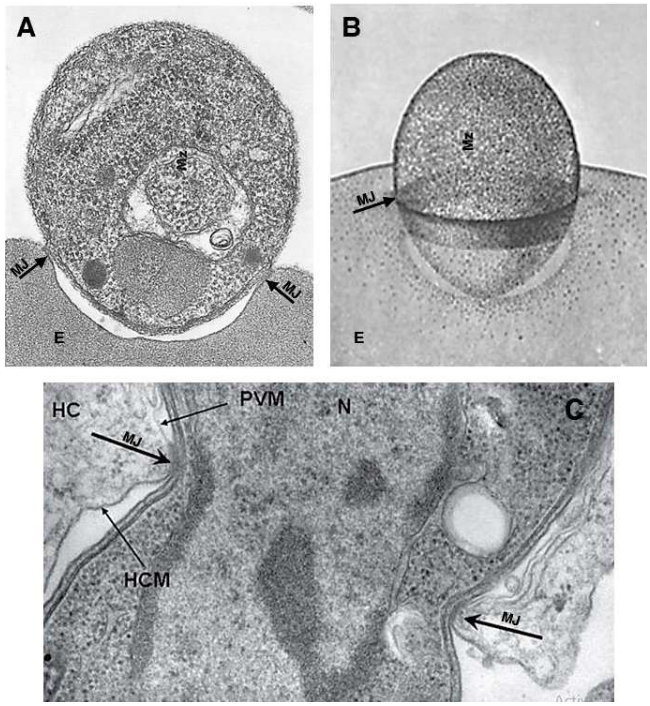


Figure 8: Moving junction formation by *Plasmodium* merozoite and *Toxoplasma* tachyzoite *in vitro*. A) Electron micrograph of *P. knowlesi* merozoite invading an erythrocyte showing erythrocyte membrane invagination upon merozoite entry through the formation of a moving junction (arrow) (Aikawa et al., 1978). B) A diagram illustrating the moving junction as an circumferential (ring shape) attachment between the invading merozoite and the erythrocyte (Aikawa et al., 1978). C) Section through an invading tachyzoite displaying the moving junction and the continuity and the difference in electron density between the HCM and the PVM. MJ, moving junction. E, erythrocyte. Mz, merozoite. HC, host cell. N, nucleus. HCM, Host cell plasmalemma; PVM, parasitophorous vacuole membrane (David J. P. Ferguson & Dubremetz, 2020)

In the following section, the main molecular components of the MJ and their role in invasion will be discussed. We will detail first the MJ complex in tachyzoites and then will present our knowledge in other stages.

1.8.2.1.1. Molecular organization of the Moving junction

The MJ is formed by rhoptry and micronemal protein assembly. The characterization of the MJ was described initially in the tachyzoites stages of *Toxoplasma*. During this stage, the microneme apical membrane antigen protein (AMA1) is secreted to the surface of the parasite and interact with the rhoptry neck protein (RON2) that is exported to the surface of the

host cell along with a pre-formed macromolecular complex of rhoptry neck proteins (RON2, RON4, $RON4_{L1}$, RON5 and RON8) (Alexander et al., 2005; J. R. Beck et al., 2014; Besteiro et al., 2011; Guérin, El Hajj, et al., 2017; Lebrun et al., 2005; Straub et al., 2011) (Figure 9). Those MJ rhoptry neck proteins are subjected to proteolytic maturation upon their translocation to their respective organelles (Besteiro et al., 2009; Guérin, Corrales, et al., 2017). RON5 and RON8 have no paralogs, however RON2 have two paralogs, $RON2_{L1}$ and $RON2_{L2}$ involved in other MJ complexes (Parker et al., 2016). Moreover, RON4 possess a homolog identified as $RON4_{L1}$ (Guérin, El Hajj, et al., 2017). Unlike, RON2, RON4 and RON5 that are conserved in Apicomplexan parasites, RON8 and $RON4_{L1}$ are specific to coccidian (Guérin, El Hajj, et al., 2017; Straub et al., 2009).

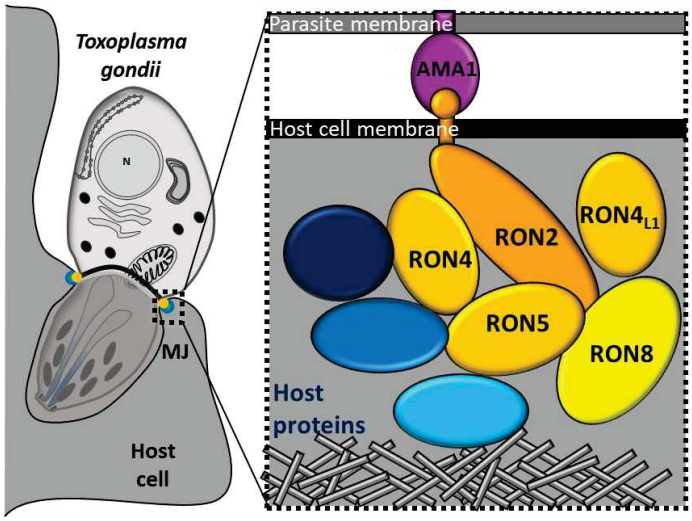


Figure 9: Scheme presenting the composition of the moving junction during invasion in tachyzoites

1.8.2.1.1.1. Moving junction composition in tachyzoites

The main micronemal protein involved in tachyzoite invasion is the type I transmembrane protein AMA1 possessing three N-terminal ectodomains (domain I, II, and III) and an intracellular C-terminal domain (Crawford et al., 2010; Hehl et al., 2000) (Figure 10). The role of AMA1 in invasion was first discovered in *Plasmodium* (M. G. Peterson et al., 1989) and next in *T. gondii*, where anti-AMA1 mouse sera were shown to inhibit tachyzoite invasion

by nearly 40% (Hehl et al., 2000). As in *T. gondii*, *Pf*AMA1 binds *Pf*RON2 to form a MJ that is essential for merozoite invasion into the red blood cells. Disruption of this MJ altered invasion and blocked the formation of the parasitophorous vacuole (M. Lamarque et al., 2011; Srinivasan et al., 2011). A resolution x-ray crystal structure showed that the ectodomain of *Toxoplasma* AMA1 has apical surface loops network which may constitute structural filters regulating entrance to a central hydrophobic groove. A DII loop forms the terminal portion of this groove to which it is anchored by a pair of tryptophan residues (Trp^{353} and Trp^{354}). Additionally, a conserved tyrosine (Tyr^{230}) forms an adjacent surface that may be essential for MJ construction. Moreover, DIII domain appears to folds into a cystine knot that is likely involved in the orientation and stabilization of an ectodomain bulk (Crawford et al., 2010). *AMA1* shares 19% to 26% identity with *P. berghei* and *P. yoelii* AMA1 and have significant levels in sequence divergence with AMA1 from *P. falciparum* and *P. vivax.* Examination of the AMA1 structure showed an apical surface loops network reorganized in size and chemistry with respect to *Pv*AMA1 and *Pf*AMA1, that appeared to function as filters preventing access to a central hydrophobic groove (Crawford et al., 2010; Normand et al., 2015).

During invasion, AMA1 is distributed on the entire surface of *T. gondii* (Donahue et al., 2000; Howell et al., 2005), thereby interacting with the C-terminal region of secreted *RON2* to the host cell membrane (M. Lamarque et al., 2011; Tyler & Boothroyd, 2011). In more details, AMA1-RON2 complex is formed by displacement of a DII extended surface loop on AMA1 which is characterized by conformational flexibility exposing a mature binding groove specific for RON2 (Tonkin et al., 2011). Notably, AMA1 DII loop is a structural gatekeeper to selectively allow ligands with only high affinity and specificity to AMA1 apical groove to bind (Parker & Boulanger, 2015). With respect to RON2, various studies reported that its C-terminal domain 3 (D3) is the region binding to AMA1 with high affinity (M. Lamarque et al., 2011; Parker & Boulanger, 2015; Tonkin et al., 2011; Tyler & Boothroyd, 2011). This

interaction with AMA1 was confirmed by a reduction in invasion efficiency upon incubating the parasites with a recombinant RON2 C-terminal region (M. Lamarque et al., 2011; Tonkin et al., 2011; Tyler & Boothroyd, 2011). Intrinsically, the association between those proteins triggers the complex organization into a ring structure surrounding the apical tip of the parasite. As the invasion proceeds, the diameter of the ring increases and decreases in dependence of the parasite's diameter, implying structural flexibility of the ring. Remarkably, the MJ structure provides a strong basis to withstand and resist the mechanical sheer forces during invasion. AMA1 and RON2 interaction is of strong and high affinity provided by a extensively buried surface structure to which those proteins bind (Tonkin et al., 2011).

One of the features of AMA1 is the proteolytic cleavage of its N-terminal ectodomain in extracellular parasites which is more enhanced upon increase in intracellular calcium levels (Donahue et al., 2000). This proteolytic process requires rhomboid protease, *Tg*ROM4, and *Tg*ROM5, that cut AMA1 within its transmembrane domain (Buguliskis et al., 2010, p. 4; Howell et al., 2005; Rugarabamu et al., 2015; Shen et al., 2014). Interestingly, the sensitivity of cleavage by rhomboid proteases is highly reduced upon binding of AMA1 to the domain 3 (D3) peptide of RON2. This would allow the two proteins to sustain an unimpaired binding during the whole invasion process (Krishnamurthy et al., 2016). Thereby, supporting MJ formation and invasion into host cell. In addition, AMA1-RON2 interaction leads to the dephosphorylation of the AMA1 cytosolic tail that is required for an outside-in signaling and efficient host cell invasion (Krishnamurthy et al., 2016).

While a small C-terminal ectodomain segment of RON2 binds to AMA1, most of RON2 is present at the cytosolic face of the host cell in complex with other RON proteins (Besteiro et al., 2009; M. Lamarque et al., 2011; Straub et al., 2009). Indeed, several co-immunoprecipitation studies revealed that RON2, RON4, RON5 and RON8 formed a complex and are all present at the MJ (Alexander et al., 2005; Besteiro et al., 2009; Lebrun et al., 2005,

p. 4; Straub et al., 2009). Notably, RON4/RON5/RON8 are secreted to the host cell membrane where they are associated to the cytosolic phase (Besteiro et al., 2009). An additional rhoptry protein, $RON4_{L1}$ was later shown to be associated with the complex and also exposed to the host cytosolic face of the MJ (Guérin, El Hajj, et al. 2017). Upon completion of the invasion process, the MJ can still be present at the parasite posterior pole for a few hours (Besteiro et al., 2009).

Interestingly, at early steps of invasion, RON4 binds β-tubulin hence providing evidence for the interaction of the parasite with the corresponding infected host cell cytoskeleton via RON4 during invasion (Takemae et al., 2013). In addition, RON4 binds to heparan sulfate (glypican 1) during invasion which may indicate a role for heparan sulfate in invasion (Takemae et al., 2018). However, this result is difficult to explain if RON4 is inserted into the host cytosol. Later, Guérin *et al* illustrated that the MJ RON complex recruits some host adaptor proteins, bringing together the underlying cytoskeleton and membrane proteins. The adaptor proteins include; CD2-associated protein (CD2AP), tumor susceptibility gene 101 protein (TSG101), ALG2-interacting protein X (ALIX; also known as programmed cell death 6-interacting protein) and CBL-interacting protein of 85 kDa (CIN85; also known as SH3 domain-containing kinase-binding protein 1) (Guérin, Corrales, et al., 2017).

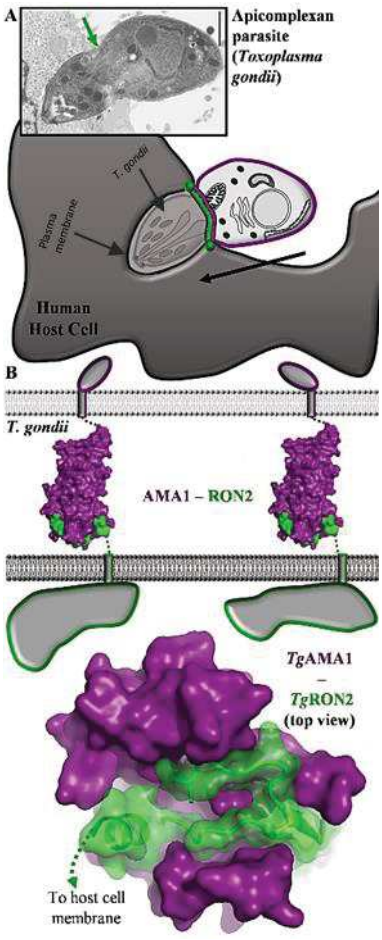


Figure 10: AMA1-RON2 complex in T. gondii (A) Electron micrograph of invading T. gondii into its host cell. (B) Top: Domains I-II-III of AMA1 (purple surface), RON2 synthetic peptide (green surface). Bottom: apical view of the AMA1 (solid purple surface)-RON2 (green cartoon) complex (Tonkin & Boulanger, 2015).

1.8.2.1.1.1.1. Importance of moving junction proteins during invasion

To decipher the role of each protein in the MJ, several conditional mutagenesis studies were conducted. Disruption of this MJ altered invasion and blocked the formation of a parasitophorous vacuole (Guérin, El Hajj, et al., 2017; M. Lamarque et al., 2011; M. H. Lamarque et al., 2014; Straub et al., 2011, p. 8; Tyler & Boothroyd, 2011). Parasites lacking RON2 were shown with severe defect in invasion (M. H. Lamarque et al., 2014). Altered expression and localization of RON4 and RON5 was noted in those KD-RON2 mutants, and both proteins were not localized to the rhoptry neck. This led to the absence of RON4 and

RON5 from the MJ during invasion. Yet, RON8 was associated with the rhoptries and was localized to the MJ during invasion in the KD-RON2 parasites (M. H. Lamarque et al., 2014). These results highlighted the importance of RON2 for *Toxoplasma* invasion and suggested that RON8 might be associated with other components contributing to build a different MJ of different composition. Moreover, in the absence of RON2, most of the mutant parasites failed to invade but leaved behind e-vacuoles in the host cell. Those e-vacuoles are the result of *T. gondii* failure to form MJ (M. H. Lamarque et al., 2014)). Conditional depletion of RON4 was also related to defect in invasion of mutant tachyzoites; RON5 and RON2 expression were reduced in that strain, while expression of RON8 was unchanged (Guérin, Corrales, et al., 2017)(M. Wang et al., 2017). This illustrated also that RON4 is not an essential gene in *Toxoplasma*. In another study, by generating a conditional mutant of RON5, the authors illustrated that the lack of RON5 led to RON2 degradation and RON4 mistargeting along the secretory pathway (J. R. Beck et al., 2014). In addition, they showed that RON5 C-terminal domain was the part involved in the stability of RON2 and in the invasion process. As seen in RON2 mutant strain, RON8 was also unaltered in the absence of RON5. Importantly, RON5 mutant parasites highlighted the requirement of an intact MJ complex and MJ formation for rhoptry bulb secretion, since e-vacuoles were not formed (J. R. Beck et al., 2014). This result was not observed for KD-RON2 (M. H. Lamarque et al., 2014) mutants, where the rhoptry proteins where shown to be properly secreted in absence of RON2.

While it was not possible to remove *RON2* and *RON5* genes (J. R. Beck et al., 2014; M. H. Lamarque et al., 2014), *RON4* (M. Wang et al., 2017), $RON4_{L1}$ (Guérin, El Hajj, et al., 2017) and *RON8* (Straub et al., 2011) are not essential. RON4 mutants showed around 60% reduction of invasion (M. Wang et al., 2017). RON8 knockout parasites were critically impaired in their ability to attach and invade host cells (80% reduction of invasion) (Straub et al., 2011). Intriguingly, during invasion of this knockout strain, the rest of the MJ proteins were

often found in trails behind the mutant parasites that managed to invade, which may indicate a malformed complex in absence of RON8 and that RON8 may play a role in forming a firm clasp between *Toxoplasma* and its host. Δ*ron8* parasites displayed like a delay in separation of the PV with an extended tether persisting between the PV and the host cell plasma membrane. That result may point to the implication of RON8 in detachment of the PV from the host plasma membrane (Straub et al., 2011). The defect in Δ*ron8* parasites *in vitro* was also translated by diminished virulence in mice model (Straub et al., 2011). However, parasites lacking $RON4_{L1}$ showed a small defect in virulence *in vivo*, yet this protein is not essential for invasion in fibroblasts *in vitro*. Like RON8, $RON4_{L1}$ trafficking to the MJ during invasion is not affected by RON2, RON4, and RON5 absence, which implies the presence of an unconventional MJ in tachyzoites (Guérin, El Hajj, et al., 2017).

Concerning AMA1, in a first study using a conditional knockout of AMA1, the tachyzoites lacking AMA1 have a strong defect in their ability to invade the host cell (10% residual invasion) (Mital et al., 2005). The initial step of attachment and microneme discharge were not affected by the depletion of AMA1, however a small decrease in ability of the mutants to secrete the content of rhoptries was noted (Mital et al., 2005). While AMA1 was predicted to be essential for the parasite, two studies were able to generate knockout for AMA1 (Bargieri et al., 2013; M. H. Lamarque et al., 2014). They also found that the absence of AMA1 induces a strong invasion defect. However, Lamarque *et al* did not confirm the defect in rhoptry secretion (M. H. Lamarque et al., 2014). Moreover, the authors showed that the cytosolic tail of AMA1 was necessary for internalization of *Toxoplasma* by unknown downstream signaling (M. H. Lamarque et al., 2014). The phenotype of the KO-AMA1 in type I strain was investigated *in vivo* and showed that mice survived the infection, demonstrating that AMA1 is involved in the parasite acute phase and dissemination *in vivo* (Lagal et al., 2015). Infection

with KO-AMA1 also resulted in a long-lasting immune response that protected mice upon challenging with high dose of type I or type II strains.

As stated before, although tachyzoites lacking AMA1 exhibit invasion defects in attachment to the host, it was possible to remove the gene (Bargieri et al., 2013; M. H. Lamarque et al., 2014). Lamarque *et al* scrutinized the ability of KO-AMA1 parasites to invade and demonstrated in this strain an upregulation of a close paralog of AMA1, called AMA2. While AMA2 protein is expressed at very low levels in tachyzoites, AMA2 is upregulated in AMA1 depleted tachyzoites, and it interacts with RON2, with a lower affinity as compared to AMA1-RON2 interaction (M. H. Lamarque et al., 2014). They next demonstrated that *AMA2* is at the MJ of invading KO-AMA1 and plays a role in residual invasion, since removing of AMA2 in KO-AMA1 parasites decreased invasion efficiency of KO-AMA1. KO-AMA1 strain also upregulated $RON2_{L1}$ that localized to the rhoptry and specifically interacted with another more distant paralog called AMA4 that was highly expressed in the mutant KO-AMA1 parasites (M. H. Lamarque et al., 2014). This complex is functional for the invasion, since a triple mutant (KO-AMA1/KO-AMA2/KO-AMA4) is less efficient to invade than the double mutant KO-AMA/KO-AMA2 and a $RON2_{L1}$ peptide that interacts with AMA4 inhibits the invasion of KO-AMA/KO-AMA2 parasites (Parker et al., 2016). This study revealed that AMA1 mutant parasites upregulated other homologues of AMA1 that supported residual invasion, highlighting the compensatory effect of other MJ complexes to sustain invasion (M. H. Lamarque et al., 2014). Interestingly, some of these up-regulated genes were shown to be important for invasion of sporozoites (detailed in section 1.8.2.1.1.2)

1.8.2.1.1.2. Moving junction in sporozoite stage

Although the MJ is extensively characterized in tachyzoites, it is poorly studied in other stages of *T. gondii*.

Three paralogs of AMA1 and two paralogs of RON2 are documented to form other functional MJ complexes; AMA2-RON2 (M. H. Lamarque et al., 2014), sporo*AMA1*-sp*oro*RON2 known as AMA3-RON2$_{L2}$ (Poukchanski et al., 2013), and AMA4- RON2$_{L1}$ (M. H. Lamarque et al., 2014; Parker et al., 2016) (Figure 11).

In oocysts, RON2$_{L2}$ ("*SporoRON2*") and AMA3 ("*SporoAMA1*") are highly expressed, but are not expressed neither in tachyzoites nor in bradyzoites, indicating a sporozoite-specific MJ that differs from that of tachyzoites (Poukchanski et al., 2013). SporoAMA1 solely and specifically interacts with sporoRON2 only. Poukchanski *et al* showed that tachyzoites and sporozoites utilize different *Tg*AMA-*Tg*RON complexes, since incubation of sporozoites with sporoRON2D3 impairs invasion of sporozoites, yet has no effect on tachyzoites. Whereas, incubation of parasites with RON2D3 has an effect only on tachyzoites (Poukchanski et al., 2013). This result highlighted the role of sporoAMA1-sporoRON2 for invasion of sporozoites and that while AMA1 and RON2 are also expressed in sporozoites, this complex does not seem to be a main component of invasion at this stage. The presence of sporoAMA1-sporoRON2 at the MJ of invading sporozoites was not investigated. Recently, a new sporoAMA1 isoform was shown to be expressed in bradyzoites during the latent chronic stage. This version is shorter than that of sporoAMA1 in sporozoites (Garfoot et al., 2019). Since this isoform has no binding site for RON2 and there is no sporoRON2 transcripts in the late bradyzoite stage, the function of the short version is thought to be involved in a regulatory role rather than invasion.

The sporozoites also express another MJ pair formed by AMA4 and RON2$_{L1}$ (Parker et al., 2016), present in the micronemes and rhoptries, respectively. However, their presence at the MJ and role in invasion of sporozoites has not been demonstrated yet.

Moreover, RON4$_{L1}$, RON2, RON4, RON5, RON8 and RON2$_{L1}$ are expressed in oocysts according to proteomic evidence (Fritz et al., 2012). As such, it is unknown whether AMA3-RON2$_{L1}$ and AMA4-RON2$_{L1}$ pairs operate in complex with RON4/5/8 or independent

of them, and whether the two pairs interact together or not. Intriguingly, a recent study detected for the firs time the presence of RON4 at the MJ of invading sporozoites, confirming that this stage use a MJ-dependent invasion process (Tartarelli et al., 2020).

While both AMA1 and AMA2 can form a complex with RON2, the other MJ complex are specific and cross-binding has not been shown (M. H. Lamarque et al., 2014; Parker et al., 2016). However, in spite of considerable sequence discrepancy, AMA1–RON2*D3* (Tonkin et al., 2011), and AMA3–*RON2*$_{L2}$D3 (Poukchanski et al., 2013) complex structures present a highly conserved architecture and binding model (Figure 11). Like AMA1, AMA3 has a three-domain architecture and RON2$_{L2}$-D3 is integrated into the apical groove of AMA3. This organization mimics the overall binding paradigm previously observed for generic AMA1-RON2 complexes from *T. gondii* tachyzoite but the co-structure of AMA3 in complex with RON2$_{L2}$ peptide reveals several divergent substructures that explain why RON2 cannot seat in the groove of DI domain of AMA3 (Poukchanski et al., 2013). Most notably, interaction of RON2$_{L2}$ with AMA3 DI/II induces alterations in the membrane-proximal AMA3 DIII indicating a possible involvement in signaling.

AMA4 and *RON2*$_{L1}$ sequence analysis and co-structure illustrated significantly different structures with an unusual assembly mechanism (Parker et al., 2016). High-resolution crystal structures of apo AMA4 and AMA4-RON2$_{L1}$-bound unraveled a unique architecture and assembly of the complex compared to other AMA-RON2 complexes. AMA4 is a type I integral membrane protein. Its ectodomain possess an expanded N-terminal AMA1 DI-like domain, AMA1 DII domain, and 15 tandem epidermal growth factor (EGF) and Cys-rich modules. Mainly, a key extended DII surface loop and deep surface groove that are needed to selectively regulate RON2 ligand binding in other *Tg*AMAs are absent in AMA4 (Parker et al., 2016) (Figure 11).

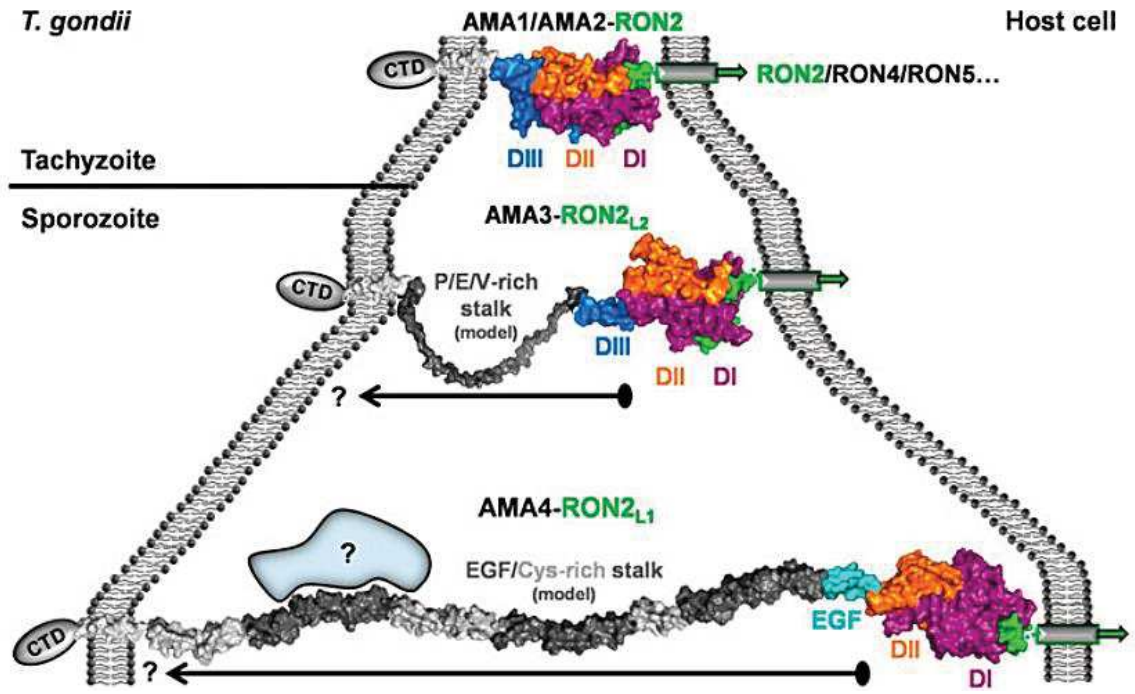


Figure 11: Structures of *Tg*AMA family members. *Tg*AMA family members possess irregular stalk regions that leads to variable distances between the parasite cell membrane and the RON2-binding head group. From the top: AMA1 (purple/orange/blue)–RON2D3 (green) complex. *AMA1* transmembrane domain in the form of seven-turn alpha-helix (white surface). CTD, C-terminal domain. At the middle, *Tg*AMA3– RON2$_{L2}$D3 complex colored the same as in Top. Stalk region (gray surface) illustrates a Pro/Glu/Val rich region; the arrow reflects the potential for considerable flexibility. At the bottom, AMA4–RON2$_{L1}$D3 complex colored the same as in Top, tandem EGF (dark gray) and Cys-rich (light gray) domains connected head to tail. Blue shape with question mark indicates the possibility for the AMA4 stalk to recruit additional proteins. Arrow with question mark indicates potential for (Parker et al., 2016).

1.9. Vaccination and Toxoplasmosis

Toxoplasmosis is one of the most prevalent diseases. It is endemic and widespread all over the world. Yet, it is reported as neglected tropical diseases by Centers for Disease Control and Prevention, CDC2019. All clinical available therapeutics targets the rapid multiplying tachyzoite stage with no notable activity on the bradyzoites tissue cysts in latent infections (Ildiko Rita Dunay et al., 2018). In humans, the main therapy is a combination of the antifolate drugs, sulfadiazine and pyrimethamine. Yet, this combination has significant failure rates (Ildiko Rita Dunay et al., 2018). Pyrimethamine was also combined with either antibiotics

including azithromycin, clarithromycin, clindamycin, or atovaquone, or monotherapy with trimethoprim–sulfamethoxazole (TMP-SMX); nevertheless, none of these regimens showed to be more potent than the pyrimethamine–sulfadiazine combination (Ildiko Rita Dunay et al., 2018). In addition, the side-effects of these drugs are of major concern (Ildiko Rita Dunay et al., 2018). For instance, treatment suing first-line therapy pyrimethamine and sulfadiazine combination has toxic side effects. It was associated with rare severe complications including hepatic necrosis, toxic epidermal necrolysis, agranulocytosis, and Stevens–Johnson syndrome (Alday & Doggett, 2017). For patients with sulfa allergy, sulfadiazine was replaced with clindamycin. However, this new combination was less efficient in suppressing relapse and accompanied with same toxicity levels as the original regimen (Alday & Doggett, 2017). Thus, vaccines can be of better replacement, and may ensure an effective long-term disease control as compared to therapeutic regimens. Up-to-date, the only commercially available vaccine is Toxovax1, solely used in sheep (Buxton & Innes, 1995). Yet, it has several limitations that are mentioned below (Buxton et al., 1991). As such, developing a safe and effective vaccine is a requisite for controlling toxoplasmosis.

1.9.1. Vaccination approaches against toxoplasmosis

Historically, substantial attempts were conducted to establish a vaccine against toxoplasmosis in humans, livestock and cats. The main objective is to develop a vaccine that is able to prevent congenital and chronic disease in humans and livestock, and inhibit oocyst shedding in cats. Those approaches aimed in targeting the origin of infection with *T. gondii* in humans including oocysts and tissue cysts (section 1.4). Lately, an immense number of vaccine candidates and vaccination strategies were examined. These include epitope vaccines, protein vaccines, DNA vaccines, live-attenuated vaccines, inactivated vaccines, and live vector-based vaccines. These different strategies were mostly inspected using murine models to assess

chronic and acute toxoplasmosis (Li & Zhou, 2018; N.-Z. Zhang et al., 2015). Some strategies were tested on cats and livestock where oocysts shedding and tissue cysts have been studied, respectively (Mévélec et al., 2020). Yet, none of these vaccine strategies could completely eradicate tissue cyst and prevent vertical transmission

Vaccines established from subunit proteins, excretory–secretory (ES) products, lysate antigen, killed organisms, and DNAs, induced effective immunity against *Toxoplasma* through activation of lymphocytes especially strong cytotoxic T lymphocytes. Various studies emphasized on antigens including, microneme antigens (MICs), rhoptry antigens (ROPs), the surface antigens (SAGs), dense granule antigens (GRAs), and several others secreted by tachyzoites and bradyzoites during replication , invasion, attachment, motility, and alteration of the host's immune response (Hiszczyńska-Sawicka et al., 2014; Li & Zhou, 2018; N.-Z. Zhang et al., 2015).

It is worth noting that the molecular composition of the vaccine and the way it is delivered, contribute to its efficacy. Many adjuvants, including interleukins, Freund's adjuvant, MHC-restricted adjuvant, CpGDNA, monophosphoryl lipid A, were introduced to the vaccination strategies to enhance immune responses (Hiszczyńska-Sawicka et al., 2014; Li & Zhou, 2018; N.-Z. Zhang et al., 2015). Interestingly, vectors including nonpathogenic viruses, protozoa or bacteria conveying *T. gondii* antigens are being used to mimic the intracellular niche of *Toxoplasma* and create an immune response in absence of additional adjuvant (S.-H. Lee et al., 2018; Machado et al., 2010; L.-J. Wang et al., 2018). As such, immunization with a vaccine based on combined virus-like particle (VLP) that expresses MIC8 and ROP18 reduced brain cyst load and improved survival through inducing strong humoral and cellular immune responses (S.-H. Lee et al., 2018). Moreover, a heterologous prime-boost immunization strategy could provide profound levels of specific cellular and humoral immune responses for therapeutic and preventative measures against toxoplasmosis. For instance, prime

immunization with a recombinant influenza viruses encoding a SAG2 antigen, followed by a booster of recombinant adenovirus expressing the same antigen, provided a strong immunity thereby protecting immunized by mice by reducing 85% of parasite burden (Machado et al., 2010).

In the section below, different vaccination approaches tested against *T. gondii* will be discussed.

1.9.1.1. Live-attenuated Vaccines

One of the most efficient vaccines are live-attenuated vaccines with their ability to grant protection since they resemble natural infection, imparting a resemblance of the microenvironment regarding antigen presentation and processing. Live-attenuated vaccines, for example TS-4, T-263, and S48 mutant parasites, have manifested high efficacy in reducing the prevalence of sheep abortion, preventing oocysts shedding from cats, and reducing tissue cyst generation in food-producing animals (Hiszczyńska-Sawicka et al., 2014; Li & Zhou, 2018; N.-Z. Zhang et al., 2015). Yet, the only commercial vaccine is Toxovax1. It is a live-attenuated tachyzoite S48 strain, licensed in the UK, New Zealand, and other European countries. Toxovax1 is used in sheep to reduce abortion incidence (Buxton & Innes, 1995). The live-attenuated S48 tachyzoites were initially isolated from an aborted lamb in New Zealand, and repeatedly passaged over 3000 times in mice which lead to the loss of tachyzoites capacity to convert into encysted bradyzoite (Buxton et al., 1991). Nevertheless, Toxovax1 cannot totally eliminate *T. gondii* and has s a short shelf life. Moreover, the attenuated S48 vaccine's molecular basis is not well understood. Spontaneous mutations could occur, thus reverting to a pathogenic strain, which can be highly risky especially to vulnerable individuals (Buxton et al., 1991). Recently, with the rise and progress of genetic engineering methods, live-attenuated vaccines based on gene editing are investigated and several procedures are applied to reach a

safe and attenuated toxoplasmosis vaccine (J.-L. Wang et al., 2016). These attenuated parasites are created by deleting particular genes. In that sense, immunization with AMA1 knockout parasites showed protection of BALB/c, C57BL/6 and CD-1 mice against chronic and acute toxoplasmosis after challenge with type II Me49 and type I RH strains, respectively (Lagal et al., 2015; Moiré et al., 2009; J.-L. Wang et al., 2019).

Another live attenuated vaccine of *T. gondii* type I RH strain lacking two micronemal genes, *MIC1* and *MIC3,* known as Mic1-3KO was tested for its ability to protect against toxoplasmosis (Ismael et al., 2006; Le Roux et al., 2020; Mévélec et al., 2010). This strain was developed in 2005 and showed reduction in host cell invasion (Cérède et al., 2005). Importantly, *MIC1-3*KO parasites did not revert into the virulent strain unlike the S48 strain that could potentially revert (Buxton et al., 1991). Interestingly, vaccination with *MIC1-3*KO strain showed significant protection against chronic toxoplasmosis in mice. Thereby reducing cyst burden by around 96% in vaccinated mice brains. Moreover, it protected against congenital toxoplasmosis whereby all born pups from vaccinated dams survived with reduced brain cyst burden (>91%) compared to non-vaccinated dams (Ismael et al., 2006). This live attenuated vaccine was also tested in sheep and showed reduction in aborted lambs of immunized ewes by around 90% and was as effective as S48 in vaccination of sheep (Mévélec et al., 2010). Yet, vaccinating cats with *MIC1-3*KO strain did not prevent oocyst shedding after challenge (Le Roux et al., 2020). This highlight the unique difference in interaction of *T. gondii* with its corresponding host.

In general, most of the live-attenuated vaccines are 100% efficient, where vaccinated mice survived for more than 30 days (Table 3). Yet, their use in humans might be dangerous due to the possibility of reverting to their virulent origin.

No.	Vaccination Approach	Immune Responses	Challenge Strain/ Amount	Protection	Animal/Strain	Immunisation Approach
1	Nonreverting, nonreplicating, live attenuated uracil auxotroph vaccine strains in the type II *KU80* knockout background		RH – 1×10^3 tachyzoites PRU *KU80* knockout strain – 2×10^7 tachyzoites	100% survival- 30 days 0 cyst	C57BL/6 mice	i.p.
2	RH strain with AMA1 knockout (AMA1KO) tachyzoites		RH *KU80* knockout strain BALB/C (10^5 tachyzoites) C57B/6J (10^3 tachyzoites) ME49 CD-1 (10^5 tachyzoites) BALB/C (10^3 tachyzoites)	100% survival until 60 days 100% survival until 45 days 100% survival until 45 days reduction in number of parasites	BALB/C, C57B/6J, CD-1 mice	i.p., s.c.
3	Lactate dehydrogenase knockout in PruΔKu80::hxgprt parental strain		RH – 1×10^4 tachyzoites	double knockout of LDH1/LDH2- 100% survival in 30 days reduction in brain cyst number	BALB/c mice	i.p.
4	GRA17 knockout in RH strain	predominance of IgG2a over IgG1; higher level of IFN-ɤ, IL-2, IL-12, and IL-10	RH – 1×10^3 tachyzoites PRU – 20 cysts	100% survival in 35 days reduction in brain cyst number	Kunming mice	i.p.
5	CDPK2 deficient tachyzoites of Pru strain	higher level of IgG; higher level of IFN-ɤ, IL-2, IL-12, and IL-10	RH – 1×10^3 tachyzoites PRU – 20 cysts	100% survival in 35 days reduction in brain cyst number	Kunming mice	i.p.

Table 3: Summary of most effective live-attenuated vaccines (Loh et al., 2019)

1.9.1.2. Protein vaccines

Up to date, recombinant protein candidates for vaccination belong to surface antigens (SAG), microneme antigens (MICs), rhoptry antigens (ROPs) or dense granule antigens (GRAs) families. Several protein vaccine candidate including MIC1, 4, 6, and 8 (Foroutan et al., 2018; Pinzan et al., 2015), SAG1 (Allahyari et al., 2016, p. 2), GRA2 and GRA5 (Ching et al., 2016), and ROP1, ROP2, ROP4, ROP5, ROP16, ROP17, ROP18, and ROP38 (Foroutan et al., 2019) were evaluated. Other protein candidates including, actin depolymerizing factor (ADF) (Z. Liu et al., 2016), phosphoglycerate mutase 2 (PGAM 2) (H.-L. Wang et al., 2016), HSP70 (Czarnewski et al., 2017), elongation factor 1 alpha *Tg*EF-1α (S. Wang et al., 2017), aspartic protease 3 (*Tg*ASP3) (G. Zhao et al., 2017) and peroxiredoxin 1 (*Tg*Prx1) (Fereig et al., 2017), were also studied. Vaccination with *Tg*CDPK3 induced cellular and humoral response in vaccinated mice, however induced partial protection against chronic (46.5%) and acute against toxoplasmosis after challenging with type II Pru cysts and type I RH, respectively (Wu et al., 2019, p. 3). Immunization with *Tg*CDPK1 protein only prolonged survival of vaccinated mice after challenge with RH strain, thereby partially protecting against acute toxoplasmosis (S.-Y. Huang et al. 2019). Table 4 summarizes some of the most effective protein vaccines. Most single protein subunits or antigen vaccines were unable to support full protection against the different stages of toxoplasmosis. This may be related to the complex

life cycle of *T. gondii,* hence constraining those vaccines to stage-limited protection. Consequently, several multivalent and multi-antigenic vaccines were developed. Another difficulty accompanied with protein vaccines is their short-lived or weak immunogenicity, however this issue may be resolved by using appropriate delivery systems and adjuvants to induce long lasting-protective immunity (Fereig & Nishikawa, 2016; Q. Liu et al., 2012; Loh et al., 2019).

No.	Types of Antigen	Antigen/Adjuvant/Delivery Approach	Immune Responses	Challenge Strain/ Amount	Protection	Mouse Strain	Immunisation Approach
1	Tachyzoite lysate antigen	*T. gondii* antigens Adjuvant - Loading of porous nanoparticles (DGNP)	mixed IgG1/IgG2a response; higher levels of IFN-ν, TNF-α, IL-2, IL-4, IL-6, and IL-17	76 K strain – 30 cysts	70% brain cyst reduction	CBA/J (H-2 k)	mucosal vaccine
		Toxoplasma lysate Adjuvant - chitosan nanospheres, Freund's incomplete adjuvant	increase in IgG and IgM; higher level of IFN-γ	RH – 2500 tachyzoites ME49 – 10 cysts	80 days survival 76.8% reduction in parasitic count	Swiss strain albino	Intraperitoneal (i.p.)
2	Rhoptry protein	ROP17 Fusion with glutathione S-transferase (GST)	greater IgG2a than IgG1, higher SIgA antibody; higher levels of IFN-γ, IL-2, and IL-4	RH – 4×10^4 tachyzoites	75% survival rate in 30 days	BALB/c	i.n.
		ROP38 and ROP18 Adjuvant – polylactide-co-glycolide (PLG) encapsulation	higher ratio of IgG2a to IgG1; higher level of IFN-γ and IL-2	PRU – 10 cysts	81.3% of cyst reduction	Kunming	Subcutaneous (s.c.)
3	Enzymes	Phosphoglycerate mutase (PGAM)2	higher IgG2a/IgG1 ratio, higher IgA antibody; Higher levels of IFN-γ, IL-2 and IL-4	RH- 4×10^4 tachyzoites	70% survival in 30 days	BALB/c	i.n.
4	Actin-binding protein	Profilin Adjuvant - encapsulated in oligomannose-coated liposomes	higher total IgG (higher IgG2c than IgG1); increase of IFN-γ	RH – 1×10^3 tachyzoites	66.7% survival in 30 days	C57BL/6	s.c.
5	Surface antigen	Actin depolymerizing factor (ADF)	higher sIgA and IgG; higher levels of IFN-γ and IL-2	RH – 4×10^4 tachyzoites	36.3% survival in 30 days	BALB/c	i.n.
		SAG1 fused with an antibody fragment scFv directed against DEC205 endocytic receptors Adjuvant- Poly I:C	predominance of IgG1 over IgG2a; higher levels of IL-12, TNF-α, and IL-6	76 K – 15 cysts	80% reduction in brain cyst number	CBA/J (H-2 k)	s.c., i.n.
6	Dense granule protein	GRA7 self-assembling polypeptide nanoparticles (SAPNs) Adjuvant- PADRE	increase of IFN-γ secretion	ME49 –2 $\times$ 10^3 tachyzoites	72% reduction in brain cysts	HLA-B*0702	s.c.
7	Scaffold protein	Receptor for activated C kinase (RACK)1	higher sIgA antibody titers, predominance of IgG2a; Higher levels of IFN-ν, IL-2, and IL-4	RH - 1×10^4 tachyzoites	45% survival in 30 days	BALB/c	i.n.
8	Inner membrane complex (IMC)	IMC sub-compartment proteins 3 (ISP3) Virus-Like Nanoparticle Vaccine	higher levels of IgA and IgG (higher IgG2a than IgG1); higher levels of IFN-γ, IL-6 and IL-11	ME49- 20 cysts	75% reduction in brain cysts	BALB/c	i.n.
9	Combination of different types of antigens	CDPK6 and ROP18 Adjuvant - encapsulated in PLG microspheres	higher level of IgG and IFN-γ	PRU – 10 cysts	73.6% reduction in brain cyst	Kunming	s.c.

Table 4: Summary of most effective protein vaccines (Loh et al., 2019)

1.9.1.3. DNA vaccines

The advantage of DNA vaccines is that it enables the expression of specific encoded antigen by host cells and thus inducing humoral and cellular immune responses (Hiszczyńska-Sawicka et al., 2014; Wolff & Budker, 2005). Moreover, DNA vaccines are relatively inexpensive, highly efficient, easy to produce and more importantly heat stable. Interestingly, DNA vaccines significantly elicit cellular immunity, which has been hard to provoke by protein vaccines (Hiszczyńska-Sawicka et al., 2014; Wolff & Budker, 2005). Since, *Toxoplasma* is an obligate intracellular parasite, cellular immune response is key to clear this parasite. Lately,

enormous antigen candidates were identified for DNA vaccines against toxoplasmosis (N.-Z. Zhang et al., 2015). A DNA vaccine construct encoding GRA14 antigen induced specific immune response and protected mice against acute toxoplasmosis from a lethal RH infection by enhancing the survival time BALB/c mice (Ahmadpour et al., 2017). SAG1 was used as a target by a DNA vaccine encoding SAG1 in combination with a gene sequence encoding a Toll-like receptor 5 agonist FliC of *Salmonella typhimurium*, to confer better protection. Yet, it slightly enhanced the survival of mice during acute toxoplasmosis upon infection with virulent RH strain (Maraghi et al., 2019). Additionally, a DNA vaccine expressing multi-epitopes of ROP8 along with IL-12 as genetic adjuvant, enhanced cellular immune response, lymphocyte proliferation and protected immunized mice against acute toxoplasmosis by enhancing survival of infected mice (Foroutan et al., 2020). Multiple studies clarified that multi-antigenic DNA vaccines provide an outstanding protection against toxoplasmosis when compared to immunity attained with single-antigenic DNA vaccines. In consequence, several recombinant DNA vaccines encoding *Tg*ROP5 and *Tg*ROP18 (Grzybowski et al., 2015), *Tg*ROP18 and *Tg*PLP1 (Y. Chen et al., 2018), *Tg*ROP5 and *Tg*GRA15 (J. Chen et al., 2015), *Tg*GRA1 and TgMIC3 (Gong et al., 2016), *Tg*SAG1 and *Tg*ROP2 (Sun et al., 2020), *Tg*PF, *Tg*ROP16, *Tg*ROP18, *Tg*MIC6, and *Tg*CDPK3 (N.-Z. Zhang et al., 2018) and many other cocktail DNA vaccines were established and tested *in vivo* (Rahimi et al., 2017). Furthermore, co-immunization generated stronger immunity and protection as compared to single-antigen vaccines. DNA vaccine encoding GRA17 and GRA23 elicited stronger specific cellular and humoral immune responses, with higher levels of Th1-type cytokines, and extended survival time in immunized BALB/c mice (Zhu et al., 2017). These findings demonstrate that co-immunization provides greater protective efficacy against toxoplasmosis. Table 5 summarizes some of the most efficient DNA vaccines. Predominantly, DNA vaccines exhibited effective immune responses and protection in small animals like mice and hamsters. However, immunity

induced in large animals like goats and sheep were less efficient. Hence, cytokines, novel adjuvants, and CpG are being integrated into DNA vaccines to strengthen the immune response and effectively protect against toxoplasmosis (Carvalho et al., 2010) .

No.	Types of Antigen	Antigen/Adjuvant/Delivery Approach	Immune Responses	Challenge Strain/ Amount	Protection	Mouse Strain	Immunisation Approach
1	Rhoptry proteins (ROP)	ROP38	higher ratio of IgG2a to IgG1; higher levels of IFN-γ and IL-2	PRU – 10 cysts	76.6% reduction in brain cysts	Kunming	Intramuscular (i.m.)
		ROP18 Expressed by recombinant canine adenovirus type-2	higher ratio of IgG2a to IgG1; higher levels of IFN-γ, IL-2 and IL-4	RH – 1×10^3 tachyzoites	40% protection in 60 days	Kunming	i.m.
		ROP16 Expressed by recombinant canine adenovirus type-2	predominance of IgG2a; higher levels of IFN-γ, IL-2, and TNF-α	RH – 1×10^3 tachyzoites	25% survival in 80 days	BALB/c	i.m.
2	Enzymes	Calcium dependent protein kinase (CDPK)1 Adjuvant - IL-21 and IL-15	predominance of IgG2a over IgG1; higher levels of IFN-γ and IL-2	PRU – 20 cysts	72.7%, reduction in cysts	Kunming	i.m.
		CDPK1 Adjuvant - IL-7 and IL-15	higher IgG2a/IgG1 ratio; higher levels of IFN-γ and IL-2	PRU – 10 cysts	73.5% reduction in cysts	Kunming	i.m.
		Nucleoside triphosphate hydrolase-II (TgNTPase-II) Using DNA-based alphaviral RNA replicon vectors	predominance of IgG2a; higher levels of IFN-γ, IL-2, IL-4 and IL-10	PRU – 20 cysts	71% reduction in brain cysts	BALB/c	i.m., electroporation
3	Rhomboid (ROM) proteins	ROM5 Adjuvant - emulsified in Freund's complete adjuvant	higher IgG2a to IgG1 ratio; higher levels of IFN-γ, IL-2 and IL-12	RH – $1X10^3$ tachyzoites PRU – 10 cysts	20% survival in 35 days 72.04% reduction in brain cysts	Kunming	i.m.
4	Surface antigen (SAG)	SAG5B and SAG5C	predominance of IgG2a over IgG1; higher level of IFN-γ	PRU-20 cysts	75% reduction in brain cyst	BALB/c	i.m.
5	Combination of different types of antigens	SAG3, ROP18, microneme protein (MIC)6, dense granule antigen (GRA)7, matrix antigen (MAG)1, bradyzoite specific antigen (BAG)1, sporozoite surface antigen (SPA) Expressed by recombinant adenovirus vaccine Adjuvant – ubiquitin	higher level of IgA; higher level of IL-2, IFN-γ, low level of IL-10	PRU – 20 cysts	78.6% reduction in brain cyst	BALB/c	Intranasal (i.n.)
		Perforin-like Protein (PLP)1 and ROP18 Adjuvant- IL-18	higher IgG2a to IgG1 ratio; higher levels of IFN-γ, IL-2, IL-12, IL-4, and IL-10	PRU- 20 cysts	72.4% reduction in brain cysts	Kunming	i.m.

Table 5: Summary of most effective DNA vaccines (Loh et al., 2019)

1.9.1.4. RNA vaccines

Unlike DNA vaccines, an advantage of RNA vaccines lies on their inability to integrate into the host chromosomes. Moreover, RNA can act as an adjuvant by inducing an immune response upon the activation of toll like receptor that recognize single stranded RNA (Heil et al. 2004). Yet, RNA vaccines can be quickly degraded by nucleases *in vivo* and need an intracellular delivery system. The use of mRNA replicons that was encapsulated and delivered without any adjuvant with a single dose (Chahal et al., 2016) was tested in the context of toxoplasmosis. This RNA vaccine conveys multiple replicons that encoded *T. gondii* GRA6, ROP2A, ROP18, SAG1, SAG2A, and AMA1. Immunized mice with a single dose of the mRNA replicon nanoparticle vaccine, induced 100% protection against acute toxoplasmosis after challenging with a lethal dose of the type II Pru strain. The example of this mRNA

replicon vaccine demonstrates that *T. gondii* vaccines are in continuous development and more time is needed for RNA vaccines to be put in use (Chahal et al., 2016).

1.9.1.5. Nanoparticle-Based Vaccines

A safer replacement for live-attenuated vaccines are recombinant subunit vaccines which contain one or several target antigens of the parasite, however they are of low immunogenicity and hence less efficient in eliciting a protective immune response (Hiszczyńska-Sawicka et al., 2014; Li & Zhou, 2018; N.-Z. Zhang et al., 2015). Lately, progress in nanomaterial engineering provided new approaches for developing novel vaccines (Fang & Zhang, 2016). Nanoparticles (NPs) are composed of virus-like particles, lipids, several polymers, metals or nonmetal inorganics and have a notable capacity as a delivery system. Encapsulation of the antigen within NPs, or covalently attaching it to the NPs, aids in protecting the antigen integrity from enzymatic degradation, improving the plausibility of antigen presentation to immune cells and extending time of systemic circulation (Diaz-Arévalo & Zeng, 2020; Fang & Zhang, 2016). Additionally, NP delivery system can transport antigens to the required targeted cells. For example, through NPs coupled with antibodies that recognize certain receptors on the surface of target cells, antigens can be directly delivered to specific cells such as DCs (Mintern et al., 2013). Another advantage of NPs is the utilization of lower doses of adjuvant and antigens, hence minimizing the possibility of side effects and toxicity (Skwarczynski et al., 2010). Some NPs are naturally immunogenic and can trigger an immune response without the use of adjuvants (Dacoba et al., 2017). NPs were used in vaccination against *Toxoplasma* and enhanced the elicitation of a potent immune response. For instance, a multiepitope recombinant vaccine containing predicted B and T cell expressed epitopes of ROP2, AMA1, SAG1, and GRA4 and encapsulated within a delivery vehicle of poly lactic-co-glycolic acid NPs was studied. Mice immunized with this vaccine possessed an enhanced Th1

immune response with a significant reduction in parasitic load which extended survival of mice by around 10 days after infected with *T. gondii* RH strain (Roozbehani et al., 2018). Moreover, mice immunized with cocktail DNA vaccines, holding GRA14 and ROM4 along with calcium phosphate nanoparticles (CaPNs), augmented immunity against acute toxoplasmosis and enhanced survival by few days (Rahimi et al., 2017). Whilst NP vaccines showed a higher protective efficacy compared to conventional subunit vaccines, yet it is less efficient than live-attenuated vaccines.

1.9.1.6. Exosome-Based Vaccines

Exosomes are membrane-bound vesicles of a size ranging between 30 nm to 200 nm in diameter and are liberated by fusion of multivesicular bodies with the plasma membrane of many eukaryotic cells (Théry et al., 2002). They constitute a mean of intercellular communication between cells, and play several functions including the establishment of immune homeostasis through transferring proteins, mRNA, and miRNA (Raposo & Stoorvogel, 2013). Notably, exosomes possess pathogen-derived antigens, and they constitute novel means for targeting infectious diseases (Coakley et al., 2015). Mice immunized with exosomes acquired from *T. gondii*-pulsed DCs elicited a protective T-cell immune response against congenital toxoplasmosis. Cysts were decreased by around 70% in the brain of pups (Beauvillain et al., 2009). Recent studies revealed that exosomes generated by *T. gondii* are able to protect immunized mice against acute toxoplasmosis by prolonging survival around 20 days through the induction of cellular and humoral responses (Li et al., 2018). As such, these studies highlight exosomes as potential vaccine delivery system in vaccines against toxoplasmosis.

1.9.1.7. Carbohydrate-Based Vaccines

In the context of toxoplasmosis, TLR-2 and TLR-4 of immune cells recognize *Toxoplasma* glycosylphosphatidylinositols (GPIs) leading to the induction of an inflammatory response and production of TNF-α (Debierre-Grockiego et al., 2007). Two major *T. gondii* GPI glycoforms were proposed as potential vaccine candidates against toxoplasmosis. However, immunized mice were not protected against challenge with a virulent RH strain. This was highly due to the fact that mice serum antibodies were directed to the linker which attach the carbohydrate to the carrier protein, rather than to the expected carbohydrate side-branch of the parasite GPI (Götze et al., 2015). Considering that some carbohydrate vaccines were successful in restraining diverse microbial infections, further assortment of more immunogenic carbohydrate antigens, may aid in the development of an efficient carbohydrate-based vaccine against toxoplasmosis.

1.9.1.8. AMA1 vaccines

Several studies stressed on AMA1 as a potential vaccine candidate in diverse apicomplexan diseases including malaria (Srinivasan et al., 2014, 2017), *Eimeria* caused-coccidiosis (Pastor-Fernández et al., 2018, 2020; X. Tang et al., 2019), babesiosis (AbouLaila, 2019), and more importantly, in toxoplasmosis (Beghetto et al., 2005; Dautu et al., 2007; M.-J. Kim et al., 2020; Roozbehani et al., 2018; Yu et al., 2012; T.-E. Zhang et al., 2015). A DNA vaccine encoding for a mixture of micronemal protein fragments (*Tg*MIC2a, *Tg*MIC2b, *Tg*MIC3, *Tg*MIC4, *Tg*M2AP, and *AMA1*) led to a significant decrease of brain cysts burden in around 85% of challenged mice (Beghetto et al., 2005). Another DNA vaccine encoding AMA1, *Tg*MIC2, *Tg*M2AP and *Tg*BAG1 showed that *AMA1* gene had greater efficiency in protection against toxoplasmosis (Dautu et al., 2007). A prime-boost vaccination strategy, using an *AMA1* plasmid and a recombinant adenovirus expressing AMA1 led to a partial

protection of mice against acute toxoplasmosis, with a 50% reduction in mortality (Yu et al., 2012). A mucosal multi-peptide vaccine of AMA1, RON2 and RON4 containing T-and B-cell epitopes administered by intranasal route, yielded a partial protection against a lethal type I RH strain of *T. gondii* in mice, with around 50% less mortality and 55% less parasite burden to the liver and to the brain (T.-E. Zhang et al., 2015). More recently, a multi-epitope peptide with selective MHC-binding capabilities, containing *Tg*GRA4, *Tg*ROP2, *Tg*SAG1 and *Tg*AMA1, and encapsulated in poly (lactic-co-glycolic acid) (PLGA) nanoparticles, conferred partial protection against acute toxoplasmosis through enhancing survival by around 10 days upon challenging with the virulent RH *T. gondii* strain (Roozbehani et al., 2018). Moreover, a virus-like particle vaccine containing AMA1 partially protected against acute toxoplasmosis in mice and led to 50% reduction in their brain cysts (M.-J. Kim et al., 2020). Interestingly, the interaction between AMA1 and RON2 positioned this complex as a promising vaccine candidate against *Plasmodium* (Srinivasan et al., 2014). This vaccine strategy was based on immunization with rAMA1 D1-D2-D3 domains, in complex with the fragment of RON2 that is deeply anchored into the AMA1 groove (Srinivasan et al., 2014). Strikingly, a complete protection of mice was obtained upon challenge with a lethal *Plasmodium yoelli* strain, only when immunization was performed with the complex AMA1-RON2. The un-complexed rAMA1 did not yield any protection. Extended to primates, this promising strategy showed that the AMA1-RON2 complex protects *Aotus* monkeys against a virulent *P. falciparum* infection, while vaccination with AMA1 alone could only confer a partial protection (Srinivasan et al., 2017). This approach had never been tested for toxoplasmosis. The x-ray crystal structures of *P. vivax* (Pizarro et al., 2005) , *P. falciparum* (Bai et al., 2005) and *T. gondii* AMA1 (Crawford et al., 2010) displayed polymorphic loops surrounding a conserved hydrophobic groove, which might be the target of the vaccination strategy used our study against toxoplasmosis.

1.9.2. Challenges for developing vaccines

Although numerous preclinical studies on *Toxoplasma* vaccine candidates has been assessed, none of those vaccines were effectively able to block transmission and eliminate tissue cysts. There are several factors that play a role in hindering the development of effective vaccines including the complex life cycle of *T. gondii*, strain variability, the ability of the parasite to evade the immune system, absence of standardized vaccine protocol and several others. *T. gondii* has three infectious stages; tachyzoites, bradyzoites and sporozoites. Every stage is characterized by their specific profile of protein expression (Z.-X. Wang et al., 2017). As such, developed vaccines that target certain epitopes or proteins of one stage can't protect against other stages. In addition, *T. gondii* strains are variant and divided into 6 major clades containing more than 16 haplo-groups with evident geographical distribution worldwide (Shwab et al., 2018; Su et al., 2012). Previous studies showed that genetically different strains may infect the same host proposing that immunization from a single strain is insufficient to cross protect against another (Dao et al., 2001; Jensen et al., 2015). Thus introducing multi-antigen vaccine could aid in cross talk immunity and protect against several stages of strains of the parasite (Onile et al., 2020).

Moreover, cross species difference makes it hard to translate vaccines that are protective in murine models to humans. For instance, a *T. gondii* protein profilin is recognized by the innate immune system in mice via TLR11 and TLR12 (Koblansky et al., 2013). In humans TLR12 is not expressed and TLR11 is a pseudogene (Yarovinsky, 2014). Thus, verified antigens that are protecting mice models may not be able to protect humans. Furthermore, the genetic background of mice model used can bias the outcome of the vaccination strategy. In mice, H-2 regions of the MHC complex determine the outcome of an immune response and hence the susceptibility to toxoplasmosis (Y Suzuki et al., 1991). H-2d

MHC haplotypes mice including outbred mice (NMRI strain) and inbred mice (BALB/c), were associated with less severe chronic infection. Whereas H-2 k (C3H/HeOuJ) or H-2b (C57BL/6) MHC haplotype mice were susceptible to chronic toxoplasmosis (D. Schlüter et al., 1991).

One of the complicated aspects of *T. gondii* is its ability to convert into a latent phase which allows its escape from the immune system (described in section 7), hence making it harder to target. Until now there is no defined protocol used in the vaccine studies and each with their drawbacks. As such, immunization of the livestock to reduce the amount of tissue cysts consumed, and cats to prevent the spread of oocysts in the environment is essential.

Most of the studies are using intraperitoneal injections rather than oral infection which is the main route of infection in humans. In addition, the used strains are usually type I (RH) and type II (76k, Me49, Pru) strains that have been passed in cell culture for several years and thereby lost their naïve origin. Furthermore, most studies focus on infection with tachyzoites and much fewer with the infective cyst and oocyst form using cat model. Hence, future vaccination strategies should challenge with naïve *T. gondii* strains by natural route of infection, using other animal models that are more relevant. In addition of targeting several *T. gondii* stages to induce protection against different forms of infection.

CHAPTER 2: MATERIALS AND METHODS

2.1. Parasite and cell culture

Tachyzoites were serially passaged in human foreskin fibroblasts (HFFs) (American Type Culture Collection (ATCC)-CRL 1634) cultured in Dulbecco's Modified Eagle's Medium (DMEM) (GIBCO, Invitrogen) and supplemented with 10% of fetal bovine serum (FBS), 1% penicillin-streptomycin, and 1% glutamine. Tachyzoites of *T. gondii* type I stains RH deleted for the *ku80* gene (RH *Δku80*), RH deleted for the *ku80* gene and *AMA1* gene (RH *KO-AMA1*) RH deleted for the *ku80* gene and *AMA4* gene (RH KO-AMA4), and type II strains (76K, Prugnaud (Pru), Pru deleted for *AMA4* gene (Pru KO-AMA4) were used throughout this study.

2.2. Generation of parasite lines

2.2.1. Knock out strategy

2.2.1.1. KO-AMA4 in RH*Δku80*

The generation of KO-AMA4 was performed in RH*Δku80* background using the disruption strategy (M. H. Lamarque et al., 2014). In more details, a pLIC-*KO-AMA4* plasmid containing the first 1300bp of the AMA4 coding sequence, three HA epitopes followed by a stop codon and the chloramphenicol acetyltransferase (CAT) resistance was used to truncate the *AMA4* wild type locus. After single homologous recombination, the pLIC-*KO-AMA4* plasmid is integrated yielding the truncated *AMA4* locus in the parasites. For transfection, $20x10^6$ freshly egressed RH*Δku80* tachyzoites were electroporated at 2.02 kV, 25µF, 50Ω to introduce the linearized pLIC-*KO-AMA4* plasmid using an Electro Cell Manipulator 630 (BTX). Mutant parasites were selected with 20µM of chloramphenicol for CAT integration. Clones were then isolated by limiting dilution and integration was verified by PCR using ML1648 and ML1863 primers to check the integration of the new veriosn of *AMA4* (disrupted) and ML1648 and ML1864 to check the absence of the wild type (Table 6, Figure 18*B*).

2.2.1.2. KO-AMA4 in Pru

The generation of KO-AMA4 was performed in Pru background using the CRISPR/*Cas9* strategy (Guérin, El Hajj, et al., 2017). The parasites were transfected with a DNA donor sequence and two pU6-Cas9-YFP vectors. The DNA donor sequence possesses a dihydrofolate reductase (DHFR) resistance cassette flanked by 30bp homology arms corresponding to *AMA4.* The pU6-Cas9-YFP vectors (guide RNA) contain a protospacer that targets 20bp before the start codon and 20bp downstream the stop codon of *AMA4* locus. Transfection was performed as described above. The mutant parasites were selected with 1µM pyrimethamine for DHFR integration. Integration was verified by PCR using ML3236 and ML2454 primers to check the integration of DHFR cassette at the 5' end, ML2602 and ML3237 to check the integration of of DHFR cassette at the 3' end and ML3403 and ML3404 to check the absence of the wild type *AMA4* locus (Table 6, Figure 18*D*).

Primer	Target	Description	Sequence
Generation of RH KO-AMA4			
ML1821	*AMA4* Locus	Forward to amplify first 1300bp of *AMA4* coding sequence	TACTTCCAATCCAATTTAATGCACGGTCACGAAAATCCTACAAGC
ML1822	*AMA4* Locus	Reverse to amplify first 1300bp of *AMA4* coding sequence	TCCTCCACTTCCAATTTTAGCGTTACCGCCACTTTTGTATGGC
ML1863	pLIC cassette	Reverse to verify integration of 1300bp of AMA4	CATTCGCAGACGGATCGTCT
ML1864	*AMA4* Locus	Reverse to verify integration of 1300bp of AMA4	CAGGGAAGTGAAGGCCATGC
ML1648	5' UTR of *AMA4*	Forward to verify integration of 1300bp of *AMA4* and WT loss	CTGGGGCCCCCAGTCGACACC
Generation of Pru KO-AMA4			
ML3232	5' gRNA	Forward	aagttGCTCTCAGCCGTCCAAAATGAg
ML3233	5' gRNA	Forward	aaaacTCATTTTGGACGGCTGAGAGCa

ML3230	3' gRNA	Forward	aagttGCCATTATTTGCACAGGGCTg
ML3231	3' gRNA	Reverse	aaaacAGCCCTGTGCAAATAATGGCa
ML3234	DHFR cassette	Forward to amplify cassette 30bp tail homology on AMA4 5'	TGGAGCGGTGTAACTAAACATCCTGTACCCAGATCCGATCTTGCTGCTG
ML3235	DHFR cassette	Reverse to amplify cassette 30bp tail homology onAMA4 3'	ATGTGTCTGCTTAGTCTTGCGAAGGCTGGCTGGCGGCCGCTCTAGAACTA
ML3236	5' UTR of *AMA4*	Forward to check 5' integration	CATCGGTCAAACTGCGCC
ML2454	DHFR cassette	Reverse to check 5' integration	ACGGGAGGCCGTTGTTGAT
ML2601	DHFR cassette	Forward to check 3' integration	ACCGAGACCGTTCCCCATT
ML3237	3' UTR of *AMA4*	Reverse to check 3' integration	GTCACACGGAAGCTAGAGTC
ML3403	WT locus	Forward	GTGCTGCTATGCTCGGCA
ML3404	WT locus	Reverse	CAGCGGCCAAGTAGATTGC

Table 6: List of primers used for the generarion of KO-AMA4 in RH*Δku80* and Pru backgrounds.

2.2.2. Tagging strategy

2.2.2.1. *RON4$_{L1}$-HA$_3$* tagging

Tagging of *RON4$_{L1}$* at the N-terminal was done in Pru strain using CRISPR/Cas9 strategy as described by Guerin *et al* in *RHΔku80* strain (Guérin, El Hajj, et al. 2017). Pru tachyzoites were transfected with a template that corresponds to a 442 bases pairs PCR product containing HA3 sequence. In addition to a protospacer sequence GACAATGCCGCCACGTGTGA that would recruit Cas9 to cut 21 bases pairs downstream the end of the signal sequence. The insertion of the HA3 Tag in Pru genome was verified by PCR using ML2059 and ML2060 primers (Table 7, Figure 14).

2.2.2.2. *AMA2-HA$_3$* tagging

Tagging of *AMA2* at the C-terminal was done in Pru strain using CRISPR/Cas9 strategy as described by Lamarque *et al* (M. H. Lamarque et al., 2014). The parasites were transfected with pU6-Cas9 containing gRNA that cleaves at the C-terminal end of *AMA2* to insert *HA$_3$* sequence using a DNA donor sequence. The DNA donor sequence possess 30 bp homology specific for the 3′ end of *ama2* fused with a *HA$_3$* sequence, a chloramphenicol selection cassette and 30pb of the 3'UTR downstream of the *ama2* generated in a pLIC-*HA$_3$-CAT* vector. The insertion of the *HA3* Tag in Pru genome was verified by PCR using ML887 and ML1476 primers (Table 7, Figure 17).

Primer	Target	Description	Sequence
Verification of RON4$_{L1}$-HA$_3$ tagging			
ML2059	5' UTR of *RON4$_{L1}$-HA$_3$*	Forward to check integration of *RON4$_{L1}$-HA$_3$* donor fragment	AAGTTGCTGAATTCGAC CAGCAGTTAG
ML2060	*HA$_3$* Locus	Reverse to check integration of *RON4$_{L1}$-HA$_3$* donor fragment	CAGCGTAGTCCGGGACG TCGTAC
Verification of AMA2-HA$_3$ tagging			
ML877	3' UTR of *AMA1*	Forward to check integration of *HA$_3$* sequence	GGCATTGCATATGGTGG GCT
ML1476	*HA$_3$* Locus	Reverse to check integration of *HA$_3$* sequence	CAGCGTAGTCCGGGACG TCGTAC

Table 7: List of primers used for the verification of *RON4$_{L1}$* and *AMA2 HA3* tagging in Pru background.

2.3. Immunofluorescence assay (IFA)

Immunofluorescence assay on HFF cells infected with intracellular tachzyoites, bradyzoite cysts or invading bradyzoites was conducted. Cells were fixed with 4% paraformaldehyde in PBS for 30 minutes followed by permeabilization with 0.2% Triton for 15 min. Following bradyzoites differentiation assay, coverslips of infected HFF with cysts were fixed with 4% paraformaldehyde in PBS for 30 minutes then permeabilized with 0.2% Triton for 15 min. Infected cells were later stained with the appropriate primary antibody listed below

followed by secondary antibody conjugated to Alexa Fluor (Table 8). Images were acquired using a Zeiss Axiocam MRm CCD camera driven at the 'Montpellier resources imagerie' facility and Zeiss LSM 710 confocal microscope (Zeiss, Oberkochen, Germany). All images were analyzed using Zeiss Zen software.

Antibody	Species	Dilution	Reference
Primary antibodies			
Anti-AMA1(anti-folded ectodomain I,II,III)	Rabbit	1:5000	(M. H. Lamarque et al., 2014)
Anti-AMA4	Rabbit	1:1000	(Parker et al., 2016)
Anti-AMA2	Mouse	1:200	Gift from Spano Furio
Anti-RON2-4	Rabbit	1:500	(Besteiro et al., 2009)
Anti-RON4	Mouse T5AH1	Undiluted hybridoma	(Leriche & Dubremetz, 1991)
Anti-RON5	Rat	1:200	(Besteiro et al., 2009)
Anti-RON8 rec2	Rat	1:200	(Besteiro et al., 2009)
Anti-RON2$_{L1}$	1:100	1:300	Gift from Spano Furio
DBA-FITC	-	1:300	Vector Laboratories
Anti-AMA1-RON2 (anti-complex)	Mouse	1:2000	this study
Anti-AMA4-RON2$_{L1}$ (anti-complex)	Mouse	1:2000	this study
Anti-AMA1	Mouse	1:2000	this study
Anti-AMA4	Mouse	1:2000	this study
Anti-HA	Mouse	1:300	Roche
Secondary antibodies			
Alexa fluor, green 488, Anti-mouse		1:4000	Invitrogen
Alexa fluor, green 488, Anti-rabbit		1:10000	Invitrogen
Alexa fluor, green 488, Anti-rat		1:200	Invitrogen
Alexa fluor, red 594, Anti-mouse		1:4000	Invitrogen
Alexa fluor, red 594, Anti-rabbit		1:4000	Invitrogen

Alexa fluor, red 594, Anti-rat	1:4000	Invitrogen

Table 8: List of antibodies used in IFA.

2.4. Western blot analysis

Pellets of freshly egressed tachyzoites or cysts following in vitro switch in HFF were lysed in 1x Laemmli buffer and proteins were separated on a 10% SDS PAGE (sodium dodecyl sulphate–polyacrylamide gel electrophoresis) and transferred to nitrocellulose membranes. Membranes were then probed with appropriate primary antibodies listed below (Table 9), followed by secondary antibodies conjugated to alkaline phosphatase. Bands were revealed with 5-bromo-4-chloro-3-indolyl phosphate/nitro blue tetrazolium (BCIP/NBT; Promega).

Antibody	Species	Dilution	Reference
Primary antibodies			
Anti-AMA1 (anti-unfolded ectodomain I,II,III)	Rabbit	1:2000	(M. H. Lamarque et al., 2014)
Anti-AMA4	Rabbit	1:1000	(Parker et al., 2016)
Anti-AMA1-RON2 (anti-complex)	Mouse	1:3000	this study
Anti-AMA4-RON2$_{L1}$ (anti-complex)	Mouse	1:3000	this study
Anti-AMA1	Mouse	1:3000	this study
Anti-AMA4	Mouse	1:3000	this study
Anti-actin	Mouse	1:10	Gift from Dominique Soldati
Anti-HA	Mouse	1:300	Roche
Secondary antibodies			
Anti-mouse AP		1:7500	Promega
Anti-rabbit AP		1:2500	Promega

Table 9: List of antibodies used in western blot analysis

2.5. *In vitro* bradyzoite differentiation assay

HFF cells were cultured on coverslips in a 24-well plate and infected with 1000 Pru tachyzoites in DMEM complete media. After 24h incubation under 37°C and 5% CO2 conditions, infected cells were cultured at 37°C in induction medium (RPMI 1640 without NaHCO3, 3% FBS, 50mM HEPES, adjusted at pH 8.2), but under ambient CO2 conditions (Weiss et al., 1995). In order to maintain the basic pH, medium was changed every other day. After 10 days, coverslips were fixed in 4% paraformaldehyde for immunofluorescence assay (IFA). Cells infected with cysts were harvested and lysed with 1x Laemmli buffer for western blot analysis.

2.6. Generation of individual proteins and complexes

2.6.1. Cloning and purification of individual proteins

The sequences encoding the mature ectoplasmic region of *AMA1* (amino acids 64 to 484, TGME49_255260 and AMA4 (amino acids 58 to 553, TGME49_294330 were synthesized and subcloned into a modified pAcGP67b vector (Pharmingen) with a C-terminal Tobacco Etch Virus (TEV) cleavage site and a hexa-histidine tag. AMA1 and AMA4 encoding virus for insect cell protein production was generated and amplified as described (Parker et al., 2016). 65-hr post-infection, the supernatant was harvested, concentrated, and proteins were purified by nickel-nitrilotriacetic acid (Ni-NTA) chromatography. The hexa-histidine tag was removed by TEV cleavage, and the protein was further purified by size exclusion chromatography (SEC) (Superdex 16/60 75) in HEPES buffered saline (HBS: 20 mM HEPES pH 7.5, 150 mM NaCl).

Sequences encoding a portion of *RON2*D3 (TGME49_300100; amino acids 1297 to 1333) and *RON2*D3L1 (TGME49_294400; amino acids 1292 to Ser1324) were synthesized and subcloned into a modified pET32a vector (Novagen) with an N-terminal hexa-histidine, a

thioredoxin (TRX) tag and a TEV cleavage site. The fusion proteins were produced in *Escherichia coli* (*E. coli*) BL21 cells and purified by Ni-NTA and SEC as described above.

2.6.2. Purification of the complexes

E. coli pellets expressing RON2D3 and $RON2_{L1}$ D3 TRX were thawed on ice, lysed in a French Press, and the insoluble material was removed by centrifugation. Purified, cleaved AMA1 and AMA4 were added directly to RON2D3 and $RON2_{L1}$D3 clarified cell lysate, respectively, and incubated at 4°C for 30 min. AMA1-RON2D3 and AMA4-$RON2D3_{L1}$ complexes were then purified using Ni-NTA pull down. Last, the TRX tag was removed after an overnight TEV cleavage, and the complexes were purified by SEC and analyzed by SDS-PAGE.

2.7. *In vivo* studies: Ethics statement

All mice protocols were approved by the Institutional Animal Care and Utilization Committee (IACUC) of the American University of Beirut (AUB) (Permit Number IACUC#19-02-RN464). Mice were housed in specific pathogen-free facilities and monitored on a daily basis. Humane endpoints were used according to AUB IACUC which follows the guidelines of the Association for Assessment and Accreditation of Laboratory Animal Care International (AAALAC) and guide of animal care use book (Guide, NRC 2011). Mice were sacrificed for any of the following reasons: 1) impaired mobility (the inability to reach food and water); 2) inability to remain upright; 3) clinical dehydration and/or prolonged decreased food intake; 4) weight loss of 15–20%; 5) self-mutilation; 6) lack of grooming behavior/rough/unkempt hair coat for more than 48 hours; 7) significant abdominal distension; 8) unconsciousness with no response to external stimuli. To verify acute toxoplasmosis, eye

pricks were performed following deep anesthesia with isoflurane, and sera of infected mice were collected. For sacrifice, mice were deeply anesthetized before cervical dislocation.

2.8. Brain cyst purification using Percoll gradient

C57BL/6 mice were sacrificed either 4 weeks post-infection intraperitoneally with 250 tachyzoites of the 76K, Pru or Pru KO-AMA4 strain, or oral challenged with 15 cysts of the same strains. Brains were harvested and cyst were purified for the Percoll gradient method as previously described (E. A. Watts, Dhara, and Sinai 2017). Briefly, every two brains were processed using a 100 μm cell strainer in 1xPBS. Afterwards, the homogenate were sheared with through a 16-G needle Luer-Lok syringe. The shearing process was repeated with 20-G and 23-G needles to completely release cysts from brain homogenate.

Brain homogenate was layered on top of the Percoll (GE Healthcare) gradient (90%, 40% and 20%). Following centrifugation at 1200 xg, the 40%-20% fraction containing the desired cysts was collected and diluted with 1X PBS. The cysts were washed frequently by centrifugation at 1500 xg. The final pellet was collected with Hanks' Balanced Salt Solution (HBSS) and cysts were enumerated using a hemocytometer.

2.9. Mice survival and burden of cysts in the brains of infected mice

To assess virulence during acute phase, eight- to ten-week-old female BALB/c mice (Jackson Laboratories) were intraperitoneally infected with 100 tachyzoites of type I RH*Δku80* or RH KO-AMA4 strains, or with 1000 tachyzoites of type II Pru *HX* or Pru *KOAMA4* strains (N=1, 5 mice per group). Seropositivity against *Toxoplasma* infection was systematically tested by immunoblotting of sera of infected mice against tachyzoites lysates. Mice were monitored on a daily basis throughout the course of infection.

To assess cyst burden during chronic toxoplasmosis, BALB/c mice were intraperitoneally injected with 250 tachyzoites of Pru or Pru KO-AMA4 strains (N=1, 10 mice per condition). One month post-infection, brain cysts were harvested as previously described (E. A. Watts, Dhara, and Sinai 2017). Cysts were enumerated using a hemocytometer. To further illustrate the role of AMA4 in in invasion, BALB/c mice were orally infected with 15 cysts of Pru or Pru KO-AMA4 strains (N=1, 10 mice per condition). Cyst load was addressed one month after infection with cysts as described above.

2.10. Immunization study

Five to six weeks old female C57BL/6 mice were divided into two groups, a control group receiving only Freund's adjuvant and an immunized group receiving the adjuvant along with one of the complexes (rAMA1-RON2D3 or rAMA4-RON2$_{L1}$D3), or one of the peptides (rAMA1 or rAMA4). 40 µg of the complexes or peptides were added to 50 µl of PBS, then emulsified with an equal volume of adjuvant. The control mice group received 50 µL of PBS emulsified with 50 µL of adjuvant. For mice receiving the two complexes together, mice were injected in separate site with 40 µg of rAMA1-RON2D3 and 40 µg of rAMA4-RON2$_{L1}$D3.

Mice were immunized subcutaneously three times, at a two-week interval between injections. The first immunization was performed in Freund's complete adjuvant, followed by two injections in Freund's incomplete adjuvant (Timeline, Figure 21 and Figure 22).

To check the protection against acute toxoplasmosis following immunization with the complexes or peptides, mice were challenged intraperitoneally (IP), two weeks after the last immunization, with a lethal dose of 1000 Pru tachyzoites, and their mortality was monitored for one month (N=2, 7 mice per group) .

To assess the protection against chronic toxoplasmosis, following immunization with the complexes or peptides, mice were challenged with 15 cysts of the type II 76K strain, by

oral route of infection (gavage), two weeks post-immunization. Mice were allowed to establish the chronic phase for one month after challenge (E. A. Watts et al., 2017), then cyst extraction from brains was performed using the Percoll gradient method as previously described (N=1, 10 mice per group).

2.11. Bradyzoite isolation and invasion assay

Bradyzoites were released from cysts by incubating the cyst solution with pepsin /HCl (pH= 2) in a final concentration of 0.05%, for 37 C for 15 minutes. Pepsin was then neutralized by adding complete DMEM (Gibco) supplemented with 10% FBS, 1 mM Glutamine and 1 mM Penicillin/Streptomycin and centrifuged for 15 minutes, at room temperature, 2200 RPM (Popiel et al., 1996). Released bradyzoites were then washed with 1X PBS and resuspended in the necessary amount of complete DMEM to proceed with intended experiments.

Confluent human foreskin fibroblasts (HFF) on coverslips were put on ice and infected with $2x10^6$ freshly isolated bradyzoites in 300 µl of medium. Parasites were allowed to settle for 20 minutes with the plate on ice. The plate was then moved to a water bath at 38°C where it was kept for 2, 3 or 10 minutes to allow invasion. After invasion, cells were immediately fixed with 4% PFA in PBS and immunofluorescence assay (IFA) was conducted.

2.12. Invasion Inhibition Assay and e-vacuoles quantification

For invasion assay, $5x10^6$ Pru or Pru KO-AMA4 tachyzoites were incubated on coverslips seeded with confluent HFF cells, in a 24 well plate on ice for 20 min. The plate was later placed in a water bath at 38.5°C to allow the parasites to invade for 5 min. IFA was later performed on 4% paraformaldehyde -fixed parasites .

For invasion inhibition assay, total IgG was purified from sera of mice immunized with rAMA1 or rAMA4 peptides, rAMA1-RON2D3 or rAMA4-RON2$_{L1}$D3 complexes, using

protein G agarose beads (GE Health Sciences) and dialyzed against RPMI 1640 medium. $5x10^6$ tachyzoites of Type *I T. gondii* (RH*Δku80* or RH *KO-AMA1*) were incubated with 0.5, 1 or 2 mg/ml of total IgG for 30 min at 37°C. Subsequently, an invasion assay was performed.

Following the invasion inhibition assay, coverslips of cells were fixed with 4% paraformaldehyde in HBSS for 30 min. Coverslips were then blocked with 10% FBS in HBSS. Mouse anti-SAG1 (Mab T4 1ES, 1/2000) antibody (Couvreur et al., 1988) was used to stain the extracellular parasites. After 2h, permeabilization was performed using 0.2% saponin for 10 min and coverslips were blocked again for 30 min with 10% FBS in HBSS. Rabbit anti-ROP1 (1/3000) antibody (M. H. Lamarque et al., 2014) was used to stain intracellular parasites. Intracellular parasites and e-vacuoles were counted using Zeiss Axioimager epifluorescence microscope. The experiment was done three independent times and 20 fields were counted on each coverslip.

2.13. Plaque assay

For plaque assays, confluent HFF cells in 24-well plates were infected with ≈50 synchronized Pru or Pru KO-AMA4 tachyzoites per well and incubated for 7 days at 37°C. They were then fixed with cold methanol for 10 min and stained with Giemsa. Images were obtained usign Olympus MVX10 macro zoom microscope equipped with an Olympus XC50 camera. Plaque area measurements were analyzed using Zeiss Zen software (M. H. Lamarque et al., 2014).

For bradyzoite inhibition assay, HFF cells were cultured in a 6-well plates and infected with 1000 76K tachyzoites in DMEM complete media. After 24h incubation under 37°C and 5% CO^2 conditions, infected cells were cultured at 37°C in induction medium without CO^2, as described above. After 10 days, cells infected with cysts were harvested and lysed by pepsin as illustrated previously. Released 76K braydzoites were enumerated using a hemocytometer.

After which, confluent HFFs monolayers in 24-well plates were infected with ≈500 bradyzoites in DMEM complete media along with 1mg/ml of control, anti-rAMA1, anti-rAMA1-RON2D3, anti-rAMA4 or anti-rAMA4-RON2$_{L1}$D3 IgG for 10 days at 37°C. They were then fixed and images were analyzed as illustrated above.

2.14. ELISA (Enzyme-linked Immunosorbent Assay)

Sera was collected from non-immunized control or from immunized mice with rAMA1, rAMA1-RON2D3, rAMA4 or rAMA4-RON2$_{L1}$D3 two weeks after the last immunization. Total IgG was assessed using an ELISA protocol as previously described in Malkin et al (Malkin et al., 2005). 96-well plates were coated with 100 µl/well of either complexes (rAMA1-RON2D3 or rAMA4-RON2$_{L1}$D3) or with single peptides (rAMA1 or rAMA4) peptides at the concentration of 1 µg/ml, diluted in coating buffer (15mM sodium carbonate, 35mM sodium bicarbonate). After an overnight incubation at 4°C, plates were blocked with 5% skimmed milk in Tris-Buffered Saline (TBS) for 2h at room temperature (RT). Sera from respective mice were diluted at 1:5000 in dilution buffer (0.1% BSA, 0.05% Tween-20 in TBS), added (100 µl/well) to detect total IgG, 1:8000 for IgG2a or 1:50000 for IgG1, and incubated for 2h at RT. Following extensive washing in TBS-0.1% Tween-20, plates were incubated with 100 µl/well of anti-mouse IgG antibody conjugated with peroxidase (Sigma), anti-mouse IgG1 antibody conjugated with peroxidase (Sigma), or anti-mouse IgG2a antibody conjugated with peroxidase (Sigma) for 2h at RT. After similar washing, peroxidase substrate 3, 3′,5,5′-Tetramethylbenzidine (Sigma) was added for 20 min and the reaction was stopped by 2M HCl. The optical density was read at 450 nm using an ELISA reader (Multiskan EX).

2.15. Statistical Analysis

All results are presented as mean value with standard deviation. All in vivo experiments, ELISA and invasion inhibition assay were analyzed using two-tailed Student's t-tests to determine the statistical significance. For in vivo survival experiments, statistical significance was determined by Log-rank test using GraphPad. Statistical significance is indicated as * for p-value < 0.05, ** for p-value < 0.01, and *** for p-value < 0.001.

CHAPTER 3: RESULTS

The bradyzoite is the stage that initiates an infection by consummation of uncooked meat and is the causative agent of latent toxoplasmosis. This chronic phase of the infection associates with several disorders in immunocompetent patients and may evolve into fatality in immunocompromised individuals. As invasion is essential for the successful propagation and persistence of the disease, we focused on the characterization and targeting of this key step in *T. gondii* life cycle, particularly on the MJ and its molecular components. Whilst the MJ formation and molecular composition has been extensively characterized in tachyzoites, the MJ in other parasitic stages was poorly tackled. In particular, only a single report addressed the invasion of bradyzoites using electron microscopy, yet the study was not conclusive. Herein, we focused on whether bradyzoites use an MJ to invade, and if yes, what would be the molecular players of their invasion.

To date, there are no gold-standard treatment for chronic toxoplasmosis and no licensed vaccine available for humans. In the second part of the thesis, we explored the potential vaccination against invasion complexes, expressed in either tachyzoite or bradyzoite stages. We also focused on the invasion inhibitory effect of antibodies produced by the vaccines, to reveal the potential mechanism by which protection against toxoplasmosis was conferred, and to further straighten our conclusions on the molecular components of the MJs involved in invasion of tachyzoites and bradyzoites.

Our results were designed to tackle two main aims:

Aim I: Deciphering the invasion process and molecular players in bradyzoites

Aim II. Vaccination using AMA-RON MJ complexes

The Results presented below are part of a collaborative work.

The contributions of each of the authors is defined in the text and the legends of corresponding figures.

The results' section will be followed by a general discussion and will then open up on the perspectives of the work.

Part I: Deciphering the invasion process and molecular players in bradyzoites

3.1.1. Moving Junction proteins are expressed in bradyzoites

One of the earliest steps of infection following oral ingestion of undercooked or raw infected meat by humans or other intermediate hosts, is the entry of bradyzoites into intestinal cells. Our knowledge of the invasion of bradyzoites remains rudimentary. To better understand the molecular mechanisms of bradyzoites invasion, we first investigated whether the MJ proteins, well characterized in tachyzoites, were also expressed in bradyzoites. Indeed, *in vivo* transcriptome analysis of *T. gondii* stages during acute and chronic infection, predicted that RON2, RON4, RON4$_{L1}$, RON5, RON8 and AMA1 proteins are all expressed in the bradyzoite stages (Figure 12) (Pittman et al., 2014).

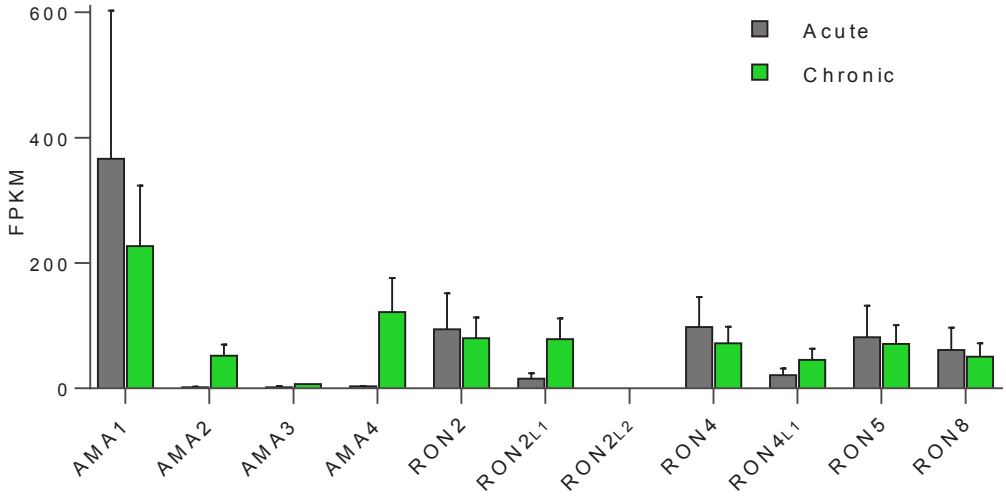


Figure 12: *In vivo* transcriptome analysis of *T. gondii* during acute and chronic infection. Prediction of *T. gondii RON2*, *RON2$_{L1}$*, *RON2$_{L2}$*, *RON4*, *RON4$_{L1}$*, *RON5*, *RON8*, *AMA1*, *AMA2* and *AMA4* genes expression during acute and chronic infection (Pittman et al., 2014).

To corroborate these results, we performed IFAs using anti-AMA1 and anti-RON2, anti-RON4, anti-RON5 and anti-RON8 antibodies on differentiated bradyzoites *in vitro* using the kystogenic strain Pru. Briefly, HFF were infected with tachyzoites of the type II Pru strain. 24h post-infection (p.i.), alkaline medium with low-serum and a subsequent culture at ambient CO_2 pressure were used to induce bradyzoite differentiation, as previously described (Silva et

al., 1998; Weiss et al., 1995). 10 days p.i., monolayers were fixed and stained using the fluorescein-labeled *Dolichos biflorus* agglutinin (DBA), which specifically binds the wall of cyst containing bradyzoites (Fux et al., 2007). Consistent with the transcriptomic data, we showed that *T. gondii* AMA1, RON2, RON4, RON5 and RON8 are all well expressed in the bradyzoite stage (Fig. 13A).

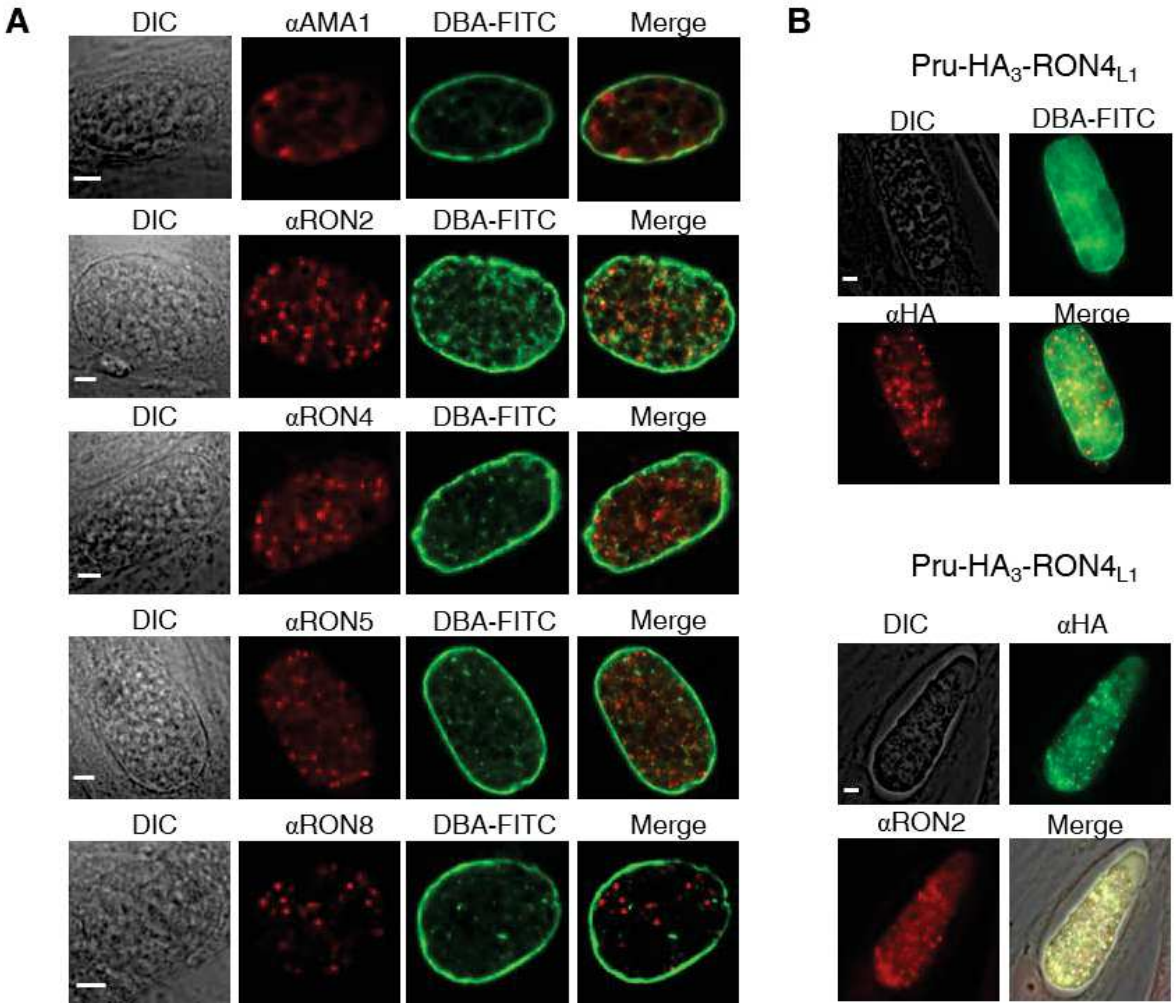


Figure 13: Expression of AMA1, RON2, RON4, RON5, RON8 and RON4$_{L1}$ in the bradyzoite stage. (A) IFAs Pru bradyzoite cysts following induction of conversion *in vitro*, and using anti-AMA1, anti-RON2, anti-RON4, anti-RON5, anti-RON8 (red) antibodies; (B) Staining of HA3-RON4$_{L1}$ with anti-HA antibodies (red), and cyst wall with DBA-FITC (green) (Upper Panel). Colocalization of RON4$_{L1}$ (green) with RON2 (red) (Lower panel). DIC: Differential Interference Contrast. Scale bars, 5μm.

Since we did not have specific sera for RON4$_{L1}$, we epitope tagged the endogenous locus of RON4$_{L1}$ at the N-terminus after the signal sequence, with three copies of the HA tag (3×HA) in the Pru strain, using CRISPR/Cas9, as previously described for tagging RON4$_{L1}$ in type I RH strain (Guérin, El Hajj, et al., 2017) (Figure 14*A*). The correct integration of the sequence encoding for HA epitope was verified by PCR (Figure 14*B*) and the expression of the protein in tachyzoite was verified using both IFA and western blot (Figure 14*C* and Figure 14*D*). To check the expression of RON4$_{L1}$ in bradyzoites, we followed the same *in vitro* approach described above and demonstrated that this protein is also expressed in bradyzoites. Moreover, this protein colocalized with RON2 (Figure 13*B*).

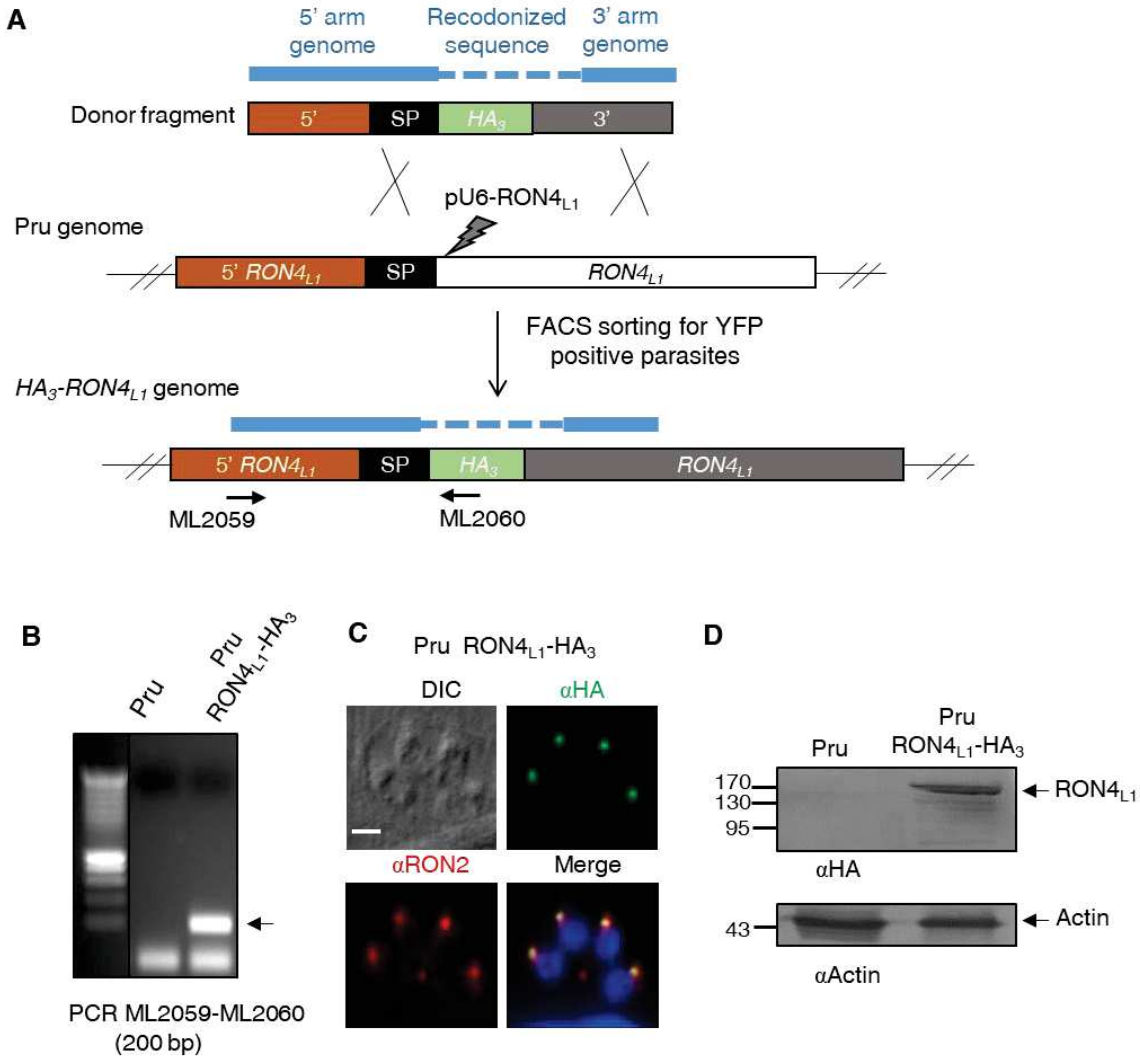


Figure 14: Tagging of the rhoptry neck protein RON4$_{L1}$ at its N-terminal end. (A) Schematic representation illustrating the approach used to endogenously tag RON4$_{L1}$ at its N-

terminus end, in the Pru background using CRISPR/Cas9 nuclease mediated gene recombination strategy. Pru parasites were transfected with cas9-yfp-*RON4$_{L1}$* gRNA expression plasmid (pU6-*RON4$_{L1}$* Tag) and a linear 442 bp donor DNA fragment containing *RON4$_{L1}$* homology regions to introduce a HA_3-tag by double homologous recombination. YFP-positive parasites were sorted by FACS. (B) Verification of HA_3-tag integration at the 5′end of *RON4$_{L1}$* coding sequence by PCR, using ML2059 and ML2060 primers. (C) IFA on intracellular tachyzoites Pru *HA$_3$-RON4$_{L1}$* parasites using anti-HA and anti-RON2 antibodies. Scale bar, 4µm. (D) Western blot Pru and Pru *HA$_3$-RON4$_{L1}$* tachyzoites using anti-HA antibodies. Dictyostelium actin recognizing *T. gondii* actin was used as loading control.

3.1.2. Bradyzoites invade in a moving junction-dependent fashion

A single study addressed the invasion of bradyzoites by electron microscopy and suggested that these stages invade in a MJ-independent manner, yet the results were not conclusive (Sasono & Smith, 1998). Our demonstration that MJ RON proteins were present in bradyzoites prompted us to test for the MJ formation upon bradyzoite invasion by IFA. To avoid any potential discrepancy between the MJ of reminiscent tachyzoites following *in vitro* switch, and differentiated bradyzoites upon invasion, we opted to study the MJ of invading bradyzoites using freshly harvested cysts from brains of infected mice. In more details, cysts were purified from the brain of mice infected with the 76K strain. Bradyzoites were collected after cyst digestion with pepsin as previously described (Popiel et al., 1996). One million of bradyzoites were allowed to invade HFF cells, fixed and then stained for the respective MJ proteins. Remarkably, a typical MJ-ring staining was observed using anti-RON2, anti-RON4, anti-RON5, anti-RON8 antibodies and anti-HA_3 antibody for Pru $RON4_{L1}$-HA_3 tagged bradyzoites (Figure 15*A*).

It was previously documented that visualization of AMA1 at the MJ of invading tachyzoites is hard (Alexander et al., 2005; M. Lamarque et al., 2011). We recently noticed while using a new batch of rabbit anti-AMA1 antibodies, directed against domains D1-D2-D3 of this protein, that AMA1 is systematically associated with the residual MJ of newly invaded tachyzoites (Figure 15*B*, left panel). Using the same batch of antibodies, we detected a faint

residual dot in invaded bradyzoites (Figure 15*B*, right panel). It is important to stress that AMA1 seems to be more abundant in tachyzoites than in bradyzoites. This was illustrated by the higher signal of anti-AMA1 in the un-secreted micronemal bulk of invading tachyzoite (Figure 15*B*, left panel) as compared to that of invading bradyzoite (Figure 15*B*, right panel). Interestingly when the bradyzoites are intracellular, RON2 and RON5 (Figure 15*C* and 15*D*) staining sometimes appears like a trail at the posterior end that evokes the trails observed at the posterior ends of invading sporozoites (Tartarelli et al., 2020). These trails varied in length and are always characterized by a straight line, marked by a more intense fluorescent dot at the end. They are also more frequently observed with immunofluorescence performed after 10 (Figure 15*C*)or 30min (Figure 15*D*) post-invasion, whereby tails observed at 30 min are longer than that observed at 10 min. This observation is absent in tachyzoites and might suggest a possible cell traversal mechanism as proposed for sporozoites (Tartarelli et al., 2020).

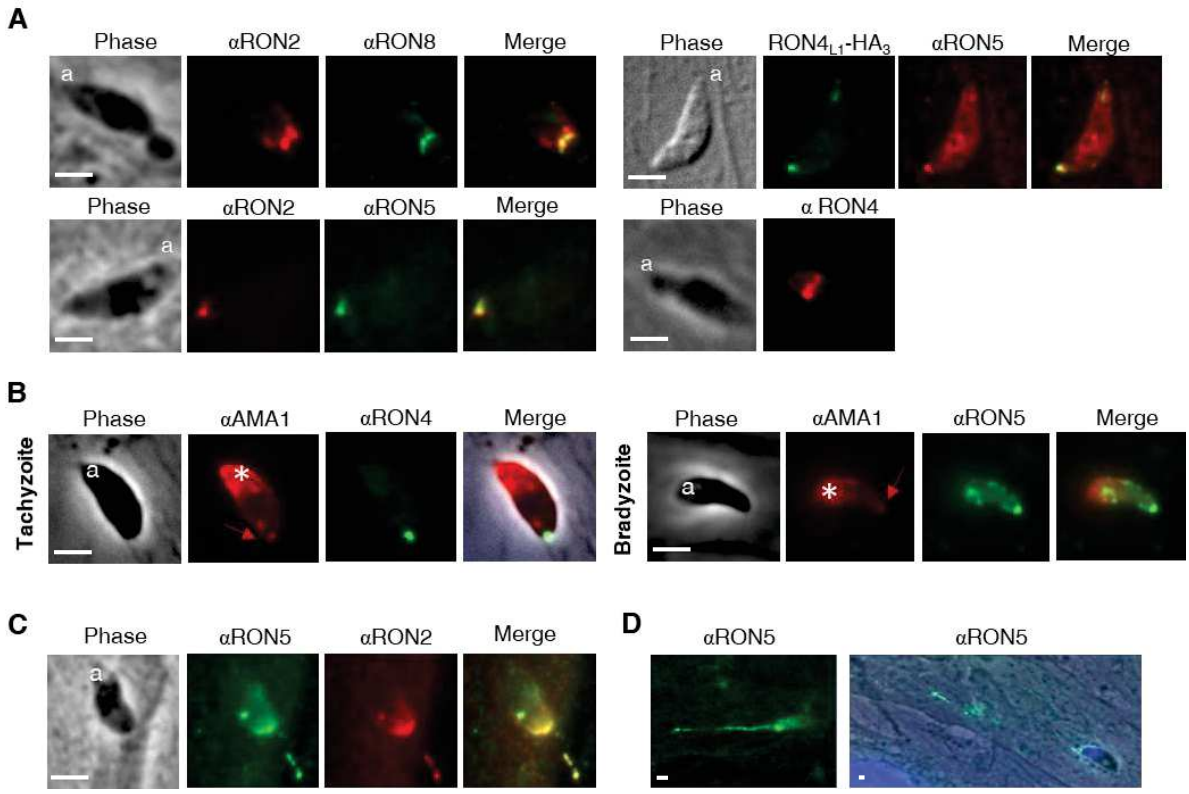


Figure 15: Localization of AMA1, RON2, RON4, RON5, RON8, and RON4$_{L1}$ at the moving junction of invading bradyzoites. (A) IFAs on Pru bradyzoites invading HFF monolayer using anti-RON2 (red), anti-RON4 (red), anti-RON5 (green) and anti-RON8 (green). For IFA of RON4$_{L1}$, bradyzoites are extracted from the brains of mice infected with the Pru *RON4$_{L1}$-HA$_3$* tagged line and RON4$_{L1}$ revealed with anti-HA$_3$ antibody for. (B) Left panel: IFAs on newly invaded RH tachyzoites in HFF monolayer using anti-AMA1 (red) and anti-RON4 (green) antibodies. Right panel: IFAs on newly invaded Pru bradyzoites in HFF monolayer using anti-AMA1 (red) and anti-RON4 (green) antibodies (C) IFAs on Pru bradyzoites after 10 min invasion in HFF monolayer using anti-RON5 (green), and anti-RON2 (red) antibodies. a: apical end of invading bradyzoites. (D) IFAs on Pru bradyzoites after 30 min invasion in HFF monlayer using anti-RON5 (green). Scale bars, 2µm.
*: bulk of un-secreted micronemes. IFAs were performed by Margarida Ruivo.

3.1.3. AMA2, AMA4 and RON2$_{L1}$ are up-regulated in the bradyzoite stage and AMA2 and AMA4 decorate the moving junction of invading bradyzoites

We next investigated if alternative AMA-RON complexes are present in bradyzoites. Proteomic and transcriptomic analyses of acute, early and late-chronic *T. gondii* infection indicated stage specific increase of transcription of AMA4, its partner RON2$_{L1}$ and AMA2 in bradyzoites (Figure 12). An alternative isoform of AMA3 (sporoAMA1) is also predicted to be expressed only during late-chronic infection (Garfoot et al., 2019). Since it would generate a non-invasive truncated AMA3 version and that there are almost no transcript corresponding to its partner RON2$_{L2}$ (sporoRON2), we focused our analysis on AMA4, RON2$_{L1}$ and AMA2. Using specific antibodies against AMA4 and RON2$_{L1}$ proteins, we showed that they are well expressed in bradyzoites (Figure 16*A*). We endogenously tagged AMA2 at the C-terminal end, with a triple haemagluttinin epitope (3×HA) in the Pru strain, using CRISPR/*Cas9* (Figure 17*A*). Correct integration of the sequence encoding for HA epitope was verified by PCR (Figure 17*B*) and expression of the protein in tachyzoite and bradyzoite was verified by western blot (Figure 17*C*). We concluded that AMA2 is also highly expressed in bradyzoites (Figure 16*A*).

A faint staining of AMA4 in the micronemes of invaded tachyzoites was detected (Figure 16*D*, right panel) as compared to the strong signal in bradyzoite (Figure 16*D*, left panel). This

further confirms the low expression of AMA4 in tachyzoites. Strikingly, anti-AMA4 antibodies labelled the MJ of invading bradyzoites (Figure 16*B,* upper panel), while we could not depict any MJ staining in the tachyzoite stage (Figure 16*D*, right panel). Indeed, we could only obtain one suggestive picture of the presence of AMA4 at the MJ, when the bradyzoite is half-way through the invasion process (Figure 16*B*, upper panel). However, we frequently detected AMA4 at the residual dot of the MJ, and only when the parasite is completely intracellular (Figure 16*B*, middle panel). This is reminiscent to the staining of AMA1 in tachyzoites, which we could not visualize at the MJ during the invasion process, but appears systematically as a strong posterior dot of newly invaded parasites (Figure 15*B*, left panel). In some parasites, AMA4 appears also as a trail, dragging behind newly invaded bradyzoites (Figure 16*B*, lower panel), and this trail colocalized with RONs.

We also checked if $RON2_{L1}$ and AMA2 were present at the MJ. We did not detect $RON2_{L1}$ using specific antibodies, but AMA2 nicely decorated the MJ during the invasion of AMA2-HA_3 tagged bradyzoites (Figure 16*C*, upper panel). AMA2 was also detected at the residual dot of the MJ in invaded bradyzoites (Figure 16*C*, middle panel). Moreover, trails of AMA2 were also observed behind newly invading parasites (Figure 16*C*, lower panel).

Altogether, these results show that bradyzoites form a MJ during invasion, but yet, with a different molecular composition from that of invading tachyzoites.

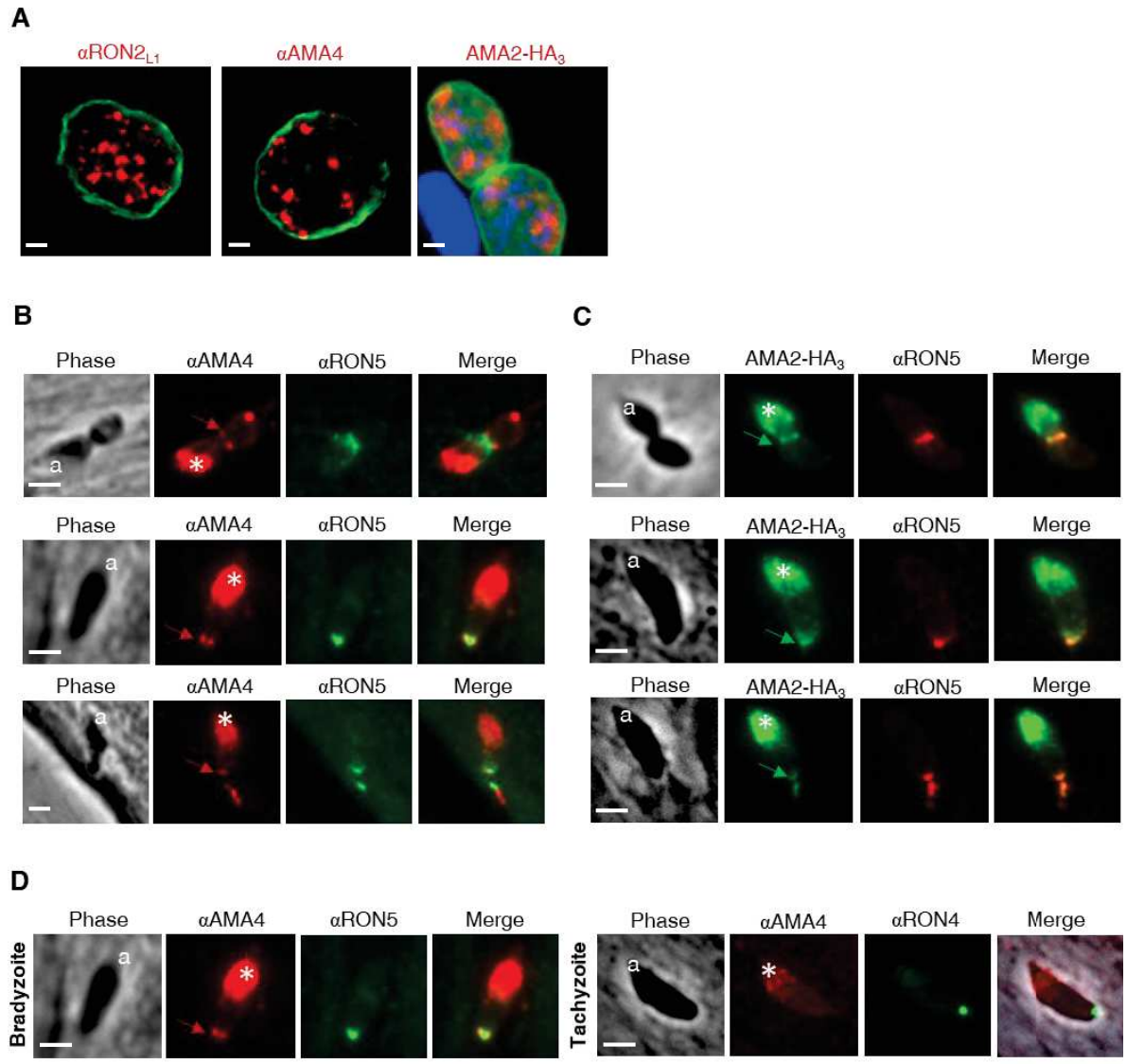


Figure 16: Expression of alternative *Tg*AMA-*Tg*RON complex in bradyzoites. (A) IFAs on *in vitro* converted Pru cysts using anti-RON2$_{L1}$, anti-AMA4, and anti-HA antibodies. anti-HA (red) antibodies are used for staining of AMA2-HA$_3$. Cyst wall was stained using DBA-FITC (green). Scale bars, 5µm. (B) IFAs on Pru bradyzoites invading HFF monolayer using anti-AMA4 (red), and anti-RON5 (green) antibodies. Upper panel corresponds to mid-invasion with AMA4 and RON5 stained MJ, middle panel refers to invaded bradyzoite with residual MJ dot, and lower panel corresponds to AMA4 trails with RON5 at the posterior end of invaded bradyzoites. (C) IFAs on Pru bradyzoites invading HFF monolayer using anti-AMA2 (green), and anti-RON5 (red) antibodies. Upper panel corresponds to mid-invasion with AMA2 and RON5 stained MJ, middle panel refers to invaded bradyzoite with residual MJ dot, and lower panel corresponds to AMA2 trails with RON5 at the posterior end of invaded bradyzoites. (D) Left panel: IFAs on newly invaded Pru bradyzoites in HFF monolayer using anti-AMA4 (red) and anti-RON4 (green) antibodies. Right panel: IFAs on newly invaded RH*HX* tachyzoites in HFF monolayer using anti-AMA4 (red) and anti-RON4 (green) antibodies. a: apical end of invading bradyzoites. *: bulk of un-secreted micronemes.(B-D) Scale bars, 2µm.

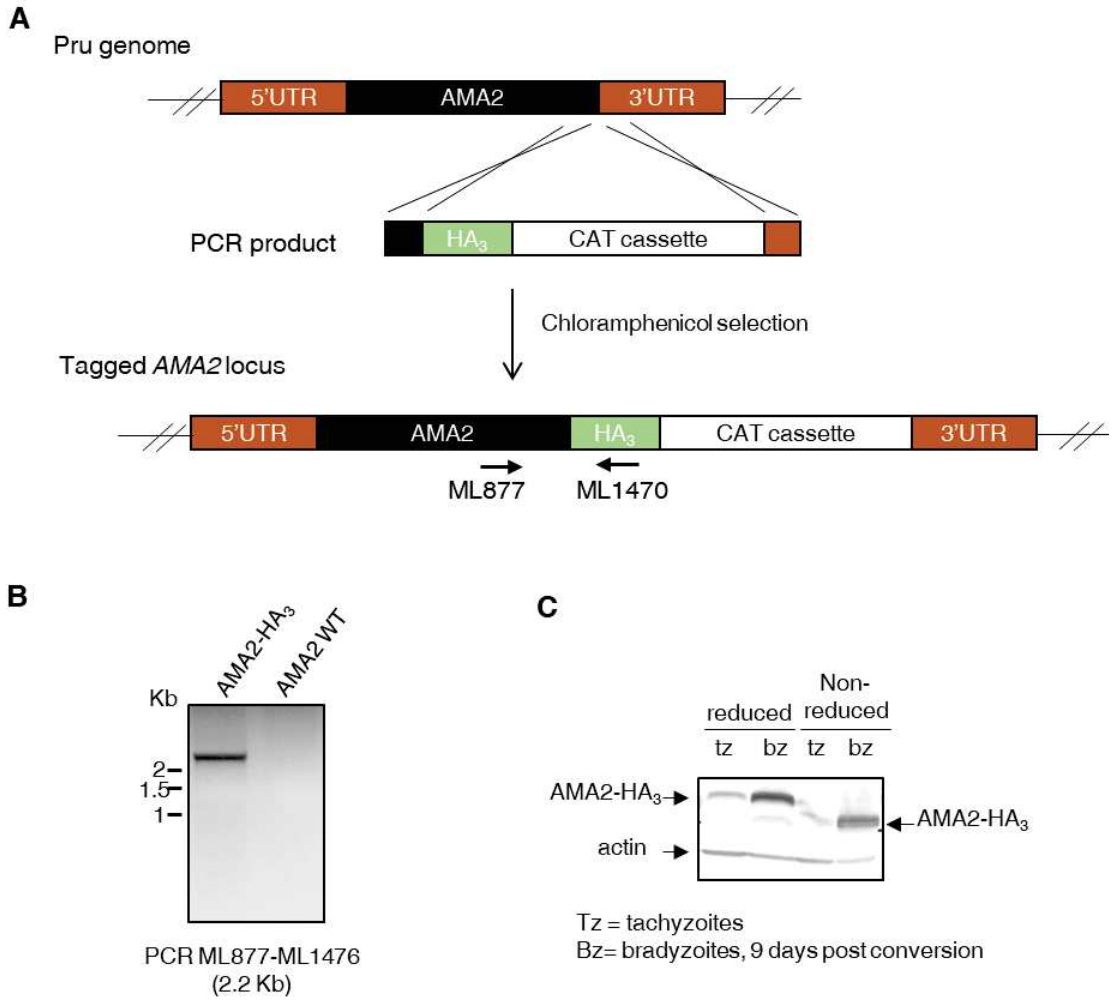


Figure 17: Tagging of the microneme protein AMA2 **at the C-terminal end. (A)** Schematic illustration of the approach used to endogenously tag AMA2 at its C-terminus end in the Pru background using CRISPR/*cas9* nuclease mediated gene recombination strategy. Pru parasites were transfected with pU6-Cas9-*AMA2* CtTag and a donor DNA sequence containing 30 bp homology specific for the 3′ end of *AMA2* in fusion with a sequence encoding for HA_3 sequence, a chloramphenicol selection cassette and 30pb of the 3'UTR downstream of the *ama2* gene to introduce HA_3-tag. Stable transformants were selected with chloramphenicol and clones were isolated by limiting dilution. (B) Verification of HA_3-tag sequence integration at the 3′end of *AMA2* coding sequence with PCR using primers ML877 and ML1476 for 3' integration. (C) Western blot of Pru and AMA2-HA_3 strains using anti-HA antibodies in tachyzoites and bradyzoites. Dictyostelium actin recognizing *T. gondii* actin was used as loading control. The AMA2-HA3 line has been generated by Margarida Ruivo.

3.1.4. AMA4 plays a role in invasion and establishment of chronic infection

AMA4 is expressed in all different developmental stages of *T. gondii*. It exhibits a low expression in tachyzoites but its expression is high in sporozoites (M. H. Lamarque et al., 2014) and bradyzoites (Figure 16). To address the role of AMA4 in tachyzoites, we first generated a knock out strain of AMA4 in a type I RH *Δku80* background (RH KO-AMA4). Gene disruption strategy by single homologous recombination was performed and was similar to the strategy used to generate the RH *KO-AMA1* (M. H. Lamarque et al., 2014) (Figure 18*A*). Gene disruption was verified by PCR (Figure 18*B*). In contrast to RH KO-AMA1 (M. H. Lamarque et al., 2014), removal of *AMA4* locus was easily obtained. Moreover, no signs of adaptation were observed during sustained passages, showing that AMA4 is not essential for the tachyzoites. We then assessed the effect of long-term depletion of AMA4 by evaluating the viability of the parasites on plaque assay. Tachyzoites of the RH KO-AMA4 strain generated less lysis plaques as compared to control parasites, and these plaques were significantly smaller, clearly indicating an invasion defect (Figure 19*A*). This result was further confirmed using invasion assay whereby, invasion of tachyzoites of the RH KO-AMA4 was significantly disrupted by around 20% as compared to the wild type parasites (Figure 19*B*). This defective invasion phenotype prompted us to examine the virulence of RH KO-AMA4 parasites in BALB/c mice. Mice were infected with 100 tachyzoites of either the RH*Δku80* or the RH KO-AMA4 strains, by intraperitoneal injection, and monitored through the course of acute phase. Of note, 100 tachyzoites is a lethal dose for type I RH*Δku80* strain. Our results showed that, mice infected with RH *Δku80* or RH KO-AMA4 succumbed to infection within 8 days. Although, RH KO-AMA4 tachyzoites had an invasion defect *in vitro*, yet the mutant parasites still possess the same virulence as the wild type strain *in vivo* (Fig. 19*C*). This may imply that the virulent RH *Δku80* strain is not affected by this small defect in invasion, and AMA1-RON2 MJ is mainly utilized at this stage.

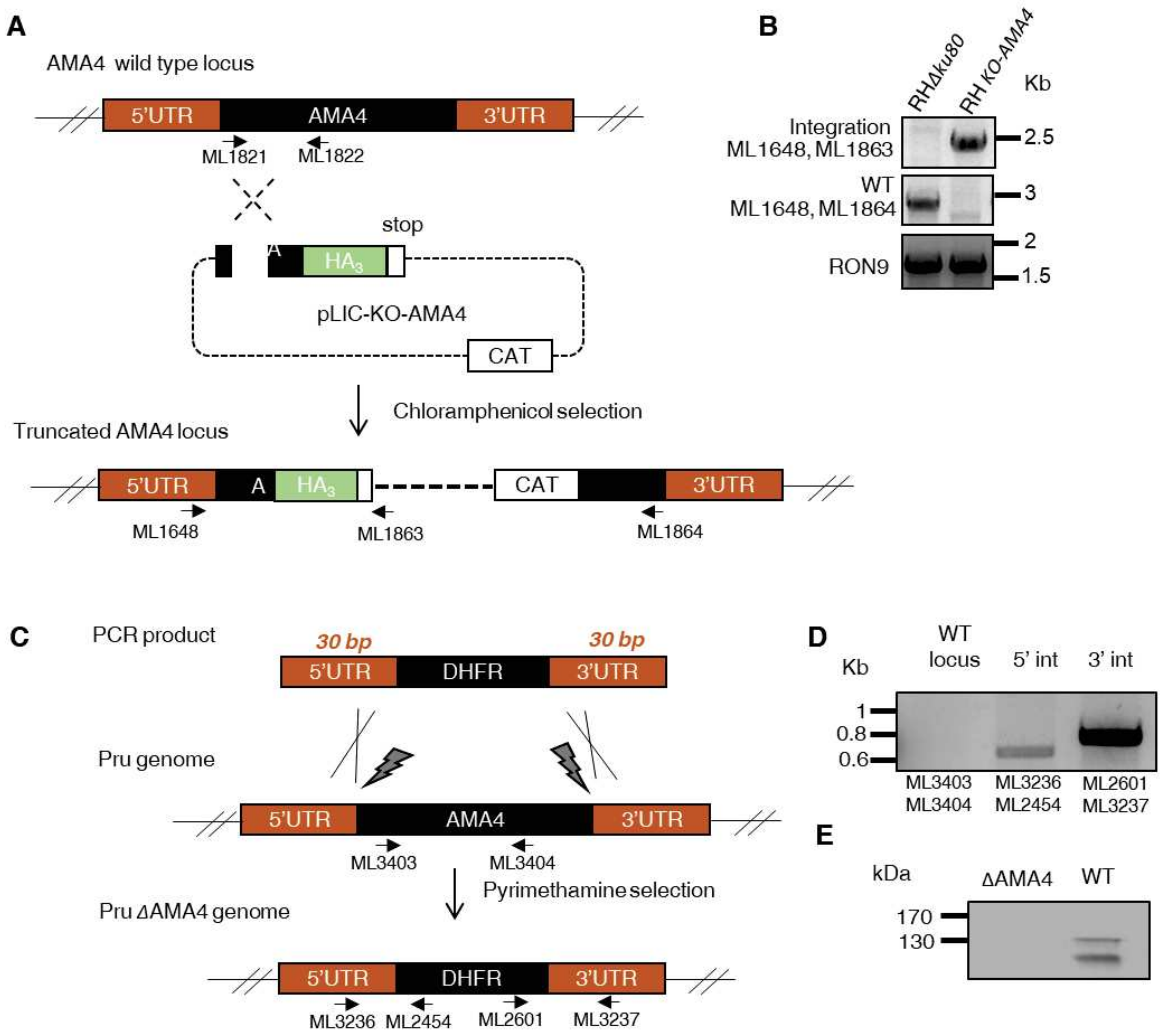


Figure 18: Disruption and knock out of *AMA4* locus in RH*Δku80* and Pru respectively. (A) Schematic representation illustrating the strategy of disruption of *AMA4* locus in the RH *Δku80* background. RH*Δku80* parasites were transfected with pLIC-KO-AMA4 plasmid containing the first 1300bp of the *AMA4* coding sequence, three HA epitopes and the chloramphenicol acetyltransferase resistance to truncate the *AMA4* wild type locus by a single homologous recombination. Stable transformants were selected with chloramphenicol and clones were isolated by limiting dilution. (B) Verification of *KO-AMA4* integration in RH *Δku80* by PCR using ML1648 and ML1863 primers. Amplification of the wild type locus (using ML1648 and ML1864 primers) and RON9 locus were used as controls. (C) Scheme illustrating *AMA4* locus knock out strategy in Pru background. Pru parasites were transfected with two gRNA guides targeting the 5' and 3'of AMA4 to remove the entire *AMA4* gene by double homologous recombination. Stable transformants were selected with pyrimethamine and clones were isolated by limiting dilution. (D) Verification of *AMA4* locus knock out by PCR though amplification of 5' integration using ML3403 and ML3404 and 3' integration using ML3236 and ML2454 primers. Amplification of the wild type locus using ML2601 and ML3237 primers was performed as a control. (E) Western blot of Pru and Pru KO-

AMA4 strains using anti-AMA4 antibodies. The KO-AMA4 in RH *Δku80* strain has been generated by Diana Penarete-Vargas and in Pru *HX* by Margarida Ruivo.

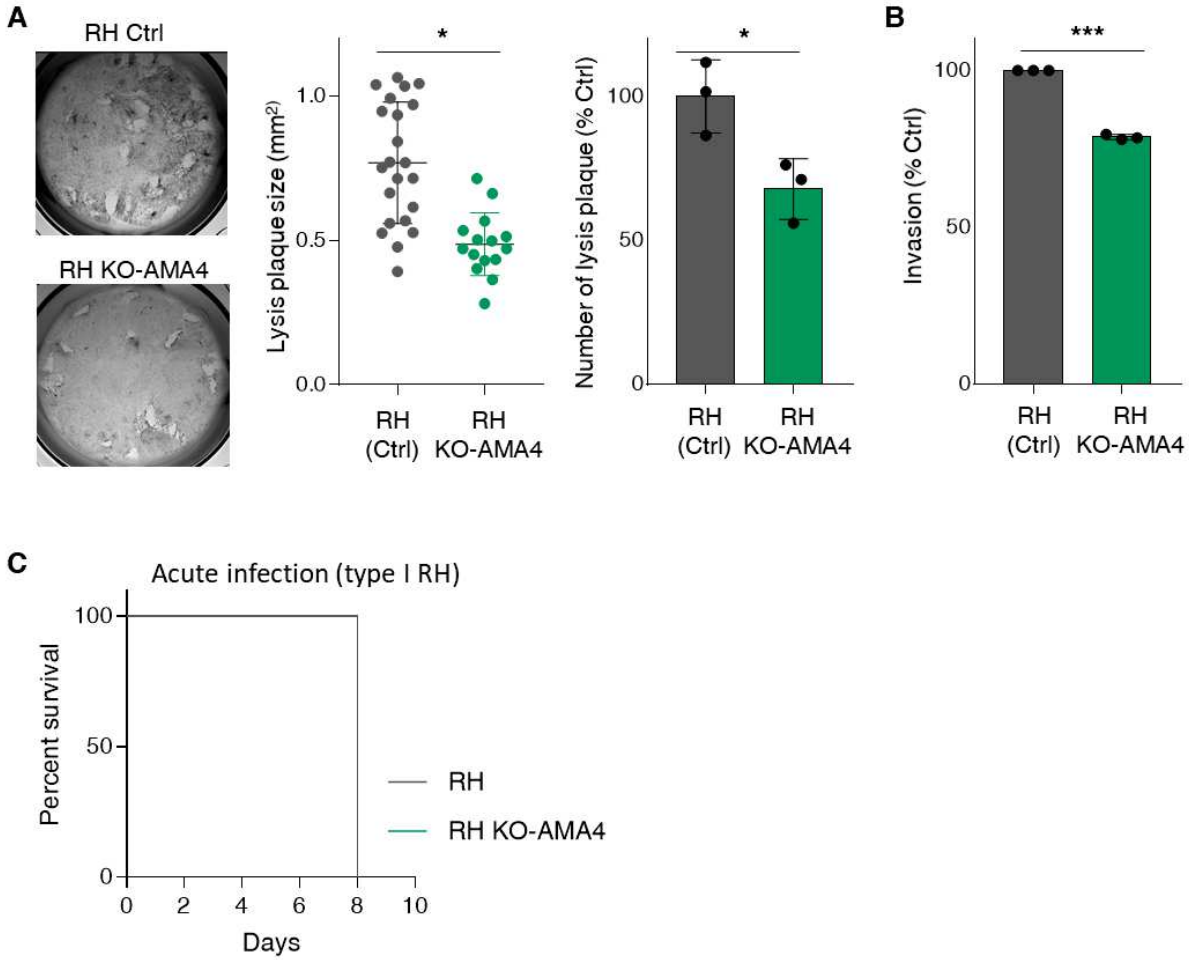


Figure 19: AMA4 does not have a role during acute phase in type I RH *Δku80* strain. (A) Plaque assays of HFFs monolayers infected with either RH*Δku80* or RH KO-AMA4 tachyzoites and grown for 7 days. Quantification of the number and size of the lysis plaques are shown in the graphs. Student's t-test, *P<0.05; Results are presented as mean±S.E.M for triplicates of one experiment representative of three independent ones. (B) Invasion assay for 5 min of RH *Δku80* and RH KO-AMA4 tachyzoites. Student's t-test, **P<0.01; Results are presented as mean±S.E.M representative of three independent experiments (C) *In vivo* virulence of RH Δ*ku80* and RH KO-AMA4 after intraperitoneal injection of 100 tachyzoites in BALB/c mice (One experiment, 5 mice per group). Panel C was done by M. Gissot (Lille).

To investigate the role of AMA4 in bradyzoites, we next generated a KO-AMA4 in the type II Pru strain. The knockout of *AMA4* locus was obtained by double homologous

recombination (Figure 18*C*) and verified by PCR (Figure 18*D*) and western blot (Figure 18*E*). The effect of depletion of invasion was then assessed by plaque assay. Tachyzoites of the RH KO-AMA4 strain generated less lysis plaques as compared to control parasites, and these plaques were significantly smaller. This indicates an invasion defect (Figure 20*A*). To study the virulence of the knockout strain during the acute phase, BALB/c mice were infected intraperitoneally with 1000 tachyzoites from either Pru or Pru KO-AMA4 and monitored during the acute phase. Of note, 1000 tachyzoites is the lethal dose of type II Pru strain. Interestingly, 100% of mice infected with the Pru KO-AMA4 strain survived whereas 60% of mice infected with the control Pru strain succumbed to infection at day 14 (P=0.051) (Figure 20*B*). This may imply a function of AMA4 in type II parasites, which are more prone to develop the latent phase of the disease. In order to establish a chronic infection, BALB/c mice were inoculated intraperitoneally with an optimized dose of 250 tachyzoites from wild-type Pru and Pru KO-AMA4 parasites. Brain cysts were harvested one-month post-infection. Interestingly, mice infected with the Pru KO-AMA4 strain significantly exhibited a lower percentage of cyst burden (around 50%) in their brains, as compared to mice infected with the wild type parasites (Figure 17C). This illustrates an important role of AMA4 to establish a chronic infection.

We next assessed the ability of the cysts from Pru KO-AMA4 to induce a new infection. Cysts were harvested from the brains of BALB/c mice infected with either Pru or Pru KO-AMA4 strains. Following counts, 15 cysts of harvested cysts of either strain were injected by oral gavage to new BALB/c mice. 15 cysts were used to obtain a mild acute infection, thus tachyzoites reaching the brain would infect neural cells and convert to bradyzoites to obtain a chronic infection. One-month post infection, mice infected with the Pru KO-AMA4 cysts showed a significant decrease in cyst burden (50%) as compared to mice infected with the Pru strain (Figure 20*C*). These results were consistent with those generated upon injection of mice with tachyzoites of the Pru KO-AMA4 (Figure 20*C*). To prove the importance of AMA4 in the

invasion of the bradyzoite stage, we performed a plaque assay using freshly harvested bradyzoites from the brains cysts of mice infected with Pru or Pru KO-AMA4 strains, following pepsin digestion (Popiel et al., 1996). 12 days post-infection with these bradyzoites, Pru KO-AMA4 strain significantly yielded less plaques as compared to the wild type, demonstrating fewer invading parasites (Figure 20*D*). This result further confirms the involvement of AMA4 in bradyzoite invasion. Altogether these findings showed that AMA4 has a minor role in the tachyzoite invasion, as reflected by the lack of difference of an *in vivo* phenotype of the acute phase, upon inoculation of type I wild type or AMA4 mutant tachyzoites. In contrast, removal of AMA4 from type II parasites induced a mild phenotype during acute phase, even if AMA4 is expressed at low levels in tachyzoites. In stark contrast, AMA4 has a more pronounced role during chronic infection. The observed reduction of cysts in Pru KO-AMA4 infected mice, might not only be the result of a defective tachyzoite stage, but also due to the high expression of AMA4 and its role in invasion of bradyzoites. This highlights that AMA4 is an invasion protein utilized for invasion in both tachyzoites and bradyzoites but with a more predominant role in bradyzoites.

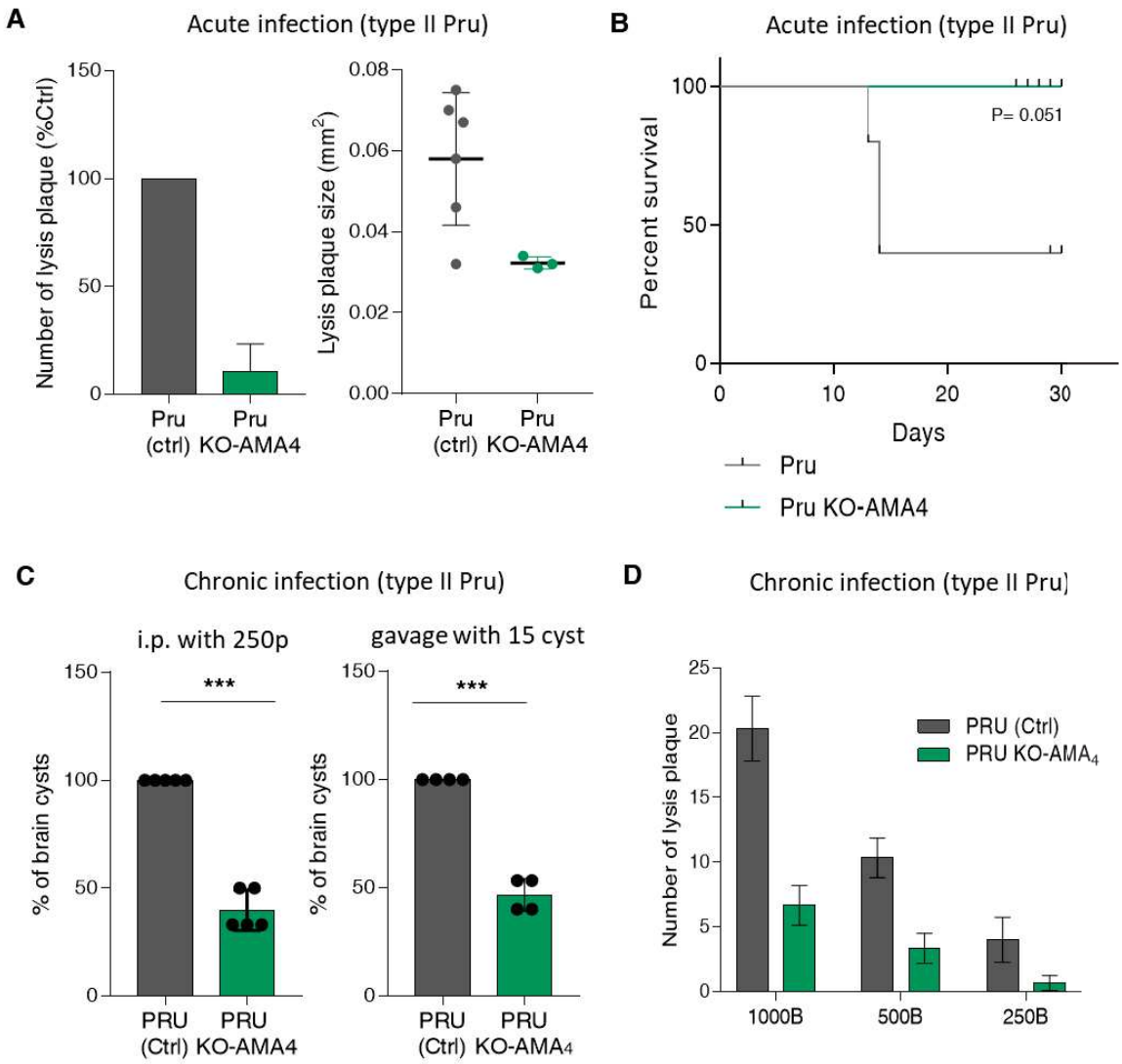


Figure 20: *AMA4* plays are role in tachyzoite invasion and establishment of chronic toxoplasmosis. (A) Plaque assays of HFFs monolayers infected with either Pru or Pru KO-AMA4 tachyzoites and grown for 7 days. Quantification of the number and size of the lysis plaques are shown in the graphs. Results are presented as mean±S.E.M. representative of triplicates of one experiment). (B) *In vivo* virulence of Pru and Pru KO-AMA4 after intraperitoneal injection of 1000 tachyzoites in Balb/c mice. Log-rank test, P=0.051 (One experiment, 5 mice per group) (C) Percentage of cyst load in brains of BALB/c mice one month after intraperitoneal infection of 250 tachyzoites of Pru or Pru KO-AMA4 tachyzoites (left) or after oral gavage with 15 cysts (right). Student's t-test, ***P<0.001; Results are presented as mean±S.E.M. representative of one experiment (10 mice per group). (D) Plaque assay of HFFs monolayers infected with 1000, 500, or 250 bradyzoites of either Pru or Pru KO-AMA4 strains obtained from brain cysts after gavage and allowed to grow for 12 days. Quantification of the number of plaques are shown in the graphs. Results are presented as mean±S.E.M. for triplicate of one experiment representative of two independent experiments. (Panel A done by Margarida Ruivio. Panels C and D were generated by Maguy Hamie at AUB, Hiba El Hajj's laboratory).

In part I, we unraveled the composition of bradyzoite moving junction. Although RON proteins of tachyzoite MJ are present in bradyzoites, this latent stage also possesses other MJ complexes. AMA4 and AMA2 proteins are the additional MJ components incorporated into the repertoire of bradyzoites invasion machinery. Herein, we focused on AMA4 and showed its importance in invasion in both type I and type II strains *in vitro*. Yet its role during invasion was only adapted in type II strain *in vivo*. As such, AMA4 had a prominent role during the chronic phase marked by a significant reduction in cyst load in the brains of infection mice.

Since disrupting the MJ marks an obstruction in the propagation of infection, thus targeting it might present remarkable vaccine candidates to the fight against toxoplasmosis. A profound study in Plasmodium shed the light on the success of targeting the MJ in this parasite by using AMA and RON proteins in a complex upon vaccination (Srinivasan et al., 2014, 2017). Mice and *Aotus* monkeys vaccinated by AMA-RON complex were protected from a challenge with a lethal dose of *Plasmodium* (Srinivasan et al., 2014, 2017). In part II, we focused on designing new vaccine candidates against acute and more importantly chronic toxoplasmosis. Since AMA1-RON2 and AMA4-RON2$_{L1}$ MJ complexes are highly expressed in tachyzoites and bradyzoites, respectively, we took advantage of those two MJ complexes and targeted the acute and more importantly the chronic phase of toxoplasmosis.

Part II. Vaccination using AMA-RON MJ complexes

3.2.1. AMA1 in complex with RON2 exhibits a strong protective effect against acute and chronic infection with *Toxoplasma gondii*

The strong protective effect of immunization with AMA1-RON2 complex against *Plasmodium yoelii* (Srinivasan et al., 2017) prompted us to interrogate the efficacy of targeting *Toxoplasma* AMA1 alone or in complex with RON2, as a vaccination approach against toxoplasmosis. All recombinant proteins were generated by Martin Boulanger at the University of Victoria, Canada. C57BL/6 mice were randomly divided into three groups corresponding to adjuvant control (group 1, *n*=17), immunized with recombinant D1-D2-D3 domains of AMA1, referred thereafter as rAMA1 (group 2, *n*=17) or immunized with rAMA1 in complex with D3 domain of RON2 (rAMA1-RON2D3) (group 3, *n*=17) (Figure 21). Each group received a first dose formulated with complete Freund's adjuvant (on day 0), followed by two doses formulated with incomplete Freund's adjuvant (on days 14 and 28, respectively). Sera from immunized C57BL/6 mice were collected 14 days after the last immunization.

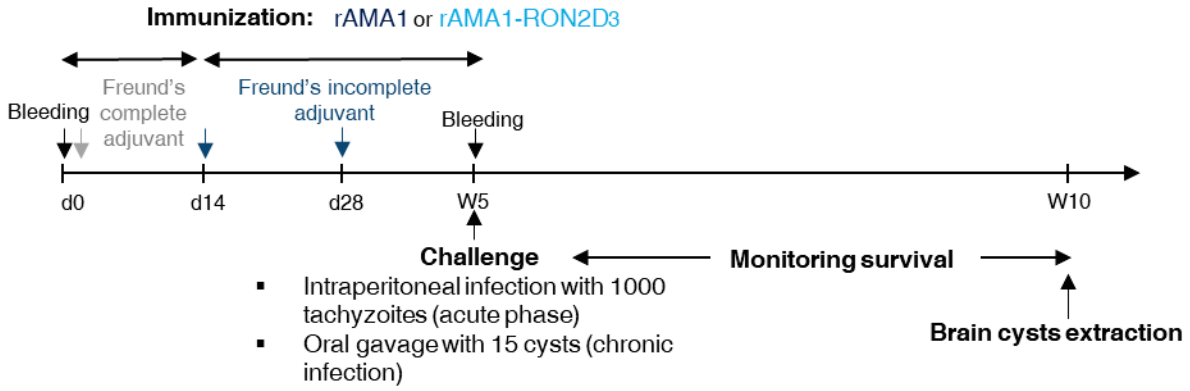


Figure 21: Vaccination strategy using rAMA$_1$ protein or rAMA1-RON$_2$D3 complex. Schematic representation illustrating the vaccination strategy of C57BL/6 mice receiving 40 µg of rAMA1 peptides or 40 µg of rAMA1-RON2D3 complex with adjuvant or adjuvant alone as a control. Mice were immunized subcutaneously three times, at a two-week interval between injections. The first immunization was performed in Freund's complete adjuvant, followed by

two injections in Freund's incomplete adjuvant. Two weeks following the last immunization, mice were challenged intraperitoneally (IP) by a lethal dose of 1000 Pru tachyzoites and their mortality was monitored for one month, or challenged by oral route with 15 cysts of the type II 76K strain and brain cyst was quantified one month after challenge.

Immunization of all mice was confirmed by ELISA using coated wells with recombinant proteins, and assessing the levels of total IgG, IgG subclass isotypes IgG1 and IgG2a in sera. Both rAMA1 and rAMA1-RON2D3 induced high immune response of similar amplitude in C57BL/6 mice (Figure 22*A*). Moreover, the levels of both IgG1 and IgG2a significantly increased in the immunized groups (Figure 22*A*), implying a mixed Th1/Th2 immune response. The specificity of sera from rAMA1 or rAMA1-RON2D3 immunized mice was verified by IFA (Figure 22*B,* right panel) and western blot (Figure 22*C*). Both sera recognized a band at the expected size for AMA1 in the control but not in the mutant parasites, which do not express AMA1 (RH *KO-AMA1*) (M. H. Lamarque et al., 2014) (Figure 22*C*). IFAs on intracellular parasites showed that anti-rAMA1 and anti-rAMA1-RON2D3 antibodies display a micronemal staining, which was absent in control sera and that completely disappeared in the RH *KO-AMA1* parasites (Figure 22B, left panel). This result confirms thereby, that the sera are specific for the micronemal protein AMA1 (Figure 22*B* and Figure 22*C*) and that antibodies induced by the rAMA1-RON2D3 complex target AMA1 but not RON2 since we do not see any signal in the rhoptry of RH *KO-AMA1* by IFA (Figure 22*B,* left panel). The lack of detection of RON2 with this complex is presumably due to the fact that rAMA1-RON2D3 complex is only formed of a small RON2 D3 peptide bound (36 aa) to the full ectodomain of AMA1.

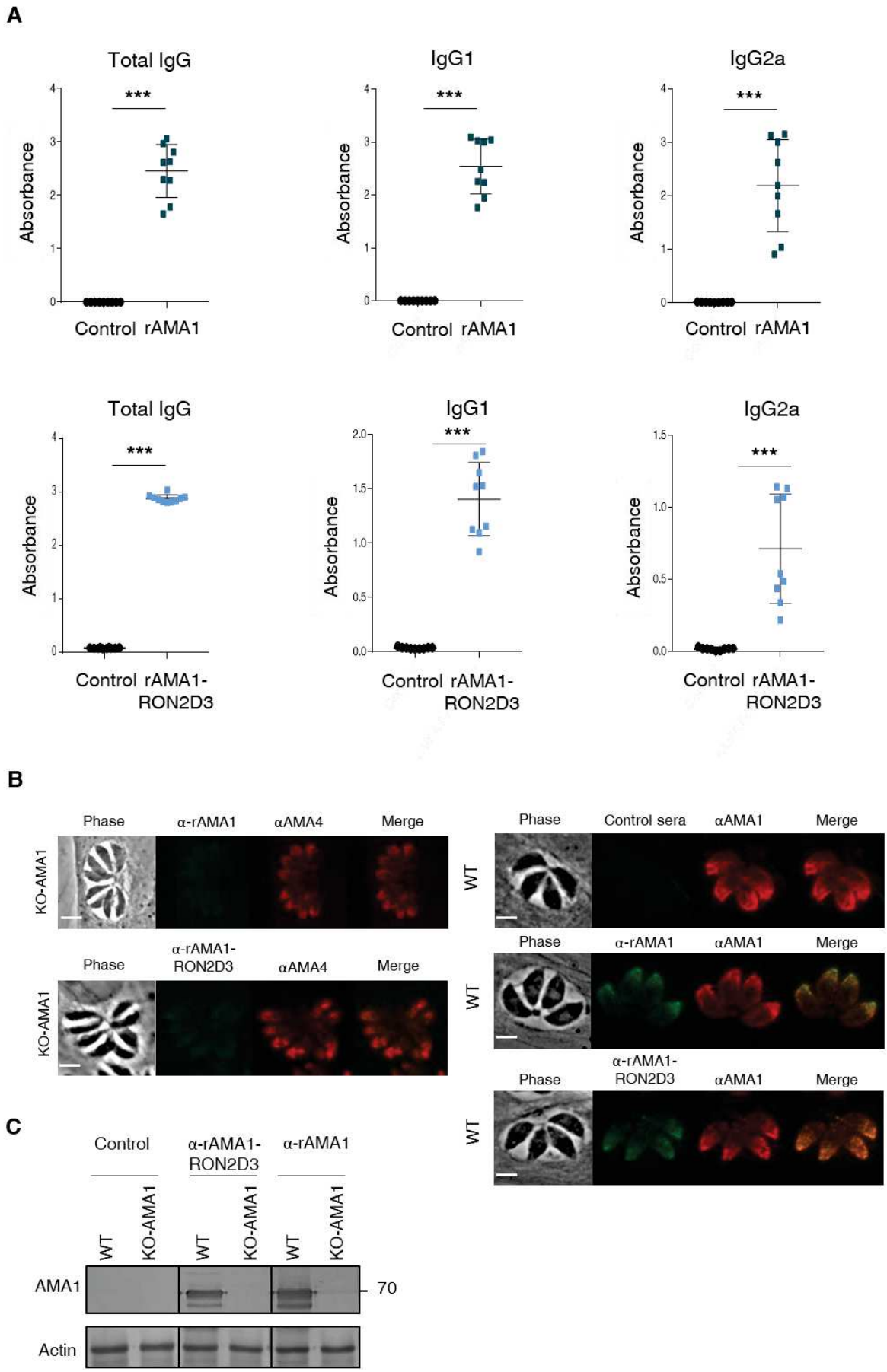

A
Total IgG
IgG1
IgG2a
Absorbance
***
Control rAMA1
Control rAMA1-RON2D3
B
Phase
α-rAMA1
αAMA4
Merge
KO-AMA1
α-rAMA1-RON2D3
Control sera
αAMA1
WT
C
Control
α-rAMA1-RON2D3
α-rAMA1
WT
KO-AMA1
AMA1
70
Actin

Figure 22: Immunization with rAMA1 or rAMA1-RON2D3 induce a strong and specific immune response against AMA1 in C57BL/6 mice. (A) ELISA showing levels of total IgG, IgG1 and IgG2a in mice immunized with rAMA1 or rAMA1-RON2D3 as compared to non-immunized mice. Student's t-test, ***P<0.001; Results are presented as mean±S.E.M.of one experiment (sera of 10 individual mice per group) (B) IFAs on intracellular RH *Δku80* and RH *KO-AMA1* using sera from mice immunized with rAMA1, rAMA1-RON2D3. Control sera (green), anti-AMA4 (red) and anti-AMA1 (red) antibodies. Scale bars, 4µm (B) Western blot of RH*Δku80* and RH *KO-AMA1* tachyzoites using sera from mice immunized with rAMA1, rAMA1-RON2D3 or control sera. Dictyostelium actin recognizing *T. gondii* actin was used loading control. These results are representative of one experiment out of two independent ones.

3.2.2. AMA1 in complex with RON2 peptide induces a protective immunization for acute and chronic phase

To explore the protective effect of rAMA1 alone or in complex with RON2D3 against the acute infection, mice were challenged with a lethal dose of tachyzoites of Pru type II parasites. In more details, 1000 tachyzoites were injected by intraperitoneal route, following the last immunization (timeline described in Figure 21) and animals were monitored for survival. Indeed, injection of 1000 tachyzoites induces death of mice only few days p.i., due to the important replication of tachyzoites and even before the establishment of any chronic phase. Hence, this lethal dose of parasites allows to estimate the efficiency of a vaccine strategy against the tachyzoite dissemination or acute phase.

All animals receiving only adjuvants or rAMA1 succumbed to the infection by only few days (Figure 23*A*). Yet this short delay of mortality between mice immunized with rAMA-1 alone or with control adjuvant was significant (P=0.017). Strikingly, more than 70% of mice immunized with rAMA1-RON2D3 complex survived against the lethal challenge (Figure 23*A*), illustrating the great protective efficacy of the complex over AMA1 alone against acute toxoplasmosis.

Our next aim was to verify whether this complex yields a similar protective efficacy against a more natural route of infection. Animals were thus challenged by oral gavage with 15

cysts of 76K strain, two weeks post last immunization, then sacrificed one month later. This period allows mice to establish the chronic phase of the disease (Haroon et al., 2012) (Figure 21). The number of cysts in brain was then quantified to assess protection against chronic toxoplasmosis.

Immunization with rAMA1 induced a significant decrease in the number of cysts in the brains of 56% of immunized mice, as compared to the control group (Figure 23*B*). Notably, rAMA1-RON2D3 incited a stronger protection against chronic toxoplasmosis, with a decrease of 80% in the number of cysts in the brains of immunized mice with this complex (Figure 23*B*).

Altogether these results mirror those obtained in the context of malaria, and infer the higher protective efficacy of the complex rAMA1-RON2D3, as compared to rAMA1 alone, against both acute and chronic toxoplasmosis, highlighting the potential value of this vaccine strategy against another apicomplexan infection.

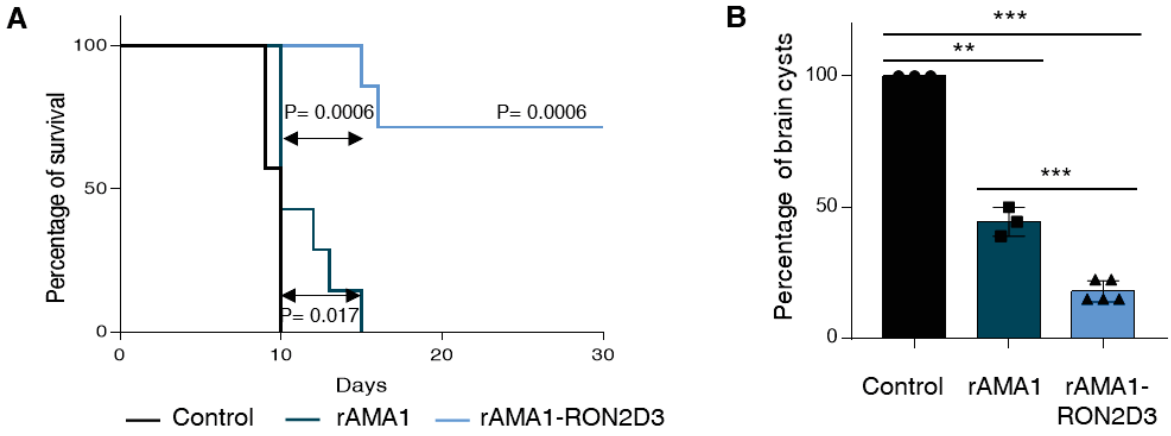


Figure 23: Immunization with rAMA1-RON2D3 induces higher protective efficacy against acute and chronic toxoplasmosis. (A) Percentage of survival in C57BL/6 mice immunized with rAMA1, and rAMA1-RON2D3 as compared to control mice upon an intraperitoneal challenge with a lethal dose of tachyzoites. Log-rank test. These results are of a representative experiment out of two independent experiments (7 mice per group). (B) Percentage of cyst load in brains of C57BL/6 mice immunized with rAMA1, and rAMA1-RON2D3 as compared to control mice after one month of challenging with 15 cysts by gavage.

Student's t-test, **P<0.01, ***P<0.001; Results are presented as mean±S.E.M. of one experiment (10 mice per group).

3.2.3. AMA4-RON2$_{L1}$ complex is another vaccine candidate against chronic toxoplasmosis

The up-regulation of AMA4 and its RON2$_{L1}$ partner, the specific association of AMA4 at the MJ of bradyzoites, and its role for invasion, particularly that of the bradyzoite, underlines the potential of improving the vaccine strategy by targeting a broader range of AMA-RON2 pairs of *Toxoplasma* invasive stages. We thus conducted similar vaccine experiments with recombinant AMA4 containing D1, D2 and D3 domains (rAMA4), alone or in complex with the D3 domain of RON2$_{L1}$ (rAMA4-RON2$_{L1}$D3) (Figure 24).

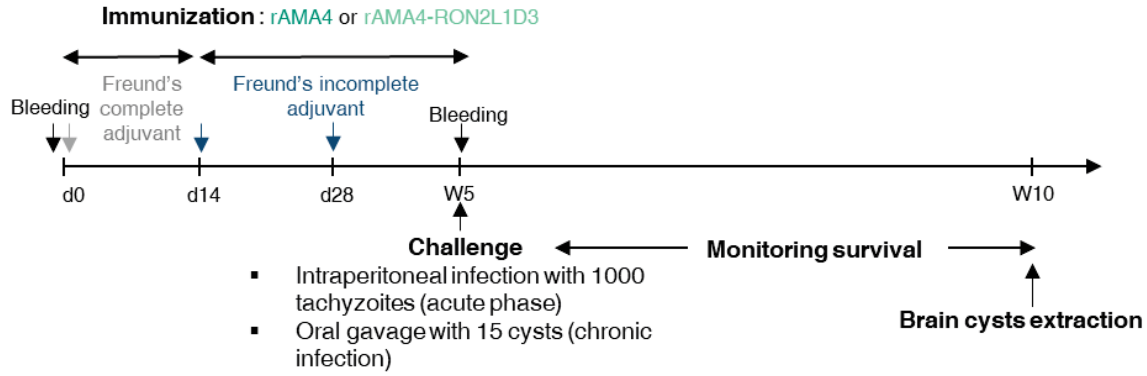
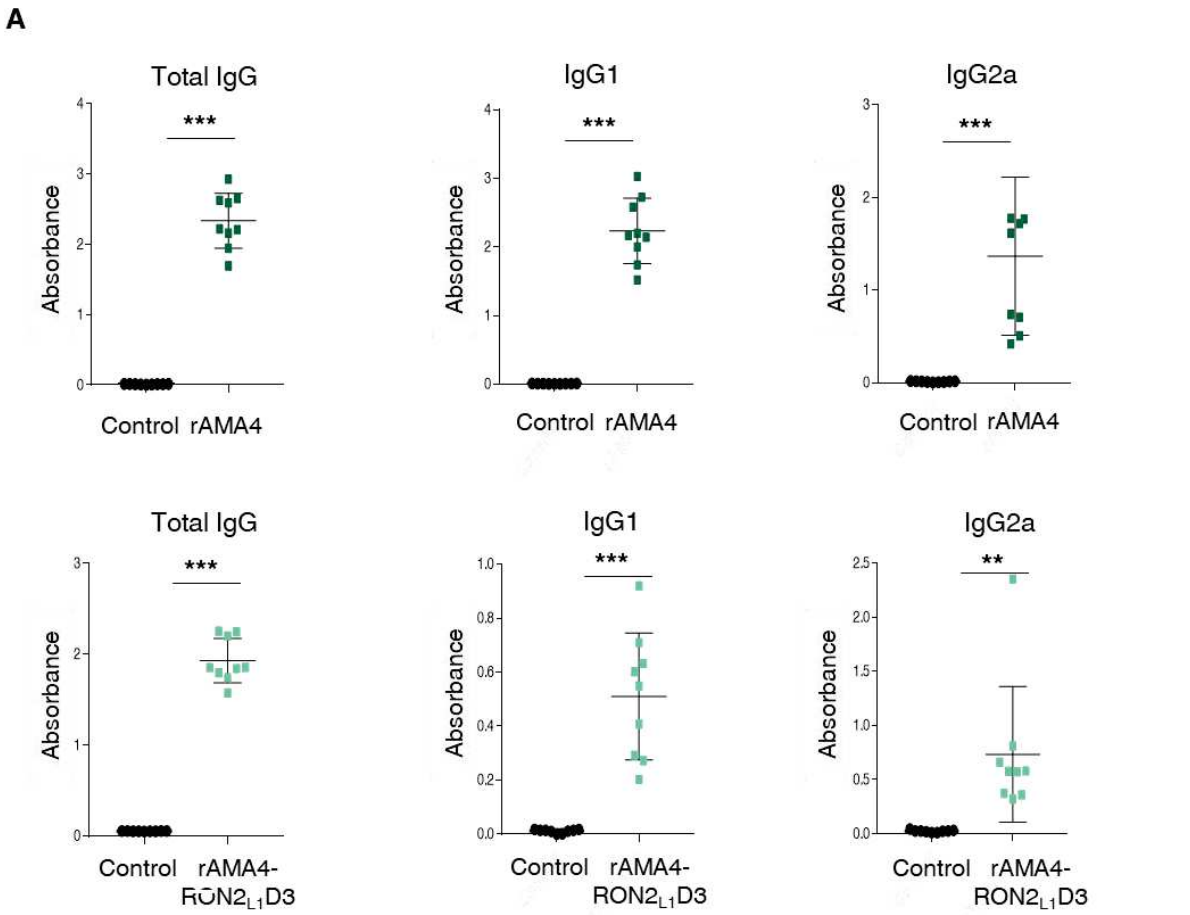


Figure 24: Vaccination strategy using rAMA4 protein or rAMA1-RON2$_{L1}$D3 complex. Schematic illustration of the vaccination strategy of C57BL/6 mice receiving 40 µg of rAMA4 peptides or 40 µg of rAMA4-RON2$_{L1}$D3 complex with adjuvant or adjuvant alone as a control. Mice were immunized subcutaneously three times, at a two-week interval between injections. The first immunization was performed in Freund's complete adjuvant, followed by two injections in Freund's incomplete adjuvant. Two weeks following the last immunization, mice were challenged either intraperitoneally (IP) by a lethal dose of 1000 Pru tachyzoites and their mortality was monitored for one month, or challenged by oral route with 15 cysts of the type II 76K strain and brain cyst was quantified one month after challenge.

Similar to our aforementioned results with rAMA1 and rAMA1-RON2D3, both rAMA4 and rAMA4-RON2$_{L1}$D3 induced high immune response by ELISA (Figure 25*A*), as indicated by significantly high level of IgG total in the immunized groups. In addition, both IgG1 and IgG2a levels significantly increased as compared to the control group (Figure 25*A*). To confirm the specificity of the sera against AMA4, we took advantage of the overexpression of AMA4 in absence of AMA1 (M. H. Lamarque et al., 2014) and tested the reactivity of sera against RH *KO-AMA1* by IFAs. As expected, both sera against rAMA4 or rAMA4-RON2$_{L1}$D3 complex gave an apical staining in RH *KO-AMA1* that co-localized with anti-AMA4 antibodies, while no signal was observed in control sera (Figure 25*B*, right panel). We did not detect any signal on WT parasites, confirming the low expression of AMA4 in tachyzoites (Figure 25*B*, left panel). This result was also supported by western blot analysis (Figure 25*C*). Interestingly, anti-rAMA4-RON2$_{L1}$D3 sera was able to stain the moving junction of RH *KO-AMA1* invading tachyzoites (Figure 25D). This confirms the presence of AMA4 at the MJ (Figure 16*B*) and that RH *KO-AMA1* uses AMA4 for invasion in the absence of AMA1.


A
Total IgG
IgG1
IgG2a
Absorbance
***
**
Control
rAMA4
rAMA4-RON2L1D3

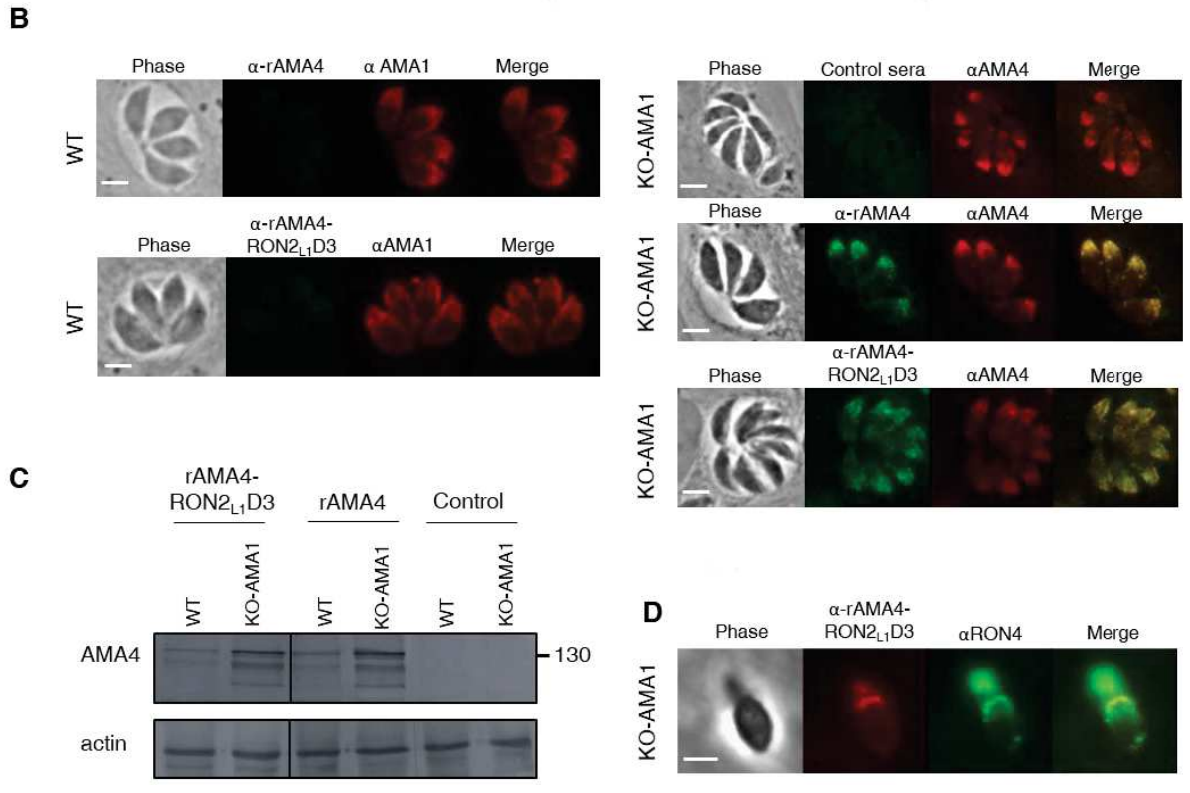

B
Phase
α-rAMA4
α AMA1
Merge
WT
α-rAMA4-RON2L1D3
αAMA1
Control sera
αAMA4
KO-AMA1
C
rAMA4-RON2L1D3
rAMA4
Control
WT
KO-AMA1
AMA4
130
actin
D
αRON4

Figure 25: Immunization with rAMA4 or rAMA4-RON2$_{L1}$D3 induce a strong and specific immune response in C57BL/6 mice. (A) ELISA showing levels of total IgG, IgG1 and IgG2a in mice immunized with rAMA1 or rAMA1-RON2D3 compared to non-immunized mice. Student's t-test, **P<0.01, ***P<0.001; Results are presented as mean±S.E.M.of one experiment (sera of 10 individual mice per group) (B) IFAs on intracellular RH *Δku80* and RH KO-AMA1 using sera from mice immunized with rAMA4, rAMA4-RON2$_{L1}$D3, or control sera (green), anti-AMA4 (red) and anti-AMA1 (red) antibodies to verify the specific of produced mice sera. Scale bars, 4µm. (C) Western blot of RH *Δku80* and RH *KO-AMA1* tachyzoites using sera from mice immunized with rAMA4, rAMA4-RON2$_{L1}$D3 or control sera. Dictyostelium actin recognizing *T. gondii* actin was used as a loading control.) (D) IFAs on invading RH KO-AMA1 using sera from mice immunized with rAMA4-RON2$_{L1}$D3 (red) and anti-RON4 (green). Scale bar, 2µm.

We then explored the protective efficacy of rAMA4 or rAMA4-RON2$_{L1}$D3 against acute and chronic toxoplasmosis. Two weeks post immunization, mice were challenged either with a lethal dose of type II tachyzoites or by oral route with cysts containing bradyzoites (Figure 24). While AMA4 alone did not induce any protection against acute infection, rAMA4-RON2$_{L1}$D3 induced a slight protection delay in the mortality of mice (Figure 26*A*), a result that correlates with the very low expression of AMA4 in tachyzoites (Figure 16*D*, right panel), the middle role of AMA4 for invasion of tachyzoite (Figure 19*A*) and the acute infection (Figure 19*B*). Remarkably, immunization with rAMA4-RON2$_{L1}$D3 significantly decreased cyst burden in the brains of around 60% of C57BL/6 mice challenged orally with bradyzoite cysts, while rAMA4 did not induce any effect as compared to the control group (Figure 26*B*). These results corroborate the results obtained under Part I and highlight a predominant role for AMA4 in the bradyzoites stage. Our results also support the role of AMA4 in complex with RON2$_{L1}$.

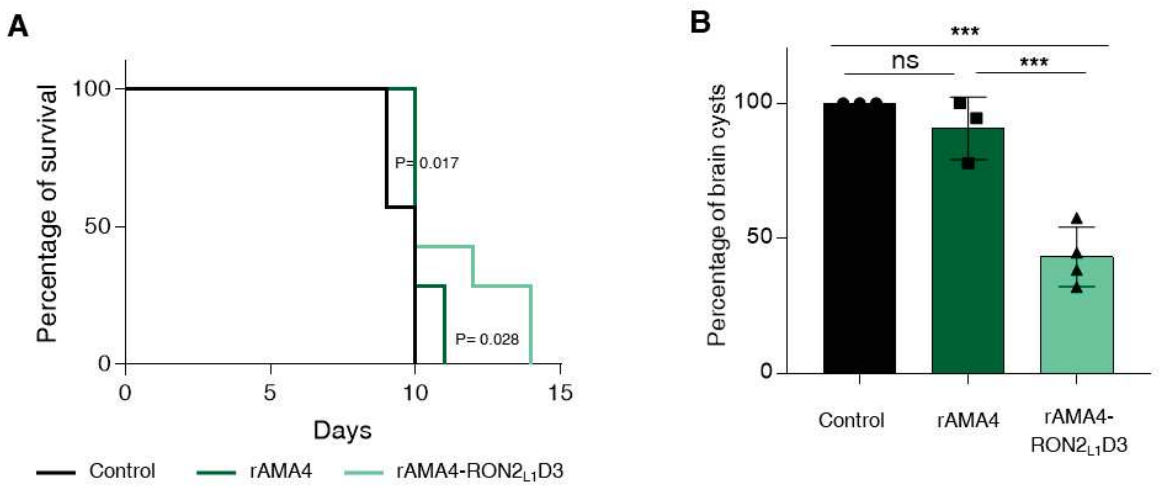


Figure 26: Immunization with rAMA4-RON2$_{L1}$D3 induces higher protective efficacy after oral challenge with cysts. (A) Percentage of survival (Log-rank test) in C57BL/6 mice immunized with rAMA4, and rAMA4-RON2$_{L1}$D3 compared to control mice upon an intraperitoneal challenge with a lethal dose of tachyzoites. Log-rank test. The depicted results are those of one representative experiment out of two independent ones (7 mice per group) (B) Percentage of cyst load in brains of C57BL/6 mice immunized with rAMA4, and rAMA4-RON2$_{L1}$D3 compared to control mice after one month of challenging with 15 cysts by gavage. Student's t-test, ***P<0.001; Results are presented as mean±S.E.M. of one experiment (10 mice per group).

The next logic approach was to evaluate whether protection can be enhanced upon immunizing mice with both complexes together. Surprisingly, challenging with a lethal dose of tachyzoites by intraperitoneal route showed that mice immunized with both complexes do not display statistically significant increase in survival as compared to mice immunized the single complex rAMA1-RON2D3 (p=0.49) (Figure 27*A*). However, we obtained a better protection after oral challenge with cysts when mice were immunized with both complexes, with an 82% reduction in cyst burden as compared to immunization with rAMA1-RON2D3 (77%) alone (p=0.05) (Figure 27*B*).

Altogether these results demonstrate the potential of the AMA4-RON2$_{L1}$ complex to protect against an oral challenge with cysts which can be used in combination with AMA1-RON2 complex to maximize the vaccine strategy against toxoplasmosis.

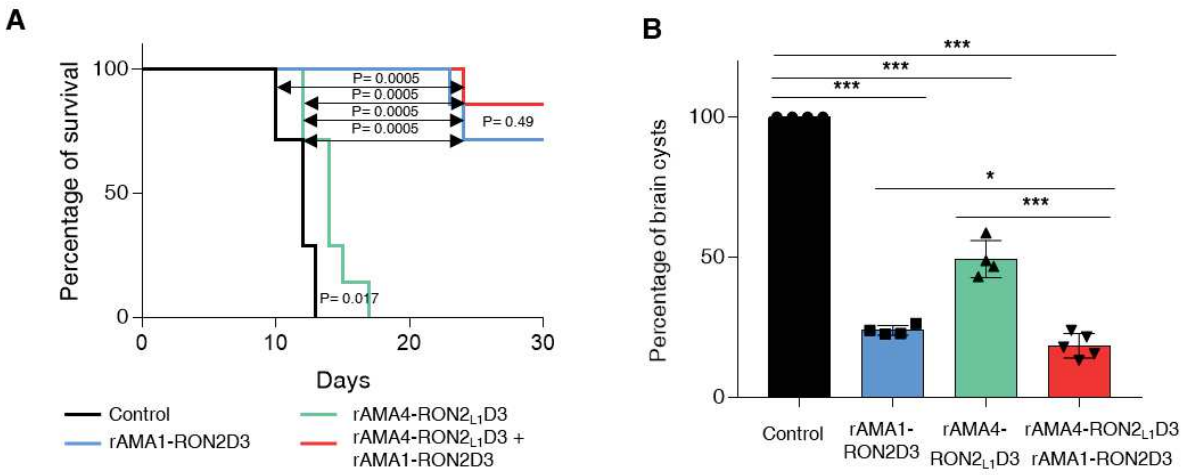


Figure 27: Immunization with both rAMA1-RON2D3 and rAMA4-RON2$_{L1}$D3 enhances protection against chronic toxoplasmosis. (A) Percentage of survival in C57BL/6 mice immunized with rAMA1-RON2D3, rAMA4-RON2$_{L1}$D3 or both complexes compared to control mice upon an intraperitoneal challenge with a lethal dose of tachyzoites. Log-rank test. (Experiment performed once with 7 mice per group) (B) Percentage of cyst load in brains of C57BL/6 mice immunized with rAMA1-RON2D3, rAMA4-RON2$_{L1}$D3 or both complexes compared to control mice after one month of challenging with 15 cysts by gavage. Student's t-test, *P<0.05, ***P<0.001; Results are presented as mean±S.E.M. of one experiment (10 mice per group).

3.2.4. AMA-RON complexes induce invasion inhibitory antibodies

For malaria vaccine, the efficiency of AMA1-RON2 vaccine was due to a significantly higher neutralization activity of anti-*Pf*AMA1 antibodies that better mimic the *Pf*AMA1 structure when complexed with *Pf*RON2 during *Plasmodium* merozoite invasion (Srinivasan et al., 2014). In an attempt to study the potential mechanism by which the antibodies are protecting mice against acute and chronic toxoplasmosis, we performed an invasion inhibition assay with total IgG purified from immunized mice sera. Briefly, tachyzoites were incubated with control sera, anti-rAMA1, anti-rAMA4, anti-rAMA1-RON2D3 or anti-rAMA4-RON2$_{L1}$D3 antibodies at 1mg/ml for 30 min. Parasites were then allowed to invade HFF cells for 5 min in presence of the sera and intracellular tachyzoites were counted as previously described using the in/out color assay (Huynh et al., 2003). As expected, anti-rAMA4 and

rAMA4-RON2$_{L1}$D3 antibodies were not able to inhibit the invasion of WT tachyzoites (Figure 28*A*), a stage that does not particularly express this complex. A moderate inhibition of 20% was only observed at a higher dose (Figure 28**C**). In stark contrast, anti-rAMA1 antibodies significantly inhibited the invasion of tachyzoites, an effect which was potentialized by complexing rAMA1 with RON2D3 (Figure 28*A*). The effect of antibodies on inhibition of invasion of tachyzoites was specific (Figure 28*B*) and was dose dependent (Figure 28*C*), reaching around 70% at a dose of 2mg/ml. Furthermore, in accordance with the up-regulation of AMA4 and RON2$_{L1}$ in the KO-AMA1 parasites (M. H. Lamarque et al., 2014), the anti-rAMA4-RON2$_{L1}$D3 antibodies inhibited the invasion of the mutants (Figure 28*B*). These results imply that one plausible mechanism of protection in immunized mice might be the partial inhibition of invasion by the parasites through targeting the formation of the respective complexes.

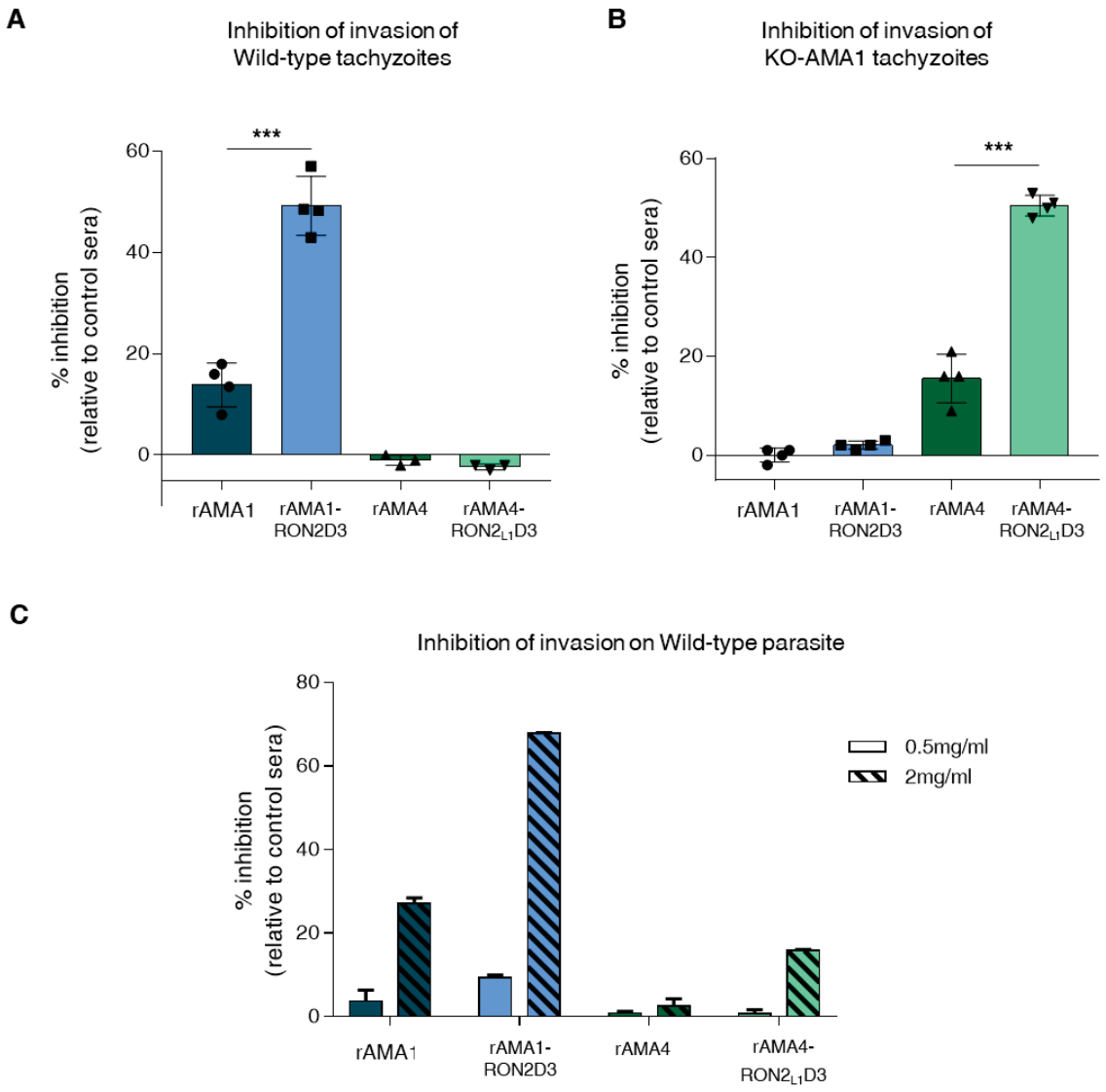


Figure 28: Immunization with the complexes induce more potent inhibitory antibodies. (A) Invasion inhibition assay of RH *Δku80* tachyzoites treated with 1mg/ml total IgG extracted from sera of mice immunized with proteins or their complexes and allowed to invade HFFs monolayers for 5 min. The percentage of inhibition was calculated with respect to their relative control sera. Student's t-test, ***P<0.001; Results are presented as mean±S.E.M. representing average of three independent experiments. (B) Invasion inhibition assay of RH KO-AMA4 tachyzoites treated with 1mg/ml total IgG extracted from sera of mice immunized with proteins or their complexes and allowed to invade HFFs monolayers for 5 min. The percentage of inhibition was calculated with respect to their relative control sera. Student's t-test, ***P<0.001; Results are presented as mean±S.E.M. representing average of four independent experiments. (C) Invasion inhibition assay of RH *Δku80* tachyzoites treated with 0.5mg/ml or 2mg/ml total IgG extracted from sera of mice immunized with proteins or their complexes and allowed to invade HFFs monolayers for 5 min. The percentage of inhibition was calculated with respect to their relative control sera. Results are presented as mean±S.E.M. of duplicates (experiment performed once).

We previously showed that interfering with AMA1 and RON2 function induces a failure to establish a firm junction and lead to parasite detachment from the host cell. Yet, the content of the rhoptry remains discharged in the host cells as a cluster of vesicles—or e-vacuoles—labelled with rhoptry marker ROP1, although no parasite could be observed in the vicinity. These e-vacuoles reflect unsuccessful MJ-dependent intimate attachment (Håkansson et al., 2001; M. H. Lamarque et al., 2014). To test whether sera from immunized mice are targeting the MJ formation, we assessed the number of e-vacuoles in presence of sera. The mean value of e-vacuoles per field significantly increased upon incubation of tachyzoites with anti-rAMA1 purified IgG (Figure 29*A*). Consistent with our results of inhibition of invasion, the rise of e-vacuoles was even more pronounced by incubating tachyzoites with anti-rAMA1-RON2D3 antibodies (Figure 29*A*), and was shown to be dose-dependent (Figure 29*C*). Moreover, the sera against rAMA4 and rAMA4-RON2$_{L1}$D3 inhibited the invasion of RH *KO-AMA1* by interfering with MJ formation (Figure 29*B*). This reveals that inhibitory IgGs target specifically MJ formation during invasion and are with higher efficiency when produced against rAMA-RON2 complex. We also performed IFA on invading RH *KO-AMA1*, and detected the MJ using rAMA4-RON2$_{L1}$D3 (Figure 25*D*), supporting the role of AMA4 during invasion of tachyzoites, when AMA1 was removed.

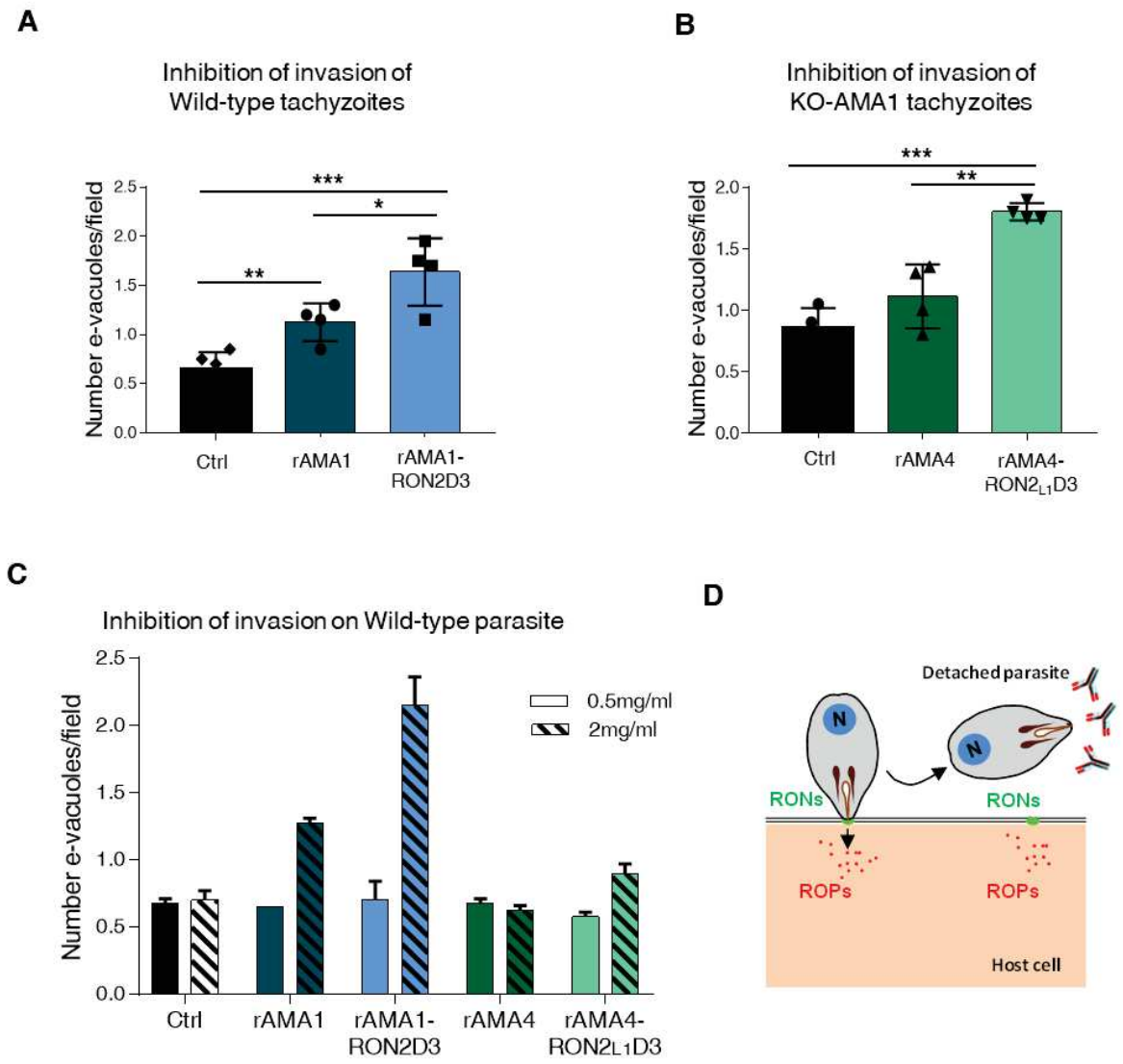


Figure 29: Inhibitory antibodies induces abortive invasion. (A) Invasion inhibition assay of RH *Δku80* tachyzoites treated with 1mg/ml total IgG extracted from sera of mice immunized with proteins or their complexes and allowed to invade HFFs monolayers for 5 min. The number of e-vacuoles produced per field was enumerated. Student's t-test, *P<0.05, **P<0.01, ***P<0.001; Results are presented as mean±S.E.M. representing average of three independent experiments. (B) Invasion inhibition assay of RH KO-AMA4 tachyzoites treated with 1mg/ml total IgG extracted from sera of mice immunized with proteins or their complexes and allowed to invade HFFs monolayers for 5 min. The number of e-vacuoles produced per field was enumerated. Student's t-test, **P<0.01, ***P<0.001; Results are presented as mean± S.E.M. representing average of four independent experiments. (C) Invasion inhibition assay of RH *Δku80* tachyzoites treated with 0.5mg/ml or 2mg/ml total IgG extracted from sera of mice immunized with proteins or their complexes and allowed to invade HFFs monolayers for 5 min. The number of e-vacuoles produced per field was enumerated. Results are presented as mean±S.E.M. of duplicates (experiment performed once). (D) Scheme illustrating the formation of the e-vacuoles upon inhibition of *T. gondii* invasion to the host cell (M. H. Lamarque et al., 2014).

3.2.5. AMA1-RON2 but mostly AMA4-RON2$_{L1}$ are involved in bradyzoite invasion

AMA1 (Mital et al., 2005) and AMA4 (Figure 19*A* and 20*A*; Part I) are both used for invasion of tachyzoites, but AMA1 has a more prevalent role for this stage as compared to AMA4 (Figure 19*C*; Part I) which is barely expressed in tachyzoites (M. H. Lamarque et al., 2014). Accordingly, we found that immunization with rAMA4-RON2$_{L1}$D3 was not efficient to protect against the acute phase caused by tachyzoites, while the rAMA1-RON2 vaccine generated a strong protection against this phase of the infection. Conversely, both proteins are well expressed in the bradyzoite stage (Figure 16*D*; Part I); yet AMA4 was more easily found to decorate the MJ. Albeit the evidence we obtained demonstrating that AMA4 was required for invasion of bradyzoites (Figure 20*D*; Part I), our results did not allow us to conclude on the contribution of AMA1-RON2 in the invasion of bradyzoites. To address this question and confirm the role of rAMA4-RON2$_{L1}$D3 in invasion of bradyzoites, we took advantage of both the specificity and potent inhibitory effect of antibodies generated after immunization with rAMA1 or rAMA4 alone or in complex with their respective RON2 (Figure 28 and 29), to inhibit the invasion of bradyzoites *in vitro*. To this end, we induced the conversion of the 76K into tissue cysts *in vitro* during 10 days, and the cysts were liberated from the infected HFF monolayers by mechanical disruption of the host cells. This allows also the liberation of unconverted tachyzoites that we removed by pepsin digestion as described previously (Mayoral et al., 2020), while keeping intact the bradyzoites that are protected from enzymatic digestion by their cyst wall. Parasites were enumerated and 500 parasites were incubated with either control sera, rAMA1, rAMA1-RON2D3, rAMA4 and rAMA4-RON2$_{L1}$D3 purified IgG prior to be added to 24-well plates containing confluent monolayers of HFFs. After 10 days on HFF monolayers, the number of plaques in each well was determined (Figure 30*A*). The number of plaques reflects the efficiency to invade, while the size of the plaque reflects both the ability of

the parasite to initially replicate and to successively reinvade performing the successive steps of the lytic cycle.

Strikingly, when bradyzoites were incubated with anti-rAMA1 purified IgG, we did not observe any decrease in the number of lysis plaque, while the anti-rAMA1-RON2D3 IgG showed less lysis plaques compared to the control (Figure 30*B*). This showed that AMA1-RON2 is important for invasion of bradyzoites. As expected, the size of the lysis plaques was reduced for both conditions, a result that is likely explained by the fact that bradyzoites rapidly convert into tachyzoites, which mostly use AMA1 to invade in the next steps of invasion (Figure 30*C*). More importantly, bradyzoites incubated with IgG targeting AMA4 alone exhibited an important lower number, as compared to the control (Figure 30*A, B*), or even no plaques when incubated with anti-rAMA4-RON2$_{L1}$D3 IgG.

Altogether, these findings suggest the involvement of AMA1-RON2 and to more extent AMA4-RON2$_{L1}$ complexes in bradyzoite invasion and progression of chronic toxoplasmosis.

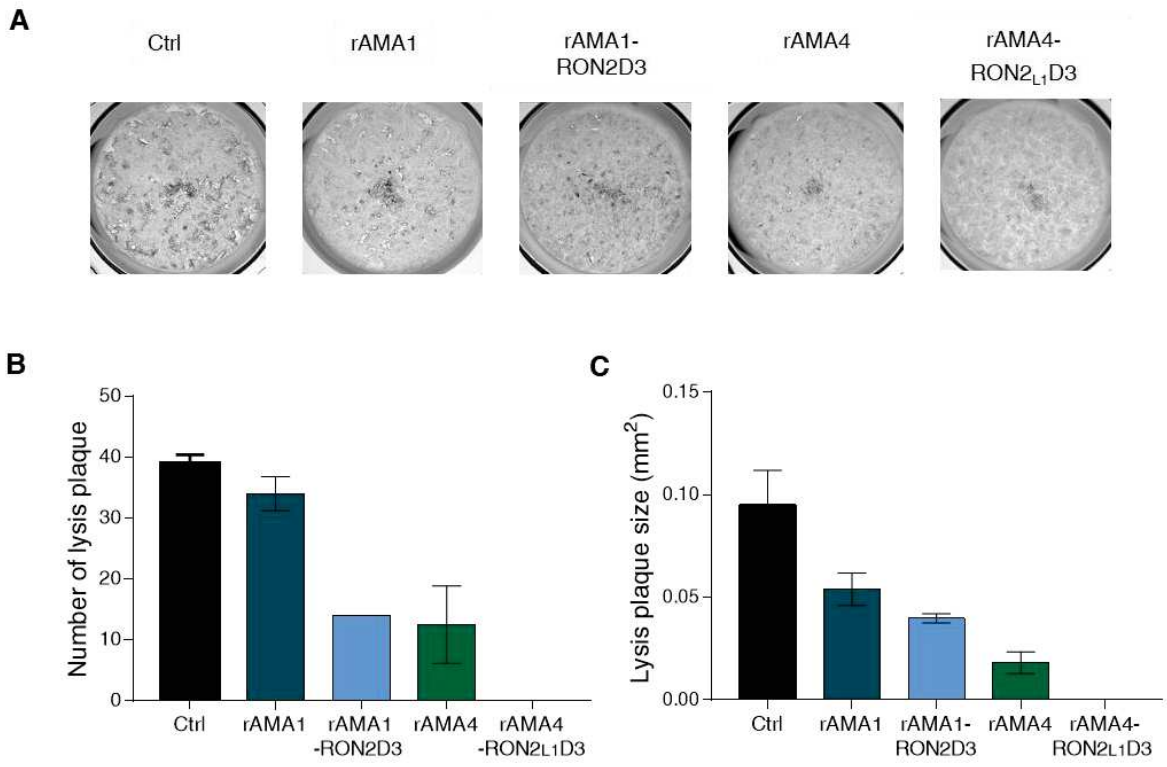


Figure 30: Inhibitory antibodies targeting the invasion complexes inhibit bradyzoite invasion. (A) Plaque assays of HFFs monolayers infected with 500 purified 76K bradyzoites and treated with total IgG from sera of mice immunized with rAMA1, rAMA1-RON2D3, rAMA4, and rAMA4-RON2$_{L1}$D3, and grown for 10 days. (B) Quantification of the number and (C) size of the lysis plaques are shown in the graphs. Results are presented as mean±S.E.M. of duplicates (experiment performed once).

CHAPTER 4: DISCUSSION AND PERSPECTIVES

Members of the Apicomplexan phylum are obligate intracellular parasites. These parasites' survival fully depends on their successful invasion, which encompasses multiple steps, including the crucial formation of the MJ (Besteiro et al., 2011; V. Carruthers & Boothroyd, 2007; Kato, 2018). The assembly of the MJ involves several complexes, which in *T. gondii* seem to be stage specific (Fritz et al., 2012; M. H. Lamarque et al., 2014; Poukchanski et al., 2013). Invasion of *Toxoplasma* takes place at different occasions of the life cycle and is equally necessary for the survival of different stages. The fast-replicative stage tachyzoite invades many different cells types, including immune cells (Lima & Lodoen, 2019; Swierzy et al., 2017), while both sporozoites and bradyzoites use enterocytes as a route for infection after oral ingestion of uncooked meat containing cysts or vegetable/water contaminated by oocysts. Bradyzoites invasion can also take place after rupture of cysts in the context of reactivation of CT, and possibly in immunocompetent individuals when bradyzoites exit from cysts and reinvade new host cells creating new cysts (A. M. Sullivan et al., 2013). However, the extent of this event is poorly understood. Invasion was extensively studied in tachyzoites, less known about in sporozoites, and unexplored in bradyzoites.

Herein, we demonstrated that bradyzoites use a MJ-dependent process and deciphered the components that are implicated in bradyzoite invasion. In addition, we designed a vaccine procedure to target two recombinant MJ complexes, rAMA1-RON2D3 and rAMA4-$RON2_{L1}$D3. This strategy did not only show an efficient protection against acute and chronic toxoplasmosis, but also helped in our understanding of the implication of several invasion effectors during different stages of the parasite. In this section, we will discuss how our study bring clue about the mechanism of invasion of bradyzoites and what are the common features and differences with the invasion of other stages. We will also put our results of vaccination

with AMA-RON complexes in the context of others vaccine strategies for toxoplasmosis and highlight how these results improve our understanding of invasion in tachyzoites and bradyzoites.

4.1. Bradyzoites use a MJ to invade but its molecular composition is slightly different than that of tachyzoites

Although the invasion of bradyzoites is particularly important in toxoplasmosis, MJ components are less studied in bradyzoite invasion. Bradyzoites undergo invasion either when they quit the ingested cysts to invade the intestine's epithelium, or when bradyzoites are released from cysts to reinvade cells. Furthermore, it was not concluded whether bradyzoites use a MJ-dependent invasion process to enter the host cell (Sasono & Smith, 1998), since electron-microscopy was used to capture the invading bradyzoites. As such, it is challenging to use electron-microscopy to investigate the invasion process of the parasite and in particular for bradyzoites due to the limited number of parasites obtained for this stage. Herein, we demonstrated that all MJ proteins of tachyzoites are highly expressed in bradyzoites. Importantly, we detected the characteristic ring-shape staining of RONs at the MJ of invading bradyzoites, demonstrating for the first time that bradyzoites use a MJ-dependent process in their invasion. All the RONs were detected at the MJ. We also detected AMA1 at the MJ of bradyzoites, but the staining of the protein at the MJ was more difficult to detect than in tachyzoites. We initially did not detect AMA1 at the MJ of tachyzoites but with a new batch of anti-AMA1 antibodies, we now clearly detect AMA1 at the residual dot of MJ when the parasite is fully intracellular. This might suggest that the epitopes on AMA1 become accessible only at the end of the invasion process, when the protein is not engaged with RON2 and with the gliding machinery. Using this serum, we also detected AMA1 at the residual MJ of bradyzoites appearing as a small dot thus implying its involvement during invasion. We also

noticed that the staining of AMA1 in micronemes of bradyzoites is less intense than in tachyzoites, which may explain the faint residual dot at the MJ of bradyzoites that might be due to the expression level of AMA1.

We further decorticated the expression of alternate MJ complexes in bradyzoites and showed that AMA2, AMA4 and $RON2_{L1}$ are highly expressed in bradyzoites, and detected both AMA2 and AMA4 associated with bradyzoites MJ. In contrast we failed to detect AMA4 at the MJ of tachyzoites. On another hand, AMA4 was found in the micronemes of tachyzoites but with a lower fluorescent intensity, which might point to the fact that AMA-RON complexes are stage specific but that doesn't deny the fact that they are expressed in other stages even at low levels. These findings also propose that bradyzoites do not primarily use AMA1 to invade. Indeed, our results showed that targeting AMA1-RON2 complex with mice sera had less impact on invading bradyzoites, than targeting AMA4-$RON2_{L1}$. Furthermore, AMA1 might be replaced by AMA2 in bradyzoites. As we showed that AMA2 is abundant and present at the MJ of invading bradyzoites. This scenario would be plausible because AMA2 can interact directly with RON2 (M. H. Lamarque et al., 2014), although with lower affinity than AMA1-RON2 interaction. Additionally, RON2 is present at the MJ of bradyzoites, together with all the members of the complex RON5, RON4, RON8, and $RON4_{L1}$. The presence of the full MJ RONs complex suggests some common functional aspects of invasion with tachyzoite MJ (Besteiro et al., 2009; Guérin, El Hajj, et al., 2017). Although, the macromolecular RON complex was detected in bradyzoites, assuming that it interacts with either AMA1 or AMA2, we have no evidence that it might interact with AMA4. We cannot exclude that the two complexes may be linked. In that regard, an immunoprecipitation assay would be helpful to fish out all proteins interacting with AMA4, and test if other RONs, like RON2, RON4, RON5 and RON8 may be also part of the complex with $RON2_{L1}$. In addition to that, AMA2 prominent presence at the bradyzoite MJ may infer its essential role in invasion during this stage that

might complement AMA4. Future investigations using mutant AMA2 parasites must be done to unravel its function in bradyzoite stage.

Intriguingly, the staining of the MJ proteins of bradyzoites at the end of the invasion process is quite different from what is observed in tachyzoites. In tachyzoites, the end of invasion is marked by a well-defined residual dot visible by IFAs, corresponding to junction proteins at the posterior end of the parasite. However, our data did not only show a punctate spot at the posterior end of newly invaded bradyzoites, but also a trail of AMA2, AMA4, RON2, and RON5. These trails were more frequently observed when staining is done at 5 min or 10 minutes post-invasion. Interestingly, ROP1, a rhoptry protein translocated to the PVM at the early step of PVM formation (Saffer et al., 1992), also decorated a trail with RON5 at the posterior end on an intracellular bradyzoite 30 min after invasion (Figure 31). This observation may suggest that the trails corresponds to the PVM which might be translocated away from the original site of invasion due to bradyzoite high motility (Dzierszinski et al., 2004). Moreover, this observation is reminiscent to the trails observed at the posterior end of invading sporozoites (Tartarelli et al., 2020). During sporozoites invasion, the trails were shown to be decorated by dense granule proteins released during invasion and were suggested to be derived from the tubulovesicular network formed at the posterior end of the parasite. These trails defined the routes followed by individual sporozoites during their intracellular migration. Additionally, ultrastucture analysis of the sporozoite trails by transmission electron-micrscopy revealed that they either appear as membranous strands stemming from the center of the PVM posterior pole, or as clusters of vesicles and tubules released in the host cell cytoplasm from the sporozoite back. In our study, the trails observed in bradyzoites showed similar sturcture to that of sporozoites. Furhter investigations should be performed to check whether bradyzoites trails possess similar morphology and contain dense granules proteins as that of sporozoite, in addition to whether they are the result from migrating.

Remarkably, the authors found extracelluar parasites surrounding by two membranes; the innermost membrane corresponding to the PVM generated during the first MJ-invasion event and the second aquired by the sporozoite during the escape from the host cell and deriving from the host cell membrane. They also found occasionally double-layered sporozoites in the process of invading a new host cell. Altogether, these observations strongly support that sporozoites are able to do cell traversal and cell-to-cell passage, as previously suggested (Dubey, 1997; Speer & Dubey, 1998) and that this process might contribute to reach suitable replicative site in the intestine. Indeed, At 2 h post-infection most of the sporozoites were found in ileal enterocytes and occasionally in goblet cells, while later at 6–12 h post-infecion, sporozoites were not detected in the intestinal epithelium, but found exclusively in cells of the underlying lamina propria, which support parasite migation (Dubey, 1997; Speer & Dubey, 1998). Furtur work is needed to establish whether bradyzoites also use cell-to-cell traversal in intestin and if the trails production has an essential role in generating the force to propel the parasite during cell traversal as suggested (Tartarelli et al., 2020) or if they are only the consequence of the parasites migration.

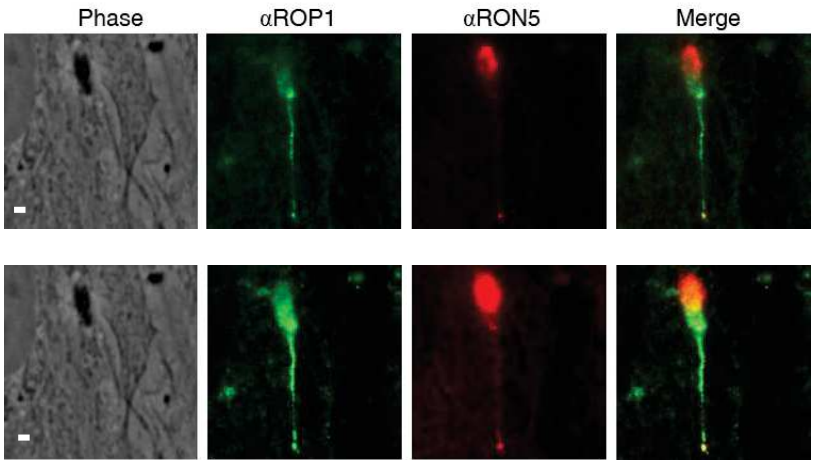


Figure 31: Localization of ROP1 and RON5 in bradyzoites 30 min after invasion. IFAs on Pru bradyzoites invading HFF monolayer using anti-RON1 (green), and anti-RON5 (red). Scale bars, 2µm.

4.2. Role of AMA4 in invasion of bradyzoites

In order to emphasize on the role of AMA4 in invasion, we generated AMA4 knockouts in type I (RH*Δku80*) and type II (Pru) tachyzoites and checked first the potential role of AMA4 in invasion of tachyzoites. To our surprise, lysis plaques obtained by RH KO-AMA4 parasites are fewer and smaller compared to those of the wild type, which could implicit the involvement of AMA4 in the invasion of tachyzoites, despite the fact that AMA4 is not well expressed in tachyzoites. We next confirmed a slight reduction of invasion of tachyzoites in the absence of AMA4 using a specific invasion assay. This result definitively demonstrated the implication of AMA4 during the invasion step. Indeed, its role until now was only defined by inhibition of invasion of KO-AMA1 using $RON2_{L1}$ peptide (Parker et al., 2016). Even though RH KO-AMA4 tachyzoites showed a significant (20%) defect in invasion *in vitro*, this phenotype had no impact on virulence in mice model, since mice infected with RH KO-AMA4 succumbed to infection at the same time as control mice. This discrepancy between *in vivo* and *in vitro* studies could be simply due to the multiple parameters of parasite dissemination and clearance *in vivo* that would mask the small defect in invasion. More resolution of the impact of AMA4 in acute phase of type I strain might be obtained by injection of lower dose of parasites.

The presence of AMA4 at the MJ of bradyzoites prompted us to investigate its role during invasion of bradyzoites. For this, we generated a KO-AMA4 in the type II Pru strain, a cyst-forming strain. We confirmed that AMA4 is important for invasion of tachyzoites in this strain type, and that resembles the importance of KO-AMA1 in type I RH*Δku80* strain. In addition, a plaque assay using bradyzoites purified from brain cysts showed a reduction in the number of plaques of Pru KO-AMA4 strain compared to wild type stain, highlighting the importance of AMA4 in invasion of bradyzoites. In contrast to type I strain, mice infected with Pru KO-AMA4 tachyzoites survived the acute phase which may suggest a more profound role of AMA4 in acute phase of type II Pru parasites. However, this result needs to be repeated.

We next determined the ability of Pru KO-AMA4 parasites to generate a chronic infection. Mice infected with a non-lethal dose of Pru KO-AMA4 tachyzoites showed a marked reduction in the number of cysts in the brain, as compared to wild type strain. This observation might be due to an alteration of invasion in reinvading bradyzoites in the brain, since bradyzoites are motile entities that exist cyst during the chronic phase to reinvade and form new cysts thereby increasing the parasitic burden (Dzierszinski et al., 2004; E. Watts et al., 2015). It might be also the consequence of a reduced parasitemia during the acute phase of infection (due to the small defect in invasion of Pru KO-AMA4 tachyzoites), that eventually leads to less tachyzoites reaching the brain and developing a chronic infection. Both hypotheses are not mutually exclusive. At this stage, and in order to obtain better clue about the role of AMA4 *in vivo*, it is particularly important to confirm a role of AMA4 during the acute phase. Even though we were not able to detect AMA4 at the moving junction of tachyzoite, it might be due to its low amounts in tachyzoites and does not deny its probable presence and involvement in invasion at this stage. Yet, targeting AMA4 in tachyzoites by 2mg/ml IgG from mice immunized with AMA4-RON2L1D3, inhibited the parasite invasion by around 20%. This result opens the door for more speculation on the limited role that AMA4 plays in tachyzoites.

We then infected mice with Pru KO-AMA4 cysts. Surprisingly, we observed that mice infected peritoneally with Pru KO-AMA4 tachyzoites or by oral gavage of cysts containing bradyzoites showed nearly the same level of reduction (50%) in cyst burden in the brain. Those experiments should be repeated in order to confirm the observed phenotype, but several explanations may interpret these results. First, we can't exclude that bradyzoites does not use AMA4 to invade enterocytes. We can also speculate that they use it but other AMA-RONs pairs may be also functional at this step. In consequence, some mutants KO-AMA4 bradyzoites would still invade the enterocytes, and then will differentiate into tachzyoites and exponentially replicate leading to acute toxoplasmosis. At the end of the acute phase, the number of mutants

that reach the brain would become comparable to the number of mutants reaching the brain after an intraperitoneal injection of tachyzoites.

As such, it is still not conclusive whether AMA4 has a profound role during the acute phase and if the decrease in cysts burden is due mostly to a defect in acute phase or mainly to a defect in reinvasion of bradyzoites after cysts rupture during chronic infection. While our overall results support the second hypothesis, further work are needed to prove it. Histopathology of the brains of mice infected by Pru or Pru *KO-AMA1* may help to support this assumption. Indeed, the presence of cyst clusters in some region of the brain was proposed to be linked to the exit and reinvasion of bradyzoites from cysts. One might therefore expect to see less clusters in the brain of mice infected with KO-AMA4.

Deciphering the function of AMA4-RON2$_{L1}$ would also require the generation of KO-RON2$_{L1}$ strain, and the conduction of all the required *in vitro* and *in vivo* experiments for its characterization. Another approach to study the contribution of AMA4 in tachyzoite invasion is though immunosuppression of mice infected with AMA4 mutant parasites during chronic toxoplasmosis. This could be attained by treating mice with dexamethasone, an immunosuppressant, a month post immunization. In a normal scenario, reactivation will occur during treatment by which bradyzoites will differentiate into tachyzoites. In case of a defect in tachyzoite invasion a delay in mortality should be observed in comparison with wild type strain.

4.3. AMA-RON2 complexes as a strategy to vaccinate against toxoplasmosis

To date there is no licensed vaccine available for human use. Yet, it is essential to develop one along with a vaccination strategy against toxoplasmosis due to the complications accompanied with latent phase reactivation. It has dire consequences not only in immunocompromised patients, but it might have as well in immunocompetent individuals on the long run. As such, we focused in our study on finding vaccine candidates that target both

chronic and acute toxoplasmosis. Due to our interest in the invasion machinery of *T. gondii*, we targeted the MJ of the invading parasites to prevent the initial stage of infection and other rounds of reinvasion upon dissemination of the parasite through its host. One of the key players in invasion is the MJ complex AMA1-RON2. As mentioned in introduction, AMA1 has been used in several studies to target toxoplasmosis either by protein, multi-epitope or DNA vaccines. Studies using AMA1 to vaccinate against malaria is also widely investigated (Berry et al., 2019; Laurens et al., 2017; Sirima et al., 2017). Yet, AMA1 is mostly specific to tachyzoites and proteins that are stage specific are less likely to protect against other stages in context of a vaccine. Moreover, the main route of infection is by ingestion of cysts or oocytes containing bradyzoites or sporozoites, respectively. Consequently, we tried to target different stages of the *T. gondii* by not only using AMA1 but to vaccinate with AMA4 as well since we showed its importance in bradyzoite invasion. One promising AMA1 vaccination approach was published recently for *Plasmodium* (Srinivasan et al., 2014). Srinivasan *et al.* introduced the significance of using recombinant complex (AMA1-RON2L) instead of AMA1 or RON2 protein alone in providing protection a lethal *Plasmodium* challenge in mice (Srinivasan et al., 2014) and *Aotus* monkeys (Srinivasan et al., 2017). Following a similar strategy, we obtained comparable results whereby the vaccine strategy was significantly enhanced against toxoplasmosis when rAMA1 was put in complex with the peptide RON2D3. Interestingly, rAMA1-RON2D3 generated protection against acute and chronic toxoplasmosis with a significant reduction in brain cysts (around 80%) and 70% survival rate compared to rAMA1 alone. One important aspect of vaccination in protecting against toxoplasmosis is the production of protective antibodies that block parasitic infection (Sayles et al., 2000). We showed that immunization with rAMA1-RON2D3 elicited a strong immune response which was illustrated by high specific antibody secretion that we revealed to be curtail for protection. We detected high levels of IgG1 and IgG2a that corresponds to a Th2 and Th1 immune

response, respectively (Snapper & Paul, 1987; Stevens et al., 1988). Cell mediated immunity is marked by Th1 pro-inflammatory cytokines, including gamma interferon (Dong & Flavell, 2000). On the contrary, humoral immunity is induced by Th2 anti-inflammatory cytokines, including IL-4, IL-5, IL-6, and IL-10 (Dong & Flavell, 2000). As such, further experiments must be done in order to address the type of provoked immune response that is aiding in protection against toxoplasmosis.

To explain a better protection when AMA1 is complexed with RON2, a plausible scenario of this enhanced protection by the complex may be due to the exposure of AMA1 immunogenic epitopes upon binding of RON2D3 to rAMA1 pocket. A similar hypothesis was proposed by Srinivasan *et al.* who showed a switch in antibodies that target a newly exposed loop upon binding of RON2 to AMA1 hydrophobic groove aiding in improved AMA1-RON2L vaccination efficacy against malaria (Srinivasan et al., 2014). Our data showed that sera from mice immunized with rAMA1-RON2D3 specifically recognize AMA1 protein only, not RON2, which is likely explained by the small RON2 peptide used. This could further emphasize that protection might be induced by targeting mainly AMA1 exposed loops. Furthermore, we demonstrated that anti-rAMA1-RON2D3 IgG are better in inhibiting tachyzoites invasion when compared to anti-rAMA1 IgG. Interestingly, when incubated with sera the parasites were able to somehow reversibly attach after secreting their rhoptry content inside the host cell, suggesting that in presence of inhibitory antibodies the parasites were not able to form properly the tight attachment (MJ) and proceed in invading, as observed by removing either AMA1 or RON2 or by disrupting the AMA1-RON2 interaction (M. H. Lamarque et al., 2014). As such, IgG produced against the complex is possibly preventing AMA1 and RON2 binding leading to MJ disruption and inhibition of invasion.

We also tested the protection using AMA4 alone or in complex with $RON2_{L1}$. Strikingly, protection against both acute and chronic phases of toxoplasmosis was improved

upon immunization with the rAMA4-RON2$_{L1}$D3 complex. Survival time was prolonged by few days in rAMA4-RON2$_{L1}$D3 immunized mice and number of brain cysts significantly reduced by 54% with a mixed Th1/Th2 immune response as that induced by rAMA1-RON2D3. Yet, the data suggest that the chronic phase of the disease was the main target upon using rAMA4-RON2$_{L1}$D3 complex in vaccination. Anti-rAMA4-RON2$_{L1}$D3 IgG were specifically targeting AMA4-RON2$_{L1}$ MJ and inhibiting invasion of KO-AMA1 parasites. Moreover, antibody from mice immunized with rAMA4-RON2$_{L1}$D3 were specifically recognizing AMA4 protein, not RON2$_{L1}$. Once again, the protection was enhanced by coupling AMA4 with its partner RON2$_{L1}$, illustrating the importance of vaccination using the complex. Likewise, this enhanced protection might be due to the exposure of immunogenic epitopes that were accessible with rAMA4 alone. Interestingly, the combination of rAMA1-RON2D3 and rAMA4-RON2$_{L1}$D3 enhanced protection against chronic toxoplasmosis. This result might be due to the fact that we targeted two forms of the parasite that act through different routes of infection. In contrast, immunization with both complexes was of comparable protection as of rAMA1-RON2D3 during the acute phase.

We repeatedly observed a better protection to chronic phase using vaccination with rAMA1-RON2D3 than using the rAMA4-RON2$_{L1}$D3 complex. While counterintuitive because AMA4 is mainly used for invasion of bradyzoites and AMA1 for tachyzoites, this could be related to the duration at which each stage lasts. Upon challenging mice with oral gavage of cysts, bradyzoites transform to tachyzoites and disseminate from the intestinal mucosa. It was suggested that invasion of intestinal enterocytes occurs within 2 hours after oral gavage and switching to tachyzoites form is complete within 18 hours. Later, tachyzoites are detectable within 24 hours and dissemination to the brain, lungs, and other organs is verified in 4 days (Dubey, 1997; Sekandarpour et al., 2018; Weiss & Kim, 2000). As such, time of tachyzoites exposure to the immune system is longer than that of bradyzoites, rendering

immunization by rAMA1-RON2D3 more effective in protection against acute toxoplasmosis. Additionally, less tachyzoites at the end of acute phase is immediately translates in less parasites reaching the brain and eventually less cysts. Moreover, the rAMA1-RON2D3 might take part also in protection during bradyzoite invasion of the intestinal epithelium or during the chronic phase when bradyzoite invade neighboring neurons.

Taking into consideration that we tried only one dose for immunization (40μg) of C57BL/6 mice, it would be interesting to test higher doses in an attempt to enhance protection against toxoplasmosis. Additionally, long-term immunity is what is needed out of a vaccine. As such, challenging after several months post-immunization is an ideal way to study the efficiency of MJ complexes as successful vaccine candidates. Importantly, a study suggested the use AMA1 recombinant protein can be used in human diagnosis for toxoplasmosis (Ferra et al., 2020), providing evidence of its high specificity and efficiency in detecting *Toxoplasma* IgG and IgM in patients serum. Thereupon, AMA1 is one of the most targeted proteins to provide protection against toxoplasmosis in humans. In the future, it would be also of great importance to test if sera from patient with acquired immunity against *Toxoplasma*, have antibodies against the different recombinant proteins. Fundamentally, our complexes should also be examined with adjuvants that are approved in humans including aluminium salts, emulsions, Toll-like receptor agonists (CpG ormonophosphoryl lipid A) and several others (Del Giudice et al., 2018).

By using rAMA1-RON2D3 and rAMA4-RON2$_{L1}$D3 for immunization, we were able to target the asexual forms of *T. gondii*; bradyzoites and tachyzoites, as concluded from the challenge experiments with either stages. Vaccination to target the sexual stage in felines would be of equal interest. *In vivo* transcriptome analysis from ToxoDB, predicted a high expression of mainly *AMA4* in addition to *RON2$_{L1}$ and AMA2*, with a complete absence of *AMA1, AMA3 and RON4* together with a very low expression of *RON2*, *RON4$_{L1}$*, *RON5* and *RON8* in

merozoites (Figure 32). This result suggests that merozoites use MJ-dependent process mainly driven by AMA4-RON2$_{L1}$ pair and involving also AMA2, possibly in complex with RON2/RON4$_{L1}$/RON5/RON8. Interesting preliminary data from collaborators showed the expression of AMA4 in late schizont using an organoid model (Bruno Martorelli Di Genova and Laura Knoll, University of Madison, USA; personal communication). Therefore, it would be interesting to assess the protection against merozoites especially using rAMA4-RON2$_{L1}$D3 that seems to be dominant among other moving junction complexes. Even though the sexual life cycle of *Toxoplasma* only takes place in feline intestine, it is now possible to study this stage in mice. A recent study showed that the lack of delta-6-desaturase activity, involved in lipid metabolism, in feline intestine is essential for *T. gondii* sexual cycle (Genova et al., 2019). Based on this finding, they developed a mice model capable of inducing the sexual stage though inhibiting this enzyme. It is interesting to use this model in future studies to assess the protection induced upon immunization with rAMA4-RON2$_{L1}$D3 against the merozoites.

Another form of the parasite released into the environment by felids is sporozoite stage, another key contributor to the transmission of the parasite. Sporozoites express AMA1-RON2 (Fritz et al., 2012; Poukchanski et al., 2013), AMA4-RON2$_{L1}$ (Parker et al., 2016) and AMA3-RON2$_{L2}$ (M. H. Lamarque et al., 2014; Poukchanski et al., 2013). As such, using recombinant complexes of those three MJ proteins for immunization of mice to target sporozoites would be interesting.

We showed that AMA2 decorates the moving junction of bradyzoites. Hence, using recombinant AMA2-RON2 complex to immunize mice and check for protection against acute and chronic toxoplasmosis should be considered. As this strategy will not only test the efficiency of a vaccine in protection but will give as well an insight on the role of AMA2 in bradyzoite invasion.

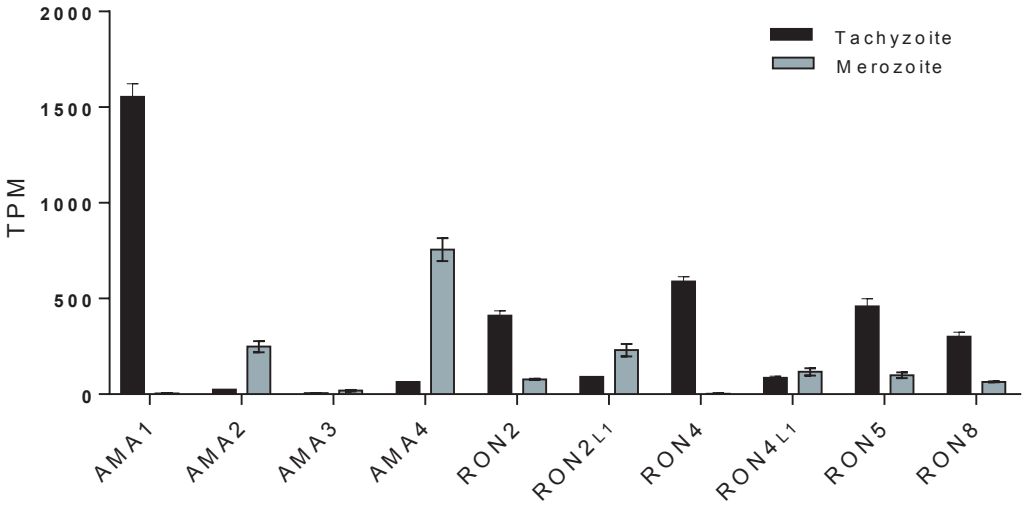


Figure 32: *In vivo* transcriptome analysis of *T. gondii* in tachyzoite and day 5 merozoite stages. Prediction of *T. gondii AMA1, AMA2, AMA3, AMA4, RON2, RON2$_{L1}$, RON4, RON4$_{L1}$, RON5* and *RON8* gene expression in tachyzoite and day 5 merozoite stages.

4.4. The vaccine study as a tool to decipher the function of AMA-RONs complexes at different stages

In the protocol of immunization with rAMA1-RON2D3 complex or with rAMA4-RON2$_{L1}$D3 complex, following by challenge with high dose of tachyzoites by intraperitoneal route, the parasites remain as tachyzoites and replicate to the point of inducing death of mice. Yet, we measure the efficiency of the recombinant proteins to mount a protective immunity against tachyzoite form only. We obtained a good protection after immunization by rAMA1-RON2D3 but not with rAMA4-RON2$_{L1}$D3. This result corroborates well the level of expression and respective implication of the two complexes at tachyzoite stage. While AMA1-RON2 is functionally necessary (M. Lamarque et al., 2011; M. H. Lamarque et al., 2014), and used as the main complex for invasion of tachyzoites, AMA4-RON2$_{L1}$ is barely expressed and contribute partially to invasion and the acute phase (discussed above). Even though Pru KO-AMA4 reduced the virulence of the strain in mice during acute phase, giving AMA4 a potential role in tachyzoites. However, the case of immunization might be different since we challenged

with a wild type strain, highly expressing AMA1 and presumably masking in function the low expressed AMA4. Consequently, AMA1 might be the main target upon immunization in both complexes in the acute phase.

In the second protocol of immunization with rAMA1-RON2D3 or rAMA4-RON2$_{L1}$D3 complexes, followed by challenge with non-lethal dose of cyst to measure brain cysts load during chronic toxoplasmosis, the interpretation of the results is more challenging. Indeed, the protection may be due to immunity acting at the level of intestinal enterocytes upon bradyzoite release to infect. Consequently, less invading bradyzoites leads to lower conversion to tachyzoites stage, less dissemination of tachyzoites and ultimately less cyst formation. The second part of protection might be during acute phase by inhibition of invasion of tachyzoites when they successively invade cells. The third part of protection might be at the level of the brain, since bradyzoites in dormant cyst are motile, able to escape then reinvade forming more cysts (Dzierszinski et al., 2004) and replication within mature tissue cysts (E. Watts et al., 2015). When we immunized with rAMA4-RON2$_{L1}$D3, we obtained an important decrease in parasite burden in brain. Knowing that this complex did not protect well against acute phase, this suggests that the control of infection might be at the initial invasion of bradyzoites in intestine and/or at the step of reinvasion of bradyzoites following cysts rupture. Both cases suggest a prime role of AMA4 at bradyzoite stage, a conclusion also supported by the fact we showed that AMA4-RON2$_{L1}$ is mainly expressed in the bradyzoite stage. In support of this conclusion are also our results of inhibition of invasion using anti-AMA4-RON2$_{L1}$ antibodies. While the anti-rAMA4-RON2$_{L1}$D3 IgG did not inhibit the invasion of tachyzoites, they inhibited efficiently the invasion of bradyzoites whereby no plaques were obtained. Conversely, anti-rAMA1-RON2D3 IgG was able to inhibit the invasion of bradyzoites *in vitro*. Altogether these astonishing results illustrate that both AMA1-RON2 and AMA4-RON2$_{L1}$ are involved during bradyzoite invasion but AMA4-RON2$_{L1}$ being likely the most utilized.

For both complexes, we obtained a better protection after immunization with complexes that by injection of AMA alone. Equally the antibodies generated are better to inhibit the invasion when they are targeted AMA in complex with its specific partner. This result indirectly reinforces the importance of the interaction of AMA1 with RON2 and AMA4 with $RON2_{L1}$ for invasion. Since AMA2 is highly expressed in bradyzoites, compared to tachyzoites, and are present at the MJ of bradyzoites; it is possible that it acts in complex with RON2 (as discussed before) and then it might be worth trying protection with the AMA2-RON2 complex and see if antibodies produced are able to inhibit the invasion of bradyzoites more specifically than tachyzoites. This might be, in addition to the characterization of a KO-AMA2, a way to address the respective role of AMA2 in tachyzoites and bradyzoites.

4.5. Presence of different MJ paralogs in the same parasitic stage

The main reason for the expression of AMA1-RON2, AMA2-RON2 and AMA4-$RON2_{L1}$ complexes is still unknown. In our study, we showed that AMA4-$RON2_{L1}$ is mainly utilized by bradyzoites unlike AMA1-RON2 complex. We can speculate that during reactivation of cysts, the bradyzoites use different pairs of AMA-RONs to overcome the huge humoral response mounted against AMA1, allowing to escape the inhibitory effect of anti-AMA1 antibodies generated during the acute phase of the initial infection. Furthermore, the fast switch from bradyzoite to tachyzoite stage during invasion of the intestinal epithelium or reactivation hold a transitional phase. Hence, the expression of AMA1-RON2 is not completely suppressed in bradyzoites. This low expression of AMA1-RON2 might be important to support the newly differentiated tachyzoites that later highly upregulates AMA1.

Different complexes may be used for invasion of different cell types. AMA4-$RON2_{L1}$ is expressed and utilized significantly in both bradyzoites (this study) and sporozoites (M. H. Lamarque et al., 2014). It also seems to be expressed in merozoites (Figure 30). What is

common between those three stages is the they both infect the intestinal epithelium containing enterocytes with microvilli at their apical surface and mucus (Allaire et al., 2018). This tough barrier might require special MJ complexes and AMA4 allocates a unique structure characterized by a long stalk that might aid in invasion (Parker et al., 2016). Indeed, tachyzoites mainly express AMA1-RON2, however bradyzoite and sporozoite and merozoites have a repertoire of MJs (as mentioned before) with a revolutionary imprint reflecting their unique feature for invading barriers and different types of cells. In addition, RON8, $RON2_{L1}$, $RON2_{L2}$ and $RON4_{L1}$ are coccidian specific (Guérin, El Hajj, et al., 2017; Parker et al., 2016; Poukchanski et al., 2013, p. 22013; Straub et al., 2009) and are mainly expressed at the stages that are involved in breaching the enterocytes barrier. This highlight the functional specificity of each stage and the variability of their targets to attain a successful infection.

Another reason for the expression of several AMA/RON pair might be due to plasticity. When one MJ is not able to be formed due to certain external barriers, for instance being highly targeted by the immune response, or because of physical barriers with no close association between the parasite and the host cell, another MJ assembles to allow the parasite to invade.

CHAPTER 5: CONCLUSION

We reported for the first time the presence of a MJ during bradyzoite invasion and marked the presence of MJ proteins that are unique to this stage or characterized previously in other stages. We mainly focused on AMA4 which is essential for bradyzoite propagation. Future work must focus on revealing the RON complex associated with AMA4 and study the role of AMA2 expressed at the chronic phase. Furthermore, we targeted the formation of two MJ complexes (AMA1-RON2 and AMA4-RON2$_{L1}$). The efficacy of rAMA1-RON2D3 in protection against chronic and acute toxoplasmosis, and rAMA4-RON2$_{L1}$D3 specifically against chronic toxoplasmosis, highlighted both complexes for being successful vaccine candidates. We illustrated that the complex of AMA and RON protein provides better protection than AMA protein alone. In addition, we studied the potential role of immunized mice IgG in protection against toxoplasmosis through the targeting of MJ. Interestingly, treating tachyzoites and bradyzoites with those IgGs helped unravel the specific MJs used by those stages. More MJs must be included like AMA2-RON2 and AMA3-RON2$_{L2}$ in an attempt to target all *T. gondii* stages. Further studies must be done in order to translate this vaccination strategy for higher primates, like injection intervals, adjuvants, and immunization routes.

List of References

AbouLaila, M. (2019). Identification, Characterization, and Protective Effect of the Apical Membrane Antigen-1 (AMA-1) Homolog from the Argentina Strain of Babesia bigemina. 1(1), 7.

Afonso, E., Thulliez, P., & Gilot-Fromont, E. (2006). Transmission of Toxoplasma gondii in an urban population of domestic cats (Felis catus). International Journal for Parasitology, 36(13), 1373–1382. https://doi.org/10.1016/j.ijpara.2006.07.010

Ahmadpour, E., Sarvi, S., Hashemi Soteh, M. B., Sharif, M., Rahimi, M. T., Valadan, R., Tehrani, M., Khalilian, A., Montazeri, M., Fasihi-Ramandi, M., & Daryani, A. (2017). Enhancing immune responses to a DNA vaccine encoding Toxoplasma gondii GRA14 by calcium phosphate nanoparticles as an adjuvant. Immunology Letters, 185, 40–47. https://doi.org/10.1016/j.imlet.2017.03.006

Aikawa, M., Miller, L., Johnson, J., & Rabbege, J. (1978). Erythrocyte entry by malarial parasites. A moving junction between erythrocyte and parasite. Journal of Cell Biology, 77(1), 72–82. https://doi.org/10.1083/jcb.77.1.72

Ajzenberg, D., Bañuls, A. L., Su, C., Dumètre, A., Demar, M., Carme, B., & Dardé, M. L. (2004). Genetic diversity, clonality and sexuality in Toxoplasma gondii. International Journal for Parasitology, 34(10), 1185–1196. https://doi.org/10.1016/j.ijpara.2004.06.007

Alday, P. H., & Doggett, J. S. (2017). Drugs in development for toxoplasmosis: advances, challenges, and current status. Drug Design, Development and Therapy, 11, 273–293. https://doi.org/10.2147/DDDT.S60973

Alexander, D. L., Mital, J., Ward, G. E., Bradley, P., & Boothroyd, J. C. (2005). Identification of the moving junction complex of Toxoplasma gondii: a collaboration between distinct secretory organelles. PLoS Pathogens, 1(2), e17. https://doi.org/10.1371/journal.ppat.0010017

Allahyari, M., Mohabati, R., Amiri, S., Esmaeili Rastaghi, A. R., Babaie, J., Mahdavi, M., Vatanara, A., & Golkar, M. (2016). Synergistic effect of rSAG1 and rGRA2 antigens formulated in PLGA

microspheres in eliciting immune protection against Toxoplasama gondii. Experimental Parasitology, 170, 236–246. https://doi.org/10.1016/j.exppara.2016.09.008

Allaire, J. M., Crowley, S. M., Law, H. T., Chang, S.-Y., Ko, H.-J., & Vallance, B. A. (2018). The Intestinal Epithelium: Central Coordinator of Mucosal Immunity. Trends in Immunology, 39(9), 677–696. https://doi.org/10.1016/j.it.2018.04.002

Andenmatten, N., Egarter, S., Jackson, A. J., Jullien, N., Herman, J.-P., & Meissner, M. (2013). Conditional genome engineering in Toxoplasma gondii uncovers alternative invasion mechanisms. Nature Methods, 10(2), 125–127. https://doi.org/10.1038/nmeth.2301

Bai, T., Becker, M., Gupta, A., Strike, P., Murphy, V. J., Anders, R. F., & Batchelor, A. H. (2005). Structure of AMA1 from Plasmodium falciparum reveals a clustering of polymorphisms that surround a conserved hydrophobic pocket. Proceedings of the National Academy of Sciences, 102(36), 12736–12741. https://doi.org/10.1073/pnas.0501808102

Balaji, S., Babu, M. M., Iyer, L. M., & Aravind, L. (2005). Discovery of the principal specific transcription factors of Apicomplexa and their implication for the evolution of the AP2-integrase DNA binding domains. Nucleic Acids Research, 33(13), 3994–4006. https://doi.org/10.1093/nar/gki709

Bannoura, S., El Hajj, R., Khalifeh, I., & El Hajj, H. (2018). Acute disseminated encephalomyelitis and reactivation of cerebral toxoplasmosis in a child: Case report. IDCases, 13, 4. https://doi.org/10.1016/j.idcr.2018.e00434

Bargieri, D. Y., Andenmatten, N., Lagal, V., Thiberge, S., Whitelaw, J. A., Tardieux, I., Meissner, M., & Ménard, R. (2013). Apical membrane antigen 1 mediates apicomplexan parasite attachment but is dispensable for host cell invasion. Nature Communications, 4, 2552. https://doi.org/10.1038/ncomms3552

Beauvillain, C., Juste, M. O., Dion, S., Pierre, J., & Dimier-Poisson, I. (2009). Exosomes are an effective vaccine against congenital toxoplasmosis in mice. Vaccine, 27(11), 1750–1757. https://doi.org/10.1016/j.vaccine.2009.01.022

Beck, H.-P., Blake, D., Dardé, M.-L., Felger, I., Pedraza-Díaz, S., Regidor-Cerrillo, J., Gómez-Bautista, M., Ortega-Mora, L. M., Putignani, L., Shiels, B., Tait, A., & Weir, W. (2009). Molecular approaches to diversity of populations of apicomplexan parasites. International Journal for Parasitology, 39(2), 175–189. https://doi.org/10.1016/j.ijpara.2008.10.001

Beck, J. R., Chen, A. L., Kim, E. W., & Bradley, P. J. (2014). RON5 Is Critical for Organization and Function of the Toxoplasma Moving Junction Complex. PLOS Pathogens, 10(3), e1004025. https://doi.org/10.1371/journal.ppat.1004025

Beghetto, E., Nielsen, H. V., Del Porto, P., Buffolano, W., Guglietta, S., Felici, F., Petersen, E., & Gargano, N. (2005). A combination of antigenic regions of Toxoplasma gondii microneme proteins induces protective immunity against oral infection with parasite cysts. The Journal of Infectious Diseases, 191(4), 637–645. https://doi.org/10.1086/427660

Berry, A. A., Gottlieb, E. R., Kouriba, B., Diarra, I., Thera, M. A., Dutta, S., Coulibaly, D., Ouattara, A., Niangaly, A., Kone, A. K., Traore, K., Tolo, Y., Mishcherkin, V., Soisson, L., Diggs, C. L., Blackwelder, W. C., Laurens, M. B., Sztein, M. B., Doumbo, O. K., … Lyke, K. E. (2019). Immunoglobulin G subclass and antibody avidity responses in Malian children immunized with Plasmodium falciparum apical membrane antigen 1 vaccine candidate FMP2.1/AS02A. Malaria Journal, 18(1), 13. https://doi.org/10.1186/s12936-019-2637-x

Besteiro, S., Dubremetz, J.-F., & Lebrun, M. (2011). The moving junction of apicomplexan parasites: a key structure for invasion. Cellular Microbiology, 13(6), 797–805. https://doi.org/10.1111/j.1462-5822.2011.01597.x

Besteiro, S., Michelin, A., Poncet, J., Dubremetz, J.-F., & Lebrun, M. (2009). Export of a Toxoplasma gondii Rhoptry Neck Protein Complex at the Host Cell Membrane to Form the Moving Junction during Invasion. PLOS Pathogens, 5(2), e1000309. https://doi.org/10.1371/journal.ppat.1000309

Bichet, M., Joly, C., Hadj Henni, A., Guilbert, T., Xémard, M., Tafani, V., Lagal, V., Charras, G., & Tardieux, I. (2014). The toxoplasma-host cell junction is anchored to the cell cortex to sustain parasite invasive force. BMC Biology, 12(1), 773. https://doi.org/10.1186/s12915-014-0108-y

Blader, I. J., & Saeij, J. P. (2009). Communication between Toxoplasma gondii and its host: impact on parasite growth, development, immune evasion, and virulence. APMIS: Acta Pathologica, Microbiologica, et Immunologica Scandinavica, 117(5–6), 458–476. https://doi.org/10.1111/j.1600-0463.2009.02453.x

Blanchard, N., Dunay, I. R., & Schlüter, D. (2015). Persistence of Toxoplasma gondii in the central nervous system: a fine-tuned balance between the parasite, the brain and the immune system. Parasite Immunology, 37(3), 150–158. https://doi.org/10.1111/pim.12173

Boothroyd, J. C. (2009). Toxoplasma gondii: 25 years and 25 major advances for the field. International Journal for Parasitology, 39(8), 935–946.

Bougdour, A., Maubon, D., Baldacci, P., Ortet, P., Bastien, O., Bouillon, A., Barale, J.-C., Pelloux, H., Ménard, R., & Hakimi, M.-A. (2009). Drug inhibition of HDAC3 and epigenetic control of differentiation in Apicomplexa parasites. The Journal of Experimental Medicine, 206(4), 953–966. https://doi.org/10.1084/jem.20082826

Brown, K. M., Long, S., & Sibley, L. D. (2017). Plasma Membrane Association by N-Acylation Governs PKG Function in Toxoplasma gondii. MBio, 8(3). https://doi.org/10.1128/mBio.00375-17

Brown, K. M., Lourido, S., & Sibley, L. D. (2016). Serum Albumin Stimulates Protein Kinase G-dependent Microneme Secretion in Toxoplasma gondii. The Journal of Biological Chemistry, 291(18), 9554–9565. https://doi.org/10.1074/jbc.M115.700518

Buchholz, K. R., Fritz, H. M., Chen, X., Durbin-Johnson, B., Rocke, D. M., Ferguson, D. J., Conrad, P. A., & Boothroyd, J. C. (2011). Identification of tissue cyst wall components by transcriptome analysis of in vivo and in vitro Toxoplasma gondii bradyzoites. Eukaryotic Cell, 10(12), 1637–1647. https://doi.org/10.1128/EC.05182-11

Buguliskis, J. S., Brossier, F., Shuman, J., & Sibley, L. D. (2010). Rhomboid 4 (ROM4) Affects the Processing of Surface Adhesins and Facilitates Host Cell Invasion by Toxoplasma gondii. PLOS Pathogens, 6(4), e1000858. https://doi.org/10.1371/journal.ppat.1000858

Bullen, H. E., Jia, Y., Yamaryo-Botté, Y., Bisio, H., Zhang, O., Jemelin, N. K., Marq, J.-B., Carruthers, V., Botté, C. Y., & Soldati-Favre, D. (2016). Phosphatidic Acid-Mediated Signaling Regulates Microneme Secretion in Toxoplasma. Cell Host & Microbe, 19(3), 349–360. https://doi.org/10.1016/j.chom.2016.02.006

Bullen, H. E., & Soldati-Favre, D. (2016). A central role for phosphatidic acid as a lipid mediator of regulated exocytosis in apicomplexa. FEBS Letters, 590(15), 2469–2481. https://doi.org/10.1002/1873-3468.12296

Buxton, D., & Innes, E. A. (1995). A commercial vaccine for ovine toxoplasmosis. Parasitology, 110 Suppl, S11-16.

Buxton, D., Thomson, K., Maley, S., Wright, S., & Bos, H. J. (1991). Vaccination of sheep with a live incomplete strain (S48) of Toxoplasma gondii and their immunity to challenge when pregnant. Veterinary Record, 129(5), 89–93. https://doi.org/10.1136/vr.129.5.89

Cabral, C. M., Tuladhar, S., Dietrich, H. K., Nguyen, E., MacDonald, W. R., Trivedi, T., Devineni, A., & Koshy, A. A. (2016). Neurons are the Primary Target Cell for the Brain-Tropic Intracellular Parasite Toxoplasma gondii. PLOS Pathogens, 12(2), e1005447. https://doi.org/10.1371/journal.ppat.1005447

Carey, K. L., Westwood, N. J., Mitchison, T. J., & Ward, G. E. (2004). A small-molecule approach to studying invasive mechanisms of Toxoplasma gondii. Proceedings of the National Academy of Sciences, 101(19), 7433–7438. https://doi.org/10.1073/pnas.0307769101

Carme, B., Demar, M., Ajzenberg, D., & Dardé, M. L. (2009). Severe acquired toxoplasmosis caused by wild cycle of Toxoplasma gondii, French Guiana. Emerging Infectious Diseases, 15(4), 656–658. https://doi.org/10.3201/eid1504.081306

Carruthers, V. B., & Sibley, L. D. (1997). Sequential protein secretion from three distinct organelles of Toxoplasma gondii accompanies invasion of human fibroblasts. European Journal of Cell Biology, 73(2), 114–123.

Carruthers, V. B., & Sibley, L. D. (1999). Mobilization of intracellular calcium stimulates microneme discharge in Toxoplasma gondii. Molecular Microbiology, 31(2), 421–428. https://doi.org/10.1046/j.1365-2958.1999.01174.x

Carruthers, V., & Boothroyd, J. C. (2007). Pulling together: an integrated model of Toxoplasma cell invasion. Current Opinion in Microbiology, 10(1), 83–89. https://doi.org/10.1016/j.mib.2006.06.017

Carruthers, Vern B., Håkansson, S., Giddings, O. K., & Sibley, L. D. (2000). Toxoplasma gondii Uses Sulfated Proteoglycans for Substrate and Host Cell Attachment. Infection and Immunity, 68(7), 4005–4011.

Carvalho, J. A., Rodgers, J., Atouguia, J., Prazeres, D. M. F., & Monteiro, G. A. (2010). DNA vaccines: a rational design against parasitic diseases. Expert Review of Vaccines, 9(2), 175–191. https://doi.org/10.1586/erv.09.158

Cérède, O., Dubremetz, J. F., Soête, M., Deslée, D., Vial, H., Bout, D., & Lebrun, M. (2005). Synergistic role of micronemal proteins in Toxoplasma gondii virulence. The Journal of Experimental Medicine, 201(3), 453–463. https://doi.org/10.1084/jem.20041672

Cerutti, A., Blanchard, N., & Besteiro, S. (2020). The Bradyzoite: A Key Developmental Stage for the Persistence and Pathogenesis of Toxoplasmosis. Pathogens, 9(3). https://doi.org/10.3390/pathogens9030234

Chahal, J. S., Khan, O. F., Cooper, C. L., McPartlan, J. S., Tsosie, J. K., Tilley, L. D., Sidik, S. M., Lourido, S., Langer, R., Bavari, S., Ploegh, H. L., & Anderson, D. G. (2016). Dendrimer-RNA nanoparticles generate protective immunity against lethal Ebola, H1N1 influenza, and Toxoplasma gondii challenges with a single dose. Proceedings of the National Academy of

Sciences of the United States of America, 113(29), E4133-4142. https://doi.org/10.1073/pnas.1600299113

Chao, C. C., Anderson, W. R., Hu, S., Gekker, G., Martella, A., & Peterson, P. K. (1993). Activated microglia inhibit multiplication of Toxoplasma gondii via a nitric oxide mechanism. Clinical Immunology and Immunopathology, 67(2), 178–183. https://doi.org/10.1006/clin.1993.1062

Chen, J., Li, Z.-Y., Petersen, E., Huang, S.-Y., Zhou, D.-H., & Zhu, X.-Q. (2015). DNA vaccination with genes encoding Toxoplasma gondii antigens ROP5 and GRA15 induces protective immunity against toxoplasmosis in Kunming mice. Expert Review of Vaccines, 14(4), 617–624. https://doi.org/10.1586/14760584.2015.1011133

Chen, Y., Yu, M., Hemandez, J. A., Li, J., Yuan, Z.-G., & Yan, H. (2018). Immuno-efficacy of DNA vaccines encoding PLP1 and ROP18 against experimental Toxoplasma gondii infection in mice. Experimental Parasitology, 188, 73–78. https://doi.org/10.1016/j.exppara.2018.04.003

Child, M. A., Garland, M., Foe, I., Madzelan, P., Treeck, M., Linden, W. A. van der, Bender, K. O., Weerapana, E., Wilson, M. A., Boothroyd, J. C., Reese, M. L., & Bogyo, M. (2017). Toxoplasma DJ-1 Regulates Organelle Secretion by a Direct Interaction with Calcium-Dependent Protein Kinase 1. MBio, 8(1). https://doi.org/10.1128/mBio.02189-16

Ching, X. T., Fong, M. Y., & Lau, Y. L. (2016). Evaluation of Immunoprotection Conferred by the Subunit Vaccines of GRA2 and GRA5 against Acute Toxoplasmosis in BALB/c Mice. Frontiers in Microbiology, 7, 609. https://doi.org/10.3389/fmicb.2016.00609

Coakley, G., Maizels, R. M., & Buck, A. H. (2015). Exosomes and Other Extracellular Vesicles: The New Communicators in Parasite Infections. Trends in Parasitology, 31(10), 477–489. https://doi.org/10.1016/j.pt.2015.06.009

Coleman, B. I., Saha, S., Sato, S., Engelberg, K., Ferguson, D. J. P., Coppens, I., Lodoen, M. B., & Gubbels, M. J. (2018). A member of the ferlin calcium sensor family is essential for toxoplasma gondii rhoptry secretion. MBio, 9(5), e01510-18. https://doi.org/10.1128/mBio.01510-18

Combe, C. L., Curiel, T. J., Moretto, M. M., & Khan, I. A. (2005). NK cells help to induce CD8(+)-T-cell immunity against Toxoplasma gondii in the absence of CD4(+) T cells. Infection and Immunity, 73(8), 4913–4921. https://doi.org/10.1128/IAI.73.8.4913-4921.2005

Cong, W., Liu, G.-H., Meng, Q.-F., Dong, W., Qin, S.-Y., Zhang, F.-K., Zhang, X.-Y., Wang, X.-Y., Qian, A.-D., & Zhu, X.-Q. (2015). Toxoplasma gondii infection in cancer patients: prevalence, risk factors, genotypes and association with clinical diagnosis. Cancer Letters, 359(2), 307–313. https://doi.org/10.1016/j.canlet.2015.01.036

Couvreur, G., Sadak, A., Fortier, B., & Dubremetz, J. F. (1988). Surface antigens of Toxoplasma gondii. Parasitology, 97 (Pt 1), 1–10. https://doi.org/10.1017/s0031182000066695

Crawford, J., Tonkin, M. L., Grujic, O., & Boulanger, M. J. (2010). Structural Characterization of Apical Membrane Antigen 1 (AMA1) from Toxoplasma gondii. The Journal of Biological Chemistry, 285(20), 15644–15652. https://doi.org/10.1074/jbc.M109.092619

Czarnewski, P., Araújo, E. C. B., Oliveira, M. C., Mineo, T. W. P., & Silva, N. M. (2017). Recombinant TgHSP70 Immunization Protects against Toxoplasma gondii Brain Cyst Formation by Enhancing Inducible Nitric Oxide Expression. Frontiers in Cellular and Infection Microbiology, 7. https://doi.org/10.3389/fcimb.2017.00142

Dacoba, T. G., Olivera, A., Torres, D., Crecente-Campo, J., & Alonso, M. J. (2017). Modulating the immune system through nanotechnology. Seminars in Immunology, 34, 78–102. https://doi.org/10.1016/j.smim.2017.09.007

Dao, A., Fortier, B., Soete, M., Plenat, F., & Dubremetz, J. F. (2001). Successful reinfection of chronically infected mice by a different Toxoplasma gondii genotype. International Journal for Parasitology, 31(1), 63–65. https://doi.org/10.1016/s0020-7519(00)00151-x

Däubener, W., Gutsche, M., Nockemann, S., MacKenzie, C., Seghrouchni, S., & Hadding, U. (1996). Protamine enhances the activity of human recombinant interferon-gamma. Journal of Interferon & Cytokine Research: The Official Journal of the International Society for Interferon and Cytokine Research, 16(7), 531–536. https://doi.org/10.1089/jir.1996.16.531

Däubener, W., Spors, B., Hucke, C., Adam, R., Stins, M., Kim, K. S., & Schroten, H. (2001). Restriction of Toxoplasma gondii growth in human brain microvascular endothelial cells by activation of indoleamine 2,3-dioxygenase. Infection and Immunity, 69(10), 6527–6531. https://doi.org/10.1128/IAI.69.10.6527-6531.2001

Dautu, G., Munyaka, B., Carmen, G., Zhang, G., Omata, Y., Xuenan, X., & Igarashi, M. (2007). Toxoplasma gondii: DNA vaccination with genes encoding antigens MIC2, M2AP, AMA1 and BAG1 and evaluation of their immunogenic potential. Experimental Parasitology, 116(3), 273–282. https://doi.org/10.1016/j.exppara.2007.01.017

de Boer, J., Wulffraat, N., & Rothova, A. (2003). Visual loss in uveitis of childhood. The British Journal of Ophthalmology, 87(7), 879–884.

Debierre-Grockiego, F., Campos, M. A., Azzouz, N., Schmidt, J., Bieker, U., Resende, M. G., Mansur, D. S., Weingart, R., Schmidt, R. R., Golenbock, D. T., Gazzinelli, R. T., & Schwarz, R. T. (2007). Activation of TLR2 and TLR4 by Glycosylphosphatidylinositols Derived from Toxoplasma gondii. The Journal of Immunology, 179(2), 1129–1137. https://doi.org/10.4049/jimmunol.179.2.1129

Del Giudice, G., Rappuoli, R., & Didierlaurent, A. M. (2018). Correlates of adjuvanticity: A review on adjuvants in licensed vaccines. Seminars in Immunology, 39, 14–21. https://doi.org/10.1016/j.smim.2018.05.001

Deneris, E. S., & Hobert, O. (2014). Maintenance of postmitotic neuronal cell identity. Nature Neuroscience, 17(7), 899–907. https://doi.org/10.1038/nn.3731

Diaz-Arévalo, D., & Zeng, M. (2020). Nanoparticle-based vaccines. Nanopharmaceuticals, 135–150. https://doi.org/10.1016/B978-0-12-817778-5.00007-5

Divanovic, S., Sawtell, N. M., Trompette, A., Warning, J. I., Dias, A., Cooper, A. M., Yap, G. S., Arditi, M., Shimada, K., Duhadaway, J. B., Prendergast, G. C., Basaraba, R. J., Mellor, A. L., Munn, D. H., Aliberti, J., & Karp, C. L. (2012). Opposing biological functions of tryptophan catabolizing

enzymes during intracellular infection. The Journal of Infectious Diseases, 205(1), 152–161. https://doi.org/10.1093/infdis/jir621

Donahue, C. G., Carruthers, V. B., Gilk, S. D., & Ward, G. E. (2000). The Toxoplasma homolog of Plasmodium apical membrane antigen-1 (AMA-1) is a microneme protein secreted in response to elevated intracellular calcium levels. Molecular and Biochemical Parasitology, 111(1), 15–30. https://doi.org/10.1016/s0166-6851(00)00289-9

Dong, C., & Flavell, R. A. (2000). Cell fate decision: T-helper 1 and 2 subsets in immune responses. Arthritis Research & Therapy, 2(3), 179. https://doi.org/10.1186/ar85

Drewry, L. L., & Sibley, L. D. (2015). Toxoplasma Actin Is Required for Efficient Host Cell Invasion. MBio, 6(3). https://doi.org/10.1128/mBio.00557-15

Dubey, J. P. (1997). Bradyzoite-induced murine toxoplasmosis: stage conversion, pathogenesis, and tissue cyst formation in mice fed bradyzoites of different strains of Toxoplasma gondii. The Journal of Eukaryotic Microbiology, 44(6), 592–602. https://doi.org/10.1111/j.1550-7408.1997.tb05965.x

Dubey, J. P. (1998). Advances in the life cycle of Toxoplasma gondii. International Journal for Parasitology, 28(7), 1019–1024.

Dubey, J. P., & Frenkel, J. K. (1972). Cyst-Induced Toxoplasmosis in Cats*. The Journal of Protozoology, 19(1), 155–177. https://doi.org/10.1111/j.1550-7408.1972.tb03431.x

Dubey, J. P., Lindsay, D. S., & Speer, C. A. (1998). Structures of Toxoplasma gondii Tachyzoites, Bradyzoites, and Sporozoites and Biology and Development of Tissue Cysts. Clinical Microbiology Reviews, 11(2), 267–299.

Dubremetz, J. F. (2007). Rhoptries are major players in Toxoplasma gondii invasion and host cell interaction. Cellular Microbiology, 9(4), 841–848. https://doi.org/10.1111/j.1462-5822.2007.00909.x

Dubremetz, J. F., & Lebrun, M. (2012). Virulence factors of Toxoplasma gondii. Microbes and Infection, 14(15), 1403–1410. https://doi.org/10.1016/j.micinf.2012.09.005

Dumètre, A., & Dardé, M. L. (2003). How to detect Toxoplasma gondii oocysts in environmental samples? FEMS Microbiology Reviews, 27(5), 651–661. https://doi.org/10.1016/S0168-6445(03)00071-8

Dunay, Ildiko R., Chan, W. C., Haynes, R. K., & Sibley, L. D. (2009). Artemisone and Artemiside Control Acute and Reactivated Toxoplasmosis in a Murine Model. Antimicrobial Agents and Chemotherapy, 53(10), 4450–4456. https://doi.org/10.1128/AAC.00502-09

Dunay, Ildiko Rita, Gajurel, K., Dhakal, R., Liesenfeld, O., & Montoya, J. G. (2018). Treatment of Toxoplasmosis: Historical Perspective, Animal Models, and Current Clinical Practice. Clinical Microbiology Reviews, 31(4). https://doi.org/10.1128/CMR.00057-17

Dunn, D., Wallon, M., Peyron, F., Petersen, E., Peckham, C., & Gilbert, R. (1999). Mother-to-child transmission of toxoplasmosis: risk estimates for clinical counselling. Lancet (London, England), 353(9167), 1829–1833. https://doi.org/10.1016/S0140-6736(98)08220-8

Dupont, C. D., Christian, D. A., & Hunter, C. A. (2012). Immune response and immunopathology during toxoplasmosis. Seminars in Immunopathology, 34(6), 793–813. https://doi.org/10.1007/s00281-012-0339-3

Dzierszinski, F., Nishi, M., Ouko, L., & Roos, D. S. (2004). Dynamics of Toxoplasma gondii Differentiation. Eukaryotic Cell, 3(4), 992–1003. https://doi.org/10.1128/EC.3.4.992-1003.2004

Egarter, S., Andenmatten, N., Jackson, A. J., Whitelaw, J. A., Pall, G., Black, J. A., Ferguson, D. J. P., Tardieux, I., Mogilner, A., & Meissner, M. (2014). The Toxoplasma Acto-MyoA Motor Complex Is Important but Not Essential for Gliding Motility and Host Cell Invasion. PLOS ONE, 9(3), e91819. https://doi.org/10.1371/journal.pone.0091819

Falih, D., & Saheb, E. (2017). The Association of Toxoplasma gondii Infection in Breast and Colorectal Cancer Patients. International Journal of Clinical Oncology and Cancer Research, 2, 86–92. https://doi.org/10.11648/j.ijcocr.20170204.13

Fang, R. H., & Zhang, L. (2016). Nanoparticle-Based Modulation of the Immune System. Annual Review of Chemical and Biomolecular Engineering, 7, 305–326. https://doi.org/10.1146/annurev-chembioeng-080615-034446

Fekadu, A., Shibre, T., & Cleare, A. J. (2010). Toxoplasmosis as a cause for behaviour disorders--overview of evidence and mechanisms. Folia Parasitologica, 57(2), 105–113.

Fereig, R. M., Kuroda, Y., Terkawi, M. A., Mahmoud, M. E., & Nishikawa, Y. (2017). Immunization with Toxoplasma gondii peroxiredoxin 1 induces protective immunity against toxoplasmosis in mice. PLOS ONE, 12(4), e0176324. https://doi.org/10.1371/journal.pone.0176324

Fereig, R. M., & Nishikawa, Y. (2016). Towards a Preventive Strategy for Toxoplasmosis: Current Trends, Challenges, and Future Perspectives for Vaccine Development. Methods in Molecular Biology (Clifton, N.J.), 1404, 153–164. https://doi.org/10.1007/978-1-4939-3389-1_10

Ferguson, D. J., & Hutchison, W. M. (1987a). An ultrastructural study of the early development and tissue cyst formation of Toxoplasma gondii in the brains of mice. Parasitology Research, 73(6), 483–491. https://doi.org/10.1007/BF00535321

Ferguson, D. J., & Hutchison, W. M. (1987b). The host-parasite relationship of Toxoplasma gondii in the brains of chronically infected mice. Virchows Archiv. A, Pathological Anatomy and Histopathology, 411(1), 39–43.

Ferguson, D. J., Hutchison, W. M., & Pettersen, E. (1989). Tissue cyst rupture in mice chronically infected with Toxoplasma gondii. An immunocytochemical and ultrastructural study. Parasitology Research, 75(8), 599–603. https://doi.org/10.1007/BF00930955

Ferguson, D. J. P. (2004). Use of molecular and ultrastructural markers to evaluate stage conversion of Toxoplasma gondii in both the intermediate and definitive host. International Journal for Parasitology, 34(3), 347–360. https://doi.org/10.1016/j.ijpara.2003.11.024

Ferguson, David J. P. (2002). Toxoplasma gondii and sex: essential or optional extra? Trends in Parasitology, 18(8), 355–359.

Ferguson, David J. P. (2009). Toxoplasma gondii: 1908-2008, homage to Nicolle, Manceaux and Splendore. Memorias Do Instituto Oswaldo Cruz, 104(2), 133–148. https://doi.org/10.1590/s0074-02762009000200003

Ferguson, David J. P., & Dubremetz, J.-F. (2020). Chapter 2 - The ultrastructure of Toxoplasma gondii. In L. M. Weiss & K. Kim (Eds.), Toxoplasma gondii (Third Edition) (pp. 21–61). Academic Press. https://doi.org/10.1016/B978-0-12-815041-2.00002-5

Ferra, B., Holec-Gąsior, L., Gatkowska, J., Dziadek, B., & Dzitko, K. (2020). Toxoplasma gondii Recombinant antigen AMA1: Diagnostic Utility of Protein Fragments for the Detection of IgG and IgM Antibodies. Pathogens, 9(1). https://doi.org/10.3390/pathogens9010043

Flegr, J. (2007). Effects of toxoplasma on human behavior. Schizophrenia Bulletin, 33(3), 757–760. https://doi.org/10.1093/schbul/sbl074

Foroutan, M., Barati, M., & Ghaffarifar, F. (2020). Enhancing immune responses by a novel multi-epitope ROP8 DNA vaccine plus interleukin-12 plasmid as a genetic adjuvant against acute Toxoplasma gondii infection in BALB/c mice. Microbial Pathogenesis, 147, 104435. https://doi.org/10.1016/j.micpath.2020.104435

Foroutan, M., Ghaffarifar, F., Sharifi, Z., Dalimi, A., & Jorjani, O. (2019). Rhoptry antigens as Toxoplasma gondii vaccine target. Clinical and Experimental Vaccine Research, 8(1), 4–26. https://doi.org/10.7774/cevr.2019.8.1.4

Foroutan, M., Zaki, L., & Ghaffarifar, F. (2018). Recent progress in microneme-based vaccines development against Toxoplasma gondii. Clinical and Experimental Vaccine Research, 7(2), 93–103. https://doi.org/10.7774/cevr.2018.7.2.93

Frade, J. M., & Ovejero-Benito, M. C. (2015). Neuronal cell cycle: the neuron itself and its circumstances. Cell Cycle (Georgetown, Tex.), 14(5), 712–720. https://doi.org/10.1080/15384101.2015.1004937

Frénal, K., Dubremetz, J.-F., Lebrun, M., & Soldati-Favre, D. (2017). Gliding motility powers invasion and egress in Apicomplexa. Nature Reviews Microbiology, 15(11), 645–660. https://doi.org/10.1038/nrmicro.2017.86

Frénal, K., Marq, J.-B., Jacot, D., Polonais, V., & Soldati-Favre, D. (2014). Plasticity between MyoC- and MyoA-Glideosomes: An Example of Functional Compensation in Toxoplasma gondii Invasion. PLOS Pathogens, 10(11), e1004504. https://doi.org/10.1371/journal.ppat.1004504

Frénal, K., Polonais, V., Marq, J.-B., Stratmann, R., Limenitakis, J., & Soldati-Favre, D. (2010). Functional dissection of the apicomplexan glideosome molecular architecture. Cell Host & Microbe, 8(4), 343–357. https://doi.org/10.1016/j.chom.2010.09.002

Frenkel, J. K. (1973). Toxoplasma In and Around Us. BioScience, 23(6), 343–352. https://doi.org/10.2307/1296513

Frenkel, J. K., Dubey, J. P., & Miller, N. L. (1970). Toxoplasma gondii in cats: fecal stages identified as coccidian oocysts. Science (New York, N.Y.), 167(3919), 893–896. https://doi.org/10.1126/science.167.3919.893

Fritz, H. M., Buchholz, K. R., Chen, X., Durbin-Johnson, B., Rocke, D. M., Conrad, P. A., & Boothroyd, J. C. (2012). Transcriptomic Analysis of Toxoplasma Development Reveals Many Novel Functions and Structures Specific to Sporozoites and Oocysts. PLOS ONE, 7(2), e29998. https://doi.org/10.1371/journal.pone.0029998

Furtado, J. M., Bharadwaj, A. S., Chipps, T. J., Pan, Y., Ashander, L. M., & Smith, J. R. (2012). Toxoplasma gondii tachyzoites cross retinal endothelium assisted by intercellular adhesion molecule-1 in vitro. Immunology and Cell Biology, 90(9), 912–915. https://doi.org/10.1038/icb.2012.21

Furtado, J. M., Winthrop, K. L., Butler, N. J., & Smith, J. R. (2013). Ocular toxoplasmosis I: parasitology, epidemiology and public health. Clinical & Experimental Ophthalmology, 41(1), 82–94. https://doi.org/10.1111/j.1442-9071.2012.02821.x

Fux, B., Nawas, J., Khan, A., Gill, D. B., Su, C., & Sibley, L. D. (2007). Toxoplasma gondii Strains Defective in Oral Transmission Are Also Defective in Developmental Stage Differentiation. Infection and Immunity, 75(5), 2580–2590. https://doi.org/10.1128/IAI.00085-07

Garcia, C. R. S., Alves, E., Pereira, P. H. S., Bartlett, P. J., Thomas, A. P., Mikoshiba, K., Plattner, H., & Sibley, L. D. (2017). InsP3 Signaling in Apicomplexan Parasites. Current Topics in Medicinal Chemistry, 17(19), 2158–2165. https://doi.org/10.2174/1568026617666170130121042

Garfoot, A. L., Wilson, G. M., Coon, J. J., & Knoll, L. J. (2019). Proteomic and transcriptomic analyses of early and late-chronic Toxoplasma gondii infection shows novel and stage specific transcripts. BMC Genomics, 20. https://doi.org/10.1186/s12864-019-6213-0

Gaskins, E., Gilk, S., DeVore, N., Mann, T., Ward, G., & Beckers, C. (2004). Identification of the membrane receptor of a class XIV myosin in Toxoplasma gondii. The Journal of Cell Biology, 165(3), 383–393. https://doi.org/10.1083/jcb.200311137

Gazzinelli, R. T., Hakim, F. T., Hieny, S., Shearer, G. M., & Sher, A. (1991). Synergistic role of CD4+ and CD8+ T lymphocytes in IFN-gamma production and protective immunity induced by an attenuated Toxoplasma gondii vaccine. Journal of Immunology (Baltimore, Md.: 1950), 146(1), 286–292.

Gazzinelli, R. T., Hieny, S., Wynn, T. A., Wolf, S., & Sher, A. (1993). Interleukin 12 is required for the T-lymphocyte-independent induction of interferon gamma by an intracellular parasite and induces resistance in T-cell-deficient hosts. Proceedings of the National Academy of Sciences of the United States of America, 90(13), 6115–6119.

Gazzinelli, R. T., Wysocka, M., Hayashi, S., Denkers, E. Y., Hieny, S., Caspar, P., Trinchieri, G., & Sher, A. (1994). Parasite-induced IL-12 stimulates early IFN-gamma synthesis and resistance during acute infection with Toxoplasma gondii. Journal of Immunology (Baltimore, Md.: 1950), 153(6), 2533–2543.

Gazzinelli, R., Xu, Y., Hieny, S., Cheever, A., & Sher, A. (1992). Simultaneous depletion of CD4+ and CD8+ T lymphocytes is required to reactivate chronic infection with Toxoplasma gondii. Journal of Immunology (Baltimore, Md.: 1950), 149(1), 175–180.

Genova, B. M. D., Wilson, S. K., Dubey, J. P., & Knoll, L. J. (2019). Intestinal delta-6-desaturase activity determines host range for Toxoplasma sexual reproduction. PLOS Biology, 17(8), e3000364. https://doi.org/10.1371/journal.pbio.3000364

Gharamti, A. A., Rao, A., Pecen, P. E., Henao-Martínez, A. F., Franco-Paredes, C., & Montoya, J. G. (2018). Acute Toxoplasma Dissemination With Encephalitis in the Era of Biological Therapies. Open Forum Infectious Diseases, 5(11). https://doi.org/10.1093/ofid/ofy259

Goldman, M., Carver, R. K., & Sulzer, A. J. (1958). Reproduction of Toxoplasma gondii by internal budding. The Journal of Parasitology, 44(2), 161–171.

Gong, P., Cao, L., Guo, Y., Dong, H., Yuan, S., Yao, X., Ren, W., Yao, L., Xu, Z., Sun, Q., & Zhang, X. (2016). Toxoplasma gondii: Protective immunity induced by a DNA vaccine expressing GRA1 and MIC3 against toxoplasmosis in BALB/c mice. Experimental Parasitology, 166, 131–136. https://doi.org/10.1016/j.exppara.2016.04.003

Götze, S., Reinhardt, A., Geissner, A., Azzouz, N., Tsai, Y.-H., Kurucz, R., Varón Silva, D., & Seeberger, P. H. (2015). Investigation of the protective properties of glycosylphosphatidylinositol-based vaccine candidates in a Toxoplasma gondii mouse challenge model. Glycobiology, 25(9), 984–991. https://doi.org/10.1093/glycob/cwv040

Graindorge, A., Frénal, K., Jacot, D., Salamun, J., Marq, J. B., & Soldati-Favre, D. (2016). The Conoid Associated Motor MyoH Is Indispensable for Toxoplasma gondii Entry and Exit from Host Cells. PLOS Pathogens, 12(1), e1005388. https://doi.org/10.1371/journal.ppat.1005388

Grzybowski, M. M., Gatkowska, J. M., Dziadek, B., Dzitko, K., & Długońska, H. (2015). Human toxoplasmosis: a comparative evaluation of the diagnostic potential of recombinant Toxoplasma gondii ROP5 and ROP18 antigens. Journal of Medical Microbiology, 64(10), 1201–1207. https://doi.org/10.1099/jmm.0.000148

Guérin, A., Corrales, R. M., Parker, M. L., Lamarque, M. H., Jacot, D., El Hajj, H., Soldati-Favre, D., Boulanger, M. J., & Lebrun, M. (2017). Efficient invasion by Toxoplasma depends on the subversion of host protein networks. Nature Microbiology, 2(10), 1358–1366. https://doi.org/10.1038/s41564-017-0018-1

Guérin, A., El Hajj, H., Penarete-Vargas, D., Besteiro, S., & Lebrun, M. (2017). RON4L1 is a new member of the moving junction complex in Toxoplasma gondii. Scientific Reports, 7(1), 17907. https://doi.org/10.1038/s41598-017-18010-9

Gupta, S. L., Carlin, J. M., Pyati, P., Dai, W., Pfefferkorn, E. R., & Murphy, M. J. (1994). Antiparasitic and antiproliferative effects of indoleamine 2,3-dioxygenase enzyme expression in human fibroblasts. Infection and Immunity, 62(6), 2277–2284.

Håkansson, S., Charron, A. J., & Sibley, L. D. (2001). Toxoplasma evacuoles: a two-step process of secretion and fusion forms the parasitophorous vacuole. The EMBO Journal, 20(12), 3132–3144. https://doi.org/10.1093/emboj/20.12.3132

Håkansson, S., Morisaki, H., Heuser, J., & Sibley, L. D. (1999). Time-Lapse Video Microscopy of Gliding Motility in Toxoplasma gondii Reveals a Novel, Biphasic Mechanism of Cell Locomotion. Molecular Biology of the Cell, 10(11), 3539–3547.

Hakimi, M.-A., Olias, P., & Sibley, L. D. (2017). Toxoplasma Effectors Targeting Host Signaling and Transcription. Clinical Microbiology Reviews, 30(3), 615–645. https://doi.org/10.1128/CMR.00005-17

Halonen, S. K., Taylor, G. A., & Weiss, L. M. (2001). Gamma Interferon-Induced Inhibition of Toxoplasma gondii in Astrocytes Is Mediated by IGTP. Infection and Immunity, 69(9), 5573–5576. https://doi.org/10.1128/IAI.69.9.5573-5576.2001

Halonen, S. K., & Weiss, L. M. (2013). TOXOPLASMOSIS. Handbook of Clinical Neurology, 114, 125–145. https://doi.org/10.1016/B978-0-444-53490-3.00008-X

Harker, K. S., Ueno, N., & Lodoen, M. B. (2015). Toxoplasma gondii dissemination: a parasite's journey through the infected host. Parasite Immunology, 37(3), 141–149. https://doi.org/10.1111/pim.12163

Harker, Katherine S., Jivan, E., McWhorter, F. Y., Liu, W. F., & Lodoen, M. B. (2014). Shear forces enhance Toxoplasma gondii tachyzoite motility on vascular endothelium. MBio, 5(2), e01111-01113. https://doi.org/10.1128/mBio.01111-13

Haroon, F., Händel, U., Angenstein, F., Goldschmidt, J., Kreutzmann, P., Lison, H., Fischer, K.-D., Scheich, H., Wetzel, W., Schlüter, D., & Budinger, E. (2012). Toxoplasma gondii actively inhibits neuronal function in chronically infected mice. PloS One, 7(4), e35516. https://doi.org/10.1371/journal.pone.0035516

Hayashi, S., Chan, C. C., Gazzinelli, R., & Roberge, F. G. (1996). Contribution of nitric oxide to the host parasite equilibrium in toxoplasmosis. Journal of Immunology (Baltimore, Md.: 1950), 156(4), 1476–1481.

Heaslip, A. T., Nishi, M., Stein, B., & Hu, K. (2011). The Motility of a Human Parasite, Toxoplasma gondii, Is Regulated by a Novel Lysine Methyltransferase. PLOS Pathogens, 7(9), e1002201. https://doi.org/10.1371/journal.ppat.1002201

Hehl, A. B., Lekutis, C., Grigg, M. E., Bradley, P. J., Dubremetz, J.-F., Ortega-Barria, E., & Boothroyd, J. C. (2000). Toxoplasma gondii Homologue of Plasmodium Apical Membrane Antigen 1 Is Involved in Invasion of Host Cells. Infection and Immunity, 68(12), 7078–7086.

Heil, F., Hemmi, H., Hochrein, H., Ampenberger, F., Kirschning, C., Akira, S., Lipford, G., Wagner, H., & Bauer, S. (2004). Species-specific recognition of single-stranded RNA via toll-like receptor 7 and 8. Science (New York, N.Y.), 303(5663), 1526–1529. https://doi.org/10.1126/science.1093620

Hidano, S., Randall, L. M., Dawson, L., Dietrich, H. K., Konradt, C., Klover, P. J., John, B., Harris, T. H., Fang, Q., Turek, B., Kobayashi, T., Hennighausen, L., Beiting, D. P., Koshy, A. A., & Hunter, C.

A. (2016). STAT1 Signaling in Astrocytes Is Essential for Control of Infection in the Central Nervous System. MBio, 7(6). https://doi.org/10.1128/mBio.01881-16

Hiszczyńska-Sawicka, E., Gatkowska, J. M., Grzybowski, M. M., & Długońska, H. (2014). Veterinary vaccines against toxoplasmosis. Parasitology, 141(11), 1365–1378. https://doi.org/10.1017/S0031182014000481

Hong, D.-P., Radke, J. B., & White, M. W. (2017). Opposing Transcriptional Mechanisms Regulate Toxoplasma Development. MSphere, 2(1). https://doi.org/10.1128/mSphere.00347-16

Hosseini, S. A., Amouei, A., Sharif, M., Sarvi, S., Galal, L., Javidnia, J., Pagheh, A. S., Gholami, S., Mizani, A., & Daryani, A. (2018). Human toxoplasmosis: a systematic review for genetic diversity of Toxoplasma gondii in clinical samples. Epidemiology and Infection, 1–9. https://doi.org/10.1017/S0950268818002947

Howell, S. A., Hackett, F., Jongco, A. M., Withers-Martinez, C., Kim, K., Carruthers, V. B., & Blackman, M. J. (2005). Distinct mechanisms govern proteolytic shedding of a key invasion protein in apicomplexan pathogens. Molecular Microbiology, 57(5), 1342–1356. https://doi.org/10.1111/j.1365-2958.2005.04772.x

Hu, K., Johnson, J., Florens, L., Fraunholz, M., Suravajjala, S., DiLullo, C., Yates, J., Roos, D. S., & Murray, J. M. (2006). Cytoskeletal Components of an Invasion Machine—The Apical Complex of Toxoplasma gondii. PLOS Pathogens, 2(2), e13. https://doi.org/10.1371/journal.ppat.0020013

Hu, K., Roos, D. S., & Murray, J. M. (2002). A novel polymer of tubulin forms the conoid of Toxoplasma gondii. Journal of Cell Biology, 156(6), 1039–1050. https://doi.org/10.1083/jcb.200112086

Huang, S., Holmes, M. J., Radke, J. B., Hong, D.-P., Liu, T.-K., White, M. W., & Sullivan, W. J. (2017). Toxoplasma gondii AP2IX-4 Regulates Gene Expression during Bradyzoite Development. MSphere, 2(2). https://doi.org/10.1128/mSphere.00054-17

Huang, S.-Y., Chen, K., Wang, J.-L., Yang, B., & Zhu, X.-Q. (2019). Evaluation of protective immunity induced by recombinant calcium-dependent protein kinase 1 (TgCDPK1) protein against acute toxoplasmosis in mice. Microbial Pathogenesis, 133, 103560. https://doi.org/10.1016/j.micpath.2019.103560

Huang, Y., Huang, Y., Chang, A., Wang, J., Zeng, X., & Wu, J. (2016). Is Toxoplasma Gondii Infection a Risk Factor for Leukemia? An Evidence-Based Meta-Analysis. Medical Science Monitor: International Medical Journal of Experimental and Clinical Research, 22, 1547–1552.

Hunter, C. A., & Sibley, L. D. (2012). Modulation of innate immunity by Toxoplasma gondii virulence effectors. Nature Reviews. Microbiology, 10(11), 766–778. https://doi.org/10.1038/nrmicro2858

Huynh, M.-H., & Carruthers, V. B. (2006). Toxoplasma MIC2 Is a Major Determinant of Invasion and Virulence. PLOS Pathogens, 2(8), e84. https://doi.org/10.1371/journal.ppat.0020084

Huynh, M.-H., Rabenau, K. E., Harper, J. M., Beatty, W. L., Sibley, L. D., & Carruthers, V. B. (2003). Rapid invasion of host cells by Toxoplasma requires secretion of the MIC2-M2AP adhesive protein complex. The EMBO Journal, 22(9), 2082–2090. https://doi.org/10.1093/emboj/cdg217

Hwang, S., & Khan, I. A. (2015). CD8+ T cell immunity in an encephalitis model of Toxoplasma gondii infection. Seminars in Immunopathology, 37(3), 271–279. https://doi.org/10.1007/s00281-015-0483-7

Ibrahim, H. M., Bannai, H., Xuan, X., & Nishikawa, Y. (2009). Toxoplasma gondii Cyclophilin 18-Mediated Production of Nitric Oxide Induces Bradyzoite Conversion in a CCR5-Dependent Manner. Infection and Immunity, 77(9), 3686–3695. https://doi.org/10.1128/IAI.00361-09

Ismael, A. B., Dimier-Poisson, I., Lebrun, M., Dubremetz, J.-F., Bout, D., & Mevelec, M.-N. (2006). Mic1-3 knockout of Toxoplasma gondii is a successful vaccine against chronic and congenital toxoplasmosis in mice. The Journal of Infectious Diseases, 194(8), 1176–1183. https://doi.org/10.1086/507706

Jacot, D., Tosetti, N., Pires, I., Stock, J., Graindorge, A., Hung, Y.-F., Han, H., Tewari, R., Kursula, I., & Soldati-Favre, D. (2016). An Apicomplexan Actin-Binding Protein Serves as a Connector and Lipid Sensor to Coordinate Motility and Invasion. Cell Host & Microbe, 20(6), 731–743. https://doi.org/10.1016/j.chom.2016.10.020

Jensen, K. D. C., Camejo, A., Melo, M. B., Cordeiro, C., Julien, L., Grotenbreg, G. M., Frickel, E.-M., Ploegh, H. L., Young, L., & Saeij, J. P. J. (2015). Toxoplasma gondii superinfection and virulence during secondary infection correlate with the exact ROP5/ROP18 allelic combination. MBio, 6(2), e02280. https://doi.org/10.1128/mBio.02280-14

Jewett, T. J., & Sibley, L. D. (2004). The toxoplasma proteins MIC2 and M2AP form a hexameric complex necessary for intracellular survival. The Journal of Biological Chemistry, 279(10), 9362–9369. https://doi.org/10.1074/jbc.M312590200

Johnson, H. J., & Koshy, A. A. (2020). Latent Toxoplasmosis Effects on Rodents and Humans: How Much is Real and How Much is Media Hype? MBio, 11(2). https://doi.org/10.1128/mBio.02164-19

Johnson, L. L., & Sayles, P. C. (2002). Deficient Humoral Responses Underlie Susceptibility to Toxoplasma gondii in CD4-Deficient Mice. Infection and Immunity, 70(1), 185–191. https://doi.org/10.1128/IAI.70.1.185-191.2002

Jones, L. A., Alexander, J., & Roberts, C. W. (2006). Ocular toxoplasmosis: in the storm of the eye. Parasite Immunology, 28(12), 635–642. https://doi.org/10.1111/j.1365-3024.2006.00874.x

Jones, T. C., Bienz, K. A., & Erb, P. (1986). In vitro cultivation of Toxoplasma gondii cysts in astrocytes in the presence of gamma interferon. Infection and Immunity, 51(1), 147–156.

Jones-Brando, L., Torrey, E. F., & Yolken, R. (2003). Drugs used in the treatment of schizophrenia and bipolar disorder inhibit the replication of Toxoplasma gondii. Schizophrenia Research, 62(3), 237–244.

Jung, B.-K., Song, H., Kim, M.-J., Cho, J., Shin, E.-H., & Chai, J.-Y. (2016). High Toxoplasma gondii Seropositivity among Brain Tumor Patients in Korea. The Korean Journal of Parasitology, 54(2), 201–204. https://doi.org/10.3347/kjp.2016.54.2.201

Jung, C., Lee, C. Y.-F., & Grigg, M. E. (2004). The SRS superfamily of Toxoplasma surface proteins. International Journal for Parasitology, 34(3), 285–296. https://doi.org/10.1016/j.ijpara.2003.12.004

Kang, H., Remington, J. S., & Suzuki, Y. (2000). Decreased resistance of B cell-deficient mice to infection with Toxoplasma gondii despite unimpaired expression of IFN-gamma, TNF-alpha, and inducible nitric oxide synthase. Journal of Immunology (Baltimore, Md.: 1950), 164(5), 2629–2634. https://doi.org/10.4049/jimmunol.164.5.2629

Kang, H., & Suzuki, Y. (2001). Requirement of non-T cells that produce gamma interferon for prevention of reactivation of Toxoplasma gondii infection in the brain. Infection and Immunity, 69(5), 2920–2927. https://doi.org/10.1128/IAI.69.5.2920-2927.2001

Kano, S., Hodgkinson, C. A., Jones-Brando, L., Eastwood, S., Ishizuka, K., Niwa, M., Choi, E. Y., Chang, D. J., Chen, Y., Velivela, S. D., Leister, F., Wood, J., Chowdari, K., Ducci, F., Caycedo, D. A., Heinz, E., Newman, E. R., Cascella, N., Mortensen, P. B., … Sawa, A. (2020). Host–parasite interaction associated with major mental illness. Molecular Psychiatry, 25(1), 194–205. https://doi.org/10.1038/s41380-018-0217-z

Kato, K. (2018). How does Toxoplama gondii invade host cells? The Journal of Veterinary Medical Science, 80(11), 1702–1706. https://doi.org/10.1292/jvms.18-0344

Katris, N. J., Ke, H., McFadden, G. I., van Dooren, G. G., & Waller, R. F. (2019). Calcium negatively regulates secretion from dense granules in Toxoplasma gondii. Cellular Microbiology, 21(6). https://doi.org/10.1111/cmi.13011

Keeley, A., & Soldati, D. (2004). The glideosome: a molecular machine powering motility and host-cell invasion by Apicomplexa. Trends in Cell Biology, 14(10), 528–532. https://doi.org/10.1016/j.tcb.2004.08.002

Kessler, H., Herm-Götz, A., Hegge, S., Rauch, M., Soldati-Favre, D., Frischknecht, F., & Meissner, M. (2008). Microneme protein 8 – a new essential invasion factor in Toxoplasma gondii. Journal of Cell Science, 121(7), 947–956. https://doi.org/10.1242/jcs.022350

Khan, I. A., Hwang, S., & Moretto, M. (2019). Toxoplasma gondii: CD8 T Cells Cry for CD4 Help. Frontiers in Cellular and Infection Microbiology, 9. https://doi.org/10.3389/fcimb.2019.00136

Kim, K. (2018). The Epigenome, Cell Cycle, and Development in Toxoplasma. Annual Review of Microbiology, 72, 479–499. https://doi.org/10.1146/annurev-micro-090817-062741

Kim, K., & Weiss, L. M. (2004). Toxoplasma gondii: the model apicomplexan. International Journal for Parasitology, 34(3), 423–432. https://doi.org/10.1016/j.ijpara.2003.12.009

Kim, M.-J., Lee, S.-H., Kang, H.-J., Chu, K.-B., Park, H., Jin, H., Moon, E.-K., Kim, S. S., & Quan, F.-S. (2020). Virus-like particle vaccine displaying Toxoplasma gondii apical membrane antigen 1 induces protection against T. gondii ME49 infection in mice. Microbial Pathogenesis, 142, 104090. https://doi.org/10.1016/j.micpath.2020.104090

Koblansky, A. A., Jankovic, D., Oh, H., Hieny, S., Sungnak, W., Mathur, R., Hayden, M. S., Akira, S., Sher, A., & Ghosh, S. (2013). Recognition of profilin by Toll-like receptor 12 is critical for host resistance to Toxoplasma gondii. Immunity, 38(1), 119–130. https://doi.org/10.1016/j.immuni.2012.09.016

Kodym, P., Malý, M., Beran, O., Jilich, D., Rozsypal, H., Machala, L., & Holub, M. (2015). Incidence, immunological and clinical characteristics of reactivation of latent Toxoplasma gondii infection in HIV-infected patients. Epidemiology and Infection, 143(3), 600–607. https://doi.org/10.1017/S0950268814001253

Kollu, V., Magalhaes-Silverman, M., Tricot, G., & Ince, D. (2018). Toxoplasma Encephalitis following Tandem Autologous Hematopoietic Stem Cell Transplantation: A Case Report and Review of the Literature. Case Reports in Infectious Diseases, 2018, 9409121. https://doi.org/10.1155/2018/9409121

Konradt, C., Ueno, N., Christian, D. A., Delong, J. H., Pritchard, G. H., Herz, J., Bzik, D. J., Koshy, A. A., McGavern, D. B., Lodoen, M. B., & Hunter, C. A. (2016). Endothelial cells are a replicative niche for entry of Toxoplasma gondii to the central nervous system. Nature Microbiology, 1, 16001. https://doi.org/10.1038/nmicrobiol.2016.1

Koshy, A. A., Dietrich, H. K., Christian, D. A., Melehani, J. H., Shastri, A. J., Hunter, C. A., & Boothroyd, J. C. (2012). Toxoplasma co-opts host cells it does not invade. PLoS Pathogens, 8(7), e1002825. https://doi.org/10.1371/journal.ppat.1002825

Krishnamurthy, S., Deng, B., del Rio, R., Buchholz, K. R., Treeck, M., Urban, S., Boothroyd, J., Lam, Y.-W., & Ward, G. E. (2016). Not a Simple Tether: Binding of Toxoplasma gondii AMA1 to RON2 during Invasion Protects AMA1 from Rhomboid-Mediated Cleavage and Leads to Dephosphorylation of Its Cytosolic Tail. MBio, 7(5). https://doi.org/10.1128/mBio.00754-16

Lachenmaier, S. M., Deli, M. A., Meissner, M., & Liesenfeld, O. (2011). Intracellular transport of Toxoplasma gondii through the blood-brain barrier. Journal of Neuroimmunology, 232(1–2), 119–130. https://doi.org/10.1016/j.jneuroim.2010.10.029

Lagal, V., Dinis, M., Cannella, D., Bargieri, D., Gonzalez, V., Andenmatten, N., Meissner, M., & Tardieux, I. (2015). AMA1-Deficient Toxoplasma gondii Parasites Transiently Colonize Mice and Trigger an Innate Immune Response That Leads to Long-Lasting Protective Immunity. Infection and Immunity, 83(6), 2475–2486. https://doi.org/10.1128/IAI.02606-14

Lamarque, M., Besteiro, S., Papoin, J., Roques, M., Vulliez-Le Normand, B., Morlon-Guyot, J., Dubremetz, J.-F., Fauquenoy, S., Tomavo, S., Faber, B. W., Kocken, C. H., Thomas, A. W., Boulanger, M. J., Bentley, G. A., & Lebrun, M. (2011). The RON2-AMA1 interaction is a critical step in moving junction-dependent invasion by apicomplexan parasites. PLoS Pathogens, 7(2), e1001276. https://doi.org/10.1371/journal.ppat.1001276

Lamarque, M. H., Roques, M., Kong-Hap, M., Tonkin, M. L., Rugarabamu, G., Marq, J.-B., Penarete-Vargas, D. M., Boulanger, M. J., Soldati-Favre, D., & Lebrun, M. (2014). Plasticity and

redundancy among AMA-RON pairs ensure host cell entry of Toxoplasma parasites. Nature Communications, 5, 4098. https://doi.org/10.1038/ncomms5098

Langermans, J. A., van der Hulst, M. E., Nibbering, P. H., & van Furth, R. (1992). Endogenous tumor necrosis factor alpha is required for enhanced antimicrobial activity against Toxoplasma gondii and Listeria monocytogenes in recombinant gamma interferon-treated mice. Infection and Immunity, 60(12), 5107–5112. https://doi.org/10.1128/IAI.60.12.5107-5112.1992

Laurens, M. B., Kouriba, B., Bergmann-Leitner, E., Angov, E., Coulibaly, D., Diarra, I., Daou, M., Niangaly, A., Blackwelder, W. C., Wu, Y., Cohen, J., Ballou, W. R., Vekemans, J., Lanar, D. E., Dutta, S., Diggs, C., Soisson, L., Heppner, D. G., Doumbo, O. K., … Thera, M. A. (2017). Strain-specific Plasmodium falciparum growth inhibition among Malian children immunized with a blood-stage malaria vaccine. PloS One, 12(3), e0173294. https://doi.org/10.1371/journal.pone.0173294

Le Roux, D., Djokic, V., Morisse, S., Chauvin, C., Doré, V., Lagrée, A.-C., Voisin, D., Villain, Y., Grasset-Chevillot, A., Boursin, F., Su, C., Perrot, S., Vallée, I., Seche, E., & Blaga, R. (2020). Evaluation of immunogenicity and protection of the Mic1-3 knockout Toxoplasma gondii live attenuated strain in the feline host. Vaccine, 38(6), 1457–1466. https://doi.org/10.1016/j.vaccine.2019.11.076

Lebrun, M., Carruthers, V. B., & Cesbron-Delauw, M.-F. (2020). Chapter 14 - Toxoplasma secretory proteins and their roles in parasite cell cycle and infection. In L. M. Weiss & K. Kim (Eds.), Toxoplasma gondii (Third Edition) (pp. 607–704). Academic Press. https://doi.org/10.1016/B978-0-12-815041-2.00014-1

Lebrun, M., Michelin, A., El Hajj, H., Poncet, J., Bradley, P. J., Vial, H., & Dubremetz, J. F. (2005). The rhoptry neck protein RON4 re-localizes at the moving junction during Toxoplasma gondii invasion. Cellular Microbiology, 7(12), 1823–1833. https://doi.org/10.1111/j.1462-5822.2005.00646.x

Lee, S.-B., & Lee, T.-G. (2017). Toxoplasmic Encephalitis in Patient with Acquired Immunodeficiency Syndrome. Brain Tumor Research and Treatment, 5(1), 34–36. https://doi.org/10.14791/btrt.2017.5.1.34

Lee, S.-H., Kang, H.-J., Lee, D.-H., Kang, S.-M., & Quan, F.-S. (2018). Virus-like particle vaccines expressing Toxoplasma gondii rhoptry protein 18 and microneme protein 8 provide enhanced protection. Vaccine, 36(38), 5692–5700. https://doi.org/10.1016/j.vaccine.2018.08.016

Lek, A., Evesson, F. J., Sutton, R. B., North, K. N., & Cooper, S. T. (2012). Ferlins: regulators of vesicle fusion for auditory neurotransmission, receptor trafficking and membrane repair. Traffic (Copenhagen, Denmark), 13(2), 185–194. https://doi.org/10.1111/j.1600-0854.2011.01267.x

Lekutis, C., Ferguson, D. J., Grigg, M. E., Camps, M., & Boothroyd, J. C. (2001). Surface antigens of Toxoplasma gondii: variations on a theme. International Journal for Parasitology, 31(12), 1285–1292. https://doi.org/10.1016/s0020-7519(01)00261-2

Leriche, M. A., & Dubremetz, J. F. (1991). Characterization of the protein contents of rhoptries and dense granules of Toxoplasma gondii tachyzoites by subcellular fractionation and monoclonal antibodies. Molecular and Biochemical Parasitology, 45(2), 249–259. https://doi.org/10.1016/0166-6851(91)90092-K

Li, Y., Liu, Y., Xiu, F., Wang, J., Cong, H., He, S., Shi, Y., Wang, X., Li, X., & Zhou, H. (2018). Characterization of exosomes derived from Toxoplasma gondii and their functions in modulating immune responses. International Journal of Nanomedicine, 13, 467–477. https://doi.org/10.2147/IJN.S151110

Li, Y., & Zhou, H. (2018). Moving towards improved vaccines for Toxoplasma gondii. Expert Opinion on Biological Therapy, 18(3), 273–280. https://doi.org/10.1080/14712598.2018.1413086

Lima, T. S., & Lodoen, M. B. (2019). Mechanisms of Human Innate Immune Evasion by Toxoplasma gondii. Frontiers in Cellular and Infection Microbiology, 9, 103. https://doi.org/10.3389/fcimb.2019.00103

Lindsay, D. S., & Dubey, J. P. (2009). Long-term survival of Toxoplasma gondii sporulated oocysts in seawater. The Journal of Parasitology, 95(4), 1019–1020. https://doi.org/10.1645/GE-1919.1

Liu, Q., Singla, L. D., & Zhou, H. (2012). Vaccines against Toxoplasma gondii: Status, challenges and future directions. Human Vaccines & Immunotherapeutics, 8(9), 1305–1308. https://doi.org/10.4161/hv.21006

Liu, Z., Yin, L., Li, Y., Yuan, F., Zhang, X., Ma, J., Liu, H., Wang, Y., Zheng, K., & Cao, J. (2016). Intranasal immunization with recombinant Toxoplasma gondii actin depolymerizing factor confers protective efficacy against toxoplasmosis in mice. BMC Immunology, 17. https://doi.org/10.1186/s12865-016-0173-9

Loh, F.-K., Nathan, S., Chow, S.-C., & Fang, C.-M. (2019). Vaccination challenges and strategies against long-lived Toxoplasma gondii. Vaccine, 37(30), 3989–4000. https://doi.org/10.1016/j.vaccine.2019.05.083

Long, S., Brown, K. M., Drewry, L. L., Anthony, B., Phan, I. Q. H., & Sibley, L. D. (2017). Calmodulin-like proteins localized to the conoid regulate motility and cell invasion by Toxoplasma gondii. PLOS Pathogens, 13(5), e1006379. https://doi.org/10.1371/journal.ppat.1006379

Lourido, S., & Moreno, S. N. J. (2015). The calcium signaling toolkit of the Apicomplexan parasites Toxoplasma gondii and Plasmodium spp. Cell Calcium, 57(3), 186–193. https://doi.org/10.1016/j.ceca.2014.12.010

Lourido, S., Shuman, J., Zhang, C., Shokat, K. M., Hui, R., & Sibley, L. D. (2010). Calcium-dependent protein kinase 1 is an essential regulator of exocytosis in Toxoplasma. Nature, 465(7296), 359–362. https://doi.org/10.1038/nature09022

Lovett, J. L., Marchesini, N., Moreno, S. N. J., & Sibley, L. D. (2002). Toxoplasma gondii microneme secretion involves intracellular Ca(2+) release from inositol 1,4,5-triphosphate (IP(3))/ryanodine-sensitive stores. The Journal of Biological Chemistry, 277(29), 25870–25876. https://doi.org/10.1074/jbc.M202553200

Lüder, C. G. K., Algner, M., Lang, C., Bleicher, N., & Gross, U. (2003). Reduced expression of the inducible nitric oxide synthase after infection with Toxoplasma gondii facilitates parasite replication in activated murine macrophages. International Journal for Parasitology, 33(8), 833–844. https://doi.org/10.1016/s0020-7519(03)00092-4

Lüder, C. G. K., & Seeber, F. (2016). <Emphasis Type="Italic">Toxoplasma</Emphasis>. Molecular Parasitology, 217–239. https://doi.org/10.1007/978-3-7091-1416-2_8

Luft, B. J., & Remington, J. S. (1992). Toxoplasmic encephalitis in AIDS. Clinical Infectious Diseases: An Official Publication of the Infectious Diseases Society of America, 15(2), 211–222. https://doi.org/10.1093/clinids/15.2.211

Lütjen, S., Soltek, S., Virna, S., Deckert, M., & Schlüter, D. (2006). Organ- and disease-stage-specific regulation of Toxoplasma gondii-specific CD8-T-cell responses by CD4 T cells. Infection and Immunity, 74(10), 5790–5801. https://doi.org/10.1128/IAI.00098-06

Lyons, R. E., McLeod, R., & Roberts, C. W. (2002). Toxoplasma gondii tachyzoite-bradyzoite interconversion. Trends in Parasitology, 18(5), 198–201.

Machado, A. V., Caetano, B. C., Barbosa, R. P., Salgado, A. P. C., Rabelo, R. H., Garcia, C. C., Bruna-Romero, O., Escriou, N., & Gazzinelli, R. T. (2010). Prime and boost immunization with influenza and adenovirus encoding the Toxoplasma gondii surface antigen 2 (SAG2) induces strong protective immunity. Vaccine, 28(18), 3247–3256. https://doi.org/10.1016/j.vaccine.2010.02.003

Mahamed, D. A., Mills, J. H., Egan, C. E., Denkers, E. Y., & Bynoe, M. S. (2012). CD73-generated adenosine facilitates Toxoplasma gondii differentiation to long-lived tissue cysts in the central nervous system. Proceedings of the National Academy of Sciences of the United States of America, 109(40), 16312–16317. https://doi.org/10.1073/pnas.1205589109

Mai, K., Sharman, P. A., Walker, R. A., Katrib, M., De Souza, D., McConville, M. J., Wallach, M. G., Belli, S. I., Ferguson, D. J. P., & Smith, N. C. (2009). Oocyst wall formation and composition in

coccidian parasites. Memorias Do Instituto Oswaldo Cruz, 104(2), 281–289. https://doi.org/10.1590/s0074-02762009000200022

Malkin, E. M., Durbin, A. P., Diemert, D. J., Sattabongkot, J., Wu, Y., Miura, K., Long, C. A., Lambert, L., Miles, A. P., Wang, J., Stowers, A., Miller, L. H., & Saul, A. (2005). Phase 1 vaccine trial of Pvs25H: a transmission blocking vaccine for Plasmodium vivax malaria. Vaccine, 23(24), 3131–3138. https://doi.org/10.1016/j.vaccine.2004.12.019

Mammari, N., Vignoles, P., Halabi, M. A., Dardé, M.-L., & Courtioux, B. (2015). Interferon gamma effect on immune mediator production in human nerve cells infected by two strains of Toxoplasma gondii. Parasite, 22. https://doi.org/10.1051/parasite/2015039

Maraghi, S., Ghadiri, A. A., Tavalla, M., Shojaee, S., & Abdizadeh, R. (2019). Evaluation of immunogenicity and protective effect of DNA vaccine encoding surface antigen1 (SAG1) of Toxoplasma gondii and TLR-5 ligand as a genetic adjuvant against acute toxoplasmosis in BALB/c mice. Biologicals: Journal of the International Association of Biological Standardization, 62, 39–49. https://doi.org/10.1016/j.biologicals.2019.10.002

Marchant, J., Cowper, B., Liu, Y., Lai, L., Pinzan, C., Marq, J. B., Friedrich, N., Sawmynaden, K., Liew, L., Chai, W., Childs, R. A., Saouros, S., Simpson, P., Roque Barreira, M. C., Feizi, T., Soldati-Favre, D., & Matthews, S. (2012). Galactose recognition by the apicomplexan parasite Toxoplasma gondii. The Journal of Biological Chemistry, 287(20), 16720–16733. https://doi.org/10.1074/jbc.M111.325928

Martin, H. L., Alsaady, I., Howell, G., Prandovszky, E., Peers, C., Robinson, P., & McConkey, G. A. (2015). Effect of parasitic infection on dopamine biosynthesis in dopaminergic cells. Neuroscience, 306, 50–62. https://doi.org/10.1016/j.neuroscience.2015.08.005

Matias, M., Gomes, A., Marques, T., & Fonseca, A. C. (2014). Ocular toxoplasmosis: a very rare presentation in an immunocompetent patient. BMJ Case Reports, 2014. https://doi.org/10.1136/bcr-2014-205846

Mayoral, J., Di Cristina, M., Carruthers, V. B., & Weiss, L. M. (2020). Toxoplasma gondii: Bradyzoite Differentiation In Vitro and In Vivo. Methods in Molecular Biology (Clifton, N.J.), 2071, 269–282. https://doi.org/10.1007/978-1-4939-9857-9_15

McFadden, G. I., & Yeh, E. (2017). The apicoplast: now you see it, now you don't. International Journal for Parasitology, 47(2–3), 137–144. https://doi.org/10.1016/j.ijpara.2016.08.005

Mehlhorn, H., & Frenkel, J. K. (1980). Ultrastructural Comparison of Cysts and Zoites of Toxoplasma gondii, Sarcocystis muris, and Hammondia hammondi in Skeletal Muscle of Mice. The Journal of Parasitology, 66(1), 59–67. JSTOR. https://doi.org/10.2307/3280590

Melo, M. B., Jensen, K. D. C., & Saeij, J. P. J. (2011). Toxoplasma gondii effectors are master regulators of the inflammatory response. Trends in Parasitology, 27(11), 487–495. https://doi.org/10.1016/j.pt.2011.08.001

Melzer, T. C., Cranston, H. J., Weiss, L. M., & Halonen, S. K. (2010). Host Cell Preference of Toxoplasma gondii Cysts in Murine Brain: A Confocal Study. Journal of Neuroparasitology, 1. https://doi.org/10.4303/jnp/N100505

Mévélec, M.-N., Ducournau, C., Bassuny Ismael, A., Olivier, M., Sèche, É., Lebrun, M., Bout, D., & Dimier-Poisson, I. (2010). Mic1-3 Knockout Toxoplasma gondii is a good candidate for a vaccine against T. gondii-induced abortion in sheep. Veterinary Research, 41(4). https://doi.org/10.1051/vetres/2010021

Mévélec, M.-N., Lakhrif, Z., & Dimier-Poisson, I. (2020). Key Limitations and New Insights Into the Toxoplasma gondii Parasite Stage Switching for Future Vaccine Development in Human, Livestock, and Cats. Frontiers in Cellular and Infection Microbiology, 10. https://doi.org/10.3389/fcimb.2020.607198

Miller, L. H., Aikawa, M., Johnson, J. G., & Shiroishi, T. (1979). Interaction between cytochalasin B-treated malarial parasites and erythrocytes. Attachment and junction formation. The Journal of Experimental Medicine, 149(1), 172–184. https://doi.org/10.1084/jem.149.1.172

Mintern, J. D., Percival, C., Kamphuis, M. M. J., Chin, W. J., Caruso, F., & Johnston, A. P. R. (2013). Targeting dendritic cells: the role of specific receptors in the internalization of polymer capsules. Advanced Healthcare Materials, 2(7), 940–944. https://doi.org/10.1002/adhm.201200441

Mital, J., Meissner, M., Soldati, D., & Ward, G. E. (2005). Conditional Expression of Toxoplasma gondii Apical Membrane Antigen-1 (TgAMA1) Demonstrates That TgAMA1 Plays a Critical Role in Host Cell Invasion. Molecular Biology of the Cell, 16(9), 4341–4349. https://doi.org/10.1091/mbc.E05-04-0281

Moiré, N., Dion, S., Lebrun, M., Dubremetz, J.-F., & Dimier-Poisson, I. (2009). Mic1-3KO tachyzoite a live attenuated vaccine candidate against toxoplasmosis derived from a type I strain shows features of type II strain. Experimental Parasitology, 123(2), 111–117. https://doi.org/10.1016/j.exppara.2009.06.003

Mondragon, R., & Frixione, E. (1996). Ca(2+)-dependence of conoid extrusion in Toxoplasma gondii tachyzoites. The Journal of Eukaryotic Microbiology, 43(2), 120–127. https://doi.org/10.1111/j.1550-7408.1996.tb04491.x

Montoya, J. G., & Liesenfeld, O. (2004). Toxoplasmosis. The Lancet, 363(9425), 1965–1976. https://doi.org/10.1016/S0140-6736(04)16412-X

Mordue, D. G., Desai, N., Dustin, M., & Sibley, L. D. (1999). Invasion by Toxoplasma gondii Establishes a Moving Junction That Selectively Excludes Host Cell Plasma Membrane Proteins on the Basis of Their Membrane Anchoring. The Journal of Experimental Medicine, 190(12), 1783–1792.

Morisaki, J. H., Heuser, J. E., & Sibley, L. D. (1995). Invasion of Toxoplasma gondii occurs by active penetration of the host cell. Journal of Cell Science, 108 (Pt 6), 2457–2464.

Morrissette, N. S., & Sibley, L. D. (2002). Cytoskeleton of Apicomplexan Parasites. Microbiology and Molecular Biology Reviews, 66(1), 21–38. https://doi.org/10.1128/MMBR.66.1.21-38.2002

Moudy, R., Manning, T. J., & Beckers, C. J. (2001). The loss of cytoplasmic potassium upon host cell breakdown triggers egress of Toxoplasma gondii. The Journal of Biological Chemistry, 276(44), 41492–41501. https://doi.org/10.1074/jbc.M106154200

Muniz-Feliciano, L., Van Grol, J., Portillo, J.-A. C., Liew, L., Liu, B., Carlin, C. R., Carruthers, V. B., Matthews, S., & Subauste, C. S. (2013). Toxoplasma gondii-induced activation of EGFR prevents autophagy protein-mediated killing of the parasite. PLoS Pathogens, 9(12), e1003809. https://doi.org/10.1371/journal.ppat.1003809

Murray, H. W., Szuro-Sudol, A., Wellner, D., Oca, M. J., Granger, A. M., Libby, D. M., Rothermel, C. D., & Rubin, B. Y. (1989). Role of tryptophan degradation in respiratory burst-independent antimicrobial activity of gamma interferon-stimulated human macrophages. Infection and Immunity, 57(3), 845–849. https://doi.org/10.1128/IAI.57.3.845-849.1989

Naguleswaran, A., Elias, E. V., McClintick, J., Edenberg, H. J., & Jr, W. J. S. (2010). Toxoplasma gondii Lysine Acetyltransferase GCN5-A Functions in the Cellular Response to Alkaline Stress and Expression of Cyst Genes. PLOS Pathogens, 6(12), e1001232. https://doi.org/10.1371/journal.ppat.1001232

Neves, E. S., Bicudo, L. N., Curi, A. L., Carregal, E., Bueno, W. F., Ferreira, R. G., Amendoeira, M. R., Benchimol, E., & Fernandes, O. (2009). Acute acquired toxoplasmosis: clinical-laboratorial aspects and ophthalmologic evaluation in a cohort of immunocompetent patients. Memórias Do Instituto Oswaldo Cruz, 104(2), 393–396. https://doi.org/10.1590/S0074-02762009000200039

NICOLLE, C. J. H. & L. H. M. (1865-1943). (1908). Sur une infection a corps de Leishman (ou organismes voisins) du gondi. In: Comptes Rendus Hebdomadaires des Seances de L'Academie des Sciences. . ., Vol. 147, Juillet - Decembre, 1908. Gauthier-Villars, 1908.

Normand, B. V.-L., Faber, B. W., Saul, F. A., Eijk, M. van der, Thomas, A. W., Singh, B., Kocken, C. H. M., & Bentley, G. A. (2015). Crystal Structure of Plasmodium knowlesi Apical Membrane

Antigen 1 and Its Complex with an Invasion-Inhibitory Monoclonal Antibody. PLOS ONE, 10(4), e0123567. https://doi.org/10.1371/journal.pone.0123567

Onile, O. S., Ojo, G. J., Oyeyemi, B. F., Agbowuro, G. O., & Fadahunsi, A. I. (2020). Development of multiepitope subunit protein vaccines against Toxoplasma gondii using an immunoinformatics approach. NAR Genomics and Bioinformatics, 2(lqaa048). https://doi.org/10.1093/nargab/lqaa048

Ono, T., Cabrita-Santos, L., Leitao, R., Bettiol, E., Purcell, L. A., Diaz-Pulido, O., Andrews, L. B., Tadakuma, T., Bhanot, P., Mota, M. M., & Rodriguez, A. (2008). Adenylyl Cyclase α and cAMP Signaling Mediate Plasmodium Sporozoite Apical Regulated Exocytosis and Hepatocyte Infection. PLOS Pathogens, 4(2), e1000008. https://doi.org/10.1371/journal.ppat.1000008

Opitz, C., & Soldati, D. (2002). "The glideosome": a dynamic complex powering gliding motion and host cell invasion by Toxoplasma gondii. Molecular Microbiology, 45(3), 597–604. https://doi.org/10.1046/j.1365-2958.2002.03056.x

Pace, D. A., McKnight, C. A., Liu, J., Jimenez, V., & Moreno, S. N. J. (2014). Calcium entry in Toxoplasma gondii and its enhancing effect of invasion-linked traits. The Journal of Biological Chemistry, 289(28), 19637–19647. https://doi.org/10.1074/jbc.M114.565390

Parker, M. L., & Boulanger, M. J. (2015). An Extended Surface Loop on Toxoplasma gondii Apical Membrane Antigen 1 (AMA1) Governs Ligand Binding Selectivity. PLOS ONE, 10(5), e0126206. https://doi.org/10.1371/journal.pone.0126206

Parker, M. L., Penarete-Vargas, D. M., Hamilton, P. T., Guérin, A., Dubey, J. P., Perlman, S. J., Spano, F., Lebrun, M., & Boulanger, M. J. (2016). Dissecting the interface between apicomplexan parasite and host cell: Insights from a divergent AMA–RON2 pair. Proceedings of the National Academy of Sciences, 113(2), 398–403. https://doi.org/10.1073/pnas.1515898113

Parlog, A., Schlüter, D., & Dunay, I. R. (2015). Toxoplasma gondii-induced neuronal alterations. Parasite Immunology, 37(3), 159–170. https://doi.org/10.1111/pim.12157

Pastor-Fernández, I., Kim, S., Billington, K., Bumstead, J., Marugán-Hernández, V., Küster, T., Ferguson, D. J. P., Vervelde, L., Blake, D. P., & Tomley, F. M. (2018). Development of cross-protective Eimeria-vectored vaccines based on apical membrane antigens. International Journal for Parasitology, 48(7), 505–518. https://doi.org/10.1016/j.ijpara.2018.01.003

Pastor-Fernández, I., Kim, S., Marugán-Hernández, V., Soutter, F., Tomley, F. M., & Blake, D. P. (2020). Vaccination with transgenic Eimeria tenella expressing Eimeria maxima AMA1 and IMP1 confers partial protection against high-level E. maxima challenge in a broiler model of coccidiosis. Parasites & Vectors, 13(1), 343. https://doi.org/10.1186/s13071-020-04210-2

Pavlou, G., Biesaga, M., Touquet, B., Lagal, V., Balland, M., Dufour, A., Hakimi, M., & Tardieux, I. (2018). Toxoplasma Parasite Twisting Motion Mechanically Induces Host Cell Membrane Fission to Complete Invasion within a Protective Vacuole. Cell Host & Microbe, 24(1), 81-96.e5. https://doi.org/10.1016/j.chom.2018.06.003

Pazicky, S., Dhamotharan, K., Kaszuba, K., Mertens, H. D. T., Gilberger, T., Svergun, D., Kosinski, J., Weininger, U., & Löw, C. (2020). Structural role of essential light chains in the apicomplexan glideosome. Communications Biology, 3(1), 1–14. https://doi.org/10.1038/s42003-020-01283-8

Pearce, B. D., Kruszon-Moran, D., & Jones, J. L. (2014). The association of Toxoplasma gondii infection with neurocognitive deficits in a population based analysis. Social Psychiatry and Psychiatric Epidemiology, 49(6), 1001–1010. https://doi.org/10.1007/s00127-014-0820-5

Peterson, M. G., Marshall, V. M., Smythe, J. A., Crewther, P. E., Lew, A., Silva, A., Anders, R. F., & Kemp, D. J. (1989). Integral membrane protein located in the apical complex of Plasmodium falciparum. Molecular and Cellular Biology, 9(7), 3151–3154.

Peterson, P. K., Gekker, G., Hu, S., & Chao, C. C. (1995). Human astrocytes inhibit intracellular multiplication of toxoplasma gondii by a nitric oxide-mediated mechanism. Journal of Infectious Diseases, 171(2), 516–518. https://doi.org/10.1093/infdis/171.2.516

Pfefferkorn, E. R. (1984). Interferon gamma blocks the growth of Toxoplasma gondii in human fibroblasts by inducing the host cells to degrade tryptophan. Proceedings of the National Academy of Sciences of the United States of America, 81(3), 908–912. https://doi.org/10.1073/pnas.81.3.908

Pinzan, C. F., Sardinha-Silva, A., Almeida, F., Lai, L., Lopes, C. D., Lourenço, E. V., Panunto-Castelo, A., Matthews, S., & Roque-Barreira, M. C. (2015). Vaccination with Recombinant Microneme Proteins Confers Protection against Experimental Toxoplasmosis in Mice. PLOS ONE, 10(11), e0143087. https://doi.org/10.1371/journal.pone.0143087

Pittman, K. J., Aliota, M. T., & Knoll, L. J. (2014). Dual transcriptional profiling of mice and Toxoplasma gondii during acute and chronic infection. BMC Genomics, 15(1), 806. https://doi.org/10.1186/1471-2164-15-806

Pizarro, J. C., Vulliez-Le Normand, B., Chesne-Seck, M.-L., Collins, C. R., Withers-Martinez, C., Hackett, F., Blackman, M. J., Faber, B. W., Remarque, E. J., Kocken, C. H. M., Thomas, A. W., & Bentley, G. A. (2005). Crystal structure of the malaria vaccine candidate apical membrane antigen 1. Science (New York, N.Y.), 308(5720), 408–411. https://doi.org/10.1126/science.1107449

Popiel, I., Gold, M. C., & Booth, K. S. (1996). Quantification of Toxoplasma gondii bradyzoites. The Journal of Parasitology, 82(2), 330–332.

PORCHET-HENNERE, E., & TORPIER, G. (1983). Relations entre toxoplasma et sa cellule-hôte. Relations Entre Toxoplasma et Sa Cellule-Hôte, 19(3), 357–370.

Poukchanski, A., Fritz, H. M., Tonkin, M. L., Treeck, M., Boulanger, M. J., & Boothroyd, J. C. (2013). Toxoplasma gondii sporozoites invade host cells using two novel paralogues of RON2 and AMA1. PloS One, 8(8), e70637. https://doi.org/10.1371/journal.pone.0070637

Prandota, J. (2009). The importance of toxoplasma gondii infection in diseases presenting with headaches. Headaches and aseptic meningitis may be manifestations of the Jarisch-

Herxheimer reaction. The International Journal of Neuroscience, 119(12), 2144–2182. https://doi.org/10.3109/00207450903149217

Radke, J. B., Lucas, O., De Silva, E. K., Ma, Y., Sullivan, W. J., Weiss, L. M., Llinas, M., & White, M. W. (2013). ApiAP2 transcription factor restricts development of the Toxoplasma tissue cyst. Proceedings of the National Academy of Sciences of the United States of America, 110(17), 6871–6876. https://doi.org/10.1073/pnas.1300059110

Radke, J. B., Worth, D., Hong, D., Huang, S., Sullivan, W. J., Wilson, E. H., & White, M. W. (2018). Transcriptional repression by ApiAP2 factors is central to chronic toxoplasmosis. PLoS Pathogens, 14(5). https://doi.org/10.1371/journal.ppat.1007035

Radke, J. R., Donald, R. G., Eibs, A., Jerome, M. E., Behnke, M. S., Liberator, P., & White, M. W. (2006). Changes in the Expression of Human Cell Division Autoantigen-1 Influence Toxoplasma gondii Growth and Development. PLoS Pathogens, 2(10). https://doi.org/10.1371/journal.ppat.0020105

Rahimi, M. T., Sarvi, S., Sharif, M., Abediankenari, S., Ahmadpour, E., Valadan, R., Ramandie, M. F.-, Hosseini, S.-A., & Daryani, A. (2017). Immunological evaluation of a DNA cocktail vaccine with co-delivery of calcium phosphate nanoparticles (CaPNs) against the Toxoplasma gondii RH strain in BALB/c mice. Parasitology Research, 116(2), 609–616. https://doi.org/10.1007/s00436-016-5325-6

Ramezani, M., Shojaii, M., Asadollahi, M., Karimialavijeh, E., & Gharagozli, K. (2016). Seroprevalence of Toxoplasma gondii in Iranian patients with idiopathic Parkinson's disease. Clinical and Experimental Neuroimmunology, 7(4), 361–365. https://doi.org/10.1111/cen3.12329

Raposo, G., & Stoorvogel, W. (2013). Extracellular vesicles: exosomes, microvesicles, and friends. The Journal of Cell Biology, 200(4), 373–383. https://doi.org/10.1083/jcb.201211138

Ravindran, S., Lodoen, M. B., Verhelst, S. H. L., Bogyo, M., & Boothroyd, J. C. (2009). 4-Bromophenacyl bromide specifically inhibits rhoptry secretion during Toxoplasma invasion. PloS One, 4(12), e8143. https://doi.org/10.1371/journal.pone.0008143

Robert-Gangneux, F., & Dardé, M.-L. (2012). Epidemiology of and diagnostic strategies for toxoplasmosis. Clinical Microbiology Reviews, 25(2), 264–296. https://doi.org/10.1128/CMR.05013-11

Roche, A. D., Rowley, D., Brett, F. M., & Looby, S. (2018, February 21). Concentric and Eccentric Target MRI Signs in a Case of HIV-Associated Cerebral Toxoplasmosis [Case Report]. Case Reports in Neurological Medicine. https://doi.org/10.1155/2018/9876514

Roiko, M. S., Svezhova, N., & Carruthers, V. B. (2014). Acidification Activates Toxoplasma gondii Motility and Egress by Enhancing Protein Secretion and Cytolytic Activity. PLOS Pathogens, 10(11), e1004488. https://doi.org/10.1371/journal.ppat.1004488

Roozbehani, M., Falak, R., Mohammadi, M., Hemphill, A., Razmjou, E., Meamar, A. R., Masoori, L., Khoshmirsafa, M., Moradi, M., & Gharavi, M. J. (2018). Characterization of a multi-epitope peptide with selective MHC-binding capabilities encapsulated in PLGA nanoparticles as a novel vaccine candidate against Toxoplasma gondii infection. Vaccine, 36(41), 6124–6132. https://doi.org/10.1016/j.vaccine.2018.08.068

Rugarabamu, G., Marq, J.-B., Guérin, A., Lebrun, M., & Soldati-Favre, D. (2015). Distinct contribution of Toxoplasma gondii rhomboid proteases 4 and 5 to micronemal protein protease 1 activity during invasion. Molecular Microbiology, 97(2), 244–262. https://doi.org/10.1111/mmi.13021

Saeij, J. P. J., Boyle, J. P., & Boothroyd, J. C. (2005). Differences among the three major strains of Toxoplasma gondii and their specific interactions with the infected host. Trends in Parasitology, 21(10), 476–481. https://doi.org/10.1016/j.pt.2005.08.001

Safa, G., & Darrieux, L. (2013). Cerebral toxoplasmosis after rituximab therapy. JAMA Internal Medicine, 173(10), 924–926. https://doi.org/10.1001/jamainternmed.2013.374

Saffer, L. D., Mercereau-Puijalon, O., Dubremetz, J.-F., & Schwartzman, J. D. (1992). Localization of a Toxoplasma gondii Rhoptry Protein by Immunoelectron Microscopy During and After Host

Cell Penetration. The Journal of Protozoology, 39(4), 526–530. https://doi.org/10.1111/j.1550-7408.1992.tb04844.x

Sahu, A., Kumar, S., Sreenivasamurthy, S. K., Selvan, L. D. N., Madugundu, A. K., Yelamanchi, S. D., Puttamallesh, V. N., Dey, G., Anil, A. K., Srinivasan, A., Mukherjee, K. K., Gowda, H., Satishchandra, P., Mahadevan, A., Pandey, A., Prasad, T. S. K., & Shankar, S. K. (2014). Host response profile of human brain proteome in toxoplasma encephalitis co-infected with HIV. Clinical Proteomics, 11(1), 39. https://doi.org/10.1186/1559-0275-11-39

Saksouk, N., Bhatti, M. M., Kieffer, S., Smith, A. T., Musset, K., Garin, J., Sullivan, W. J., Cesbron-Delauw, M.-F., & Hakimi, M.-A. (2005). Histone-Modifying Complexes Regulate Gene Expression Pertinent to the Differentiation of the Protozoan Parasite Toxoplasma gondii. Molecular and Cellular Biology, 25(23), 10301–10314. https://doi.org/10.1128/MCB.25.23.10301-10314.2005

Santos, J. M., Lebrun, M., Daher, W., Soldati, D., & Dubremetz, J.-F. (2009). Apicomplexan cytoskeleton and motors: key regulators in morphogenesis, cell division, transport and motility. International Journal for Parasitology, 39(2), 153–162. https://doi.org/10.1016/j.ijpara.2008.10.007

Sasono, P. M. D., & Smith, J. E. (1998). Toxoplasma gondii : an ultrastructural study of host-cell invasion by the bradyzoite stage. Parasitology Research, 84(8), 640–645. https://doi.org/10.1007/s004360050463

Sawmynaden, K., Saouros, S., Friedrich, N., Marchant, J., Simpson, P., Bleijlevens, B., Blackman, M. J., Soldati-Favre, D., & Matthews, S. (2008). Structural insights into microneme protein assembly reveal a new mode of EGF domain recognition. EMBO Reports, 9(11), 1149–1155. https://doi.org/10.1038/embor.2008.179

Sayles, P. C., Gibson, G. W., & Johnson, L. L. (2000). B Cells Are Essential for Vaccination-Induced Resistance to Virulent Toxoplasma gondii. Infection and Immunity, 68(3), 1026–1033.

Scharton-Kersten, T. M., Wynn, T. A., Denkers, E. Y., Bala, S., Grunvald, E., Hieny, S., Gazzinelli, R. T., & Sher, A. (1996). In the absence of endogenous IFN-gamma, mice develop unimpaired IL-12 responses to Toxoplasma gondii while failing to control acute infection. The Journal of Immunology, 157(9), 4045–4054.

Schlüter, D., Deckert, M., Hof, H., & Frei, K. (2001). Toxoplasma gondii infection of neurons induces neuronal cytokine and chemokine production, but gamma interferon- and tumor necrosis factor-stimulated neurons fail to inhibit the invasion and growth of T. gondii. Infection and Immunity, 69(12), 7889–7893. https://doi.org/10.1128/IAI.69.12.7889-7893.2001

Schlüter, D., Löhler, J., Deckert, M., Hof, H., & Schwendemann, G. (1991). Toxoplasma encephalitis of immunocompetent and nude mice: immunohistochemical characterisation of Toxoplasma antigen, infiltrates and major histocompatibility complex gene products. Journal of Neuroimmunology, 31(3), 185–198. https://doi.org/10.1016/0165-5728(91)90040-e

Schlüter, Dirk, Kwok, L.-Y., Lütjen, S., Soltek, S., Hoffmann, S., Körner, H., & Deckert, M. (2003). Both lymphotoxin-alpha and TNF are crucial for control of Toxoplasma gondii in the central nervous system. Journal of Immunology (Baltimore, Md.: 1950), 170(12), 6172–6182. https://doi.org/10.4049/jimmunol.170.12.6172

Schmitz, J. L., Carlin, J. M., Borden, E. C., & Byrne, G. I. (1989). Beta interferon inhibits Toxoplasma gondii growth in human monocyte-derived macrophages. Infection and Immunity, 57(10), 3254–3256.

Scholtyseck, E., & Mehlhorn, H. (1970). Ultrastructural study of characteristic organelles (paired organelles, micronemes, micropores) of sporozoa and related organisms. Zeitschrift Für Parasitenkunde, 34(2), 97–127. https://doi.org/10.1007/BF00260383

Sekandarpour, S., Mirahmadi, H., Mohammadi, M., Zaman, J., Saravani, R., & Mousavi, M. (2018, January 29). Study of Tissue Orientation and Parasite Load in Various Tissues and Blood in an Experimental Mouse Model of Acute Toxoplasmosis. Archives of Clinical Infectious Diseases. https://doi.org/10.5812/archcid.13744

Sharif, M., Amouei, A., Sarvi, S., Mizani, A., Aarabi, M., Hosseini, S.-A., & Daryani, A. (2017). Genetic diversity of Toxoplasma gondii isolates from ruminants: A systematic review. International Journal of Food Microbiology, 258, 38–49. https://doi.org/10.1016/j.ijfoodmicro.2017.07.007

Sheiner, L., Vaidya, A. B., & McFadden, G. I. (2013). The metabolic roles of the endosymbiotic organelles of Toxoplasma and Plasmodium spp. Current Opinion in Microbiology, 16(4), 452–458. https://doi.org/10.1016/j.mib.2013.07.003

Shen, B., Buguliskis, J. S., Lee, T. D., & Sibley, L. D. (2014). Functional Analysis of Rhomboid Proteases during Toxoplasma Invasion. MBio, 5(5). https://doi.org/10.1128/mBio.01795-14

Shwab, E. K., Saraf, P., Zhu, X.-Q., Zhou, D.-H., McFerrin, B. M., Ajzenberg, D., Schares, G., Hammond-Aryee, K., van Helden, P., Higgins, S. A., Gerhold, R. W., Rosenthal, B. M., Zhao, X., Dubey, J. P., & Su, C. (2018). Human impact on the diversity and virulence of the ubiquitous zoonotic parasite Toxoplasma gondii. Proceedings of the National Academy of Sciences of the United States of America, 115(29), E6956–E6963. https://doi.org/10.1073/pnas.1722202115

Shwab, E. K., Zhu, X.-Q., Majumdar, D., Pena, H. F. J., Gennari, S. M., Dubey, J. P., & Su, C. (2014). Geographical patterns of Toxoplasma gondii genetic diversity revealed by multilocus PCR-RFLP genotyping. Parasitology, 141(4), 453–461. https://doi.org/10.1017/S0031182013001844

Sibley, L. D., & Boothroyd, J. C. (1992). Virulent strains of Toxoplasma gondii comprise a single clonal lineage. Nature, 359(6390), 82–85. https://doi.org/10.1038/359082a0

Sibley, L. D., Messina, M., & Niesman, I. R. (1994). Stable DNA transformation in the obligate intracellular parasite Toxoplasma gondii by complementation of tryptophan auxotrophy. Proceedings of the National Academy of Sciences of the United States of America, 91(12), 5508–5512. https://doi.org/10.1073/pnas.91.12.5508

Sidik, S. M., Hortua Triana, M. A., Paul, A. S., El Bakkouri, M., Hackett, C. G., Tran, F., Westwood, N. J., Hui, R., Zuercher, W. J., Duraisingh, M. T., Moreno, S. N. J., & Lourido, S. (2016). Using a

Genetically Encoded Sensor to Identify Inhibitors of Toxoplasma gondii Ca2+ Signaling. The Journal of Biological Chemistry, 291(18), 9566–9580. https://doi.org/10.1074/jbc.M115.703546

Silva, N. M., Gazzinelli, R. T., Silva, D. A., Ferro, E. A., Kasper, L. H., & Mineo, J. R. (1998). Expression of Toxoplasma gondii-specific heat shock protein 70 during In vivo conversion of bradyzoites to tachyzoites. Infection and Immunity, 66(8), 3959–3963. https://doi.org/10.1128/IAI.66.8.3959-3963.1998

Singh, S. (2016). Congenital toxoplasmosis: Clinical features, outcomes, treatment, and prevention. Tropical Parasitology, 6(2), 113–122. https://doi.org/10.4103/2229-5070.190813

Sirima, S. B., Durier, C., Kara, L., Houard, S., Gansane, A., Loulergue, P., Bahuaud, M., Benhamouda, N., Nebié, I., Faber, B., Remarque, E., Launay, O., & AMA1-DiCo Study Group. (2017). Safety and immunogenicity of a recombinant Plasmodium falciparum AMA1-DiCo malaria vaccine adjuvanted with GLA-SE or Alhydrogel® in European and African adults: A phase 1a/1b, randomized, double-blind multi-centre trial. Vaccine, 35(45), 6218–6227. https://doi.org/10.1016/j.vaccine.2017.09.027

Skariah, S., McIntyre, M. K., & Mordue, D. G. (2010). Toxoplasma gondii: determinants of tachyzoite to bradyzoite conversion. Parasitology Research, 107(2), 253–260. https://doi.org/10.1007/s00436-010-1899-6

Skillman, K. M., Diraviyam, K., Khan, A., Tang, K., Sept, D., & Sibley, L. D. (2011). Evolutionarily Divergent, Unstable Filamentous Actin Is Essential for Gliding Motility in Apicomplexan Parasites. PLOS Pathogens, 7(10), e1002280. https://doi.org/10.1371/journal.ppat.1002280

Skwarczynski, M., Zaman, M., Urbani, C. N., Lin, I.-C., Jia, Z., Batzloff, M. R., Good, M. F., Monteiro, M. J., & Toth, I. (2010). Polyacrylate dendrimer nanoparticles: a self-adjuvanting vaccine delivery system. Angewandte Chemie (International Ed. in English), 49(33), 5742–5745. https://doi.org/10.1002/anie.201002221

Snapper, C. M., & Paul, W. E. (1987). Interferon-gamma and B cell stimulatory factor-1 reciprocally regulate Ig isotype production. Science (New York, N.Y.), 236(4804), 944–947. https://doi.org/10.1126/science.3107127

Soldati, D., Dubremetz, J. F., & Lebrun, M. (2001). Microneme proteins: structural and functional requirements to promote adhesion and invasion by the apicomplexan parasite Toxoplasma gondii. International Journal for Parasitology, 31(12), 1293–1302. https://doi.org/10.1016/s0020-7519(01)00257-0

Speer, C. A., & Dubey, J. P. (1998). Ultrastructure of early stages of infections in mice fed Toxoplasma gondii oocysts. Parasitology, 116 (Pt 1), 35–42. https://doi.org/10.1017/s0031182097001959

Speer, C. A., & Dubey, J. P. (2005). Ultrastructural differentiation of Toxoplasma gondii schizonts (types B to E) and gamonts in the intestines of cats fed bradyzoites. International Journal for Parasitology, 35(2), 193–206. https://doi.org/10.1016/j.ijpara.2004.11.005

Speer, C. A., Dubey, J. P., Blixt, J. A., & Prokop, K. (1997). Time lapse video microscopy and ultrastructure of penetrating sporozoites, types 1 and 2 parasitophorous vacuoles, and the transformation of sporozoites to tachyzoites of the VEG strain of Toxoplasma gondii. The Journal of Parasitology, 83(4), 565–574.

Speer, C. A., Tilley, M., Temple, M. E., Blixt, J. A., Dubey, J. P., & White, M. W. (1995). Sporozoites of Toxoplasma gondii lack dense-granule protein GRA3 and form a unique parasitophorous vacuole. Molecular and Biochemical Parasitology, 75(1), 75–86. https://doi.org/10.1016/0166-6851(95)02515-4

Splendore, A. (1908). Un nuovo protozoa parassita dei conigli: incontrato nell lesioni anatomiche d'une malattia che ricorda in molti punti kala-azar dell'uomo. 3, 109–112.

Srinivasan, P., Baldeviano, G. C., Miura, K., Diouf, A., Ventocilla, J. A., Leiva, K. P., Lugo-Roman, L., Lucas, C., Orr-Gonzalez, S., Zhu, D., Villasante, E., Soisson, L., Narum, D. L., Pierce, S. K., Long, C. A., Diggs, C., Duffy, P. E., Lescano, A. G., & Miller, L. H. (2017). A malaria vaccine protects

Aotus monkeys against virulent Plasmodium falciparum infection. Npj Vaccines, 2(1), 1–10. https://doi.org/10.1038/s41541-017-0015-7

Srinivasan, P., Beatty, W. L., Diouf, A., Herrera, R., Ambroggio, X., Moch, J. K., Tyler, J. S., Narum, D. L., Pierce, S. K., Boothroyd, J. C., Haynes, J. D., & Miller, L. H. (2011). Binding of Plasmodium merozoite proteins RON2 and AMA1 triggers commitment to invasion. Proceedings of the National Academy of Sciences of the United States of America, 108(32), 13275–13280. https://doi.org/10.1073/pnas.1110303108

Srinivasan, P., Ekanem, E., Diouf, A., Tonkin, M. L., Miura, K., Boulanger, M. J., Long, C. A., Narum, D. L., & Miller, L. H. (2014). Immunization with a functional protein complex required for erythrocyte invasion protects against lethal malaria. Proceedings of the National Academy of Sciences of the United States of America, 111(28), 10311–10316. https://doi.org/10.1073/pnas.1409928111

Stevens, T. L., Bossie, A., Sanders, V. M., Fernandez-Botran, R., Coffman, R. L., Mosmann, T. R., & Vitetta, E. S. (1988). Regulation of antibody isotype secretion by subsets of antigen-specific helper T cells. Nature, 334(6179), 255–258. https://doi.org/10.1038/334255a0

Straub, K. W., Cheng, S. J., Sohn, C. S., & Bradley, P. J. (2009). Novel components of the Apicomplexan moving junction reveal conserved and coccidia-restricted elements. Cellular Microbiology, 11(4), 590–603. https://doi.org/10.1111/j.1462-5822.2008.01276.x

Straub, K. W., Peng, E. D., Hajagos, B. E., Tyler, J. S., & Bradley, P. J. (2011). The Moving Junction Protein RON8 Facilitates Firm Attachment and Host Cell Invasion in Toxoplasma gondii. PLOS Pathogens, 7(3), e1002007. https://doi.org/10.1371/journal.ppat.1002007

Su, C., Khan, A., Zhou, P., Majumdar, D., Ajzenberg, D., Dardé, M.-L., Zhu, X.-Q., Ajioka, J. W., Rosenthal, B. M., Dubey, J. P., & Sibley, L. D. (2012). Globally diverse Toxoplasma gondii isolates comprise six major clades originating from a small number of distinct ancestral lineages. Proceedings of the National Academy of Sciences, 109(15), 5844–5849. https://doi.org/10.1073/pnas.1203190109

Sullivan, A. M., Zhao, X., Suzuki, Y., Ochiai, E., Crutcher, S., & Gilchrist, M. A. (2013). Evidence for Finely-Regulated Asynchronous Growth of Toxoplasma gondii Cysts Based on Data-Driven Model Selection. PLOS Computational Biology, 9(11), e1003283. https://doi.org/10.1371/journal.pcbi.1003283

Sullivan, W. J., Smith, A. T., & Joyce, B. R. (2009). Understanding mechanisms and the role of differentiation in pathogenesis of Toxoplasma gondii: a review. Memorias Do Instituto Oswaldo Cruz, 104(2), 155–161.

Sun, H., Li, J., Xiao, T., Huang, X.-D., Wang, L.-J., Huang, B.-C., Yin, K., Liu, G.-Z., Xu, C., & Wei, Q.-K. (2020). Protective immunity induced by a DNA vaccine cocktail expressing TgSAG1, TgROP2, and the genetic adjuvant HBsAg against Toxoplasma gondii infection. Microbial Pathogenesis, 147, 104441. https://doi.org/10.1016/j.micpath.2020.104441

Suzuki, Y., & Joh, K. (1994). Effect of the strain of Toxoplasma gondii on the development of toxoplasmic encephalitis in mice treated with antibody to interferon-gamma. Parasitology Research, 80(2), 125–130. https://doi.org/10.1007/BF00933779

Suzuki, Y, Joh, K., Orellana, M. A., Conley, F. K., & Remington, J. S. (1991). A gene(s) within the H-2D region determines the development of toxoplasmic encephalitis in mice. Immunology, 74(4), 732–739.

Suzuki, Y., Orellana, M. A., Schreiber, R. D., & Remington, J. S. (1988). Interferon-gamma: the major mediator of resistance against Toxoplasma gondii. Science, 240(4851), 516–518. https://doi.org/10.1126/science.3128869

Suzuki, Y., & Remington, J. S. (1990). The effect of anti-IFN-gamma antibody on the protective effect of Lyt-2+ immune T cells against toxoplasmosis in mice. Journal of Immunology (Baltimore, Md.: 1950), 144(5), 1954–1956.

Suzuki, Yasuhiro, Claflin, J., Wang, X., Lengi, A., & Kikuchi, T. (2005). Microglia and macrophages as innate producers of interferon-gamma in the brain following infection with Toxoplasma

gondii. International Journal for Parasitology, 35(1), 83–90. https://doi.org/10.1016/j.ijpara.2004.10.020

Swierzy, I. J., Händel, U., Kaever, A., Jarek, M., Scharfe, M., Schlüter, D., & Lüder, C. G. K. (2017). Divergent co-transcriptomes of different host cells infected with Toxoplasma gondii reveal cell type-specific host-parasite interactions. Scientific Reports, 7(1), 7229. https://doi.org/10.1038/s41598-017-07838-w

Swisher, C. N., Boyer, K., & McLeod, R. (1994). Congenital toxoplasmosis. The Toxoplasmosis Study Group. Seminars in Pediatric Neurology, 1(1), 4–25.

Takemae, H., Kobayashi, K., Sugi, T., Han, Y., Gong, H., Ishiwa, A., Recuenco, F. C., Murakoshi, F., Takano, R., Murata, Y., Nagamune, K., Horimoto, T., Akashi, H., & Kato, K. (2018). Toxoplasma gondii RON4 binds to heparan sulfate on the host cell surface. Parasitology International, 67(2), 123–130. https://doi.org/10.1016/j.parint.2017.10.008

Takemae, H., Sugi, T., Kobayashi, K., Gong, H., Ishiwa, A., Recuenco, F. C., Murakoshi, F., Iwanaga, T., Inomata, A., Horimoto, T., Akashi, H., & Kato, K. (2013). Characterization of the interaction between Toxoplasma gondii rhoptry neck protein 4 and host cellular β-tubulin. Scientific Reports, 3. https://doi.org/10.1038/srep03199

Tang, Q., Andenmatten, N., Hortua Triana, M. A., Deng, B., Meissner, M., Moreno, S. N. J., Ballif, B. A., & Ward, G. E. (2014). Calcium-dependent phosphorylation alters class XIVa myosin function in the protozoan parasite Toxoplasma gondii. Molecular Biology of the Cell, 25(17), 2579–2591. https://doi.org/10.1091/mbc.E13-11-0648

Tang, X., Wang, C., Liang, L., Hu, D., Zhang, S., Duan, C., Suo, J., Liu, X., Suo, X., & Cui, S. (2019). Co-immunization with two recombinant Eimeria tenella lines expressing immunoprotective antigens of E. maxima elicits enhanced protection against E. maxima infection. Parasites & Vectors, 12(1), 347. https://doi.org/10.1186/s13071-019-3605-6

Tartarelli, I., Tinari, A., Possenti, A., Cherchi, S., Falchi, M., Dubey, J. P., & Spano, F. (2020). During host cell traversal and cell-to-cell passage, Toxoplasma gondii sporozoites inhabit the

parasitophorous vacuole and posteriorly release dense granule protein-associated membranous trails. International Journal for Parasitology, 50(13), 1099–1115. https://doi.org/10.1016/j.ijpara.2020.06.012

Tenter, A. M., Heckeroth, A. R., & Weiss, L. M. (2000). Toxoplasma gondii: from animals to humans. International Journal for Parasitology, 30(12–13), 1217–1258.

Théry, C., Zitvogel, L., & Amigorena, S. (2002). Exosomes: composition, biogenesis and function. Nature Reviews. Immunology, 2(8), 569–579. https://doi.org/10.1038/nri855

Thirugnanam, S., Rout, N., & Gnanasekar, M. (2013). Possible role of Toxoplasma gondii in brain cancer through modulation of host microRNAs. Infectious Agents and Cancer, 8(1), 8. https://doi.org/10.1186/1750-9378-8-8

Thomas, F., Lafferty, K. D., Brodeur, J., Elguero, E., Gauthier-Clerc, M., & Missé, D. (2012). Incidence of adult brain cancers is higher in countries where the protozoan parasite Toxoplasma gondii is common. Biology Letters, 8(1), 101–103. https://doi.org/10.1098/rsbl.2011.0588

Tonkin, M. L., & Boulanger, M. J. (2015). The Shear Stress of Host Cell Invasion: Exploring the Role of Biomolecular Complexes. PLOS Pathogens, 11(1), e1004539. https://doi.org/10.1371/journal.ppat.1004539

Tonkin, M. L., Roques, M., Lamarque, M. H., Pugnière, M., Douguet, D., Crawford, J., Lebrun, M., & Boulanger, M. J. (2011). Host Cell Invasion by Apicomplexan Parasites: Insights from the Co-Structure of AMA1 with a RON2 Peptide. Science, 333(6041), 463–467. https://doi.org/10.1126/science.1204988

Tosetti, N., Dos Santos Pacheco, N., Soldati-Favre, D., & Jacot, D. (2019). Three F-actin assembly centers regulate organelle inheritance, cell-cell communication and motility in Toxoplasma gondii. ELife, 8, e42669. https://doi.org/10.7554/eLife.42669

Tussiwand, R., Behnke, M. S., Kretzer, N. M., Grajales-Reyes, G. E., Murphy, T. L., Schreiber, R. D., Murphy, K. M., & Sibley, L. D. (2020). An important role for CD4+ T cells in adaptive

immunity to Toxoplasma gondii in mice lacking the transcription factor Batf3. MSphere, 5(4), e00634-20. https://doi.org/10.1128/MSPHERE.00634-20

Tyler, J. S., & Boothroyd, J. C. (2011). The C-terminus of Toxoplasma RON2 provides the crucial link between AMA1 and the host-associated invasion complex. PLoS Pathogens, 7(2), e1001282. https://doi.org/10.1371/journal.ppat.1001282

Ueno, N., Harker, K. S., Clarke, E. V., McWhorter, F. Y., Liu, W. F., Tenner, A. J., & Lodoen, M. B. (2014). Real-time imaging of Toxoplasma-infected human monocytes under fluidic shear stress reveals rapid translocation of intracellular parasites across endothelial barriers. Cellular Microbiology, 16(4), 580–595. https://doi.org/10.1111/cmi.12239

Waldman, B. S., Schwarz, D., Wadsworth, M. H., Saeij, J. P., Shalek, A. K., & Lourido, S. (2020). Identification of a Master Regulator of Differentiation in Toxoplasma. Cell, 180(2), 359-372.e16. https://doi.org/10.1016/j.cell.2019.12.013

Walker, R., Gissot, M., Croken, M. M., Huot, L., Hot, D., Kim, K., & Tomavo, S. (2013). The Toxoplasma nuclear factor TgAP2XI-4 controls bradyzoite gene expression and cyst formation. Molecular Microbiology, 87(3), 641–655. https://doi.org/10.1111/mmi.12121

Wang, A. W., Avramopoulos, D., Lori, A., Mulle, J., Conneely, K., Powers, A., Duncan, E., Almli, L., Massa, N., McGrath, J., Schwartz, A. C., Goes, F. S., Weng, L., Wang, R., Yolken, R., Ruczinski, I., Gillespie, C. F., Jovanovic, T., Ressler, K., … Pearce, B. D. (2019). Genome-wide association study in two populations to determine genetic variants associated with Toxoplasma gondii infection and relationship to schizophrenia risk. Progress in Neuro-Psychopharmacology & Biological Psychiatry, 92, 133–147. https://doi.org/10.1016/j.pnpbp.2018.12.019

Wang, H.-L., Wen, L.-M., Pei, Y.-J., Wang, F., Yin, L.-T., Bai, J.-Z., Guo, R., Wang, C.-F., & Yin, G.-R. (2016). Recombinant Toxoplasma gondii phosphoglycerate mutase 2 confers protective immunity against toxoplasmosis in BALB/c mice. Parasite, 23. https://doi.org/10.1051/parasite/2016012

Wang, J., Dixon, S. E., Ting, L.-M., Liu, T.-K., Jeffers, V., Croken, M. M., Calloway, M., Cannella, D., Hakimi, M. A., Kim, K., & Jr, W. J. S. (2014). Lysine Acetyltransferase GCN5b Interacts with AP2 Factors and Is Required for Toxoplasma gondii Proliferation. PLOS Pathogens, 10(1), e1003830. https://doi.org/10.1371/journal.ppat.1003830

Wang, J.-L., Huang, S.-Y., Behnke, M. S., Chen, K., Shen, B., & Zhu, X.-Q. (2016). The Past, Present, and Future of Genetic Manipulation in Toxoplasma gondii. Trends in Parasitology, 32(7), 542–553. https://doi.org/10.1016/j.pt.2016.04.013

Wang, J.-L., Zhang, N.-Z., Li, T.-T., He, J.-J., Elsheikha, H. M., & Zhu, X.-Q. (2019). Advances in the Development of Anti-Toxoplasma gondii Vaccines: Challenges, Opportunities, and Perspectives. Trends in Parasitology, 35(3), 239–253. https://doi.org/10.1016/j.pt.2019.01.005

Wang, L.-J., Xiao, T., Xu, C., Li, J., Liu, G.-Z., Yin, K., Cui, Y., Wei, Q.-K., Huang, B.-C., & Sun, H. (2018). Protective immune response against Toxoplasma gondii elicited by a novel yeast-based vaccine with microneme protein 16. Vaccine, 36(27), 3943–3948. https://doi.org/10.1016/j.vaccine.2018.05.072

Wang, M., Cao, S., Du, N., Fu, J., Li, Z., Jia, H., & Song, M. (2017). The moving junction protein RON4, although not critical, facilitates host cell invasion and stabilizes MJ members. Parasitology, 144(11), 1490–1497. https://doi.org/10.1017/S0031182017000968

Wang, S., Zhang, Z., Wang, Y., Gadahi, J. A., Xu, L., Yan, R., Song, X., & Li, X. (2017). Toxoplasma gondii Elongation Factor 1-Alpha (TgEF-1α) Is a Novel Vaccine Candidate Antigen against Toxoplasmosis. Frontiers in Microbiology, 8. https://doi.org/10.3389/fmicb.2017.00168

Wang, X., & Suzuki, Y. (2007). Microglia Produce IFN-γ Independently from T Cells During Acute Toxoplasmosis in the Brain. Journal of Interferon & Cytokine Research, 27(7), 599–605. https://doi.org/10.1089/jir.2006.0157

Wang, Z.-X., Zhou, C.-X., Elsheikha, H. M., He, S., Zhou, D.-H., & Zhu, X.-Q. (2017). Proteomic Differences between Developmental Stages of Toxoplasma gondii Revealed by iTRAQ-Based

Quantitative Proteomics. Frontiers in Microbiology, 8. https://doi.org/10.3389/fmicb.2017.00985

Watts, E. A., Dhara, A., & Sinai, A. P. (2017). Toxoplasma gondii tissue cyst purification using Percoll gradients. Current Protocols in Microbiology, 45, 20C.2.1-20C.2.19. https://doi.org/10.1002/cpmc.30

Watts, E., Zhao, Y., Dhara, A., Eller, B., Patwardhan, A., & Sinai, A. P. (2015). Novel Approaches Reveal that Toxoplasma gondii Bradyzoites within Tissue Cysts Are Dynamic and Replicating Entities In Vivo. MBio, 6(5), e01155-01115. https://doi.org/10.1128/mBio.01155-15

Webster, J. P. (2001). Rats, cats, people and parasites: the impact of latent toxoplasmosis on behaviour. Microbes and Infection, 3(12), 1037–1045. https://doi.org/10.1016/S1286-4579(01)01459-9

Webster, J. P. (2007). The effect of Toxoplasma gondii on animal behavior: playing cat and mouse. Schizophrenia Bulletin, 33(3), 752–756. https://doi.org/10.1093/schbul/sbl073

Weilhammer, D. R., Iavarone, A. T., Villegas, E. N., Brooks, G. A., Sinai, A. P., & Sha, W. C. (2012). Host metabolism regulates growth and differentiation of Toxoplasma gondii. International Journal for Parasitology, 42(10), 947–959. https://doi.org/10.1016/j.ijpara.2012.07.011

Weiss, L. M., & Dubey, J. P. (2009). Toxoplasmosis: a history of clinical observations. International Journal for Parasitology, 39(8), 895–901. https://doi.org/10.1016/j.ijpara.2009.02.004

Weiss, L. M., & Kim, K. (2000). THE DEVELOPMENT AND BIOLOGY OF BRADYZOITES OF TOXOPLASMA GONDII. Frontiers in Bioscience : A Journal and Virtual Library, 5, D391–D405.

Weiss, L. M., Laplace, D., Takvorian, P. M., Tanowitz, H. B., Cali, A., & Wittner, M. (1995). A Cell Culture System for Study of the Development of Toxoplasma gondii Bradyzoites. Journal of Eukaryotic Microbiology, 42(2), 150–157. https://doi.org/10.1111/j.1550-7408.1995.tb01556.x

Wetzel, D. M., Håkansson, S., Hu, K., Roos, D., & Sibley, L. D. (2003). Actin filament polymerization regulates gliding motility by apicomplexan parasites. Molecular Biology of the Cell, 14(2), 396–406. https://doi.org/10.1091/mbc.e02-08-0458

Wetzel, Dawn M., Chen, L. A., Ruiz, F. A., Moreno, S. N. J., & Sibley, L. D. (2004). Calcium-mediated protein secretion potentiates motility in Toxoplasma gondii. Journal of Cell Science, 117(24), 5739–5748. https://doi.org/10.1242/jcs.01495

Whitelaw, J. A., Latorre-Barragan, F., Gras, S., Pall, G. S., Leung, J. M., Heaslip, A., Egarter, S., Andenmatten, N., Nelson, S. R., Warshaw, D. M., Ward, G. E., & Meissner, M. (2017). Surface attachment, promoted by the actomyosin system of Toxoplasma gondii is important for efficient gliding motility and invasion. BMC Biology, 15(1), 1. https://doi.org/10.1186/s12915-016-0343-5

Wiendl, H., Hohlfeld, R., & Kieseier, B. C. (2005). Immunobiology of muscle: advances in understanding an immunological microenvironment. Trends in Immunology, 26(7), 373–380. https://doi.org/10.1016/j.it.2005.05.003

Wiersma, H. I., Galuska, S. E., Tomley, F. M., Sibley, L. D., Liberator, P. A., & Donald, R. G. K. (2004). A role for coccidian cGMP-dependent protein kinase in motility and invasion. International Journal for Parasitology, 34(3), 369–380. https://doi.org/10.1016/j.ijpara.2003.11.019

Wohlfert, E. A., Blader, I. J., & Wilson, E. H. (2017). Brains and Brawn: Toxoplasma Infections of the Central Nervous System and Skeletal Muscle. Trends in Parasitology, 33(7), 519–531. https://doi.org/10.1016/j.pt.2017.04.001

Wolff, J. A., & Budker, V. (2005). The mechanism of naked DNA uptake and expression. Advances in Genetics, 54, 3–20. https://doi.org/10.1016/S0065-2660(05)54001-X

Wu, M., An, R., Chen, Y., Chen, T., Wen, H., Yan, Q., Shen, J., Chen, L., & Du, J. (2019). Vaccination with recombinant Toxoplasma gondii CDPK3 induces protective immunity against experimental toxoplasmosis. Acta Tropica, 199, 105148. https://doi.org/10.1016/j.actatropica.2019.105148

Xu, J., Nault, R. J., Maldonado-Naranjo, A., Frizon, L. A., John, K., Holman, K., & Nagel, S. J. (2018). Disseminated cerebral toxoplasmosis in a patient with chronic lymphocytic leukemia. Journal of Clinical Neuroscience: Official Journal of the Neurosurgical Society of Australasia, 50, 127–128. https://doi.org/10.1016/j.jocn.2018.01.057

Yamamoto, L., Targa, L. S., Sumita, L. M., Shimokawa, P. T., Rodrigues, J. C., Kanunfre, K. A., & Okay, T. S. (2017). Association of Parasite Load Levels in Amniotic Fluid With Clinical Outcome in Congenital Toxoplasmosis. Obstetrics and Gynecology, 130(2), 335–345. https://doi.org/10.1097/AOG.0000000000002131

Yap, G. S., Scharton-Kersten, T., Charest, H., & Sher, A. (1998). Decreased resistance of TNF receptor p55- and p75-deficient mice to chronic toxoplasmosis despite normal activation of inducible nitric oxide synthase in vivo. Journal of Immunology (Baltimore, Md.: 1950), 160(3), 1340–1345.

Yarovinsky, F. (2014). Innate immunity to Toxoplasma gondii infection. Nature Reviews. Immunology, 14(2), 109–121. https://doi.org/10.1038/nri3598

Yazdani, M. R., Mehrabi, Z., Ataei, B., Ghahfarokhi, A. B., Moslemi, R., & Pourahmad, M. (2018). Frequency of sero-positivity in household members of the patients with positive toxoplasma serology. Revista Española de Quimioterapia, 31(6), 506–510.

Yu, L., Yamagishi, J., Zhang, S., Jin, C., Aboge, G. O., Zhang, H., Zhang, G., Tanaka, T., Fujisaki, K., Nishikawa, Y., & Xuan, X. (2012). Protective effect of a prime-boost strategy with plasmid DNA followed by recombinant adenovirus expressing TgAMA1 as vaccines against Toxoplasma gondii infection in mice. Parasitology International, 61(3), 481–486. https://doi.org/10.1016/j.parint.2012.04.001

Zeiner, G. M., Norman, K. L., Thomson, J. M., Hammond, S. M., & Boothroyd, J. C. (2010). Toxoplasma gondii Infection Specifically Increases the Levels of Key Host MicroRNAs. PLOS ONE, 5(1), e8742. https://doi.org/10.1371/journal.pone.0008742

Zhang, N.-Z., Gao, Q., Wang, M., Elsheikha, H. M., Wang, B., Wang, J.-L., Zhang, F.-K., Hu, L.-Y., & Zhu, X.-Q. (2018). Immunization With a DNA Vaccine Cocktail Encoding TgPF, TgROP16, TgROP18, TgMIC6, and TgCDPK3 Genes Protects Mice Against Chronic Toxoplasmosis. Frontiers in Immunology, 9, 1505. https://doi.org/10.3389/fimmu.2018.01505

Zhang, N.-Z., Wang, M., Xu, Y., Petersen, E., & Zhu, X.-Q. (2015). Recent advances in developing vaccines against Toxoplasma gondii: an update. Expert Review of Vaccines, 14(12), 1609–1621. https://doi.org/10.1586/14760584.2015.1098539

Zhang, T.-E., Yin, L.-T., Li, R.-H., Wang, H.-L., Meng, X.-L., & Yin, G.-R. (2015). Protective immunity induced by peptides of AMA1, RON2 and RON4 containing T-and B-cell epitopes via an intranasal route against toxoplasmosis in mice. Parasites & Vectors, 8. https://doi.org/10.1186/s13071-015-0636-5

Zhao, G., Song, X., Kong, X., Zhang, N., Qu, S., Zhu, W., Yang, Y., & Wang, Q. (2017). Immunization with Toxoplasma gondii aspartic protease 3 increases survival time of infected mice. Acta Tropica, 171, 17–23. https://doi.org/10.1016/j.actatropica.2017.02.030

Zhao, Y., Marple, A. H., Ferguson, D. J. P., Bzik, D. J., & Yap, G. S. (2014). Avirulent strains of Toxoplasma gondii infect macrophages by active invasion from the phagosome. Proceedings of the National Academy of Sciences of the United States of America, 111(17), 6437–6442. https://doi.org/10.1073/pnas.1316841111

Zhou, N., Zhang, X. Y., Li, Y. X., Wang, L., Wang, L. L., & Cong, W. (2018). Seroprevalence and risk factors of Toxoplasma gondii infection in oral cancer patients in China: a case-control prospective study. Epidemiology and Infection, 146(15), 1891–1895. https://doi.org/10.1017/S0950268818001978

Zhu, W.-N., Wang, J.-L., Chen, K., Yue, D.-M., Zhang, X.-X., Huang, S.-Y., & Zhu, X.-Q. (2017). Evaluation of protective immunity induced by DNA vaccination with genes encoding Toxoplasma gondii GRA17 and GRA23 against acute toxoplasmosis in mice. Experimental Parasitology, 179, 20–27. https://doi.org/10.1016/j.exppara.2017.06.002

Annexe

DispatchDate: 24.12.2020 · ProofNo: 854, p.1

nature microbiology

LETTERS

https://doi.org/10.1038/s41564-020-00854-z

Check for updates

An Alveolata secretory machinery adapted to parasite host cell invasion

Eleonora Aquilini[1,7], Marta Mendonça Cova[1,7], Shrawan Kumar Mageswaran[2], Nicolas Dos Santos Pacheco[1], Daniela Sparvoli[1,3], Diana Marcela Penarete-Vargas[1], Rania Najm[1], Arnault Graindorge[1], Catherine Suarez[1], Marjorie Maynadier[1], Laurence Berry-Sterkers[1], Serge Urbach[4], Pilar Ruga Fahy[5], Amandine N. Guérin[6], Boris Striepen[6], Jean-François Dubremetz[1], Yi-Wei Chang[2], Aaron P. Turkewitz[3] and Maryse Lebrun[1]✉

Apicomplexa are unicellular eukaryotes and obligate intracellular parasites, including *Plasmodium* (the causative agent of malaria) and *Toxoplasma* (one of the most widespread zoonotic pathogens). Rhoptries, one of their specialized secretory organelles, undergo regulated exocytosis during invasion[1]. Rhoptry proteins are injected directly into the host cell to support invasion and subversion of host immune function[2]. The mechanism by which they are discharged is unclear and appears distinct from those in bacteria, yeast, animals and plants. Here, we show that rhoptry secretion in Apicomplexa shares structural and genetic elements with the exocytic machinery of ciliates, their free-living relatives. Rhoptry exocytosis depends on intramembranous particles in the shape of a rosette embedded into the plasma membrane of the parasite apex. Formation of this rosette requires multiple non-discharge (Nd) proteins conserved and restricted to Ciliata, Dinoflagellata and Apicomplexa that together constitute the superphylum Alveolata. We identified Nd6 at the site of exocytosis in association with an apical vesicle. Sandwiched between the rosette and the tip of the rhoptry, this vesicle appears as a central element of the rhoptry secretion machine. Our results describe a conserved secretion system that was adapted to provide defence for free-living unicellular eukaryotes and host cell injection in intracellular parasites.

Apicomplexan parasites are invasive and defined by the presence of an apical complex used to recognize and gain entry into host cells. The apical complex includes two types of secretory organelle: micronemes and rhoptries[3]. Microneme proteins are secreted to the parasite surface and mediate motility, host cell recognition and invasion[4]. Rhoptry proteins are injected directly into the host cell[2], where they anchor the machinery propelling the parasite into the host cell[5], facilitate nutrient import[6–8], interfere with the immune response and modulate gene expression to promote infection[9]. Rhoptry secretion requires a trigger in the form of microneme proteins binding to host cell receptors[10,11]. Importantly, rhoptry proteins not only cross the plasma membrane of the parasite (exocytosis) but also that of the host[1,12]. Rhoptry exocytosis factors identified to date[11,13,14] are mostly specific to Apicomplexa, suggesting that these cells depend on unique lineage-restricted secretory mechanisms. Consistent with this, no eukaryotic SNAREs—the main drivers for fusing vesicles to the target membrane in eukaryotic systems—have so far been associated with rhoptry exocytosis. Apicomplexa also lack genes encoding prokaryotic secretion systems[15]. Thus, how rhoptry effectors are delivered into the host cytoplasm remains unclear.

To explore the mechanisms of rhoptry secretion, we searched for examples of regulated secretion in organisms phylogenetically closely related to Apicomplexa[16]. All Alveolata bear alveolar sacs beneath the plasma membrane, which give the superphylum its name. They contain elaborate membrane-bound secretory organelles with shared evolutionary origin[6] but different morphologies and functions. Known as trichocysts in the Ciliata *Paramecium*, they function in defence, docking at the plasma membrane and discharging in response to predation[17]. Exocytic membrane fusion occurs at plasma membrane sites consisting of rosettes of eight to nine intramembranous particles (IMPs)[18,19]. Previous electron microscopy studies have described similar rosettes at the apex of several apicomplexan parasites[20–23]. Although it has been suggested to be involved in exocytic fusion[20], the function of the IMP rosette has never been experimentally addressed in Apicomplexa. Analysis of *Paramecium tetraurelia* mutants defective in both trichocyst exocytosis and rosette assembly[24,25] led to the identification of non-discharge (*nd*) genes[26–29] (Supplementary Table 1). To determine whether similar factors could be involved in exocytosis of secretory organelles in Apicomplexa, we first searched for Nd homologues in the tree of life. Genome mining for *nd* genes and phylogenetic analyses revealed that *nd6* and *nd9* are conserved in Ciliata, but also in Dinoflagellata, Chromerida and Apicomplexa (Extended Data Fig. 1). We also found an Nd9 homologue in the Perkinsozoa, a sister group of Dinoflagellata. Altogether, this analysis suggested a conserved evolution and common function of *nd* genes across Alveolata.

To define the parasite localization of Nd proteins, we tagged *nd6* (TGGT1_248640) and *nd9* (TGGT1_249730) at the endogenous loci in *Toxoplasma gondii*, an experimentally tractable apicomplexan (Extended Data Fig. 2). Both proteins displayed a punctuate signal throughout the cytoplasm, but in addition, TgNd6 accumulated at the apical tip of the parasite (Fig. 1a,b). A closer look at the

[1]Laboratory of Pathogen Host Interactions, UMR 5235, CNRS, Université de Montpellier, Montpellier, France. [2]Department of Biochemistry and Biophysics, Perelman School of Medicine, University of Pennsylvania, Philadelphia, PA, USA. [3]Department of Molecular Genetics and Cell Biology, University of Chicago, Chicago, IL, USA. [4]IGF, Université de Montpellier, CNRS, INSERM, Montpellier, France. [5]Pôle Facultaire de Microscopie Ultrastructurale, Geneva, Switzerland. [6]Department of Pathobiology, School of Veterinary Medicine, University of Pennsylvania, Philadelphia, PA, USA. [7]These authors contributed equally: Eleonora Aquilini, Marta Mendonça Cova. ✉e-mail: mylebrun@univ-montp2.fr

Uncorrected Proofs

apical tip by immunoelectron microscopy localized TgNd6 at the site of rhoptry exocytosis, in association with the parasite plasma membrane and an underlying membranous spheroid known as the apical vesicle (Fig. 1c). Despite being previously observed by electron microscopy in *Toxoplasma*[21,30] and indications that it is linked to rhoptries[22,30], the composition and function of the apical vesicle remains unknown.

Because *Tgnd6* and *Tgnd9* were predicted to be fitness-conferring genes[31], to investigate their function, we generated inducible knockdown mutants using an auxin-inducible degron for TgNd6 (ref. [32]) and tetracycline-induced repression for TgNd9 (refs. [33,34]) (Extended Data Fig. 2). Parasites conditionally depleted of TgNd6 or TgNd9 showed reduced plaque formation on fibroblast monolayers, indicating the inability of both mutants to efficiently complete the lytic cycle (Extended Data Fig. 3a). *Tgnd6* and *Tgnd9* inducible knockdown (iKD) mutants showed no detectible defects in their intracellular replication, egress, conoid protrusion, motility or host cell attachment (Extended Data Fig. 3b–g). In contrast, invasion was severely impaired for both mutants (Fig. 1d).

To understand the mechanistic basis of this invasion defect, we evaluated microneme and rhoptry secretion in the *Tgnd6* iKD and *Tgnd9* iKD mutants. Release of the micronemal protein apical membrane antigen 1 (AMA1) into the supernatant was unimpeded by the absence of TgNd6 or TgNd9 (Fig. 1e). In contrast, rhoptry secretion was significantly impaired by the loss of TgNd6 or TgNd9, as revealed by quantifying the release of the rhoptry protein ROP1 into host cells using immunofluorescence assays (IFAs)[35] (Extended Data Fig. 3h), or the delivery of Cre recombinase fused to the rhoptry protein toxofilin into the nucleus of a suitable reporter cell[36] (Fig. 1f). This was not due to defects in rhoptry biogenesis, as the mutants showed normal organelle formation and apical positioning, as judged by IFA and electron microscopy (Extended Data Fig. 4). Analysis by freeze-fracture electron microscopy of the apex of *Tgnd6* iKD mutants showed no significant reduction in the presence of the apical rosette (Fig. 1g). In contrast, *T. gondii* depleted of TgNd9 displayed a strong decrease in cells with a rosette at the parasite apex (Fig. 1g). This last result links rosette formation with rhoptry secretion and supports an evolutionarily conserved mechanism of regulated exocytosis in Alveolata.

To determine whether other Apicomplexa require *nd* genes for rhoptry function, we analysed Nd9 in *Plasmodium falciparum*, the causative agent of the deadliest form of malaria. We confirmed that *P. falciparum* intracellular merozoites possess a fusion rosette of eight IMPs (Fig. 2a). As *nd9* is also predicted to have a fitness cost in *P. falciparum*[36], we used the rapamycin-inducible dimerizable Cre recombinase (DiCre) system[37] to conditionally excise the low-expressed *Pfnd9* gene (PF3D7_1232700) (Extended Data Fig. 5a–d). DiCre-mediated ablation of *Pfnd9* resulted in substantial reduction in parasite proliferation (Fig. 2b), which was due to the inability of *Pfnd9* inducible gene knockout (iKO) mutants to reinvade host cells while their intracellular development and egress were unaffected (Fig. 2b,c and Extended Data Fig. 5e). As in *T. gondii*, microneme secretion was unaltered in *Pfnd9* iKO parasites (Fig. 2d) but rhoptry secretion was affected (Fig. 2e).

To gain a more complete understanding of the molecular composition of the rhoptry secretion machinery, we searched for Nd interacting proteins in *T. gondii*. TgNd9 displays two Armadillo repeats while TgNd6 shows homology with GDP/GTP exchange factors known to activate GTPases (Fig. 3a). We used TgNd9 for immunoprecipitation experiments as we found TgNd6 to be largely insoluble (Extended Data Fig. 2g). Mass spectrometry analysis revealed robust interaction of TgNd9 with TgNd6 and with TgFER2 (TGGT1_260470), a member of the ferlin calcium sensor family that is known to be essential for *Toxoplasma* rhoptry secretion[13] (Fig. 3a and Supplementary Table 2). The TgNd9 immunoprecipitation also enriched TGGT1_222660, a protein harbouring Armadillo repeats and leucine-rich repeats, named hereafter TgNdP1 (Nd partner 1), and TGGT1_316730 (TgNdP2 (Nd partner 2)), a protein with a C2 calcium lipid-binding domain (Fig. 3a). The genes transcribing both proteins are broadly shared among Alveolata (Extended Data Fig. 1c,d) and are predicted to be fitness conferring in *Toxoplasma*[31] and *Plasmodium*[38]. In contrast, the TgNd9-IP interactor TGGT1_277840, a GTPase, is restricted to Apicomplexa and Dinoflagellata, and TGGT1_253570 is only found in the apicomplexan subgroup Coccidia. Importantly, all of these proteins are also recovered when using reverse immunoprecipitation with tagged TgNdP1 protein (Supplementary Table 3).

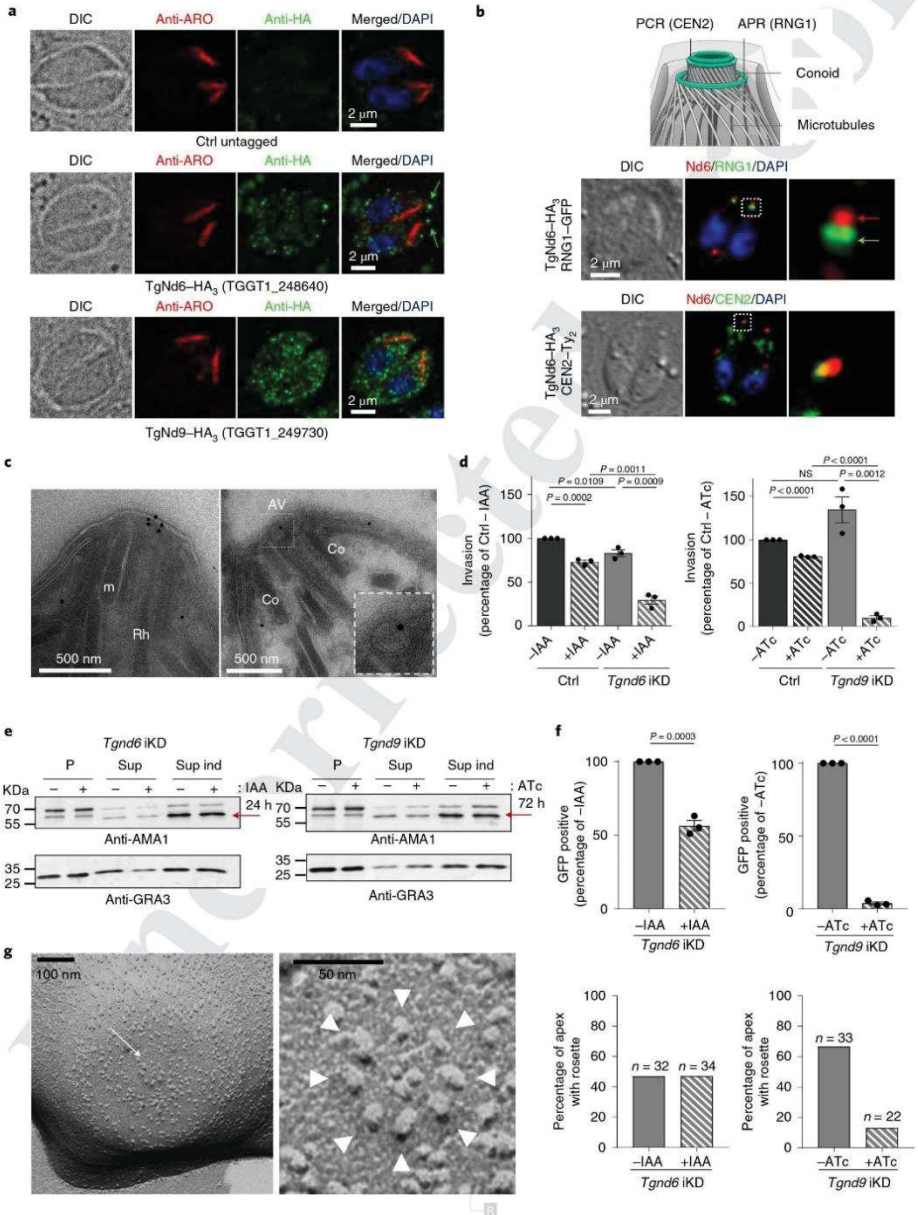
To learn more about the conserved partners of TgNd9, we generated *T. gondii* lines in which TgNdP1 or TgNdP2 was tagged by an epitope and could be ablated conditionally (Extended Data Fig. 6). Both proteins appeared as punctate cytoplasmic staining (Fig. 3b) but TgNdP2—like TgNd6—also appeared as a dot at the apical tip of the parasite, although consistently with lower intensity. Depletion of TgNdP1 or TgNdP2 resulted in a profound growth defect (Extended Data Fig. 7a) that we linked to impairment of host cell invasion and rhoptry secretion (Fig. 3c,d and Extended Data Fig. 7). Again, loss of rhoptry secretion went hand in hand with loss of the rosette in *Tgndp1* iKD and *Tgndp2* iKD parasites (Fig. 3e).

To further validate our conservation data and broaden our discoveries back to Ciliata, we generated knockouts for ortho-

Fig. 1 | Rhoptry secretion is dependent on rosette formation. a, IFAs of the control (Ctrl) untagged line and endogenously HA_3-tagged TgNd6 and HA_3-tagged TgNd9 tachyzoites. The green arrows point to TgNd6 apical puncta. ARO is a marker for rhoptries. Shown are the maximum-intensity projections of confocal *z*-stacks of fixed parasites. The results are representative of five experiments. DIC, differential interference contrast. **b**, Super-resolution microscopy of the apical dot of TgNd6. Top: schematic of the apical end of a tachyzoite. The images show maximum-intensity projections of *z*-stacks of TgNd6–HA_3 parasites transiently expressing ring-1-GFP (RNG1-GFP) (middle) and centrin 2-Ty_2 (CEN2-Ty_2) (bottom). The protein RNG1-GFP marks the apical polar ring (APR) and CEN2-Ty_2 marks pre-conoidal rings (PCR). Higher magnifications of the areas indicated by a dashed box (right) show that TgNd6–HA_3 (red arrow) localizes above the apical polar ring (green arrow) and co-localizes partially with CEN2. The results are representative of two experiments. **c**, Left: Immunogold labelling of TgNd6–HA_3. Right: TgNd6–HA_3 on the apical vesicle (AV). Inset: higher-magnification view of the apical vesicle. Micronemes (m) and rhoptries (Rh) are visible in a transverse section of the conoid (Co). The results are representative of two experiments. **d**, Quantification of invasion after depletion of TgNd6 (left) and TgNd9 (right). The data represent means ± s.e.m. ($n = 3$ independent experiments). NS, not significant. **e**, Immunoblot showing microneme secretion assessed by the release of proteolytically cleaved AMA1 (arrow = processed/secreted TgAMA1) in *Tgnd6* iKD ± IAA at 24 h (left) and *Tgnd9* iKD ± ATC at 72 h (right). P, pellet; Sup, supernatant; Sup ind, propanolol-induced supernatant. Granule protein 3 (GRA3) was used as a loading control. The results are representative of three experiments for *Tgnd6* iKD and four experiments for *Tgnd9* iKD. **f**, Rhoptry secretion assay by SeCrEt. Shown are quantification of the rhoptry secretion of *Tgnd6* iKD ± IAA (left) and *Tgnd9* iKD ± ATc (right). The data represent means ± s.e.m. ($n = 3$ independent experiments). **g**, Left: Freeze-fracture electron microscopy image of a *T. gondii* tachyzoite (P-face) showing a rosette of IMPs (white arrow) at the middle of the apex. Middle: higher-magnification view of the images shown in the left panel. The white arrowheads point to the eight IMPs of the rosette. Right: quantification of rosettes of IMPs in *Tgnd6* iKD ± IAA at 24 h (left) and *Tgnd9* iKD ± ATc at 72 h (right) using the freeze-fracture method. The results are representative of one experiment for *Tgnd6* iKD and two experiments for *Tgnd9* iKD. Statistical significance in **d** and **f** was determined by unpaired two-tailed Student's *t*-test.

logues of both NdP1 (TTHERM_01287970; *Ttn*Δ*ndp1*) and NdP2 (TTHERM_00498010; *Ttn*Δ*ndp2*) in the free-living Ciliata *Tetrahymena thermophila* (Extended Data Fig. 8a,b). The homologous organelles to *Paramecium* trichocysts in *Tetrahymena* are called mucocysts and are non-essential for laboratory growth. We found that *Ttn*Δ*ndp1* and *Ttn*Δ*ndp2* cells were defective in mucocyst secretion, which was triggered by exposure to dibucaine[39] (Fig. 3f). We further showed that the impairment of exocytosis was not due to defects in mucocyst biogenesis, given that mucocyst maturation (as measured by processing of mucocyst pro-proteins) and trafficking (monitored by IFA) remained unaltered (Extended Data Fig. 8c,d). Taken together, we identified a complex of proteins essential for organellar exocytosis and rosette assembly, conserved across Alveolata.

The exact position of the rosette relative to the apical tip of the rhoptry and the enigmatic apical vesicle remained elusive since the



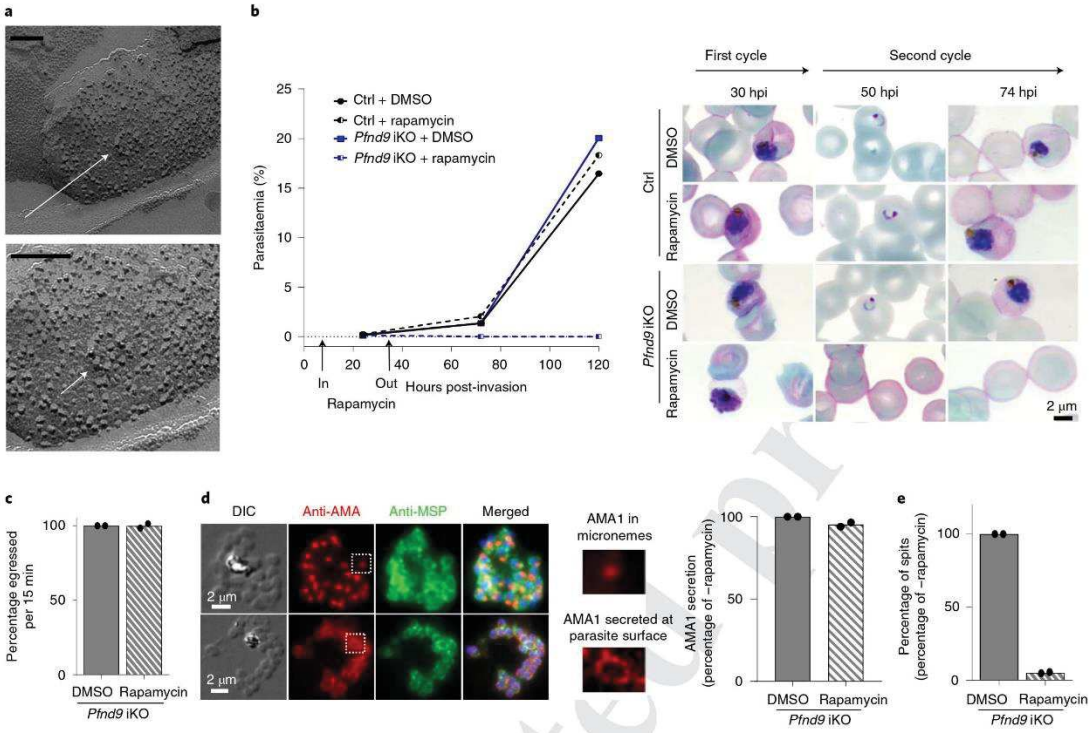


Fig. 2 | PfNd9 is essential for rhoptry secretion in *P. falciparum*. **a**, Top: freeze-fracture electron microscopy of a *P. falciparum* merozoite (P-face) showing a rosette of IMPs (white arrow). Bottom: higher-magnification view of the image shown above. Scale bars, 100 nm. The results are representative of two experiments. **b**, Left: growth curves (parasitaemias) of *p230p* DiCre (Ctrl) and the *Pfnd9* iKO mutant ± rapamycin showing that PfNd9-depleted parasites have a growth defect. The means of three technical replicates are shown. The results are representative of three independent experiments. Right: Giemsa staining of the representative growth experiment illustrating development and reinvasion of *p230p* DiCre (Ctrl) and *Pfnd9* iKO asexual parasites (along two cycles) ± rapamycin treatment. hpi, hours post-invasion. **c**, Quantification of egress of *Pfnd9* iKO ± rapamycin schizonts. The data were collected from eight videos of *Pfnd9* iKO ± rapamycin. The means of two independent experiments are shown. **d**, Left: IFA images illustrating AMA1 protein stored in micronemes (top) or secreted and translocated at the surface of the parasite before egress (bottom). Middle: Magnified images of the areas indicated by a dashed box to the left. Right: quantification of the results. The means of two independent experiments are shown. **e**, Quantification of rhoptry secretion events in *Pfnd9* iKO ± rapamycin-treated schizonts using anti-PfRAP2 antibodies to visualize rhoptry secretion events (spits of RAP2 exported into the RBC). The means of two independent experiments are shown.

freeze-fracture technique—used to image the rosette on the membrane—does not capture the internal structures at the same time. To overcome this limitation, we imaged the *Toxoplasma* apex by cryo-electron tomography (cryo-ET)—a technique combining the advantages of three-dimensional imaging with molecular resolution to reveal the ultrastructure in situ in its native biological context. We were able to simultaneously visualize and define three linked elements: (1) the rosette (dark blue); (2) the apical vesicle (magenta); and (3) the apical tip (cyan) of the rhoptry (orange) (Fig. 4a,b and Extended Data Fig. 9). The rosette showed an eightfold rotational symmetry around a central axis (Fig. 4c,d) and extended under the parasite plasma membrane (light blue) to interact with the apical vesicle (Fig. 4c). Thus, the rosette is tightly sandwiched between the apical vesicle and the plasma membrane and extensively interacts with both membranes. The apical vesicle in turn sits over the rhoptry tip (Fig. 4a,b). The contiguity of all elements from the rhoptry tip to the plasma membrane supports the idea that the rosette and apical vesicle are integral parts of the rhoptry secretion machinery. Interestingly, the connection between the apical vesicle and rosette is sometimes observed even in the absence of a docked rhoptry (Fig. 4e), suggesting that they assemble independent of rhoptry docking. Supporting this hypothesis, when we imaged the *Toxoplasma* ARO mutant in which rhoptries fail to dock and are dispersed in the cytoplasm[40], both the rosette (seen using the freeze-fracture technique; Fig. 4f) and apical vesicle (seen by electron microscopy; Fig. 4g) were still present at the apex of the parasite. Altogether, these results positioned the rosette and apical vesicle at the heart of the exocytic machinery in Apicomplexa and implied that rhoptries do not make contact and fuse directly with the plasma membrane.

Our work breaks ground on the molecular and structural mechanisms for rhoptry exocytosis in Apicomplexa. We defined the apical rosette of IMPs as the site for rhoptry exocytosis in Apicomplexa, and we characterized an Alveolata-specific Nd complex necessary for the assembly of the rosette. In *Paramecium*, physiological studies predicted PtNd6 to be active at the plasma membrane[24] while PtNd9 appeared to be a diffusible cytoplasmic component interacting with both trichocyst and plasma membranes[41,42]. However, both the

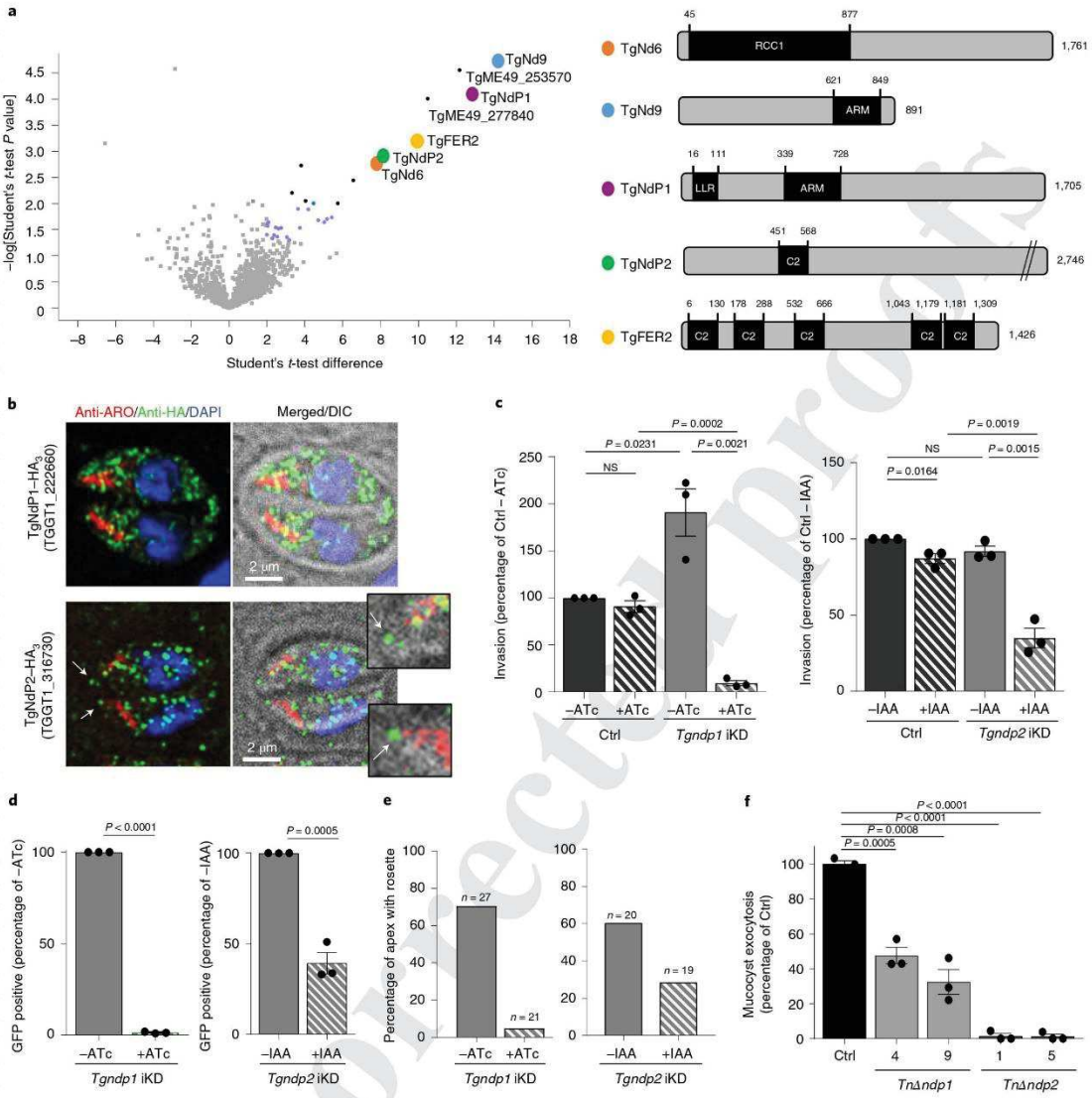
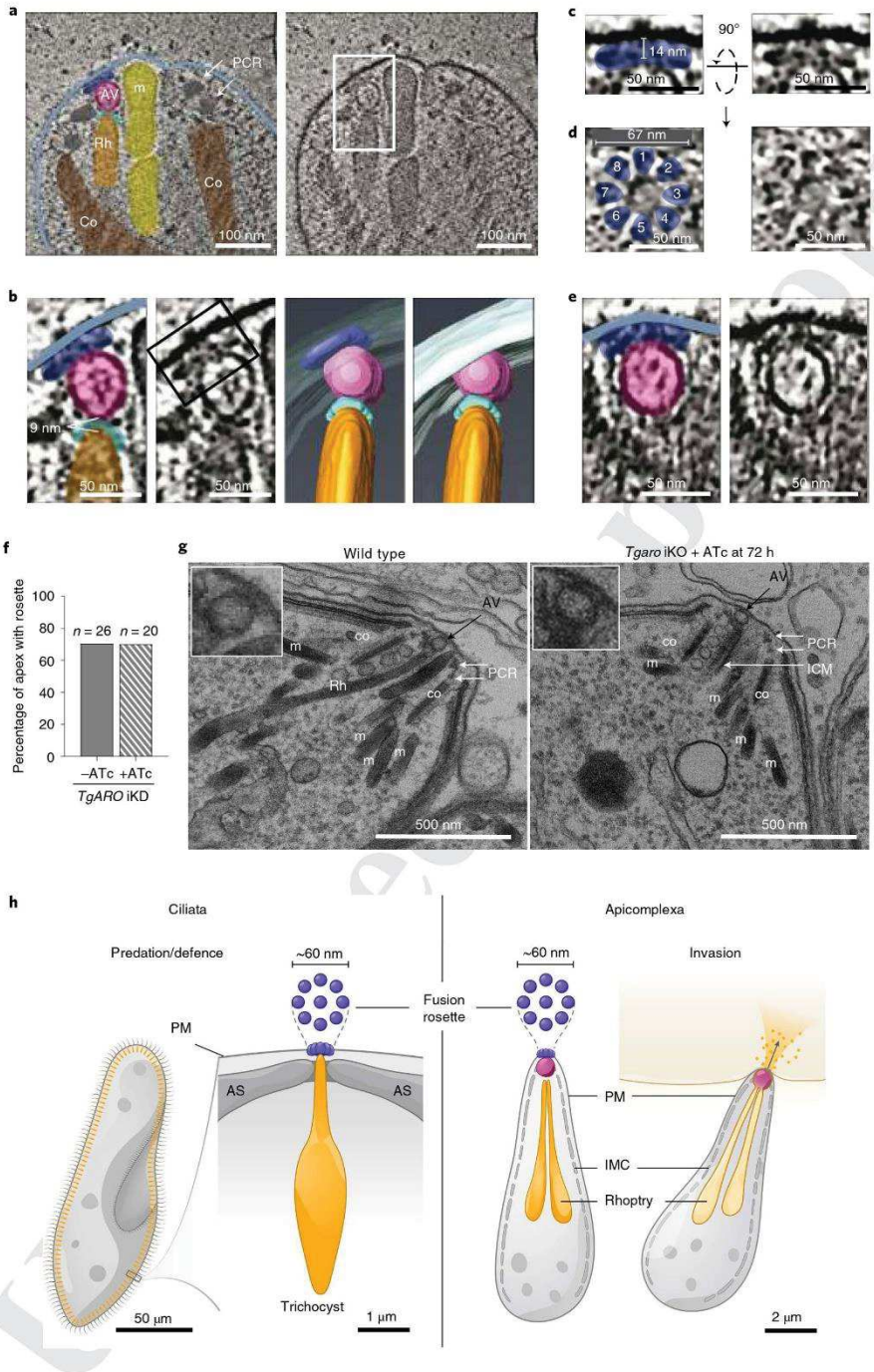


Fig. 3 | Nd6 and Nd9 are part of an Alveolata complex essential for organelle secretion in *T. gondii* (Apicomplexa) and *T. thermophila* (Ciliata). **a**, Mass spectrometry analysis of immuno-isolated TgNd9–HA_3. Left: volcano plot of the proteins differentially enriched in TgNd9 versus control immunoprecipitation. This plot presents the fold change (difference) and significance (−log[*P*]) obtained from an unpaired two-tail Student's *t*-test of three independent immunoprecipitations using LFQ intensity values. Right: schematic of TgNd proteins using SUPERFAMILY[63]. ARM, Armadillo-repeat domain; C2, lipid/calcium-binding domain; RCC1, regulator of chromosome condensation 1-like domains (a versatile domain that performs many different functions, including guanine nucleotide exchange on small GTP-binding proteins[64]); LRR, leucine-rich-repeat domain. **b**, Immunofluorescence of endogenously HA_3-tagged TgNdP1 and TgNdP2 tachyzoites. The white arrows point to TgNdP1 apical dots of two adjacent parasites, which are magnified on the right. ARO was used as a rhoptry marker and 4′,6-diamidino-2-phenylindole (DAPI) was used as a DNA marker. The results are representative of three experiments. **c**, Quantification of invasion after depletion of TgNdP1 (left; using ATc) and TgNdP2 (right; using IAA) along with negative control strains. The data represent means ± s.e.m. ($n = 3$ independent experiments). **d**, Rhoptry secretion quantification of *TgndP1* iKD ± ATc (left) and *TgndP2* iKD ± IAA (right). The data represent means ± s.e.m. ($n = 3$ independent experiments). **e**, Quantification of rosettes of IMPs in *Tgndp1* iKD ± ATc at 72 h and *Tgndp2* iKD ± IAA at 24 h using the freeze-fracture technique. The results are representative of one experiment. **f**, Quantification of mucocyst exocytosis by dibucaine assay. The date represent means ± s.e.m. ($n = 3$ independent experiments). Statistical significance in **c**, **d** and **f** was determined by unpaired two-tailed Student's *t*-test.



localization and identity of partners in Ciliata remained unknown. We localized TgNd9 to the cytoplasm and TgNd6 to the site of exocytosis in *Toxoplasma*. We found both proteins to form a complex that included TgNdP1 and TgNdP2, which we demonstrated to be essential for organelle exocytosis in both Ciliata and Apicomplexa. This complex further includes proteins with C2 domains (TgFER2

Fig. 4 | The rhoptry secretion machinery includes the apical vesicle and rosette. a, Left: tomogram slice showing a side view of the apical complex, including the conoid (brown), pre-conoidal apical rings (grey), micronemes (yellow), plasma membrane (light blue) and rhoptry secretion system (consisting of the rosette (dark blue), apical vesicle (magenta), rhoptry (orange) and rhoptry tip density (cyan)). Right: original image without annotation or colour overlays. **b**, Left: magnified images (with and without colour overlays) of the boxed region in **a**, showing the connections between the rhoptry, rhoptry tip density, apical vesicle, rosette and plasma membrane. Right: three-dimensional segmentations of the left image. In the left of the two images, the plasma membrane is rendered transparent to enable a view of the rosette. **c**, Magnified images (with and without colour overlays) of the boxed region in **b**, showing the side view of the rosette. **d**, Top views (with and without colour overlays and annotation) of the rosette in **c**, showing an eightfold rotational symmetry. **e**, Images (with and without colour overlays) of the apical vesicle connected with the plasma membrane via a rosette in the absence of docked rhoptry. All of the measurements were made in three dimensions. The images in **c** and **d** are from two different cells oriented differently on the electron microscopy grid. The results in **a**–**e** are representative of 20 tomograms produced from two independent samples. **f**, Quantification of apical rosettes in *TgARO* iKD mutants ± ATc at 72 h. The results are representative of two experiments. **g**, Left: ultrastructure of wild-type tachyzoites with the apical vesicle positioned beneath the plasma membrane and above the tip of the rhoptry neck. Right: in *Tgaro* iKD ATc-treated tachyzoites, the apical vesicle is still properly positioned at the apex (presumably under the rosette), while rhoptries are not docked on the apical vesicle. Inset: magnified images of the vesicles. The results are representative of one experiment. ICM, pair of intraconoidal microtubules. **h**, Schematic of exocytosis in Alveolata, outlined by the presence of a rosette at the exocytosis site. In Ciliata, organelle discharge can have a defensive or predatory function. Rhoptry exocytosis in Apicomplexa is critical for host cell invasion. In Apicomplexa, but not in Ciliata, the apical vesicle, present between the tip of the rhoptry and the plasmalemma, is plausibly involved in the injection of rhoptry proteins into the host cell. The alveolar sac (AS) in Ciliata is homologous to the inner membrane complex (IMC) of Apicomplexa. PM, plasma membrane; PVM, parasitophorous vacuole membrane.

and TgNdP2), a homologue of the membrane fusion ferlin family (FER2)[13], a GTPase (TGME49_277840) and a putative GDP/GTP exchange factor protein (TgNd6). These proteins and their domains yield a regulatory model in which calcium signalling and nucleotide binding and hydrolysis constitute key steps that control rosette assembly and/or organelle discharge (for more discussion, see the Supplementary Text).

In this study, we also shed light on the enigmatic apical vesicle. Described in *Toxoplasma*[22,30], it is also visible in early micrographs from other apicomplexan parasites[20,43,44] (Extended Data Fig. 10). We have shown that the apical vesicle is on one side tightly connected with the plasma membrane via the rosette, and from the other sits on the tip of the rhoptry, precluding a direct link and fusion between the rhoptry and the plasma membrane. In Ciliata, where no comparable apical vesicle is present, the docking and fusion of the trichocysts to the plasma membrane shapes the rosette. Diverging from this scenario, we have also shown that the docking of the rhoptries in *Toxoplasma* is dispensable for rosette formation (Fig. 4e–g), which suggests that the assembly of the rosette in *Toxoplasma* might instead be induced by docking of the apical vesicle.

While *Paramecium* trichocysts are discharged into the environment to thwart predators, apicomplexan rhoptries translocate their contents directly into the cytoplasm of host organisms to infect and parasitize. The difference in terms of the presence or absence of the apical vesicle (Fig. 4h) suggests that the apical vesicle is an adaptation in Apicomplexa for parasitism and cell invasion. Its presence may reflect additional complexity of the secretory machinery in apicomplexans, in which exocytosis must be coupled with injection of rhoptry content through the barrier of a host cell membrane. In support of this hypothesis, a similar vesicle is present at the apex of *Perkinsus marinus* (previously named *Dermocystidium marinum*)[45]. This organism possesses rhoptries and invades and parasitizes the cells of oysters. Phylogenetically, *Perkinsus* falls between Dinoflagellata and Apicomplexa and is viewed as a basal taxon and an example of early adaptation to parasitism.

The rosette and the set of Nd proteins highlight a common ancestry for the fusion machinery linked to secretory organelles in two groups of protists that diverged hundreds of millions of years ago and have adopted radically different lifestyles. The architecture and molecular composition of the rhoptry system that enables the intracellular parasitism of Apicomplexa is now revealed. Future studies combining high-resolution structural biology approaches with the genetics and cell biology of *Toxoplasma* will allow a full understanding of how this fascinating mechanism unfolds and is regulated. Such an understanding may find application in designing strategies against malaria, cryptosporidiosis and toxoplasmosis.

Methods

Parasite immunofluorescence microscopy. IFAs on intracellular *T. gondii* parasites were conducted as previously described[46]. Briefly, cell monolayers were washed and fixed in 4% paraformaldehyde (PFA) in phosphate-buffered saline (PBS) for 20 min. After three washes with PBS, the cells were permeabilized with 0.1% (vol/vol) Triton X-100 or with saponin 0.1% (vol/vol) (for invading parasites) in PBS for 5 min, blocked with 10% foetal bovine serum in PBS for 45 min, incubated with primary antibodies diluted in 2% foetal bovine serum in PBS, washed three times and then incubated with secondary antibody. The coverslips were mounted onto microscope slides using Immu-Mount (Calbiochem).

For IFAs on *P. falciparum*, thin blood smears of highly synchronized dimethyl sulfoxide (DMSO) and rapamycin-treated *Pfnd9* iKO schizonts were air-dried, fixed in 4% (wt/vol) PFA and permeabilized in 0.1% (vol/vol) Triton X-100. After blocking in 1.5% bovine serum albumin (BSA), samples were probed for 1 h with the suitable antibodies: rabbit anti-PfAMA1 antibody (1:1,000)[47]; mouse anti-PfMSP1 antibody (1:1,000)[48]; and mouse anti-PfRAP2 antibody (1:500)[49]. The secondary antibodies used were Alexa Fluor 488 and 594-conjugated antibodies against mouse or rabbit immunoglobulin (highly cross-adsorbed), both diluted 1:4,000 (Molecular Probes). Samples were then counterstained with Hoechst and slides were mounted with Vectashield antifade mounting medium.

Except when specified, observations were performed with a Zeiss Axioimager Z1 epifluorescence microscope equipped with a Zeiss AxioCam MRm CCD camera and a 100×/1.4 Oil Plan Apochromat objective. Images were processed using ZEN Blue 2.3 Pro (Zeiss) software. Imaging of TgNd6, TgNd9, TgNdP1 and TgNdP2 co-localization with the rhoptry protein TgARO (Figs. 1 and 3) was performed on a ZEISS confocal LSM 880 equipped with an Airyscan detector and a 63×/1.4 Oil Plan Apochromat objective. ZEN Black (Zeiss) was used for image Airyscan processing. *Z*-stack images and *z*-projection images were denoised, adjusted in brightness and contrast and coloured using the program Fiji[50].

Adjustments for brightness and contrast were applied uniformly on the entire images and, when required, matching pairs of images were recorded with the same exposure time and processed identically. All optical images were collected at the Montpellier Ressources Imagerie (MRI) facility of the University of Montpellier (www.mri.cnrs.fr).

Invasion assays. *Toxoplasma* plaque assays, replication assays and two-colour invasion assays were performed as previously described[35,51]. Briefly, to synchronize invasion, freshly egressed tachyzoites (5×10^6), pre-treated for 72 h ± ATc (*Tgnd9* iKD and *Tgndp1* iKD) or 24 h ± IAA (*Tgnd6* iKD and *Tgndp2* iKD), were harvested and settled on ice for 20 min on an HFF monolayer grown on coverslips in 24-well plates. Invasion was allowed for 5 min at 38 °C and stopped by fixation with 4% PFA in Hank's Balanced Salt Solution (HBSS) for 20 min at room temperature. To detect extracellular parasites, immunodetection was performed with the mouse monoclonal antibody T4 1E5 anti-SAG1 (dilution 1:1,000) in 2% foetal calf serum/HBSS, without previous permeabilization. After permeabilization with 0.01% saponin for 15 min, a second IFA was performed using rabbit anti-ROP1 antibody (dilution 1:1,000) to label the parasitophorous vacuole of intracellular parasites. Extracellular and intracellular parasites were counted by microscopic examination of at least 20 fields per coverslip ($n=3$ coverslips). The graphs show the mean of three independent invasion assays.

Microneme secretion assay. Microneme secretion in *T. gondii* was assayed by monitoring release into the culture medium. Freshly egressed *T. gondii* tachyzoites, pre-treated for 72 h ± ATc (*Tgnd9* iKD and *Tgndp1* iKD) or 24 h ± IAA (*Tgnd6* iKD and *Tgndp2* iKD), were harvested by centrifugation at 600*g* and washed twice

in intracellular buffer (5 mM NaCl, 142 mM KCl, 1 mM $MgCl_2$, 2 mM EGTA, 5.6 mM glucose and 25 mM HEPES (pH 7.2)) prewarmed to 37 °C. Parasites were resuspended in Dulbecco's Modified Eagle's Medium (supplemented with 2 mM glutamine) ± 500 µM propranolol and incubated at 37 °C for 20 min to induce microneme secretion. Parasites were pelleted at 1,000*g* for 5 min at 4 °C, washed once in PBS and stored at −20 °C. Supernatants were centrifuged at 2,000*g* for 5 min at 4 °C and used as excreted/secreted antigen. Pellets and excreted/secreted antigen samples were analysed for micronemal protein (AMA1) by western blot. Microneme secretion in *P. falciparum* was assayed by monitoring the surface translocation of AMA1. Highly synchronized DMSO and rapamycin-treated *Pfnd9* iKO schizonts were exposed to 10 µM E64 to block egress. IFAs were then performed with anti-PfAMA1 antibodies to analyse AMA1 translocation to the merozoite surface.

Rhoptry secretion assays. To evaluate the efficiency of rhoptry secretion in *T. gondii*, we expressed in the *Tgnd* iKD and *Tgndp* iKD lines a rhoptry secretion reporter protein consisting of the rhoptry protein toxofilin fused with Cre recombinase, a nuclear localization signal and a myc tag, collectively called secreted Cre, epitope-tagged (SeCrEt)[36]. The reporter strains generated were called *Tgnd9* iKD_SeCrEtUPRT, *Tgndp1* iKD_SeCrEtUPRT and *Tgnd6* iKD_SeCrEtHXGPRT. DsRed cells, constitutively expressing DsRed and able to switch to enhanced green fluorescent protein (GFP) expression upon Cre-mediated recombination, were used as reporter cells[36]. DsRed cells were maintained at <50% confluence (regardless of the flask size) and plated the day before parasite infection at a density of 2×10^5 cells per ml (in T25 flasks). Tachyzoites pre-treated for 72 h ± ATc (*Tgnd9* iKD and *Tgndp1* iKD) or 24 h ± IAA (*Tgnd6* iKD and *Tgndp2* iKD) were collected and used to infect the DsRed cells at a multiplicity of infection of 3. At 24 h post-invasion, infected DsRed cells were trypsinized and examined by fluorescence-activated cell sorting using FACSDiva software (BD Biosciences) to assess the percentage of cells expressing DsRed (rhoptry secretion impairment) and GFP (successful rhoptry secretion). The number of GFP-positive cells was normalized as a percentage compared with 100% in the control (−IAA or −ATc).

Additionally, rhoptry secretion has also been quantified by classical e-vacuole assay[35]. Freshly egressed parasites, pre-treated for 72 h ± ATc (*Tgnd9* iKD and *Tgndp1* iKD) or 24 h ± IAA (*Tgnd6* iKD), were preincubated with 1 µM cytochalasin D (cytD) for 10 min and then incubated with HFF cells in the presence of cytD for 15 min. IFAs were then performed with anti-ROP1 (rhoptry secretion) and anti-SAG1 (parasite surface), and the number of ROP1 stainings per field was determined by microscopic examination of at least 20 fields per coverslip ($n = 3$ coverslips).

To quantify rhoptry secretion in *P. falciparum*, the same number of DMSO- and rapamycin-treated *Pfnd9* iKO purified schizonts were arrested with 1.5 µM C2 for 4 h before being washed twice to allow them to egress. Parasites were then incubated for 30 min in complete medium with 1 µM cytD in the presence of red blood cells (RBCs). IFAs were then performed with anti-PfRAP2 antibodies to visualize rhoptry secretion events (spits of RAP2 export into the RBC). The number of secretion events was counted over the total RBCs by microscopic examination of 11 fields (~3,000 events analysed).

Freeze-fracture analysis. Cells used for the freeze-fracture analysis were harvested, pelleted and fixed in 2.5% glutaraldehyde in 0.1 M phosphate buffer at room temperature for 2 h. Following primary fixation, the samples were rinsed in the same buffer and kept overnight in 30% glycerol/0.1 M phosphate solution. The cells were then quickly frozen by immersion in liquid nitrogen under a vacuum. The frozen samples were fractured in a Bal-Tec BAF060 apparatus; subsequently, the fracture face was shadowed by evaporating platinum 45° (3.2 nm) and carbon 90° (25 nm). The replicas were then washed in 6.5% sodium hypochlorite, rinsed in a chloroform (2/3)–(1/3) solution, rinsed in distilled water and mounted on copper grids. Two different surfaces were taken in consideration when analysing the freeze-fracture technique replicas: the E-face (ectoplasmic) and the P-face (protoplasmic)[52]. The E-face is the portion of the lipid bilayer associated with the exterior of the cell or extracellular face. The P-face is the portion associated with the interior of the cell.

In vitro growth assay of *P. falciparum* parasite asexual development. The growth capability of *Pfnd9* iKO mutant parasites was assessed by comparing it with the *p230p* DiCre parental line[53] ± rapamycin in biological triplicates. DMSO (vehicle control) and rapamycin-treated cultures were synchronized at ring stages by sorbitol synchronization and parasitaemia adjusted to 0.2%, to follow growth over three cycles. Parasites around 30 h post-invasion were collected at each cycle to determine parasitaemia by counting Giemsa-stained parasites on at least 1,000 RBCs per culture.

***P. falciparum*-induced egress and time-lapse microscopy.** *P. falciparum* egress was imaged using C2 compound to tightly synchronize egress. DMSO- and rapamycin-treated *Pfnd9* iKO parasites were highly synchronized and blocked 40 h post-invasion (mature schizonts) with 1.5 µM C2 compound to prevent egress. After 40 h, the parasites were washed twice with warm RPMI 1640 medium (Gibco) to remove C2 and placed into a 35 mm dish (MatTek). The parasite suspension was sealed by adhering a 22 mm × 22 mm square coverslip to the dish and the preparation was introduced on a temperature-controlled microscope stage at 37 °C. Brightfield images were collected 5 min after washing off the C2 at 1 s intervals over a total of 15 min using a ZEISS Axio Observer microscope fitted with a CoolSNAP HQ2 digital camera and 63×/1.4 Oil Plan Apochromat objective. Images were exported to MOV videos using ZEN 2 (blue edition) software. The number of egress events in 15 min was normalized as a percentage compared with 100% in the control.

***Tetrahymena* dibucaine assay to quantify mucocyst secretion.** *Tetrahymena* cells were grown to stationary phase (10^6 cells per ml) in 25 ml SPP (2% proteose peptone, 0.1% yeast extract, 0.2% dextrose and 0.003% ferric-EDTA supplemented with 250 µg ml^{-1} penicillin G, 250 µg ml^{-1} streptomycin sulfate and 0.25 µg ml^{-1} amphotericin B fungizone) for 48 h, then concentrated by centrifugation into a lose 1.5 ml pellet. Cells were stimulated with 2.5 mM dibucaine, vigorously mixed for 30 s and diluted to 15 ml with 10 mM HEPES (pH 7.5) and 5 mM $CaCl_2$. After gently mixing, the culture was centrifuged at 1,200*g* for 2 min, resulting in the formation of a cell pellet/flocculent bilayer. Quantification of mucocyst secretion was done by weighing the flocculent layer overlying the pellet of cells.

Transmission electron microscopy. *Tgnd9* iKD and *Tgaro* iKD, together with the *Δku80*-TATi parental strain, were treated with ATc for 72 h. *Tgnd6* iKD parasites and the *Δku80*-Tir1 parental strain were treated with IAA for 24 h. Extracellular parasites were collected in the culture medium after natural egress and fixed by adding and equal volume of 0.1 M phosphate buffer containing 5% glutaraldehyde for 1 h at room temperature. Parasites were then centrifuged and resuspended in 1 ml fresh buffer with 2.5% glutaraldehyde for 2 h before being kept at 4 °C until further processing. Each of the following steps was performed in suspension followed by centrifugation steps in a tabletop microcentrifuge. Samples were post-fixed with 1% OsO_4 and 1.5% potassium ferricyanide in 0.1 M phosphate buffer for 1 h at room temperature, washed in water and then incubated in 2% uranyl acetate in water overnight at 4 °C. Tachyzoites were then dehydrated in a growing concentration of acetonitrile, followed by impregnation in epon 118/acetonitrile at a ratio of 50:50 for 2 h, 90:10 for two additional hours and then pure epon overnight. Pellets were polymerized in fresh epon for 48 h at 60 °C. Ultrathin sections (70 nm) were cut with a Leica ultracut system (Leica Microsystems) and counterstained with uranyl acetate and lead citrate.

Immunoelectron microscopy. TgNd6–HA_3 parasites and infected fibroblast monolayers were trypsinized and fixed with equal volumes of 8% formaldehyde in phosphate buffer overnight at 4 °C and resuspended in 4% fresh formaldehyde until further processing. Cells were then incubated with 0.1% glycine in phosphate buffer, pelleted and embedded in 12% gelatin, cut into small blocks (<1 mm) and infused in 2.3 M sucrose on a rotating wheel for 24 h at 4 °C. Gelatin blocks were mounted on specimen pins and frozen in liquid nitrogen. Cryo-sectioning was performed on a Leica UC7 cryo-ultramicrotome and 70 nm cryosections were picked-up in a 1:1 mixture of 2.3 M sucrose and 2% methylcellulose in water and stored at 4 °C. For on-grid immunodetection, grids were floated on 2% gelatin in PBS for 30 min at 37 °C to remove the methylcellulose/sucrose mixture, then blocked with 1% fish-skin gelatin (Sigma–Aldrich) in PBS for 5 min. Successive immunolabelling steps were performed on drops as follows: (1) rat monoclonal anti-HA antibodies (clone 3F10; Roche) in 1% BSA; (2) rabbit polyclonal anti-rat immunoglobulin antibody (Sigma–Aldrich) in 1% BSA; and (3) Protein A gold (UMC Utrecht) in 1% BSA. Four washes (2 min each) with 0.1% BSA were performed between steps. After Protein A treatment, the grids were washed four times for 2 min each with PBS, fixed for 5 min in 1% glutaraldehyde in water and washed six times for 2 min each with distilled water. The grids were then incubated with 2% methylcellulose:4% uranyl acetate at a ratio of 9:1 on ice in the dark for 15 min, picked-up on a wire loop and air-dried.

All chemicals were from Electron Microscopy Sciences and all solvents were from Sigma–Aldrich. Observations and image acquisition were performed on a Jeol 1200 EXII transmission electron microscope at the Electron Microscopy Platform of the University of Montpellier (http://mea.edu.umontpellier.fr). Transmission electron microscopy images were processed with Fiji for contrast optimization, and the Image J plugin was used to make the electron microscopy panels.

Cryo-ET. Freshly isolated *T. gondii* cells were suspended in HBSS along with fiducials (10 nm colloidal gold from Ted Pella for alignment of tilt series). A 4 µl drop of the suspension was applied onto electron microscopy grids, excess liquid was blotted away and the suspension was plunge frozen in a liquid ethane/propane mixture (pre-cooled using liquid nitrogen) using an electron microscopy GP2 automatic plunger (Leica Microsystems)[54]. The blotting chamber was set to 95–100% relative humidity at 37 °C and blotting was done either from the sample side of the grid or from the back using Whatman filter paper (No. 1). Plunge-frozen grids were subsequently loaded into AutoGrid cartridges (Thermo Fisher Scientific). Electron microscopy cartridges containing frozen grids were stored in liquid nitrogen and maintained at ≤−170 °C throughout storage, transfer and cryo-ET imaging.

Cryo-ET data collection was performed on a Thermo Fisher Scientific Krios G3i 300 keV field emission cryogenic transmission electron microscopy gun equipped with a 6k × 4k K3 direct electron detector (Gatan) at the Beckman Center for Cryo-Electron Microscopy in the Singh Center for Nanotechnology, University of Pennsylvania. The camera was operated in electron-counting mode to enable motion correction. An energy filter (Gatan Imaging Filter; Gatan) with a slit width of 20 eV was used to increase the contrast of the projection images. Additionally, a Volta phase plate was used to boost the image contrast at defocus values of −2–3 µm. A magnification of 33,000× with corresponding pixel sizes of 2.65 Å was used for imaging. SerialEM software[55] was used for all imaging. Cells were first assessed at lower magnifications for suitability of ice thickness and outer membrane integrity (the parasites sometimes tend to vesiculate their outer membrane, possibly in response to blotting). Once the target cells were identified and marked, anchor maps were used to revisit these locations and collect tilt series in an automated fashion. Each tilt series was collected from −60° to +60°, with increments of 2°, in an automated fashion using the low-dose functions of tracking and focusing. The cumulative dose of each tilt series ranged between 100 and 150 e^{-} Å^{-2}. Once acquired, tilt series were binned twice or four times before being aligned using the 10 nm colloidal gold as fiducials and reconstructed into tomograms by our in-house automated computation pipeline utilizing the IMOD software package[56]. For presentation purposes, tomograms were favourably oriented in three dimensions before averaging a few slices around the slice of interest (to enhance contrast) using the slicer window in IMOD. In a few cases (Fig. 4b–e), the contrast was further enhanced using the nonlinear anisotropic diffusion filter in IMOD.

Immunopurification and mass spectrometry analysis. Immunopurification was performed using anti-HA magnetic beads (Pierce; R88836) as previously described[57]. Purified proteins were loaded on a sodium dodecyl sulfate polyacrylamide gel electrophoresis system and digested in gel (two bands per sample) as previously described[58]. Samples were loaded onto a 25 cm reversed-phase column (75 mm inner diameter; Acclaim PepMap 100 C18; Thermo Fisher Scientific) and separated with an UltiMate 3000 RSLC system (Thermo Fisher Scientific) coupled to a Q Exactive HFX system (Thermo Fisher Scientific). Tandem mass spectrometry analyses were performed in a data-dependent mode. Full scans (375–1,500 m/z) were acquired in the Orbitrap mass analyzer with a resolution of 60,000 at 200 m/z. For the full scans, 3×10^6 ions were accumulated within a maximum injection time of 60 ms. The 12 most intense ions with charge states ≥2 were sequentially isolated (1×10^5) with a maximum injection time of 45 ms and fragmented by higher-energy collisional dissociation in the collision cell (normalized collision energy of 28%) and detected in the Orbitrap analyzer at a resolution of 30,000.

Raw spectra were processed with MaxQuant[59] using standard parameters with label-free quantification (LFQ) and matched between runs using Andromeda[60]. Tandem mass spectrometry spectra were matched against the UniProt reference proteomes of *T. gondii* and humans (proteome IDs UP000001529 and UP000005640, respectively) and 250 frequently observed contaminants, as well as reversed sequences of all entries (MaxQuant contaminant database). Statistical analyses were done using Perseus on LFQ data[61].

Amino acid sequence alignments and phylogenetic analyses, cell and parasite culture, parasite cloning strategies, parasite transfections, parasite immunoblots, *T. gondii* plaque assays, *T. gondii* intracellular growth assays, *T. gondii* immunofluorescence-based induced egress assays, *T. gondii* conoid extrusion assays, *T. gondii* gliding assays, *T. gondii* attachment assays, Ciliata culture conditions, Ciliata biolistic transformation, generation of the *Tetrahymena* knockout strain, Ciliata immunoblots, Ciliata immunofluorescence microscopy, statistical analysis, reagents and antibodies are found in the Supplementary Methods.

Reporting Summary. Further information on research design is available in the Nature Research Reporting Summary linked to this article.

Data availability

The mass spectrometry proteomics data generated during this study are available from the ProteomeXchange Consortium (http://proteomecentral.proteomexchange.org) via the PRIDE partner repository[62] with the dataset identifiers PXD022713 (Nd9 dataset) and PXD022725 (NdP1 dataset). All data generated or analysed during this study are included within the published article and its Supplementary Information files. Source data are provided with this paper.

Received: 9 April 2020; Accepted: 14 December 2020;

References

1. Dubremetz, J. F. Rhoptries are major players in *Toxoplasma gondii* invasion and host cell interaction. *Cell Microbiol.* **9**, 841–848 (2007).
2. Boothroyd, J. C. & Dubremetz, J. F. Kiss and spit: the dual roles of *Toxoplasma* rhoptries. *Nat. Rev. Microbiol.* **6**, 79–88 (2008).
3. Carruthers, V. B. & Sibley, L. D. Sequential protein secretion from three distinct organelles of *Toxoplasma gondii* accompanies invasion of human fibroblasts. *Eur. J. Cell Biol.* **73**, 114–123 (1997).
4. Frenal, K., Dubremetz, J. F., Lebrun, M. & Soldati-Favre, D. Gliding motility powers invasion and egress in Apicomplexa. *Nat. Rev. Microbiol.* **15**, 645–660 (2017).
5. Besteiro, S., Dubremetz, J. F. & Lebrun, M. The moving junction of apicomplexan parasites: a key structure for invasion. *Cell Microbiol.* **13**, 797–805 (2011).
6. Ito, D., Schureck, M. A. & Desai, S. A. An essential dual-function complex mediates erythrocyte invasion and channel-mediated nutrient uptake in malaria parasites. *eLife* **6**, e23485 (2017).
7. Counihan, N. A. et al. *Plasmodium falciparum* parasites deploy RhopH2 into the host erythrocyte to obtain nutrients, grow and replicate. *eLife* **6**, e23217 (2017).
8. Nguitragool, W. et al. Malaria parasite *clag3* genes determine channel-mediated nutrient uptake by infected red blood cells. *Cell* **145**, 665–677 (2011).
9. Hakimi, M.-A., Olias, P. & Sibley, L. D. *Toxoplasma* effectors targeting host signaling and transcription. *Clin. Microbiol. Rev.* **30**, 615–645 (2017).
10. Singh, S., Alam, M. M., Pal-Bhowmick, I., Brzostowski, J. A. & Chitnis, C. E. Distinct external signals trigger sequential release of apical organelles during erythrocyte invasion by malaria parasites. *PLoS Pathog.* **6**, e1000746 (2010).
11. Kessler, H. et al. Microneme protein 8—a new essential invasion factor in *Toxoplasma gondii*. *J. Cell Sci.* **121**, 947–956 (2008).
12. Nichols, B. A., Chiappino, M. L. & O'Connor, G. R. Secretion from the rhoptries of *Toxoplasma gondii* during host-cell invasion. *J. Ultrastruct. Res.* **83**, 85–98 (1983).
13. Coleman, B. I. et al. A member of the ferlin calcium sensor family is essential for *Toxoplasma gondii* rhoptry secretion. *mBio* **9**, e01510–e01518 (2018).
14. Suarez, C. et al. A lipid-binding protein mediates rhoptry discharge and invasion in *Plasmodium falciparum* and *Toxoplasma gondii* parasites. *Nat. Commun.* **10**, 4041 (2019).
15. Tseng, T. T., Tyler, B. M. & Setubal, J. C. Protein secretion systems in bacterial–host associations, and their description in the Gene Ontology. *BMC Microbiol.* **9**, S2 (2009).
16. Gubbels, M.-J. & Duraisingh, M. T. Evolution of apicomplexan secretory organelles. *Int. J. Parasitol.* **42**, 1071–1081 (2012).
17. Plattner, H. Trichocysts—*Paramecium*'s projectile-like secretory organelles: reappraisal of their biogenesis, composition, intracellular transport, and possible functions. *J. Eukaryot. Microbiol.* **64**, 106–133 (2017).
18. Plattner, H., Miller, F. & Bachmann, L. Membrane specializations in the form of regular membrane-to-membrane attachment sites in *Paramecium*. A correlated freeze-etching and ultrathin-sectioning analysis. *J. Cell Sci.* **13**, 687–719 (1973).
19. Knoll, G., Braun, C. & Plattner, H. Quenched flow analysis of exocytosis in *Paramecium* cells: time course, changes in membrane structure, and calcium requirements revealed after rapid mixing and rapid freezing of intact cells. *J. Cell Biol.* **113**, 1295–1304 (1991).
20. Dubremetz, J. F. & Torpier, G. Freeze fracture study of the pellicle of an Eimerian sporozoite (Protozoa, Coccidia). *J. Ultrastruct. Res.* **62**, 94–109 (1978).
21. Porchet, E. & Torpier, G. [Freeze fracture study of *Toxoplasma* and *Sarcocystis* infective stages (author's transl)]. *Z. Parasitenkd.* **54**, 101–124 (1977).
22. Porchet-Hennere, E. & Nicolas, G. Are rhoptries of Coccidia really extrusomes? *J. Ultrastruct. Res.* **84**, 194–203 (1983).
23. Dubremetz, J. F. & Entzeroth, R. in *Membrane Traffic in Protozoa* Pt. A, Vol. 2 (ed. Tartakoff, A. M. & Plattner, H.) 83–98 (Elsevier Science, 1993).
24. Lefort-Tran, M., Aufderheide, K., Pouphile, M., Rossignol, M. & Beisson, J. Control of exocytotic processes: cytological and physiological studies of trichocyst mutants in *Paramecium tetraurelia*. *J. Cell Biol.* **88**, 301–311 (1981).
25. Beisson, J., Lefort-Tran, M., Pouphile, M., Rossignol, M. & Satir, B. Genetic analysis of membrane differentiation in *Paramecium*. Freeze-fracture study of the trichocyst cycle in wild-type and mutant strains. *J. Cell Biol.* **69**, 126–143 (1976).
26. Gogendeau, D., Keller, A. M., Yanagi, A., Cohen, J. & Koll, F. Nd6p, a novel protein with RCC1-like domains involved in exocytosis in *Paramecium tetraurelia*. *Eukaryot. Cell* **4**, 2129–2139 (2005).
27. Froissard, M., Keller, A. M. & Cohen, J. ND9P, a novel protein with Armadillo-like repeats involved in exocytosis: physiological studies using allelic mutants in *Paramecium*. *Genetics* **157**, 611–620 (2001).
28. Skouri, F. & Cohen, J. Genetic approach to regulated exocytosis using functional complementation in *Paramecium*: identification of the *ND7* gene required for membrane fusion. *Mol. Biol. Cell* **8**, 1063–1071 (1997).
29. Froissard, M., Keller, A. M., Dedieu, J. C. & Cohen, J. Novel secretory vesicle proteins essential for membrane fusion display extracellular-matrix domains. *Traffic* **5**, 493–502 (2004).
30. Paredes-Santos, T. C., de Souza, W. & Attias, M. Dynamics and 3D organization of secretory organelles of *Toxoplasma gondii*. *J. Struct. Biol.* **177**, 420–430 (2012).

31. Sidik, S. M. et al. A genome-wide CRISPR screen in *Toxoplasma* identifies essential apicomplexan genes. *Cell* **166**, 1423–1435.e12 (2016).
32. Long, S. et al. Calmodulin-like proteins localized to the conoid regulate motility and cell invasion by *Toxoplasma gondii*. *PLoS Pathog.* **13**, e1006379 (2017).
33. Meissner, M., Schluter, D. & Soldati, D. Role of *Toxoplasma gondii* myosin A in powering parasite gliding and host cell invasion. *Science* **298**, 837–840 (2002).
34. Sheiner, L. et al. A systematic screen to discover and analyze apicoplast proteins identifies a conserved and essential protein import factor. *PLoS Pathog.* **7**, e1002392 (2011).
35. Lamarque, M. H. et al. Plasticity and redundancy among AMA–RON pairs ensure host cell entry of *Toxoplasma* parasites. *Nat. Commun.* **5**, 4098 (2014).
36. Koshy, A. A. et al. *Toxoplasma* secreting Cre recombinase for analysis of host–parasite interactions. *Nat. Methods* **7**, 307–309 (2010).
37. Collins, C. R. et al. Robust inducible Cre recombinase activity in the human malaria parasite *Plasmodium falciparum* enables efficient gene deletion within a single asexual erythrocytic growth cycle. *Mol. Microbiol.* **88**, 687–701 (2013).
38. Zhang, M. et al. Uncovering the essential genes of the human malaria parasite *Plasmodium falciparum* by saturation mutagenesis. *Science* **360**, eaap7847 (2018).
39. Briguglio, J. S., Kumar, S. & Turkewitz, A. P. Lysosomal sorting receptors are essential for secretory granule biogenesis in *Tetrahymena*. *J. Cell Biol.* **203**, 537–550 (2013).
40. Mueller, C. et al. The *Toxoplasma* protein ARO mediates the apical positioning of rhoptry organelles, a prerequisite for host cell invasion. *Cell Host Microbe* **13**, 289–301 (2013).
41. Beisson, J., Cohen, J., Lefort-Tran, M., Pouphile, M. & Rossignol, M. Control of membrane fusion in exocytosis. Physiological studies on a *Paramecium* mutant blocked in the final step of the trichocyst extrusion process. *J. Cell Biol.* **85**, 213–227 (1980).
42. Bonnemain, H., Gulik-Krzywicki, T., Grandchamp, C. & Cohen, J. Interactions between genes involved in exocytotic membrane fusion in *Paramecium*. *Genetics* **130**, 461–470 (1992).
43. Varghese, T. Fine structure of the endogenous stages of *Eimeria labbeana*. I. The first generation merozoites. *J. Protozool.* **22**, 66–71 (1975).
44. Sheffield, H. G. Electron microscope study of the proliferative form of *Besnoitia jellisoni*. *J. Parasitol.* **52**, 583–594 (1966).
45. Perkins, F. O. Zoospores of the oyster pathogen, *Dermocystidium marinum*. I. Fine structure of the conoid and other sporozoan-like organelles. *J. Parasitol.* **62**, 959–974 (1976).
46. El Hajj, H. et al. Molecular signals in the trafficking of *Toxoplasma gondii* protein MIC3 to the micronemes. *Eukaryot. Cell* **7**, 1019–1028 (2008).
47. Collins, C. R., Withers-Martinez, C., Hackett, F. & Blackman, M. J. An inhibitory antibody blocks interactions between components of the malarial invasion machinery. *PLoS Pathog.* **5**, e1000273 (2009).
48. Burghaus, P. A. & Holder, A. A. Expression of the 19-kilodalton carboxy-terminal fragment of the *Plasmodium falciparum* merozoite surface protein-1 in *Escherichia coli* as a correctly folded protein. *Mol. Biochem. Parasitol.* **64**, 165–169 (1994).
49. Douki, J. B. et al. Adhesion of normal and *Plasmodium falciparum* ring-infected erythrocytes to endothelial cells and the placenta involves the rhoptry-derived ring surface protein-2. *Blood* **101**, 5025–5032 (2003).
50. Schindelin, J. et al. Fiji: an open-source platform for biological-image analysis. *Nat. Methods* **9**, 676–682 (2012).
51. Cerede, O. et al. Synergistic role of micronemal proteins in *Toxoplasma gondii* virulence. *J. Exp. Med.* **201**, 453–463 (2005).
52. Branton, D. et al. Freeze-etching nomenclature. *Science* **190**, 54–56 (1975).
53. Knuepfer, E., Napiorkowska, M., van Ooij, C. & Holder, A. A. Generating conditional gene knockouts in *Plasmodium*—a toolkit to produce stable DiCre recombinase-expressing parasite lines using CRISPR/Cas9. *Sci. Rep.* **7**, 3881 (2017).
54. Iancu, C. V. et al. Electron cryotomography sample preparation using the Vitrobot. *Nat. Protoc.* **1**, 2813–2819 (2006).
55. Mastronarde, D. N. Automated electron microscope tomography using robust prediction of specimen movements. *J. Struct. Biol.* **152**, 36–51 (2005).
56. Kremer, J. R., Mastronarde, D. N. & McIntosh, J. R. Computer visualization of three-dimensional image data using IMOD. *J. Struct. Biol.* **116**, 71–76 (1996).
57. Lebrun, M. et al. The rhoptry neck protein RON4 relocalizes at the moving junction during *Toxoplasma gondii* invasion. *Cell Microbiol.* **7**, 1823–1833 (2005).
58. Skorupa, A. et al. Angiogenin induces modifications in the astrocyte secretome: relevance to amyotrophic lateral sclerosis. *J. Proteom.* **91**, 274–285 (2013).
59. Cox, J. & Mann, M. MaxQuant enables high peptide identification rates, individualized p.p.b.-range mass accuracies and proteome-wide protein quantification. *Nat. Biotechnol.* **26**, 1367–1372 (2008).
60. Cox, J. et al. Andromeda: a peptide search engine integrated into the MaxQuant environment. *J. Proteome Res.* **10**, 1794–1805 (2011).
61. Tyanova, S. et al. The Perseus computational platform for comprehensive analysis of (prote)omics data. *Nat. Methods* **13**, 731–740 (2016).
62. Perez-Riverol, Y. et al. The PRIDE database and related tools and resources in 2019: improving support for quantification data. *Nucleic Acids Res.* **47**, D442–D450 (2019).
63. Wilson, D., Madera, M., Vogel, C., Chothia, C. & Gough, J. The SUPERFAMILY database in 2007: families and functions. *Nucleic Acids Res.* **35**, D308–D313 (2007).
64. Hadjebi, O., Casas-Terradellas, E., Garcia-Gonzalo, F. R. & Rosa, J. L. The RCC1 superfamily: from genes, to function, to disease. *Biochim. Biophys. Acta* **1783**, 1467–1479 (2008).

Acknowledgements

We thank S. Lourido for the pU6-Universal plasmid, A. Scherf for the anti-PfRAP2 antibodies, D. Soldati-Favre for providing the anti-ARO antibodies and *TgARO* iKD strain, M. Blackman for the anti-PfAMA1 and anti-PfMSP1 antibodies, pDC2-Cas9-hDHFRyFCU plasmid and *p230p* DiCre strain, J. Boothroyd for the monoclonal antibody CCL2 anti-TgAMA1, E. Peterson for anti-TgSAG1, R. Waller for the ring-1–GFP plasmid, A. Koshy for the toxofilin-Cre plasmid, and H. Blau's laboratory for the Cre reporter DsRed cell line. We thank O. Billker for providing us with compound 2. We thank V. Richard and F. Godiard for technical assistance with the electron microscopy service of the University of Montpellier. We are also grateful to E. Jublanc and the imaging facility MRI at the University of Montpellier (part of the national infrastructure France-BioImaging supported by the French National Research Agency (ANR-10-INBS-04; Investments for the future)) and to C. Duperray of the MRI-Cytometry facility at the Institute for Regenerative Medicine and Biotherapy for assistance and technical support. We thank J. Marcetteau for the graphical design of Figs. 1b and 4. We acknowledge the use of instruments at the Electron Microscopy Resource Lab and Beckman Center for Cryo-Electron Microscopy at the University of Pennsylvania. M.L. is an INSERM researcher. This work was supported by the Laboratoire d'Excellence ParaFrap (ANR-11-LABX-0024), ANR (ANR-16-CE15-0010-01), Fondation pour la Recherche Medicale (Equipe FRM DEQ20170336725), European Research Council (ERC advanced grant number 833309 KissAndSpitRhoptry to M.L.), France and Chicago Collaborating in the Sciences (to A.P.T. and M.L.) and NIH (GM105783 to A.P.T.), as well as by a David and Lucile Packard Fellowship for Science and Engineering (2019-69645 to Y.-W.C.) and an EMBO fellowship (number ALTF 58-2018 to A.N.G.).

Author contributions

E.A. performed most of the work on *Toxoplasma*. M.M.C. generated the *Plasmodium* data and completed the work on *Toxoplasma* during revision. A.G. performed the phylogenetic analyses. E.A., D.S. and R.N. generated the *T. thermophila* data. C.S. generated the donor plasmid for *Pfnd9* iKO. A.N.G., N.D.S.P., R.N. and M.M. contributed to the *Toxoplasma* phenotypic analyses. D.M.P.-V. performed the immunoprecipitation analyses. S.U. performed the mass spectrometry analyses. E.A., L.B.-S. and J.-F.D. performed the electron microscopy. E.A., P.R.F. and J.-F.D. performed the freeze-fracture analyses. S.K.M. and Y.-W.C. performed the cryo-ET. A.N.G. and S.K.M. prepared the samples for cryo-ET. M.L. designed the study with support from E.A. M.L. supervised the research. E.A. and M.L. wrote the paper with editorial support from M.M.C., A.P.T., D.S., A.N.G., S.K.M., Y.-W.C. and B.S.

Competing interests

The authors declare no competing interests.

Additional information

Extended data is available for this paper at https://doi.org/10.1038/s41564-020-00854-z.

Supplementary information is available for this paper at https://doi.org/10.1038/s41564-020-00854-z.

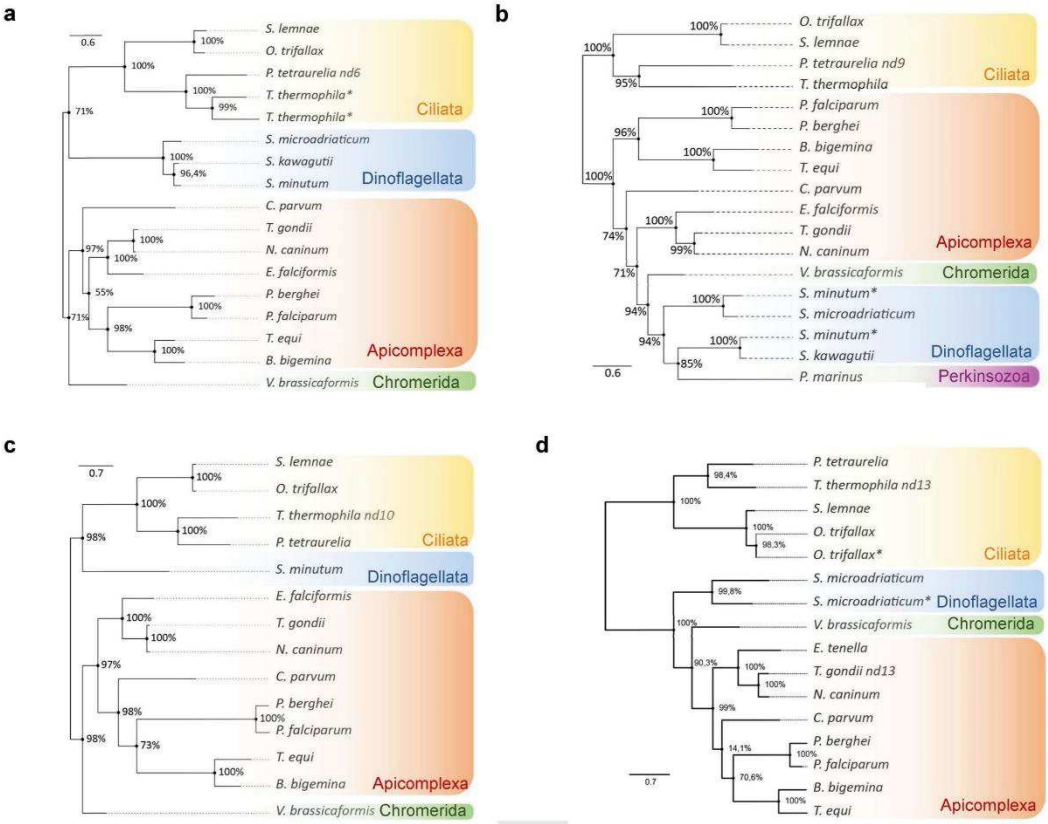
Correspondence and requests for materials should be addressed to M.L.

Peer review information *Nature Microbiology* thanks Ke Hu, Geoffrey Ian G. McFadden and the other, anonymous, reviewer(s) for their contribution to the peer review of this work.

Reprints and permissions information is available at www.nature.com/reprints.

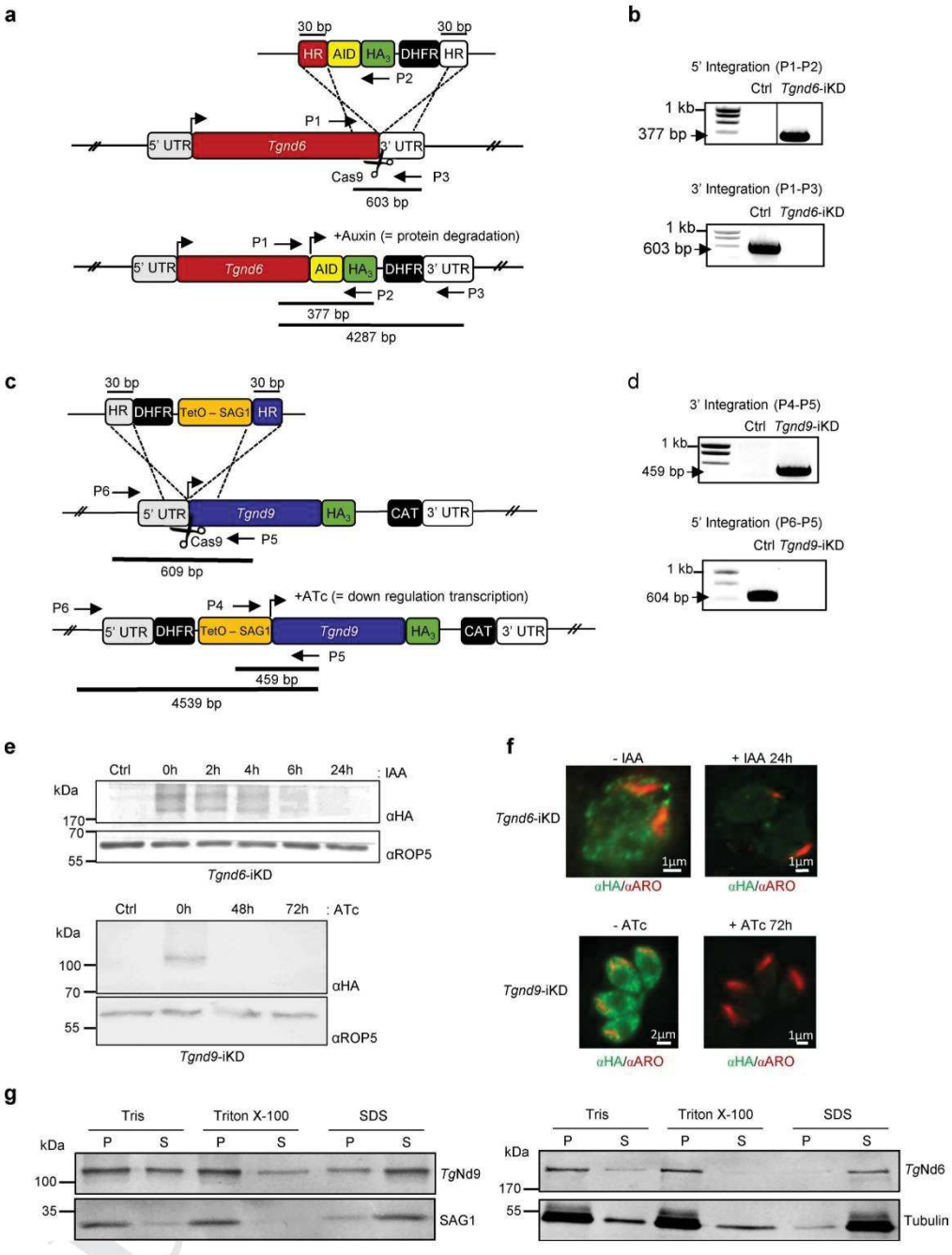
Publisher's note Springer Nature remains neutral with regard to jurisdictional claims in published maps and institutional affiliations.

© The Author(s), under exclusive licence to Springer Nature Limited 2021



Extended Data Fig. 1 | Amino acid sequence alignments and phylogenetic analyses. a–d, Maximum likelihood phylogenetic trees based on *Alveolata* non discharge (Nd) Nd6 (a) Nd9 (b) NdP1 (c) and NdP2 (d) protein sequences. Asterisks indicate two homologous genes in the same species. The scale bar represents the branch length values. Amino acids sequences, accession number and alignments used to generate phylogenetic tree of Nd6, Nd9, NdP1 and NdP2 are presented in Source Data Extended Data Fig. 1.

Uncorrected

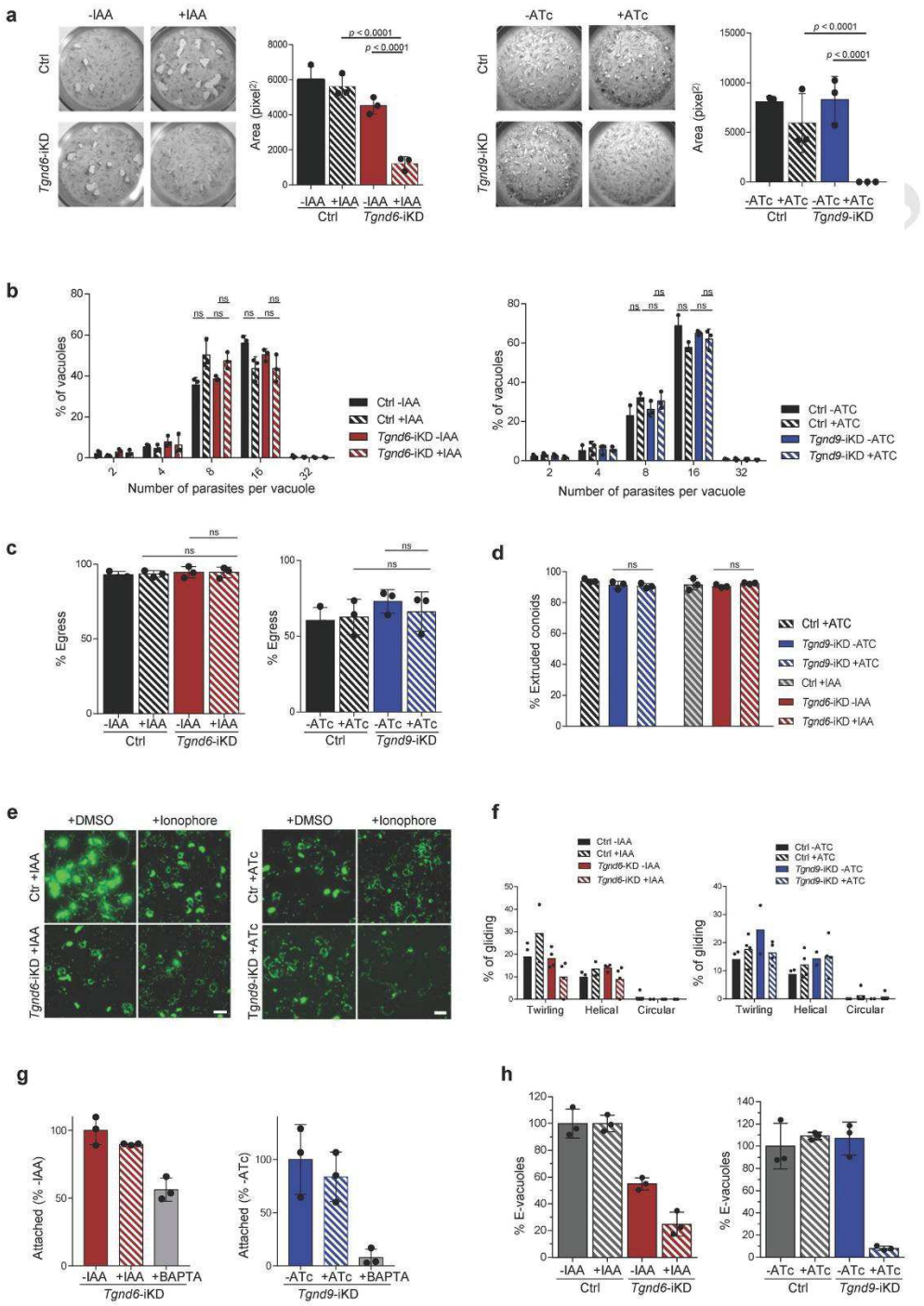


Extended Data Fig. 2 | See next page for caption.

Extended Data Fig. 2 | Generation of *Tgnd6*-iKD and *Tgnd9*-iKD. a, Strategy for conditional depletion of *Tg*Nd6 (TGGT1_248640) using the Auxin-inducible degron system. **b**, Integration PCRs showing double homologous recombination at the 5′ (top) and at the 3′ (bottom) of the *Tgnd6* locus. Representative of 3 experiments. **c**, Strategy for conditional depletion of *Tg*Nd9 (TGGT1_249730) using the Tet-OFF system. **d**, Integration PCRs showing double homologous recombination at the 3′ (top) and at the 5′ (bottom) of the *Tgnd9* locus. Representative of 3 experiments. **e**, Immunoblot of *Tgnd6*-iKD ± IAA (top) and *Tgnd9*-iKD ± ATc (bottom) showing the timing for protein depletion. ROP5, loading control. Ctrl: *ΔKu80-Tir1* (upper panel) and *ΔKu80-TaTi* (lower panel). Representative of one experiment for *Tgnd9*-iKD and 2 experiments for *Tgnd6*-iKD. **f**, IFA of *Tgnd6*-iKD shows depletion of *Tg*Nd6 after 24 hours IAA treatment (top right), IFA of *Tgnd9*-iKD shows depletion of *Tg*Nd9 after 72 hours ATc treatment (bottom right). Red, anti-ARO. Green, anti-HA. Representative of 3 experiments. **g**, Detergent extraction profile of *Tg*ND6 and *Tg*ND9 after solubilization of HA-tagged *Tg*Nds parasites with Tris 1 mM, 1% TritonX-100 or 1% SDS. Representative of 2 experiments.

Uncorrected proofs

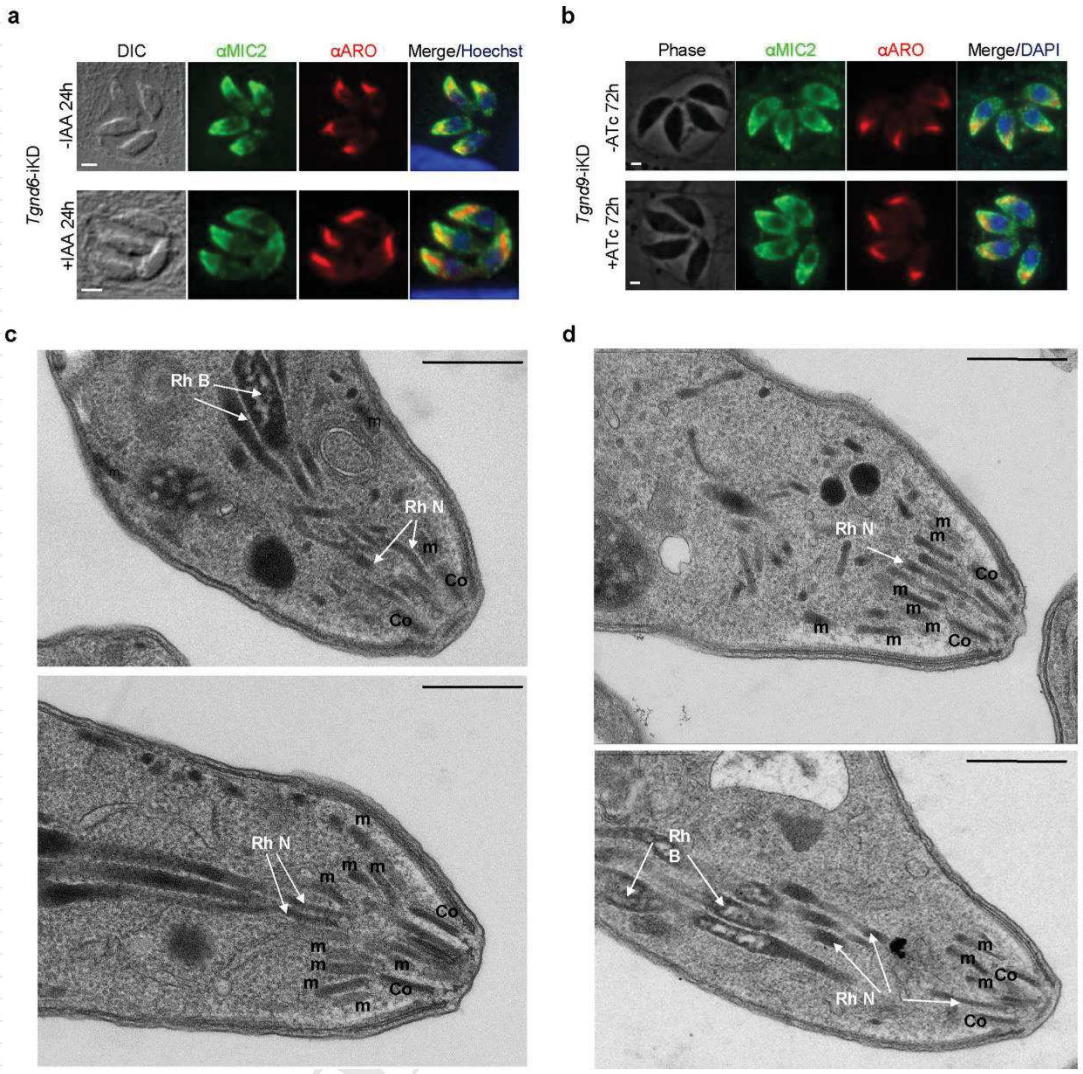
A B



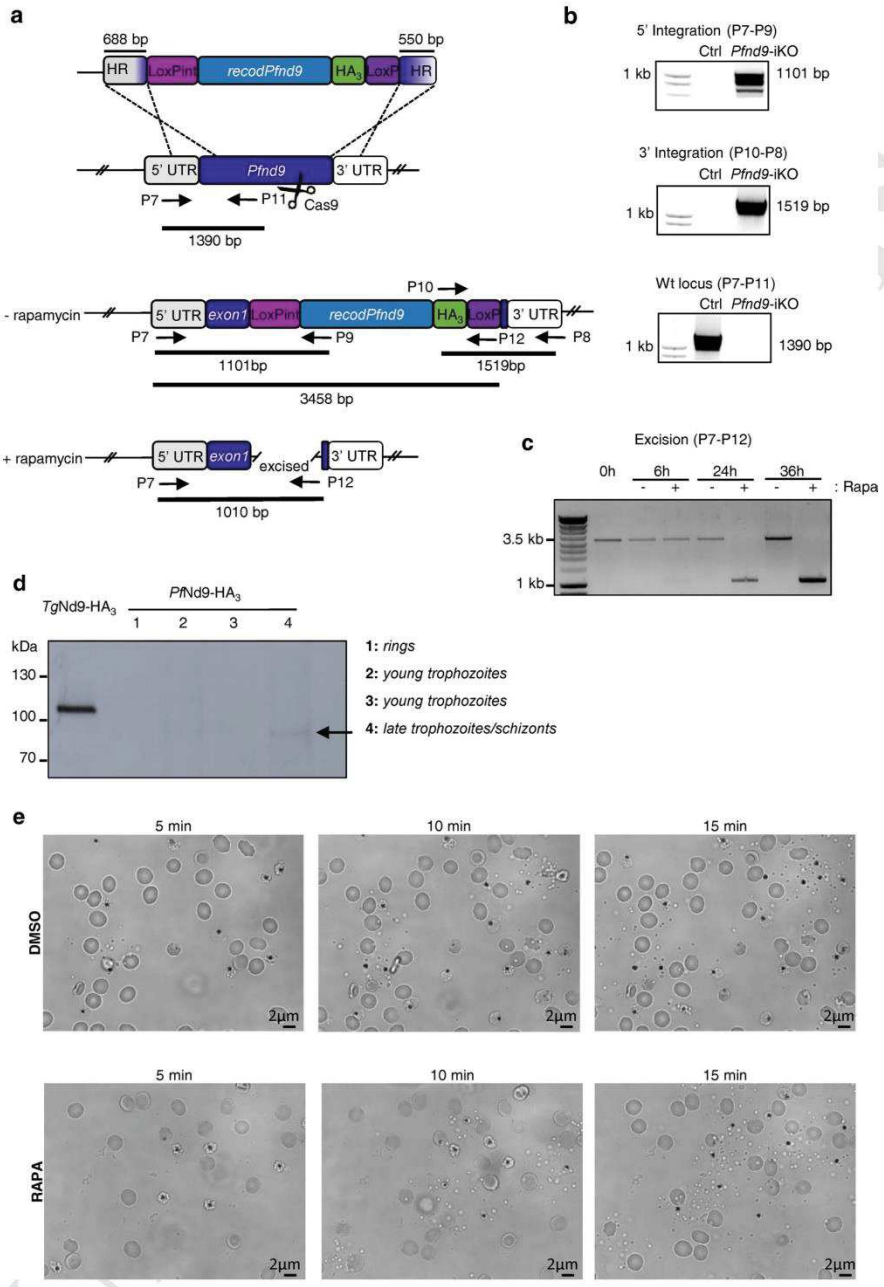
Extended Data Fig. 3 | See next page for caption.

Extended Data Fig. 3 | Depletion of Nd6 or Nd9 in *T. gondii* parasites does not affect replication, egress, gliding motility nor attachment. a, Plaque assay. Left: Δ*Ku80-Tir1* (Ctrl) ± IAA vs *Tgnd6*-iKD ± IAA. Right: Δ*Ku80-TaTi* (Ctrl) ± ATc vs *Tgnd9*-iKD ± ATc. 7 dpi lysis plaque areas were measured. No plaques were observed for *Tgnd9*-iKD +ATc. Means of plaque area ± SD of 3 biological samples. Representative of 3 independent assays. **b**, Intracellular replication. Left: Δ*Ku80-Tir1* (Ctrl) and *Tgnd6*-iKD ± IAA. Right: Δ*Ku80-TaTi* (Ctrl) and *Tgnd9*-iKD ± ATc. The percentage of vacuoles containing 2, 4, 8, 16 or 32 parasites was determined for 200 vacuoles. Means ± SD from 3 biological samples. Representative of 3 independent experiments. **c**, Percentage of egressed vacuoles. Left: Δ*Ku80-Tir1* (Ctrl) and *Tgnd6*-iKD ± IAA. Right: Δ*Ku80-TaTi* (Ctrl) and *Tgnd9*-iKD ± ATc. Egress events were quantified for 200 vacuoles. Means ± SD from 3 biological samples. Representative of 2 independent experiments. **d**, Conoid protrusion assay. The graph represents the percentage of protruded conoids induced by 5 µM A23187, or DMSO as control. Means ±SD from 3 biological samples. Representative of 3 independent experiments. **e**, Gliding assays were performed with Δ*Ku80-Tir1* (Ctrl) and *Tgnd6*-iKD parasite lines ± IAA 24 h (left) and Δ*Ku80-TaTi* (Ctrl) and *Tgnd9*-iKD parasite lines ± ATc 72 h (right). Trails were revealed by IFA using anti-SAG1 antibodies. Scale bar=10 µm. Representative of 3 experiments. **f**, Quantification of parasite motility by time–lapse video microscopy. Data are plotted as a percentage of circular, helical and twirling movements. Values represent mean of 2–4 movies. **g**, Quantification of attachment on glutaraldehyde fixed host cell. As control of microneme secretion-dependent attachment, parasites were treated with BAPTA-AM. **h**, Quantification of rhoptry secretion by e-vacuoles assay. *Tgnd6*-iKD was compared to the background line Δ*ku80-Tir1* ± IAA 24 h and *Tgnd9*-iKO was compared to the background line Δ*ku80-TATi* ± Atc 72 h. (g,h) Means ± SD from 3 biological samples. Representative of one experiment. The significance of the results was assessed using a parametric paired *t*-test (Student's two-tailed *t*-test). ns = non-significant.

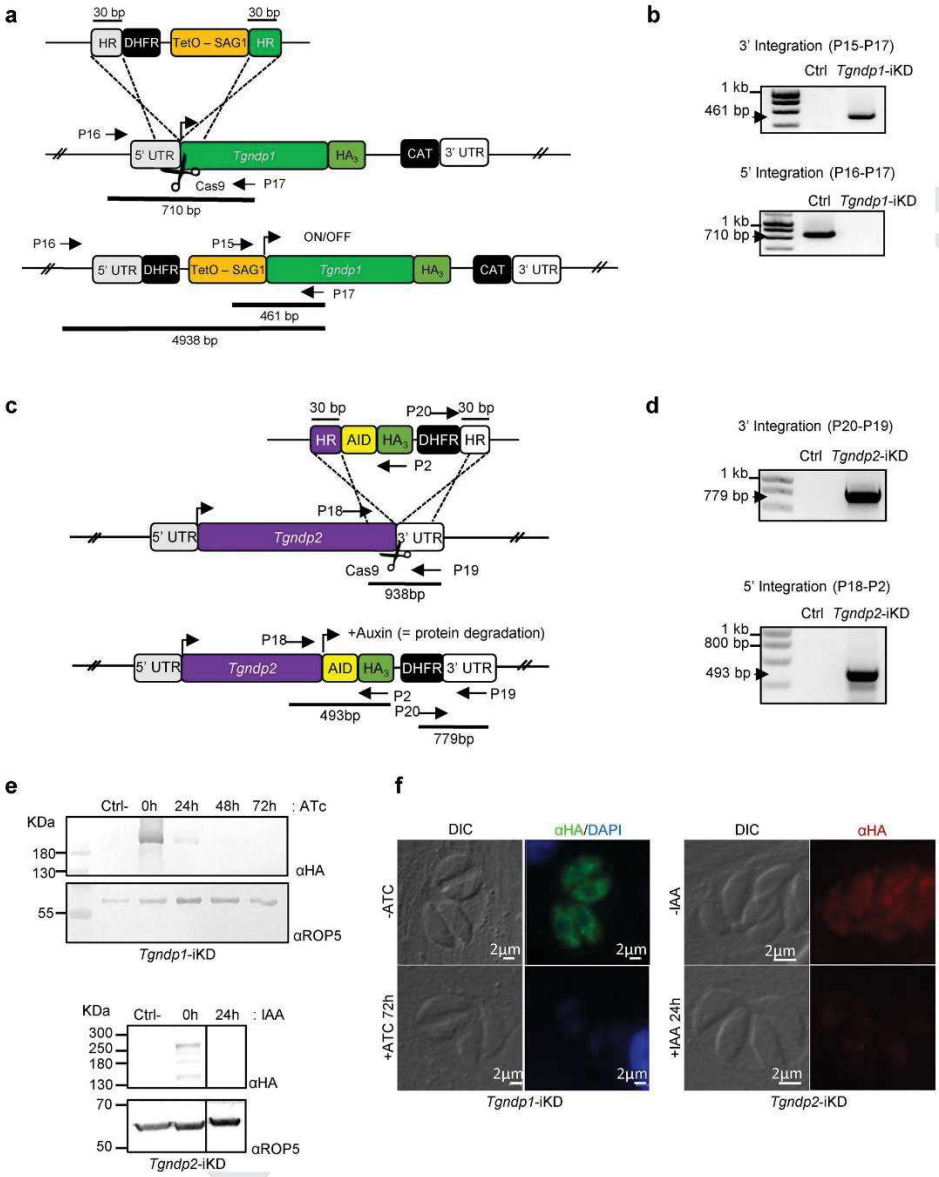
Uncorrected proofs



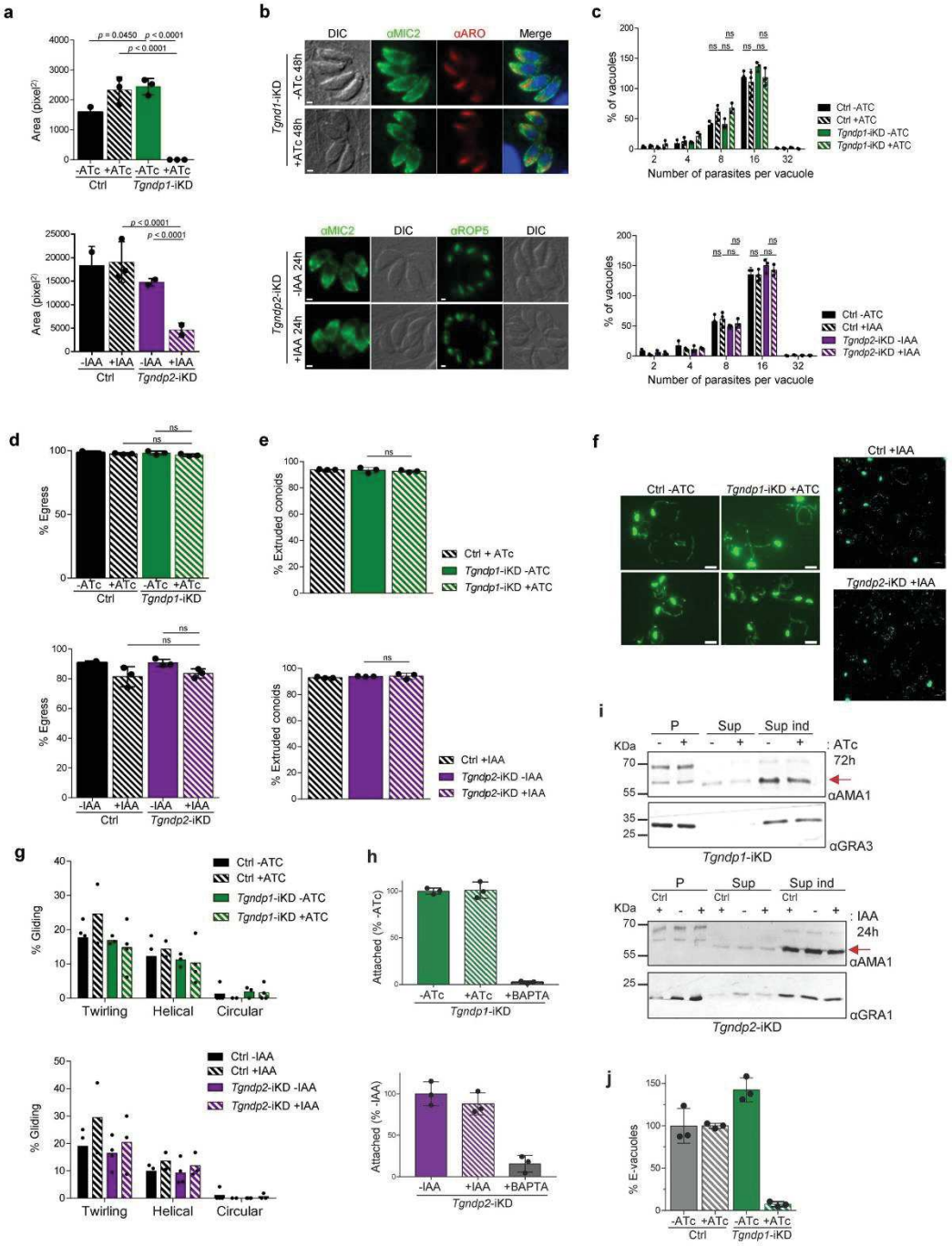
Extended Data Fig. 4 | Secretory organelles biogenesis and positioning is not affected in *Tgnd6*-iKD and *Tgnd9*-iKD. a, b, IFA using anti-ARO antibodies (rhoptry marker) and anti-MIC2 (microneme marker) on *Tgnd6*-iKD parasites ± IAA 24 h (**a**) and on *Tgnd9*-iKD parasites ± ATc 72 h (**b**). Scale bar=1 µm. Representative of 3 experiments. **c**, **d**, Electron microscopy images showing the apical complex of extracellular tachyzoites of *Tgnd6*-iKD +IAA 24 h (**c**) and of *Tgnd9*-iKD +ATc 72 h. Representative of one experiment. (**d**). Rh B = rhoptry bulb, Rh N = rhoptry neck, Co = conoid, m = microneme. Bar = 500 nm.



Extended Data Fig. 5 | Generation of *Pfnd9*-iKO. a, Strategy for conditional depletion of *Pf*Nd9 (PF3D7_1232700) using the DiCre system. **b**, Integration PCRs showing double homologous recombination at the 5′ end (top panel) and at the 3′ end (middle panel) of the *Pfnd9* locus. In the bottom panel, PCR demonstrating the absence of the wt locus in the floxed clonal population. Representative of 2 experiments. **c**, PCRs showing efficient excision of the *Pfnd9* locus upon addition of rapamycin. Representative of 3 experiments. **d**, Immunoblot on parasite lysates from *Pfnd9*-iKO mutant parasites. We could not detect the protein by IFA and only observed a faint band at the expected size in late schizonts by Western blot, both consistent with the very low transcript level of *PfNd9* (Plasmodb.org). Representative of 2 experiments. **e**, Representative images of 2 experiments from the time lapse video microscopy of merozoites egressing from schizonts in the DMSO control and in the rapamycin-treated *Pfnd9*-iKO parasites. Relative time shown in minutes.



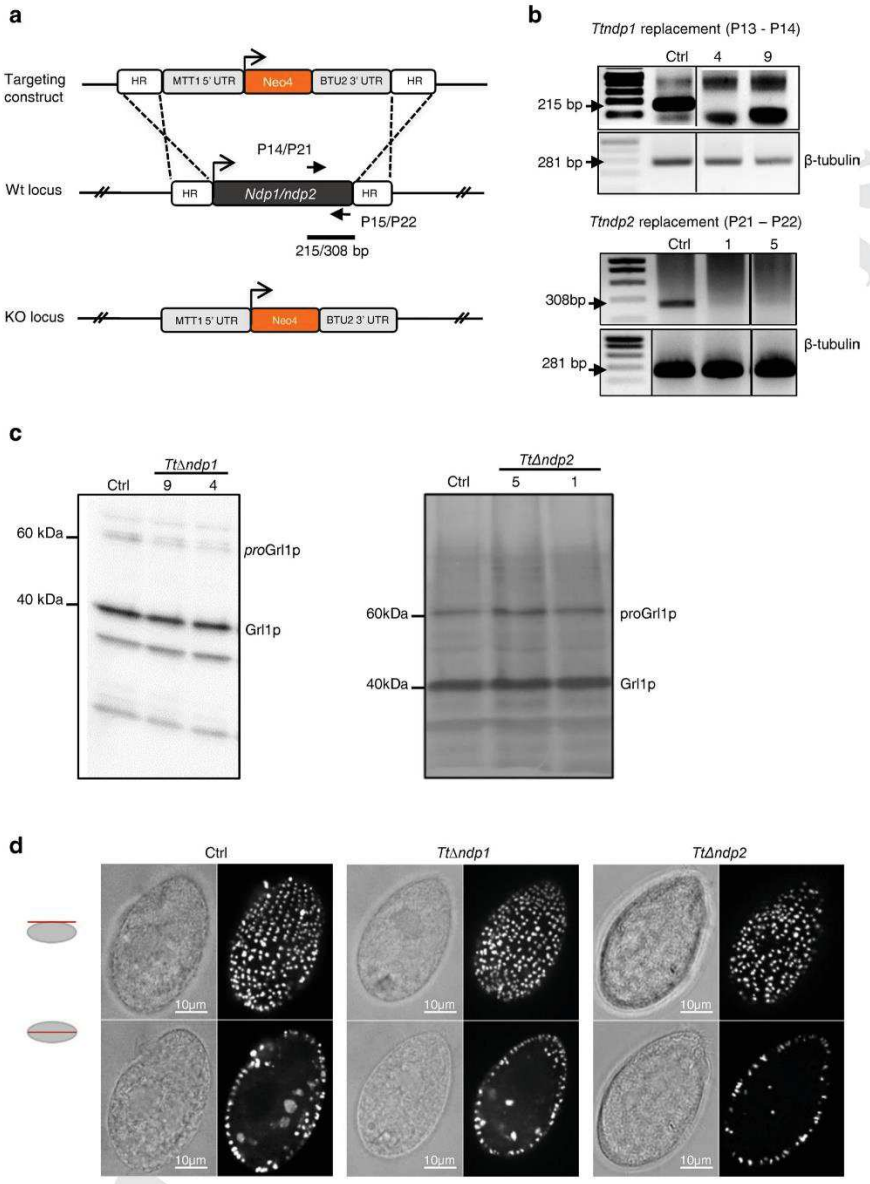
Extended Data Fig. 6 | Generation of *Tgnp1*-iKD and *Tgndp2*-iKD. a, Strategy for conditional depletion of *Tg*NdP1 (TGGT1_222660) using the Tet-OFF system. **b**, PCRs confirming integration events (double homologous recombination) at the 5′ end (top panel) and at the 3′ end (bottom panel) at the *Tgnp1* locus. Representative of 3 experiments. **c**, Strategy for conditional depletion of *Tg*NdP2 (TGGT1_ 316730) using the Auxin-inducible degron system. **d**, PCRs confirming integration events (double homologous recombination) at the 5′ end (top panel) and at the 3′ end (bottom panel) at the *Tgnp2* locus. Representative of 2 experiments. **e**, Immunoblot of *Tgndp1*-iKD +ATc and *Tgndp2*-iKD +IAA showing proteins depletion. ROP5, loading control. Ctrl: *ΔKu80-TATi* (left) and *ΔKu80-Tir1* (right). Representative of one experiment for *Tgndp1*-iKD and 2 experiments for *Tgndp2*-iKD. **f**, IFA of *Tgndp1*-iKD shows depletion of *Tg*NdP1 after 72 hours ATc treatment (left), IFA of *Tgndp2*-iKD shows depletion of *Tg*NdP2 after 24 hours IAA treatment (right). Representative of 3 experiments.



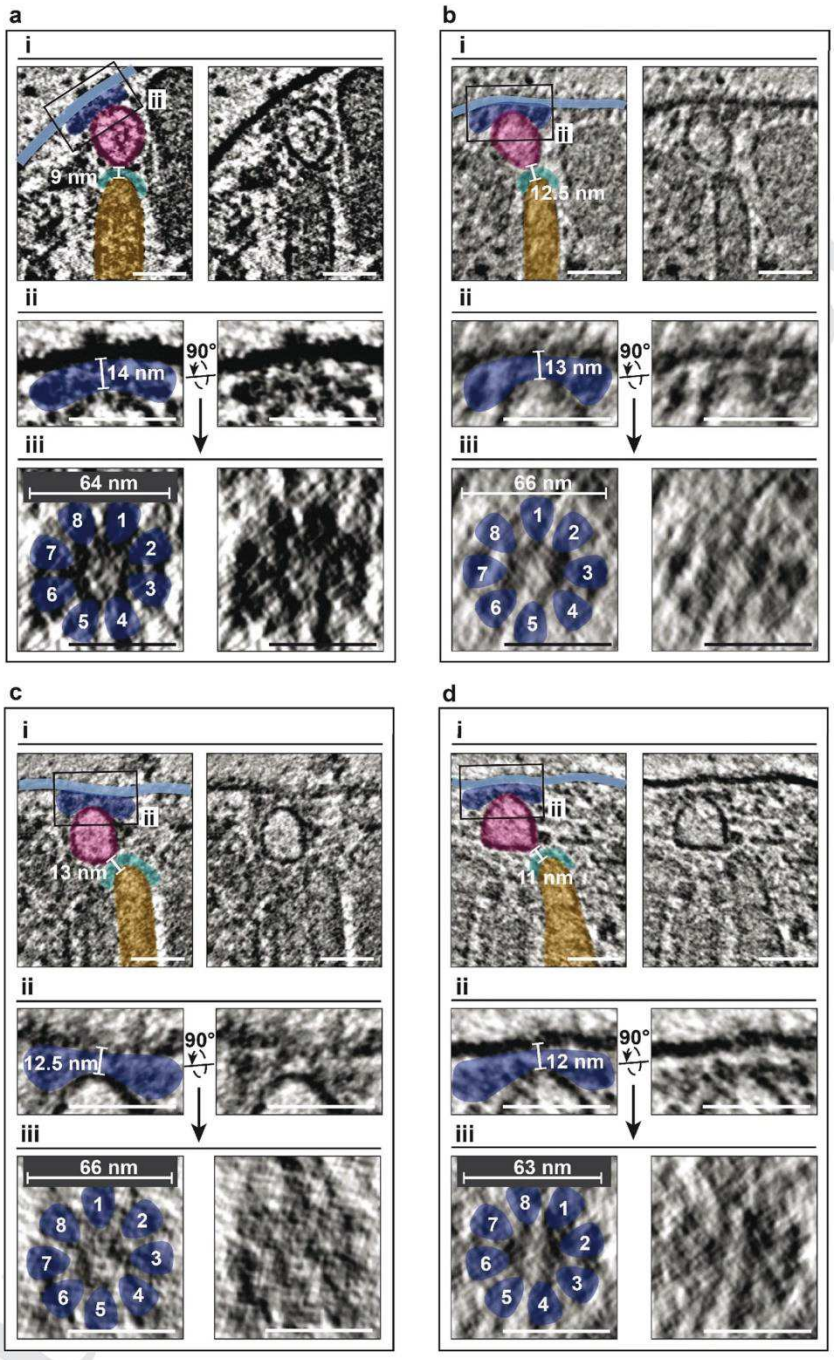
Extended Data Fig. 7 | See next page for caption.

Extended Data Fig. 7 | Depletion of NdP1 or NdP2 in *T. gondii* parasites does not affect replication, egress, gliding motility, nor attachment. a, Plaque assay. Top: *ΔKu80-TaTi* (Ctrl) ± ATc vs *Tgndp1*-iKD ± ATc. Bottom: *ΔKu80-Tir1* (Ctrl) ± IAA vs *Tgndp2*-iKD ± IAA. Means of plaque area ± SD from 3 biological samples. Representative of 3 independent experiments. **b**, IFA using anti-ROP5 and anti-ARO antibodies (rhoptry markers), and anti-MIC2 (microneme marker) on *Tgndp1*-iKD +ATc 72 h and *Tgndp2*-iKD +IAA 24 h. Scale bar=1 µm. Representative of 3 experiments. **c**, Intracellular replication. *ΔKu80-TaTi* (Ctrl) vs *Tgndp1*-iKD ±ATc and *ΔKu80-Tir1* (Ctrl) vs *Tgndp2*-iKD ±IAA. The percentage of vacuoles containing 2, 4, 8, 16 or 32 parasites was determined for 200 vacuoles. Means ± SD from 3 biological samples. Representative of 3 independent experiments. **d**, Percentage of egressed vacuoles. *ΔKu80-TaTi* (Ctrl) vs *Tgndp1*-iKD ± ATc and *ΔKu80-Tir1* (Ctrl) vs *Tgndp2*-iKD ± IAA. Egress events were quantified for 200 vacuoles. Means ± SD from 3 biological samples. Representative of 2 independent experiments. **e**, Conoid protrusion assay. The graph represents the percentage of protruded conoids induced by 5 µM A23187, and DMSO as control. Means ± SD from 3 biological samples. Representative of 3 independent experiments. **f**, Gliding assays comparing *ΔKu80-TaTi* (Ctrl) vs *Tgndp1*-iKD parasite lines ± ATc 72 h or comparing *ΔKu80-Tir1* (Ctrl) vs *Tgndp2*-iKD ± IAA 24 h. Trails were revealed by IFA using anti-SAG1 antibodies. Scale bar=10 µm. Representative of 3 experiments. **g**, Quantification of parasite motility by time-lapse video microscopy. Data are plotted as a percentage of circular, helical and twirling movements. Values represent mean of 2–4 movies. **h**, Quantification of attachment on glutaraldehyde fixed host cell. As control of microneme secretion-dependent attachment, parasites were treated with BAPTA-AM. **i**, Immunoblot showing microneme secretion assessed by the release of the processed form of AMA1 (arrow=processed/secreted *Tg*AMA1) in *Tgndp1*-iKD ± ATc 72 h and *Tgndp2*-iKD ± IAA 24 h. Ctrl = *ΔKu80-Tir1* + IAA 24. P = pellet, Sup = supernatant, Sup ind = propanolol-induced supernatant. GRA3, loading control. **j**, Quantification of rhoptry secretion by e-vacuoles assay in *Tgndp1*-iKD ±ATc 72 h. (**h**, **j**) Means ± SD from 3 biological samples. Representative of one experiment. The significance of the results was assessed using a parametric paired *t*-test (Student's two-tailed *t*-test). ns = non-significant.

Uncorrected proof



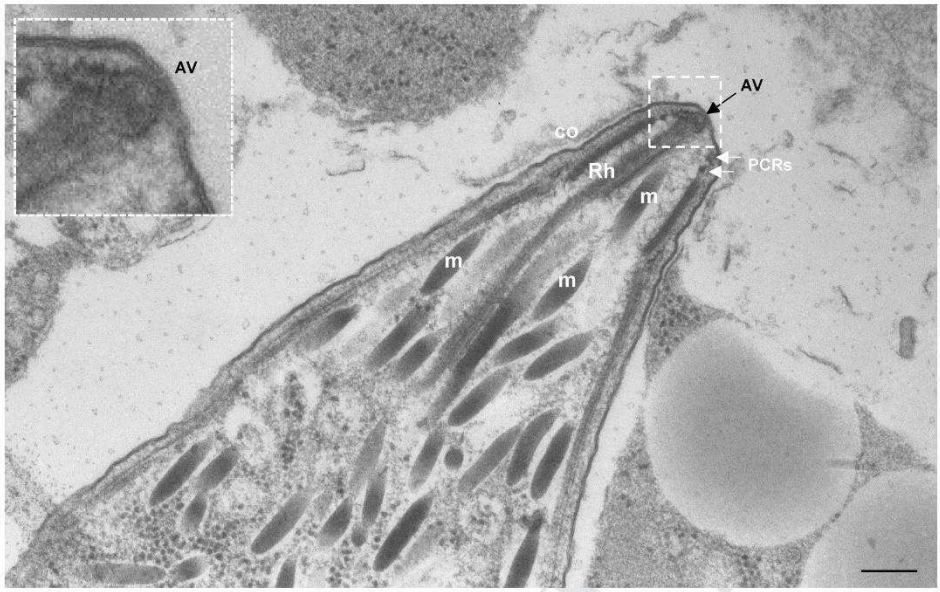
Extended Data Fig. 8 | Mucocyst biogenesis and positioning is not affected in *TtΔndp1* and *TtΔndp2*. **a**, Generation of *Ttndp1* and *Ttndp2* knockout strains in *T. thermophila* Cu428. **b**, cDNA from *TtΔndp1* (clones 4 and 9) or *TtΔndp2* (Clones 1 and 5) were PCR amplified with primers P13/P14 and P21/P22 respectively, to assay the presence of the corresponding transcripts in the knockout strain. To confirm that equal amounts of cDNA were being amplified, reactions with primers specific for β-tubulin 1 were run in parallel (loading control). Representative of 2 experiments. **c**, Immunoblot showing proGrl1p processing in wild-type and mutant strains (clones 4 and 9 for *TtΔndp1*; clones 1 and 5 for *TtΔndp2*). Representative of one experiment. **d**, Confocal cross (top) and transverse (bottom) sections, with paired differential interference contrast (DIC) images, of *TtΔndp1* (clone 9) and *TtΔndp2* (clone 5). Cells were immunostained with mAbs 5E9, which recognize the mucocyst protein Grl3p. The wild-type pattern of the docked mucocysts is maintained in *TtΔndp1* and *TtΔndp2* clones. Scale bar = 10µm. Representative of 3 experiments.



Extended Data Fig. 9 | See next page for caption.

Extended Data Fig. 9 | Cryo-ET of rhoptry secretion system. Four examples (a-d) from cryo-ET imaging of apical ends of the rhoptry secretion system. (i) vertical tomogram slices show the arrangement of the rhoptry (orange), tip density (cyan), apical vesicle (AV; magenta), rosette (dark blue) and the plasma membrane (PM; light blue). Original images (right) are annotated with color overlays (left). (ii) Magnified image of the boxed region in (i) showing the side view of the rosette. (iii) Top view of the rosette from a horizontal tomogram section through it and perpendicular to the plane in (ii) showing an 8-fold rotational symmetry. All measurements are made in 3D. Panel (a) shows images from the unfiltered version of the tomogram that is shown in Fig. 4a-c. In each of the four examples, images in (ii) and (iii) are from the same cell. Scale bars: 50 nm. Representative of 20 tomograms produced from 2 independent samples.

Uncorrected proofs



Extended Data Fig. 10 | Apical area of a *Sarcocystis tenella* cystozoite. Similarly to what was observed in literature and experimentally in *T. gondii*, cystozoites of *S. tenella* display an apical vesicle in between the apical tip of the rhoptry neck and the plasma membrane, at the site of exocytosis. PCR=posterior preconoidal ring; co = conoid; Rh = rhoptry neck; m = micronemes; AV=apical vesicle. Bar is 0.2 µm. Representative of 2 experiments.

Uncorrected Proof

Résumé français de la thèse

Les apicomplexes représentent un large groupe de parasites eucaryotes responsables de différentes infections chez l'homme et les animaux, dont le paludisme et la toxoplasmose. La toxoplasmose est considérée comme une infection parasitaire négligée nécessitant un contrôle de santé publique. Elle est due au parasite intracellulaire obligatoire, *Toxoplasma gondii*. Une des voies d'infection par ce parasite est l'ingestion de kystes tissulaires contenant des bradyzoïtes. Le bradyzoïte est une forme à multiplication lente, localisée à l'intérieur d'un kyste tissulaire retrouvé dans les tissus des animaux infectés par *Toxoplasma*. Par conséquent, l'une des voies d'infection de l'homme est donc due à la consommation des viandes peu ou pas cuites contaminées par ces kystes. Suite à l'action des sucs gastriques et intestinaux, la paroi des kystes de bradyzoïtes est rompue, et ces bradyzoïtes se retrouvent libérés dans l'estomac et l'intestin grêle de l'hôte. Ces stades parasitaires envahissent ainsi les cellules de la muqueuse intestinale où ils s'y transforment en une forme infectieuse, à multiplication rapide, appelée tachyzoïte. Le tachyzoïte est capable d'infecter toutes cellules nucléées où il se multiplie activement, entraînant la lyse des cellules parasitées. Les tachyzoïtes libérés infectent par la suite, les cellules adjacentes y compris celles du système immunitaire. La prolifération et dissémination rapide de ces tachyzoïtes dans tout l'organisme constituent la phase aiguë de l'infection. Une réponse immunitaire spécifique se met alors en place et la plupart des tachyzoïtes sont rapidement éliminés. Cependant, sous la pression de la réponse immune, certains tachyzoïtes réussissent à se différencier en bradyzoïtes et vont s'enkyster, notamment dans les muscles striés squelettiques dont le muscle cardiaque et dans les cellules du système nerveux. Cet enkystement correspond à la phase chronique de l'infection. A noter qu'un équilibre étroit est maintenu entre le parasite et l'hôte, permettant aux kystes de persister de manière "dormante" pendant toute la durée de vie de l'hôte immunocompétent. Cependant, chez les patients immunodéprimés, les bradyzoïtes présentent la capacité de se reconvertir en

tachyzoïtes. La multiplication et dissémination de ces derniers par voie hématogène dans l'organisme du patient peut conduire à une maladie potentiellement fatale, si elle n'est pas traitée.

*Toxoplasm*a, comme *Plasmodium*, sont des parasites intracellulaires obligatoires; l'entrée dans la cellule hôte représente alors un évènement crucial pour la survie de ces parasites et pour le maintien de leur cycle de développement. L'invasion est un processus unique et conservé au sein du phylum des Apicomplexes. Lors de l'invasion, les parasites établissent un contact étroit entre leur extrémité apicale et la cellule hôte. Ce processus implique la sécrétion séquentielle du contenu de deux organites uniques aux Apicomplexes: les micronèmes et les rhoptries. Lors de l'invasion, la formation d'une structure désignée la jonction mobile (JM) est primordiale, et elle correspond à une connexion étroite entre les membranes du parasite et celles de la cellule hôte. Chez les tachyzoïtes, la JM a fait l'objet de nombreuses études, et sa caractérisation moléculaire est, à ce jour, relativement bien élucidée. La JM est formée par l'interaction d'une protéine de micronème, AMA1, exposée à la surface du parasite une fois sécrétée, et d'une protéine issue du col des rhoptries, RON2, qui est quant à elle, exportée et insérée dans la membrane de la cellule hôte. RON2, forme un complexe avec d'autres protéines du col des rhoptries, RON4, $RON4_{L1}$, RON5 et RON8, qui se retrouvent également associées à la JM à la membrane de la cellule hôte. Bien que les mécanismes d'invasion et les acteurs moléculaires qui permettent d'établir la JM soient en partie élucidés chez les formes tachyzoïtes, le processus d'invasion des bradyzoïtes demeure en revanche énigmatique. Une seule étude a abordé cette question et suggérait que les bradyzoïtes ne formaient pas de JM lors de l'invasion.

Le travail de thèse présenté dans ce manuscrit avait pour ambition de caractériser le processus d'invasion des bradyzoïtes et d'évaluer la possibilité de vaccination en ciblant les protéines de la JM pour protéger contre la toxoplasmose.

Dans la première partie de cette étude, nous avons dans un premier temps évalué si les protéines de JM caractérisées au stade tachyzoïte, étaient exprimées au stade bradyzoïte. Nous avons également investi la possibilité de formation d'une JM chez ce stade parasitaire. Tout d'abord, nous avons montré que les protéines AMA1, RON2, RON4, $RON4_{L1}$, RON5 et RON8, étaient toutes exprimées au stade bradyzoïte. De plus toutes ces protéines décoraient une structure caractéristique de la JM, sur des bradyzoïtes en cours d'invasion, révélant ainsi, pour la première fois, que les bradyzoïtes établissent une JM lors de leur invasion. *Toxoplasma* possède des protéines homologues à AMA1 (AMA2, AMA3 et AMA4) et à RON2 ($RON2_{L1}$ et $RON2_{L2}$) mais qui ne sont quasiment pas exprimées au stade tachyzoïte. AMA2 est capable d'interagir avec RON2, AMA3 avec $RON2_{L2}$ et AMA4 avec $RON2_{L1}$. Ceci nous a poussée à évaluer ensuite l'expression de ces paralogues au stade bradyzoïte. Nous avons ainsi montré que les protéines AMA2, AMA4 et $RON2_{L1}$, sont en revanche fortement exprimées au stade bradyzoïte. Notamment, nous avons détecté les protéines AMA4 et AMA2 à la JM des bradyzoïtes, soulignant que la JM de ces stades-là présente une composition protéique différente de celle des tachyzoïtes. Ces résultats supportaient aussi le rôle du complexe AMA4-$RON2_{L1}$ lors de l'invasion des bradyzoïtes.

Pour aborder la fonction du complexe AMA4-$RON2_{L1}$ lors de l'invasion, nous avons entrepris une approche par génétique réverse. Nous n'avons pu obtenir de mutant pour le gène *$RON2_{L1}$*. Par contre, nous avons pu générer avec succès des parasites knock-out *AMA4*. La caractérisation phénotypique des mutants a permis de conclure que la protéine AMA4 participait à l'invasion des tachyzoïtes, mais que son rôle dans l'invasion était surtout prédominant lors de l'invasion des bradyzoïtes. Des infections chez la souris montrent également qu'AMA4 joue un rôle lors de la phase aigüe de la toxoplasmose et pour l'établissement de la phase chronique de l'infection.

En l'absence d'un vaccin approuvé contre la toxoplasmose humaine, et en vue des résultats prometteurs d'une stratégie de vaccination contre le paludisme reposant sur l'immunisation avec le complexe AMA1-RON2, nous avons en parallèle testé l'hypothèse que les complexes jonctionnels identifiés chez *Toxoplasma* pouvaient également être des candidats vaccins contre la toxoplasmose. Dans cette étude, nous avons ciblé les complexes moléculaires de la JM des tachyzoïtes et des bradyzoïtes et immunisé les souris avec les protéines AMA1 et AMA4 seules, ou en complexes avec leur partenaires RON2 et RON_{L1} respectivement. Les domaines D1-D2-D3 des protéines recombinantes AMA ont été produits et complexés avec un court peptide de RON2, correspondant spécifiquement au domaine D3 de cette protéine de col de rhoptries, et qui se lie au domaine D1 des protéines AMA. Après immunisation, la protection a été évaluée soit après une épreuve par voie intrapéritonéale d'une dose léthale de tachyzoïtes, ou après challenge par voie orale avec des kystes. Dans le premier cas de figure, la mortalité des souris a été suivie au cours du temps (suivie de la phase aigüe), alors que dans le deuxième protocole la protection de la phase chronique de la toxoplasmose a été évaluée par la mesure de la charge kystique dans le cerveau des souris immunisées.

L'immunisation par la protéine recombinante AMA1, en complexe avec un peptide RON2, a montré une efficacité protectrice élevée se manifestant par environ 80% de réduction du nombre de kystes après une épreuve par voie orale avec des kystes, et 80% de survie des souris infectées par une dose létale de tachyzoïtes. Cependant, le complexe AMA4 lié à son peptide $RON2_{L1}$ n'a pas permis de conférer une protection contre l'infection aiguë, un résultat cohérent avec sa faible expression chez les tachyzoïtes et son rôle mineur dans l'invasion des tachyzoïtes que nous lui avions attribué dans la première partie de notre étude. En revanche, le complexe AMA4-$RON2_{L1}$ protégeait principalement les souris contre l'infection chronique, après une épreuve par voie orale de kystes, supportant le rôle essentiel de ce complexe dans l'invasion des bradyzoïtes. De plus, nous avons montré que l'immunisation avec les complexes

AMA-RON2 s'avérait plus efficace que l'immunisation par les protéines AMA seules, comme observé dans le cas de la vaccination chez *Plasmodium*.

Finalement, nous avons purifié les immunoglobulines G (IgG) obtenus après immunisation avec l'un ou l'autre des complexes et montré que les IgG inhibaient la formation de la JM et de l'invasion *in vitro*, suggérant que l'inhibition de l'invasion puisse être un des mécanismes de protection *in vivo*. En outre, nous avons démontré que les anticorps générés contre le complexe AMA1-RON2 étaient plus efficaces dans l'inhibition de l'invasion des tachyzoïtes alors que les anticorps générés contre le complexe AMA4-$RON2_{L1}$ ciblaient préférentiellement l'invasion des bradyzoïtes. Ces deux résultats soutiennent le rôle prédominant du complexe AMA1-RON2 dans l'invasion des tachyzoïtes et celui du complexe AMA4-$RON2_{L1}$ dans l'invasion des bradyzoïtes. Globalement, ces résultats de vaccination supportent les résultats obtenus dans la première étude quant au rôle du complexe AMA4-$RON2_{L1}$ pour l'invasion des bradyzoïtes et identifient et valident différents complexes de JM comme candidats potentiels pour la vaccination contre la toxoplasmose.

Résumé

La toxoplasmose est une infection parasitaire négligée nécessitant un contrôle de santé publique. Elle est due au parasite intracellulaire obligatoire, *Toxoplasma gondii*. Une des voies d'infection est l'ingestion orale de kystes tissulaires contenant des bradyzoïtes. Ces derniers envahissent les entérocytes et se transforment en tachyzoïtes, responsables de la toxoplasmose aiguë. Sous le contrôle de la réponse immunitaire de l'hôte, les tachyzoïtes se retransforment en bradyzoïtes, forme dormante enkystée dans le cerveau et les muscles, et conduisant à la toxoplasmose chronique. Chez les immunodéprimés, cette forme chronique peut se réactiver et devenir fatale, si non traitée. L'invasion par le toxoplasme engage la formation d'une jonction mobile (JM), correspondant à une connexion étroite entre les membranes du parasite et de sa cellule hôte. Chez les tachyzoïtes, la JM est moléculairement bien caractérisée. Elle est formée par l'interaction d'une protéine de micronème, AMA1, et une protéine du col des rhoptries, RON2, elle-même associée à d'autres protéines RONs. Quant aux bradyzoïtes, la présence de JM et l'invasion demeurent énigmatiques. Dans cette étude, nous avons montré que les protéines de JM caractérisées chez le tachyzoïte, sont également exprimées dans la JM des bradyzoïtes, révélant pour la première fois, que les bradyzoïtes établissent une JM lors de leur invasion. Nous avons également montré qu'AMA2, AMA4 et $RON2_{L1}$, des protéines homologues à AMA1 et RON2 mais quasiment pas exprimées au stade tachyzoïte, l'étaient en revanche fortement au stade bradyzoïte. Notamment, nous avons détecté AMA4 et AMA2 à la JM des bradyzoïtes, soulignant que la JM de ces stades présente une composition protéique différente de celle des tachyzoïtes. Nous avons aussi généré des parasites knock-out AMA4 et montré l'importance d'AMA4 lors de l'invasion des tachyzoïtes, mais surtout son rôle prédominant lors de l'invasion des bradyzoïtes et de l'établissement de la toxoplasmose chronique. En absence d'un vaccin approuvé contre la toxoplasmose humaine, et en vue des résultats prometteurs de la stratégie de vaccination contre le paludisme basée sur l'immunisation avec le complexe AMA1-RON2, nous visions à cibler les complexes moléculaires de la JM des stades tachyzoïtes et bradyzoïtes, afin d'élucider la protection éventuelle contre la toxoplasmose. L'immunisation par la protéine recombinante AMA1, en complexe avec un peptide RON2, montra une efficacité protectrice élevée se manifestant par 80% de réduction du nombre de kystes après une épreuve kystique par voie orale, et 80% d'augmentation de survie des souris infectées par une dose létale de tachyzoïtes par voie intrapéritonéale. Cependant, le complexe AMA4 lié à son peptide $RON2_{L1}$ n'a conféré aucune protection contre l'infection aiguë, un résultat cohérent avec sa faible expression chez le tachyzoïte. Cependant, le complexe AMA4-$RON2_{L1}$ protégeait principalement les souris contre l'infection chronique après une épreuve par voie orale de kystes, supportant son rôle essentiel dans l'invasion des bradyzoïtes. De plus, l'immunisation avec les complexes AMA-RON2 s'avérait plus efficace que celle par les protéines AMA seules. Finalement, les immunoglobulines G contre l'un ou l'autre des complexes inhibaient la formation de la JM et l'invasion *in vitro*, suggérant que l'inhibition de l'invasion puisse être un des mécanismes de protection *in vivo*. En outre, nous avons démontré que les anticorps générés contre le complexe AMA1-RON2 ciblent surtout l'invasion des tachyzoïtes alors que ceux générés contre le complexe AMA4-$RON2_{L1}$ visent préférentiellement l'invasion des bradyzoïtes; soutenant ainsi le rôle prédominant du complexe AMA1-RON2 dans l'invasion des tachyzoïtes et celui du complexe AMA4-$RON2_{L1}$ dans l'invasion des bradyzoïtes. Globalement, nos résultats identifient et valident différents complexes de JM comme candidats potentiels pour la vaccination contre la toxoplasmose.

Mots clés: Toxoplasmose, invasion, jonction mobile, AMA4-$RON2_{L1}$, AMA1-RON2, vaccin

ABSTRACT

Toxoplasmosis is classified as a neglected parasitic infection necessitating public health control. It is due to *Toxoplasma gondii*, an obligatory intracellular parasite. One route of infection occurs following the oral ingestion of bradyzoite tissue cysts. Thereupon, bradyzoites invade enterocytes and convert rapidly to tachyzoites, leading to the acute infection. Under the tight control of host immune response, tachyzoites transform back into bradyzoites which sustain a lifelong chronic disease. If left untreated, chronic toxoplasmosis may reactivate and become fatal in immunocompromised patients. Invasion of *Toxoplasma* involves the formation of a tight connection between the parasite and the host cell membranes, referred to a structure called Moving Junction (MJ). In tachyzoites, the MJ is shaped by the assembly of a microneme protein, AMA1, and a rhoptry neck protein, RON2, as part of a complex involving additional RONs. Whilst the MJ process is well characterized in tachyzoites, invasion in bradyzoites remains underexplored. Here, we demonstrated that tachyzoite MJ proteins are also expressed at the MJ of invading bradyzoites, showing for the first time that bradyzoites do form a MJ during their invasion. We also characterized more paralogs of MJ proteins, which are barely expressed in tachyzoites, and demonstrated that AMA2, AMA4 and $RON2_{L1,}$ are highly expressed in bradyzoites. Remarkably, we found AMA4 and AMA2 at the MJ of invading bradyzoites, highlighting that bradyzoite MJ exhibits a different protein composition than that of invading tachyzoites. Moreover, we generated AMA4 knockout parasites and unraveled the importance of AMA4 for invasion in tachyzoites in some extend, but its predominant role for bradyzoite invasion and for establishing the chronic phase of infection. In light of the absence of an approved vaccine against human toxoplasmosis and the promises of a vaccine strategy based on immunization with AMA1-RON2 complex against *Plasmodium*, we built on the importance of MJ in invasion of both tachyzoite and bradyzoite stages, and interrogated the potential protection against toxoplasmosis by targeting MJ complexes. Immunization with recombinant AMA1 protein in complex with a RON2 peptide, revealed a high protective efficacy both after oral challenge of mice with bradyzoites (≈80% reduction of cysts burden) or intraperitoneal challenge with a lethal dose of tachyzoites (80% increased mice survival). Yet, AMA4 in complex with its binding $RON2_{L1}$ peptide did not protect against acute infection, a consistent result with its low expression and function in tachyzoites. In contrast, supporting its role in the invasion of bradyzoites, AMA4-$RON2_{L1}$ complex mainly protected against chronic infection. In both cases, immunization with AMA-RON2 complexes is more efficient than immunization with AMA alone. Finally, IgG against either complexes inhibited MJ formation and invasion *in vitro*, suggesting that the inhibition of invasion may be one plausible mechanism for *in vivo* protection. Importantly, antibodies against AMA1-RON2 are more efficient to inhibit the invasion of tachyzoites while antibodies against AMA4-$RON2_{L1}$ target preferentially the invasion of bradyzoites; both supporting a predominant role of AMA1-RON2 in tachyzoites and AMA4-$RON2_{L1}$ in bradyzoites. Altogether, these results validate different MJ complexes as potential vaccine candidates to protect against toxoplasmosis.

Keywords: Toxoplasmosis, invasion, moving junction, AMA4-$RON2_{L1}$, AMA1-RON2, vaccine